S.S. SHEVCHENKO
O.E. CHERNOV

MECHANICAL SEALS FOR ENERGY PUMPS

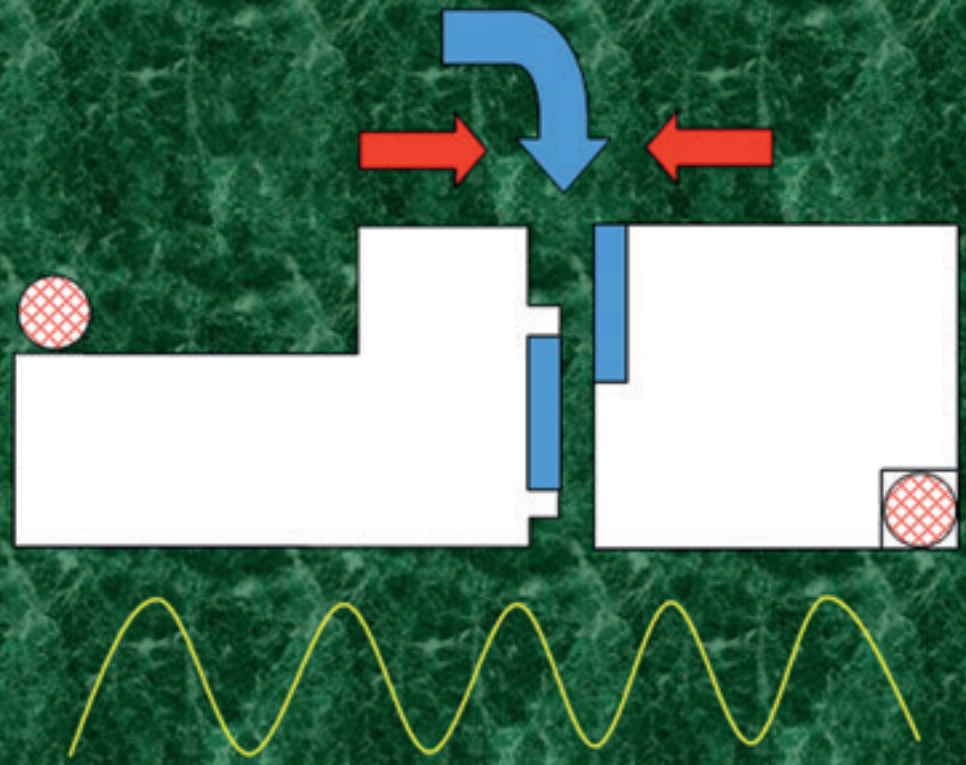

NATIONAL ACADEMY OF SCIENCES OF UKRAINE
G.E. PUKHOV INSTITUTE FOR MODELLING
IN ENERGY ENGINEERING OF THE NATIONAL ACADEMY
OF SCIENCES OF UKRAINE

НАЦІОНАЛЬНА АКАДЕМІЯ НАУК УКРАЇНИ
ІНСТИТУТ ПРОБЛЕМ МОДЕЛЮВАННЯ
В ЕНЕРГЕТИЦІ ім. Г.Є. ПУХОВА НАН УКРАЇНИ

С.С. ШЕВЧЕНКО
О.Є. ЧЕРНОВ

ТОРЦОВІ УЩІЛЬНЕННЯ ЕНЕРГЕТИЧНИХ НАСОСІВ

ПРОЄКТ
«УКРАЇНСЬКА НАУКОВА КНИГА
ІНОЗЕМНОЮ МОВОЮ»

КИЇВ
АКАДЕМПЕРІОДИКА
2024

S.S. SHEVCHENKO
O.E. CHERNOV

MECHANICAL SEALS FOR ENERGY PUMPS

PROJECT
«UKRAINIAN SCIENTIFIC BOOK
IN A FOREIGN LANGUAGE»

KYIV
AKADEMPERIODYKA
2024

https://doi.org/10.15407/akademperiodyka.503.205
UDC 62-762.8
S53

Reviewers:

V.P. KRAVCHENKO, doctor of technology sciences,
professor, head of the Department of Nuclear Power Plants,
Odesa National Polytechnic University

V.B. TARELNYK, doctor of technology sciences,
professor, head of the Technical Service Department,
Sumy National Agrarian University

S.D. VINNYCHUK, doctor of technology sciences, professor,
head of Department 8, G.E. Pukhov Institute for Modelling in Energy
Engineering of the National Academy of Sciences of Ukraine

Approved for publication by G.E. Pukhov Institute for Modelling in Energy Engineering of the NAS of Ukraine (August, 31, 2023, Protocol No. 7)

The publication was funded within the framework of the Targeted Complex Program of the NAS of Ukraine "Scientific Bases of Functioning and Providing for Conditions for the Development of the Scientific and Publishing Complex of the NAS of Ukraine"

Shevchenko S.S.

Mechanical Seals for Energy Pumps / S.S. Shevchenko,
S53 O.E. Chernov; National Academy of Sciences of Ukraine,
G.E. Pukhov Institute for Modelling in Energy Engineering of
the NAS of Ukraine. — Kyiv: Akademperiodyka, 2024. — 205 p.

ISBN 978-966-360-503-6

Physical principles are considered, and modern methods of calculating contact mechanical seals are developed. The principle of operation, calculation methods, and design features of non-contact mechanical seals are described. Modern technologies and materials used in the production of mechanical seals are presented. Directions for improving mechanical seals are proposed. The analysis of designs and features of operation of energy pumps mechanical seals was carried out. The main causes of failure were identified, and a system of maintenance and repair of mechanical seals was developed.

UDC 62-762.8

ISBN 978-966-360-503-6

CONTENTS

INTRODUCTION. Classification of sealing devices of centrifugal machines. 9

CHAPTER 1 **THE PHYSICAL BASIS OF MECHANICAL SEALS**

1.1. The history of the emergence and development of mechanical seals 13

1.2. The principle of operation and structural diagram of the mechanical seal 19

1.3. Classification of mechanical seals 23

1.4. Friction Modes of Sealing Surfaces 25

1.5. Wear mechanism of friction pairs 27

1.6. Development of a mechanical seal closed design model . . . 31

1.7. Conclusion 43

CHAPTER 2 **FUNDAMENTALS OF MECHANICAL SEALS CALCULATION**

2.1. Computing loads in the friction pair of mechanical seal . . . 45

2.2. Determination of the mechanical seal hydrodynamic characteristics 48

2.3. Computing leaks and friction power losses 51

2.4. Computing of the mechanical seal thermal state 57

2.5. Thermal deformations of friction pair rings 63

2.6. Force deformations of sealing rings 68

2.7. Conclusion. Basic recommendations for the calculation of mechanical seals 72

CHAPTER 3 **NON-CONTACT MECHANICAL SEALS**

3.1. Classification and purpose 74

3.2. Hydrostatic mechanical seals 75

3.3. Hydrodynamic mechanical seals 81

3.3.1. Hydrodynamic mechanical seals with permanent grease supply 82

3.3.2. Thermohydrodynamic mechanical seals 84

3.3.3. Hydrodynamic mechanical seals with microwaviness in circumferential direction 85
3.3.4. Hydrodynamic mechanical seals with LaserFace backflow structures 87
3.4. Impulse mechanical seals 88
3.4.1. Research on the influence of pulse compaction parameters on static characteristics 92
3.4.2. Identification of factors affecting the dynamic characteristics of the seal 99
3.4.3. An example of engineering calculations for the impulse mechanical seal 107
3.5. Designs of non-contact mechanical seals 111
3.6. Conclusions 114

CHAPTER **4** **BASIC MATERIALS OF MECHANICAL SEAL PARTS**

4.1. Designations of the main materials of mechanical seals 116
4.1.1. Basic materials of friction pair rings 116
4.1.2. Auxiliary seal materials 116
4.1.3. Spring materials 117
4.1.4. Construction materials of seal parts 117
4.2. Materials of friction pair rings 117
4.2.1. Soft carbon-graphite materials 118
4.2.2. Silicon carbide 120
4.2.3. Siliconized graphite 123
4.2.4. Metal carbides (hard alloys) 124
4.2.5. Oxide ceramics 125
4.2.6. Wear-resistant coatings and sprayings 125
4.3. Auxiliary and secondary seal materials 126
4.4. Design and materials of axial clamping devices 128
4.5. Materials of main parts of mechanical seals 130
4.6. Design and materials of driving elements 131
4.7. Selection of friction pair materials 131
4.8. Conclusion 132

CHAPTER **5** **MANUFACTURING TECHNOLOGY OF MECHANICAL SEALS**

5.1. Manufacturing of mechanical seal rings 135
5.1.1. Processing of friction pair rings 135

5.1.2. Connection of rings with reinforcing clips 137
5.2. Grinding in and checking the flatness of sealing bands 138
5.2.1. Finishing the working surfaces of friction pairs 138
5.2.2. Finishing of sealing rings made of polymer-based materials 143
5.2.3. Quality control of lapped ring surfaces..... 143
5.3. Manufacturing of main parts of mechanical seals 146
5.3.1. Manufacturing of spring elements..... 146
5.3.2. Basic requirements for pump parts 147
5.4. Leak testing of mechanical seals 148
5.5. Conclusion 151

CHAPTER **6** **DESIGNS AND OPERATING FEATURES OF MECHANICAL SEALS OF ENERGY PUMPS**

6.1. Mechanical seals for feed pumps 152
6.2. Mechanical seals for condensate pumps 156
6.3. Mechanical seals of network and circulation pumps 159
6.3.1. Mechanical seals for network pumps 159
6.3.2. Mechanical seals for circulation pumps 160
6.4. Mechanical seals for fuel oil, chemical, and auxiliary pumps 165
6.4.1. Mechanical seals for fuel oil and oil pumps 165
6.4.2. Mechanical seals for chemical pumps 167
6.5. Conclusions 167

CHAPTER **7** **ANALYSIS OF THE MAIN CAUSES OF FAILURE AND REPAIR OF MECHANICAL SEALS**

7.1. Basic provisions 169
7.2. The procedure for inspecting a mechanical seal to identify the cause of failure 170
7.3. Wear or destruction of the end rings 172
7.4. Damage to secondary seals..... 178
7.4.1. Curing 179
7.4.2. Compression effect..... 180
7.4.3. Cuts and nicks..... 180
7.4.4. Bloating 180
7.4.5. Extrusion..... 181
7.4.6. Abrasive wear 181

7.4.7. Residual compression deformation 182
7.4.8. Chemical degradation 182
7.4.9. Caisson failure. 182
7.4.10. Squeezing ring material into the gap. 182
7.4.11. Damage during installation 183
7.4.12. Outgassing of ingredients from the elastomer. 183
7.4.13. Unacceptable compression deformation. 183
7.4.14. Spiral twist. 184
7.4.15. Thermal degradation of the elastomer 184
7.4.16. Features of Teflon secondary seals. 185
7.4.17. Direction of pressure 186
7.5. Damage to leash products 186
7.5.1. Causes of damage to driving elements 186
7.5.2. Destruction of locking pins 187
7.6. Other factors affecting the performance of mechanical seals 188
7.6.1. Corrosion 188
7.6.2. Vibration 189
7.6.3. Cavitation 189
7.7. Repair and restoration of mechanical seals 189

CONCLUSIONS. 198
REFERENCES. 200

INTRODUCTION

Classification of sealing devices of centrifugal machines

Sealing, i.e., separation of media to prevent product leakage, is a universal problem for a broad range of products used by mankind. Minimizing leakage of the working medium at the exit of shafts from heavy-duty pumps and hydraulic turbines, preventing losses in technological systems of chemical production, and sealing nuclear power equipment — this is just a small list of applications for sealing technology.The problem of sealing the rotating shafts of the units is essential since leaks through the seals of the rotors of industrial pumps and compressors lead to huge losses of energy, chemicals, foodstuffs, fresh water, and so on.

According to some data [35], about 60% of emissions into the atmosphere are uncontrolled leaks through the pump seals (even for aggressive liquids, a leak rate of 0.5—2.0 l/h is considered acceptable; only through one such pump, losses are 4—16 tons of the pumped medium per year, which requires additional costs for their disposal).The technical level of modern seals is constantly growing due to the tightening of operating requirements that limit or exclude external leakage of the sealed medium. The criteria for assessing a society whose life is influenced somehow by industry, and hence the seals used in pumps, are maximum safety and minimum environmental damage. Operators want to have a minimum of worries, and entrepreneurs — a minimum of costs.

The most critical requirement is to increase the seals reliability and service life, especially considering the growth of equipment unit capacity and the automation of continuous technological processes in which forced outage due to seals failure leads to large economic losses, significantly exceeding the costs of seals directly. Forced outage of production

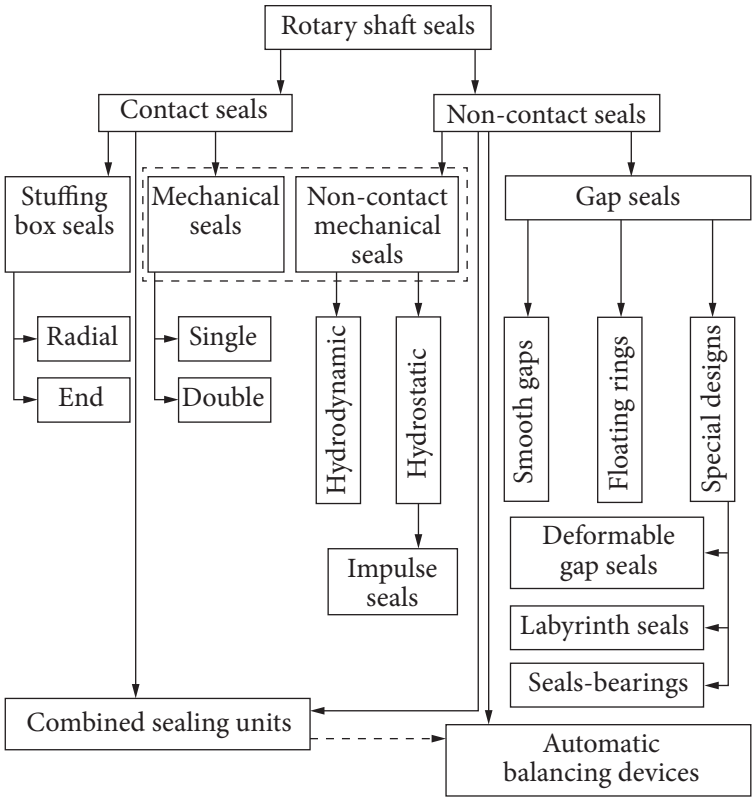

Fig. 1. Classification of rotary machines seals

lines and systems due to seal failures causes significant economic damage to enterprises, and their repair requires a lot of labor and expensive materials. In industrialized countries, where economic feasibility is a decisive factor in the choice of technical means manufacturers of pumps, compressors, and other rotary machines prefer reliable (sometimes expensive) seals, realizing that they pay off their costs.

The requirements for sealing are expressed in three seemingly simple concepts — reliability, tightness, and cost, but only a deep analysis can make it possible to find the optimal solution for each specific case. The search for a compromise between these conflicting requirements resulted in the formation of two rotor seals classes — contact and noncontact.

There are many classifications of sealing devices created by various researchers [14, 18, 25]. Since this monograph is

devoted to shaft seals of rotary machines, it is proposed to separate this segment into a separate classification, shown in Fig. 1.

Currently, pumps are equipped mainly with mechanical and radial stuffing box seals. The choice of seals is very important since up to 70% of forced shutdowns of pumps during operation occur due to failure of seals [62]. The seal costs themselves can reach 20% of the cost of the pump, so the choice of seal type is determined by the requirements for the equipment and the working conditions of the maintenance personnel, as well as economic feasibility [15].

A mechanical seal with a lapped friction pair is an unadjustable assembly, the life of which is uniquely determined by the operating time until an unacceptable leakage is reached. The existing attempts to use detachable friction pairs have not gotten widespread use due to the complexity of the design and installation. The main directions of development of this seal type are to increase the assembly resource by improving the materials of the friction pair and reducing the cost of mechanical seals. Mechanical seals are automatic components, the restoration of which is very difficult under operating conditions.

Restoration of pump performance is ensured by dismantling it and replacing the seal. Besides, the disadvantage of the mechanical seal from the point of view of operation is that its failure in the vast majority of cases is sudden. It is practically impossible to determine whether a unit has reached the maximum permissible state by diagnostic methods since the causes of failure are either loss of mobility or failure of one of the sealing elements.

Areas where mechanical seals occupy the advantageous position operating at a pressure of sealed liquids of more than 1.0 MPa are petrochemical industry, aviation and space technology, energy equipment, including nuclear power as well. The design, manufacture, and operation of seals and sealing systems require extensive knowledge. Processes in sealing slots are determined by the properties of liquids and gases, physical phenomena of heat transfer and heat transfer processes, phase changes, wear and corrosion processes, the balance of acting forces and moments, the vibrational state of machines, and other operational factors.

The book analyzes domestic and foreign experiences in the mechanical seals creation and shows ways to improve their designs.

Chapter 1 discusses the physical basis of contact mechanical seals. Chapter 2 is devoted to modern methods for calculating contact mechanical seals. Chapter 3 describes the principle of operation, calculation methods, and design features of non-contact mechanical seals, and Chapter 4 describes the materials used in the production of the main parts of mechanical seals. Chapter 5 presents modern technologies for the mechanical seals manufacture, and Chapter 6 presents the design and operation features of mechanical seals for energy pumps. Analysis of the leading causes of failure and repair of mechanical seals are presented in Chapter 7.

The book can become a practical guide for developers of mechanical seal units, engineers of operating organizations, as well as for teachers and students of technical universities.

CHAPTER 1

THE PHYSICAL BASIS OF MECHANICAL SEALS

1.1. The history of the emergence and development of mechanical seals

Mechanical seals appeared at the beginning of the 20th century in the process of world industrial development. Mayer, in his work [42], points out that the concept of mechanical seals originated in the early 1900s. Schoenherr in [57] presented several patents from 1913 [68] to 1919, which contain some features of the modern mechanical seal. The first known commercially successful mechanical seal for use on centrifugal pumps was made by the Cameron division of the Ingersoll-Rand Company in 1928 [56]. Before this, mechanical seals were used in the compressors of small refrigeration machines. The Cameron seal was installed in a range of centrifugal pipeline pumps for the first time. There was no production and sale of mechanical seals for centrifugal pumps for general use as independent units until the 1930s.

George J. Cooke invented the modern mechanical seal [7] in 1923 under the original name "Cooke Seal". He founded the Cooke Seal Company. The Cook seal was used first in refrigeration compressors. The Cooke Seal Company was sold to the Muskegon Piston Ring Company, where it became the Rotary Seal Division.

In 1929, J. M. Ryan of the Crane Packing Company developed the "Ryan Seal" mechanical seal. The seal uses a steel-bronze friction pair, one coil spring, and packing as secondary sealing elements since the rubber sealing ring had not yet been invented. The rotating ring was made of steel and mounted with an interference fit on the pump shaft. The sealing surfaces were machined.

At least three Ryan Seals seal assemblies have been implemented: one for a pipeline maintenance pump, one for a refinery pump, and one for a boiler water transfer pump.

In 1934, mechanical seals made by A.R. Tuck and J.H. Hohler were used in the pumps of a standard refinery in Whiting, Indiana. Durametallic signed an exclusive agreement with Tuck and Hohler, and within 12 years, mechanical seals became Durametallic's core product.

Early designs of pump mechanical seals often used a combination of hardened steel on ground bronze as the material combination performed satisfactorily in lubricating oils. However, when sealing "non-lubricating" fluids, a different approach is required to provide lubrication to friction surfaces. To this end, Durametallic developed the double mechanical seal [48] in 1937, which also proved to be effective in aggressive, dirty environments and high-pressure sealing. In a way, double mechanical seals were similar to conventional lantern ring seals with barrier fluid supply. Although these early mechanical seals leaked excessively, mechanical seal leakage was an order of magnitude less than gland leakage.

Mechanical seals in the 1930s used soft packing as secondary sealing elements. It was made from natural fibers, rubber, neoprene, or asbestos. The rubber o-ring was developed in the 1930s but was not used in mechanical seals until after World War II. Neil Christensen developed the optimal O-ring and groove dimensions in 1933. He applied for a patent in 1937 and received it in 1939 [6]. Before World War II, natural rubber was used to make rubber rings, although synthetic production was already developing. Synthetic rubber production became a wartime priority due to the difficulty of obtaining raw materials for natural rubber. Neoprene, Buna N, Buna S, and Butyl Rubbers were the first synthetics. Synthetic rubbers had a temperature limit of up to 120 °C.

In the mid-1930s, the Crane Packing Company patented the Chicago seal. Through several patents, this design evolved into a mechanical seal with rubber bellows. By 1938, Crane Packing Ltd in England began making mechanical seals for refinery pumps. The design used several spring elements, packing as secondary sealing elements, and a carbon-on-stellite friction pair. Later, rubber bellows began to be used as secondary seals. Some seals were applied at high pressures and speeds (one of the samples at 11,000 rpm).

The patent review shows that from the mid-30s to the mid-40s, the designs of mechanical seals were improved actively. Patents include:

1936 — First automobile compactor, John Crane.

1938 — Hanns Hornschurch, "Sealing device" (first balanced seal).

1939 — Robert Stevenson, Seal Knot (Successor of Sealol).

1941 — Olin Brummer "Liquid seal for rotating shafts" (assignee of John Crane).

In the late 1930s, around 1938 or 1939, mechanical seals began to replace oil seals on automotive water pumps. The water pump of a famous World War II Jeep uses a John Crane rubber bellows seal. After the Second World War, all automotive water pumps are equipped with mechanical seals.

In 1938, F.B. Porges, an engineer at the Manchester Refinery in England, developed mechanical seals to solve some operational problems. Within a few years, Flexibox Co., Ltd. has brought its mechanical seals to the market. The first Flexibox products use single-layer metal bellows. Flexibox soon began producing double and triple bellows seals.

The concept of load balance ratio is mentioned in a seal patented in 1913 [57]. However, the balanced seal, later known as the double mechanical seal, was developed in the late 1930s by Hanns Hornschurch [21]. In this design, the internal seal is balanced. It was the first use of the balance ratio, although the term was not in use at the time. Later, Robert Stevenson — Stevenson Engineering (later Sealol) received a patent for a hydraulically balanced mechanical seal [65]. Then, a balance ratio of about 50% was assumed based on the statement that the contact load is created by springs and does not depend on the pressure being sealed.

Teflon became commercially available in 1944, but it was not used in mechanical seals until after World War II. The inertness of Teflon made it possible to start using mechanical seals in aggressive environments. Because of its rigidity, Teflon is typically made in wedges, U-cups, chevrons, and bellows to use as secondary sealing elements. Teflon is suitable for use up to 260 °C.

After World War II, developments in carbon graphite production made it possible to use this self-lubricating material to manufacture O-rings in mechanical seals, the production of which increased in the 1950s.

In the mid-1940s, pump manufacturers started making their own mechanical seals. Ingersoll-Rand has developed single-balanced mechanical seals for pressures up to 4 MPa. This gave them an edge over their competitors, who used double seals and a lubrication system. Worthington, Pacific, Byron Jackson, United, Union, and others developed their own projects [48]. Eventually, the seal business spun off from the pump companies. Byron Jackson became Borg-Warner (now Flowserve) and Worthington were sold to ChemPro (now John Crane — Sealol).

In 1945, Crane Packing developed and patented four types of rubber bellows seals (originally Jeep water pump seals). In addition, Flexibox Ltd was founded in Manchester in 1945, specializing in the development of mechanical seals for use in the Manchester Refinery. The first seals manufactured by Flexibox used complex metal bellows. For several years, Flexibox has been making double and triple bellows.

In 1946, Jim Thayer at the Crane Packing Company developed the Type 9 seal that uses a Teflon wedge. A Teflon wedge was needed for sealing highly caustic or corrosive liquids in DuPont's chemical plants. Around the same time, the Crane Packing Company developed the Type 8B seal for pipeline pumps. Type 8B seals use Buna O-rings and are balanced for pressures up to 8.3 MPa.

The reasons that modern mechanical seals have less leakage are improvements in manufacturing processes and quality control. The first sealing surfaces of mechanical seal rings were not as flat and smooth as they are today. The lapping accuracy has evolved along with the improvement of mechanical seal designs. In 1938, Crane Packing began lapping O-rings and, in 1948, created the Lapmaster division for lapping machines and processes.

In the late 1940s, Olin Brummer left John Crane to form his own company, the Brümmer Manufacturing Company. He received several mechanical seal patents advertised for widespread use in water pumps.

Cartridge seals developed by C.E. Wiessner from Durametallic in 1942 [48] began to be used constantly from 1950.

The impeller rings used to circulate seal systems were developed in the early 1950s.

By 1954, mechanical seals were used so regularly in refining pumps that the American Petroleum Institute included seal specifications in the first edition of its 610 Centrifugal Pumps for the Refining Industry standard to address the problem of changing from stuffing boxes to mechanical seals. In 1955, the American Standards Association attempted to unify some sizes of pumping nomenclature. This work eventually led to the creation of the American ANSI standard.

By 1956, many of the mechanical seal concepts and application principles that are in use today were developed [10]. Design options include both rotating and fixed springs, balanced and unbalanced hydraulic loads, rubber and metal bellows, and a wide variety of spring designs and types. Various designs of secondary sealing elements include rings, wedges, U-cups, and various packings. Carbon-graphite is widely used as an O-ring material, and mating rings are often made of cast iron, niresist, stainless steel, stellite or alumina, ceramic, or tungsten carbide. Hard overlays, especially stellite, are often applied to stainless steel. When two rigid rings are used, carbon-graphite is usually replaced by cast iron, bronze, or sometimes tungsten carbide. Stainless steel is widely used for springs, retainers, and body parts. The range of temperature level for these seals is from 90 to 420 °C, and the nominal pressure is up to 7 MPa, depending on the design and materials. Single and multi-stage (so-called "double" or "tandem") compaction devices were used as operationally necessary to achieve the required resource. Undoubtedly, the allowable leakage for mechanical seals in the 1950s was much higher than today. Back then, mechanical seal leakage was compared to gland leakage, and the mechanical seal was definitely superior.

In 1956, the Japanese NOK Corporation developed its first mechanical seal.

Karl Schoenherr, who has made major contributions to mechanical seal technology, encourages Herbert B. Hummer, Chief Engineer of Durametallic, to develop the pressure-velocity index (*PV*) as a guideline for the design and

application of mechanical seals [2]. Hammer began work on the *PV* in the early 1950s. In addition to *PV*, the effect of shaft runout on seal performance was investigated, and the principles of limitation were determined. Schenger, chief engineer at John Crane, developed the *PV* concept and published many articles on the basics of mechanical seals.

Metal bellows have been used as sealing elements in mechanical seals, valve stems, and other equipment since the 1950s. In 1957, Sealol introduced welded metal bellows. Previously, molded bellows were used, which were much thicker and stiffer than welded metal bellows. The emphasis was on high temperatures. DuPont began producing Viton A fluor elastomers.

In the early 1960s, Crane Packing Company developed the Type 8B-1 mechanical seal, which was a version of the Type 9B with a rubber ring.

In the 1960s, theoretical research and testing of mechanical seals focused on surface effects in friction pairs and hydrodynamics. Researchers began to write about uneven sealing surfaces as a means of increasing hydrodynamic bearing force. With Burgmann seals, Mayer used circulation grooves on the sealing surface to help cool it. John Crane's Trytek has developed hydrodynamic sealing surfaces.

Rayleigh pads, which have been used in thrust bearings, were not considered rigid enough for a long time to ensure the non-contact operation of mechanical seals in a wide range of operating conditions. Muijderman improved Rayleigh pads with helical grooves. In the late 1960s, while working for the Crane Packing Company, James F. Gardner developed and patented a non-contact mechanical seal for compressors that uses spiral grooves on the sealing surface. In 1989, A.O. Lebeck [29] received a patent for an "O-ring with a wavy surface" close to a non-contact seal.

Most of the modern compressors have begun to be equipped with non-contact dry mechanical seals, and many older compressors have been retrofitted. In 1962, Burgmann began developing and manufacturing mechanical seals. Dr. Ehrhard Mayer has researched and developed thermohydrodynamic grooved mechanical seals for high-pressure applications. Tungsten carbide came into use as a sealing surface material around 1963.

Elastomer bellows, previously only made from natural rubber, neoprene, or Buna, were made from fluoropolymer in 1965.

In 1971, DuPont revolutionized elastomers again with Kalrez, a high-temperature and corrosion-resistant perfluoro elastomer.

In 1972, solid reaction-bonded silicon carbide (RBSiC) began to be used as the rings of mechanical seals.

Chesterton began manufacturing ANSI cartridge mechanical seals. Previously, due to the small size of the ANSI seal chambers, most pumps had to use stuffing box seals.

Modern metal bellows seals were developed as part of Exxon's seal reliability program. Exxon's pumping division was not satisfied with the reliability and durability of the seals in hot environments. Starting in January 1976, Exxon's metal bellows seals were mass-produced using parts from various seal manufacturers.

Until the late 1980s, the ANSI "chemical standard" was used primarily for pumps that were designed for gland packing. It was difficult to insert mechanical seals into the small sizes of stuffing boxes, especially multi-stage ones. Independent tests on several seal pumps from different manufacturers have confirmed the obvious: seals work better with larger radial chamber sizes. The size of the seal chamber in the pump design has been increased.

The environmental "Clean Air Act" of 1990 contains restrictions on fugitive leaks from pumps. Seal manufacturers have taken to refining the design using computer simulations and the use of modern materials. Particular attention was paid to the cartridge design of seals and the improvement of sealing mechanisms. As a result, the requirement of the "Clean Air Act" was met.

Non-contact mechanical gas dry seals proved so reliable and popular for compressors that variations were soon applied to pumps. In the late 1980s, Upstream Pumping used helical grooves on the sealing surfaces to create additional lift. Subsequently, the liquid seal was replaced by a gas barrier and double-dry mechanical gas seals were created, which became widely used.

In October 1994, the American Petroleum Institute issued the first edition of API 682, Shaft Seals for Centrifugal and Rotary Pumps. This standard, issued for the needs of the oil refining industry, had a significant impact on the development of sealing technology. API 682 provides guidance on seal design selection and requires seal testing by manufacturers. API 682 also sets a reliability metric of three years of continuous service.

The reliability of mechanical seals has improved significantly since their original use [13]. The service life of the first seals was several months. In the late 1940s, seal life became nine months, about the same as other major refinery pump assemblies had. From the early 1960s, seal manufacturers began using PV to provide a seal life of at least two years. In the early 1970s, most pumps were equipped with mechanical seals with an operating time between pump overhauls from 15 to 30 months. Studies have shown that the number of seals that fail due to wear has been significantly reduced. With improvements in pump and seal designs according to API 610, a replacement life of over six years has been reached.

For now, in addition to the spiral grooves and the wavy surface of the sealing rings, materials with special surfaces are being developed to increase the hydrodynamic lifting force in the mechanical sealing pair. Laser technologies are used to etch microscopic grooves and obtain the desired shape of the seal-

ing surface. Piezoelectric materials and electronic control systems are being researched to create controlled seals. The use of modern technologies for processing the surfaces of sealing rings and the introduction of automatic control elements have great prospects.

Currently, mechanical seals are used increasingly due to such important qualities such as tightness and durability. In the industry, a specialized branch of the production of mechanical seals has been formed. Leading global companies EagleBurgmann (includes Eagle, Burgmann); John Crane (Smiths Group), including Sealol (Rotary), Flexibox, Safematic, Ropac; Flowserve including BW/IP (Borg-Warner), Durametallic, Five Star, Pacific Wietz; Garlock and others supply complete seal assemblies for a wide range of parameters and operating conditions, guaranteeing tens of thousands of hours of life.

1.2. The principle of operation and structural diagram of the mechanical seal

The simplest mechanical seal (Fig. 1.1) has an offset (*2)* and rotating axially-movable (3) sealing rings made of wear-resistant material, which are caged (*1)* and (*5)*.

Preliminary contact pressure between the rings is achieved through spring force (*6)* and then enhanced due to the pressure force of the sealed liquid. The clearance between the shaft and axially-movable ring (*3)* is sealed by secondary seal (*4)*. The torque required to overcome friction on the end contact surfaces is transferred from the shaft to the rotating ring via a driving device (pin (*7)* and ring skirt with a longitudinal groove).

Sealing is completed as a result of compression of the end surfaces of offset (*2)* and rotating (*3)* rings. With the increase of contact pressure, sealing is increased, but along with this, friction power losses increase, thus increasing the wear of friction surfaces, their heating, and temperature deformations. Thus,

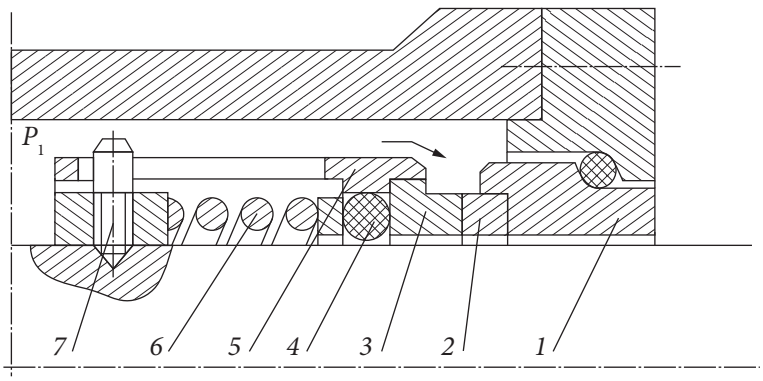

Fig. 1.1. Mechanical seal

the performance of a contact mechanical seal is determined by contact pressure and physical processes on the end surfaces in contact and moving relative to each other. Despite the seeming external simplicity of mechanical seal assembly, the processes proceeding at the joint of mating end surfaces of two parts (one of which rotates with the rotor) are extremely complicated. This is due to the simultaneous affect and communication of the friction processes, hydrodynamics, and heat processes, as well as changes in the form of mating surfaces in the sealing joint when the load parameters of the seal are changed.

According to the experimental data available [45], seal performance can be presented more simply as follows. When the whole is filled with a liquid, leakage is unavoidable, resulting in the heat being tapped from the friction pair, and under normal conditions, a heat balance is established. With increased friction power losses (for example, due to an increase in peripheral velocity), the temperature in the layer rises, and the moment might come when the liquid in this layer begins to boil. As a rule, it happens in the region adjacent to the external low-pressure chamber, where the temperature is maximal, as liquid temperature increases as it flows in the clearance gap from the high-pressure to low-pressure region. Liquid and vapor phases are formed, and the borderline between them can shift radially. The region of the liquid phase decreases as friction power losses increase.

At the interface, intense vaporization occurs due to friction energy. Therefore, the temperature in the gap stabilizes, especially since the formation of steam reduces the force of viscous friction. Under unfavorable conditions, the liquid phase may decrease so much that the liquid layer in the gap loses its continuity. This leads to a sharp increase in temperature, and the normal operation of the seal is disrupted. Therefore, if a visible leakage is permitted, it is necessary to ensure a good heat rejection to prevent vapor generation. For seals to perform without visible leakage, it is necessary to stabilize the position of the phase interface. Thus, because of small peripheral velocity and viscous liquids, even heat rejection may be appropriate. With high speed, it is necessary to ensure a reliable cooling of friction pairs. The main difficulties of calculating mechanical seals and performance prediction are conditioned by the complexity of friction and wear processes. In this case, practice is considerably in advance of theory: the immediacy of the problem of rotor sealing often forces us to search blindly for and find the proper constructive and process design solutions for various parameters of the sealed liquids, their pressures, peripheral velocity, temperature, requirements for reliability, durability, and sealing at economically sound cost.

When designing mechanical seals, it is reasonable to take a durability indicator as an optimality criterion, for example, an average resource, i.e., the mathematical expectation of the operating time before the limit state when

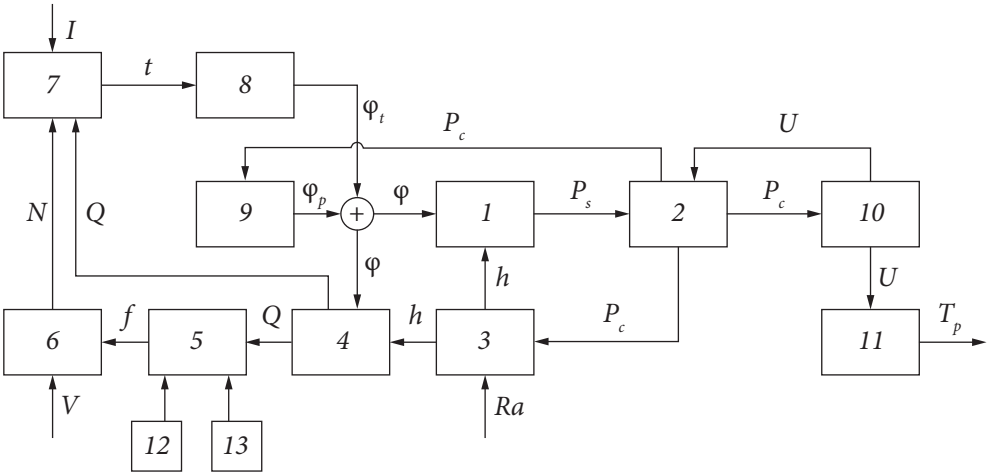

Fig. 1.2. Structural diagram of the mechanical seal: *1* — hydrostatic pressure in the gap; *2* — contact pressure; *3* — end gap; *4* — leaks; *5* — friction mode; *6* — friction losses; *7* — thermal state; *8* — temperature deformations; *9* — force deformations; *10* — wear; *11* — resource; *12* — anti-friction properties of materials; *13* — characteristics of the medium to be sealed. Let's introduce the following definitions: I — heat rejection efficiency; t — temperature; k — coefficient of load; P_1 — sealed pressure; N — friction power loss; P_c — contact pressure; P_s — hydrostatic pressure in the clearance gap; φ_t — temperature deformations; φ_p — force deformations; h — end clearance; U — wear; v — peripheral velocity; f — coefficient of friction; R_a — the roughness of friction surface; T_p — assembly resource

the further operation becomes technically impossible or unreasonable. Other important requirements — integrity, safety margin, minimum friction power losses, admissible dimensions, and cost — should be considered as limitations in the optimization problem.

The durability of mechanical seals is determined by the wear resistance of materials of friction pairs, operating conditions, and contact pressure, which, in turn, depends on a range of design and operational factors. The design factors, except for the coefficient of load and direction of radial flow, include the geometric shape of the radial section of the sealing rings, their diameter, and the manner of fastening. The main operational factors are rotor speed, physical properties, pressure and temperature of the sealed medium, the content of abrasive contaminant in it, value, and the nature of rotor vibrations.

The mechanical seal is a dynamic system [59], a simplified structural diagram of which (Fig. 1.2) gives an idea of the interaction of its main components, the nature of their transfer functions, external actions and outputs of the system, and allows the computational problems of transfer functions of components to be determined and the system reaction to external influences to be estimated. The complexity of the processes of thermal hydroelasticity, friction,

and wear does not allow to give an accurate definition of most transfer functions of the system components. Therefore, the computation has to be limited to approximate estimates and a comparison of the newly designed seals with proven-in-use analogues.

At the same time, the block diagram shows the tasks of calculation, which are reduced to determining the transfer functions of the elements and assessing the response of the system to external influences. As a reaction, one can take the resource T_p of the seal or the linear wear U of the end contact surfaces.

The papers [18, 30, 42] present an abundance of experimental data on mechanical seal friction and wear that allows seal durability to be approximately predicted during the design phase. On the basis of ideas about friction and wear processes, design formulas are proposed for assessing wear indicators, containing a number of coefficients that must be determined experimentally for specific materials and friction conditions. Unfortunately, the proposed dependencies based on empirical data are not universal. The dimensionless mode criterion [41] $G = \mu\omega \times r_c / p_c h$, corresponding to the Sommerfeld inverse number, can be used as a universal operational characteristic of seals.

The most substantiated and acceptable formulas for calculating the wear intensity for engineering calculations are given in the reference book [42]. However, the special physical and mechanical characteristics included in these formulas (the parameter of the frictional fatigue curve, the correction factor for the number of cycles corresponding to the separation of the wear particle, the coefficient characterizing the stress state on the contact patch, etc.) are partially systematized only for some common structural materials in dry friction conditions. There are no such characteristics yet for anti-friction materials of friction pairs of mechanical seals in the presence of an intermediate film of the sealing liquid.

The main factor that determines the wear of the friction pair of a mechanical seal is contact pressure, which, in turn, depends not only on the design and operating parameters but also on a range of internal processes accompanying the seal's performance. In particular, force and temperature deformations, which are determined by the geometric shape of the sealing rings, friction power losses, and the conditions of heat rejection, can have a significant effect on the processes in the friction pair. Therefore, in order to successfully design mechanical seals as dynamic systems, computational tools developed on the basis of studying the physical processes occurring in them should be used.

1.3. Classification of mechanical seals

The design of the seal and its characteristics are determined by operational factors, primarily the pressure of the sealing liquid and the average circumferential speed. The product is used as a general indicator. E. Mayer [42] conditionally subdivides mechanical seals into four groups (Table 1.1.), which makes it possible to present in general terms the difficulties associated with sealing the rotors of specific pumps. If the seals of the first and second groups are mass-produced, then the seals of the fourth, and often the third group, require individual design and manufacture.

A similar classification according to operational characteristics [23], which also includes the characteristics of the medium being sealed, is given in Table 1.2. According to this classification, the corresponding load groups have higher parameters in comparison with Table 1.1. For special-purpose seals, loading parameters are not regulated.

Table 1.1. **Classification of mechanical seals by loading**

Group	Degree of loading	Pressure, MPa	Velocity, m/s	Parameter $p_1 v$, MPa · m/s
I	Low	≤0,1	≤10	≤1
II	Average	≤1,0	≤10	≤5
III	High	≤5,0	≤20	≤50
IV	Extra high	>5,0	>20	>50

Table 1.2. **Classification by operational characteristics**

Purpose		Degree | of loading	Pressure, MPa	Circum ferential speed, m/s	Factor $p_1 v$, MPa·m/s
General purpose	For neutral and aggressive environments	Low	≤0.8	≤30	≤8
		Average	≤1.6		≤48
		High	≤20		>48
	For highly aggressive environments	Not regulated			
Specific purpose	For media with abrasive inclusions				
	For high temperatures and cryogenic technology				

Fig. 1.3. Classification of contact mechanical seals according to [37]

The dimensionless mode criterion [18] $G = \mu\omega \times r_c / p_c h$ corresponding to the reciprocal of the Sommerfeld number can be used as a universal performance characteristic of seals. The classification according to operational features implicitly reflects the design features and materials used, which ensure the operability of different groups of seals according to the operating conditions [17].

The variety of operating conditions and sealing requirements has resulted in a myriad of designs that nevertheless can be classified according to a limited number of basic design features (Figure 1.3).

In this classification, only the principal diagrams of single mechanical seals are shown, from which more complex multi-section assemblies with series or parallel connected sections can be combined.

A more detailed classification should consider the characteristic features of individual elements of the mechanical seal: secondary seals, elastic elements, locking devices, geometry of the contact end surfaces, methods of heat removal, etc.

When designing mechanical seals, it is advisable to take a durability indicator as an optimality criterion, for example, an average resource, i.e., the mathematical expectation of operating time until the limit state, when further operation becomes technically impossible or impractical. Other important requirements — tightness, failure-free operation, minimum power loss due to friction, allowable dimensions, and cost — should be considered as limitations in the optimization problem.

The durability of mechanical seals is determined by the wear resistance of friction pair materials, operating conditions, and contact pressure, which, in turn, depends on a number of design and operating factors. In addition to the load factor and the direction of the radial flow, design factors include the geometric shape of the radial section of the sealing rings, their diameter, and the fastening method. The main operational factors are rotor speed, physical properties, pressure and temperature of the medium being sealed, the content of abrasive impurities in it, and the magnitude and nature of the rotor vibrations.

1.4. Friction Modes of Sealing Surfaces

Mechanical seals work in the presence of contact spots between the end surfaces rotating relative to each other. The main reason for limiting their resource is the wear of lubricated rough surfaces as a result of friction. Thus, among other factors, wear is influenced by the friction mode and surface parameters.

The characteristic of microroughnesses that cause surface roughness, regardless of the method of its preparation, is determined by the roughness class (Table 1.3). The arithmetic mean deviation R_a of the profile at the base length l, the height of the irregularities R_z at ten points, and the highest height of the profile irregularities R_{max} are used as the main roughness parameters.

An idea of the various modes of friction is given by the generalized Stribeck curve (Fig. 1.4), depicting a qualitative relationship between the friction coefficient f and the dimensionless quantity $\mu\omega / p_c$, proportional to the ratio of the fluid friction force to the contact pressure force (μ — dynamic viscosity coefficient of the sealed liquid, ω — rotor speed).

The right section of the I curve corresponds to the liquid lubrication regime: a continuous layer of liquid is maintained between the rubbing surfaces. The value of the average gap h_0 satisfies the condition $h_0 / \overline{R} > 3 \div 5$, where $\overline{R}^2 = R_{a1}^2 + R_{a2}^2$; R_{a1}, R_{a2} are the arithmetic mean deviations of the profiles of contacting rough surfaces.

In the liquid lubrication mode, the coefficient of friction is easy to calculate since the friction force is equal to

$$F_m = \tau_c S_c = 2\pi\mu\omega r_c^2 b / h_0 \tag{1.1}$$

and the normal pressure force $P = p_c S_c$, where S_c is the contact area τ_c — shear stress p_c is the average contact pressure. As a result

$$f = \mu\omega r_c / p_c h_0 \cdot \tag{1.2}$$

As the external load P and, accordingly, the contact pressure increase, the gap decreases so much that contact occurs between the individual roughness

Table 1.3. **Characteristics of microroughnesses**

Surface roughness class	Roughness parameters		Base length *l*, mm
	R_a, micron	R_z, micron	
1	80—63—50	320—250—200	8.0
2	40—32—25	160—125—100	
3	20—16—12.5	80—63—50	
4	10—8—6.3	40—32—25	2.5
5	5—4—3.2	20—16—12.5	
6	2.5—2—1.6	—	0.8
7	1.25—1—0.8		
8	0.63—0.50—0.40		
9	0.32—0.25—0.2	—	0.25
10	0.16—0.125—1.10		
11	0.080—0.063—0.05		
12	0.040—0.032—0.025	—	0.25
13	0.02—0.016—0.012	0.100—0.080—0.063	0.08
14	0.01—0.08	0.05—0.04—0.032	

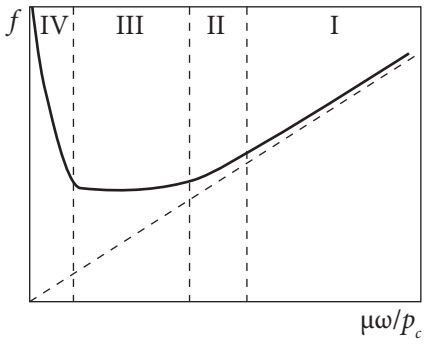

Fig. 1.4. Stribeck curve: I — liquid lubrication ($h_0/R > 3$); II — mixed lubrication; III — boundary lubrication; IV — dry friction

protrusions, and the continuity of the oil layer is broken (section II of the Stribeck curve corresponding to mixed lubrication). The characteristic relationships between the average gap and the roughness parameter are as follows: $0,4 < h / \overline{R} < 3$. The friction coefficient is still mainly determined by the lubricant viscosity, but its dependence on the antifriction properties of the materials of the friction pair is already partially manifested.

With a further increase in the load and the approach of the contact pairs $\left(h_0 / \overline{R} < 0,4\right)$, some volumes of lubricant remain only in the depressions; the rest of the contact surface is covered with an adsorbed film, the thickness of which is several molecular layers $\left(h_0 = 10^{-3} \div 10^{-1}\,\mu m\right)$. The friction coefficient in the boundary lubrication regime (section III) is determined by the anti-friction properties of the materials and the physicochemical structure of the adsorbed lubricant films. Boundary friction is the most characteristic friction mode of mechanical seals. At the same time, seals retain high tightness: visible leaks are either absent at all (they have time to evaporate), or only drip leaks are observed.

There is no lubrication in dry friction (section IV of the Striebeck curve), so the adsorbed film is destroyed without recovery. Between the irregularities of rubbing rough surfaces, episodic touches occur, accompanied by plastic deformations with a significant increase in local pressures and temperatures, which ultimately leads to fatigue failure of friction surfaces. In addition, the molecular bond (adhesion) between rubbing bodies is enhanced, which can lead to seizing and seizing. Dry friction is rare, particularly when a vacuum is being sealed.

There are no clear boundaries between the considered modes of friction since the process of friction is determined by random factors and is of a random nature itself, just like the process of wear of rubbing surfaces.

1.5. Wear mechanism of friction pairs

Wear is a process of gradual change in body dimensions during friction, which manifests itself in the separation of the material from the friction surface and (or) its permanent deformation. Wear is the result of the wear process and its quantitative expression. As wear indicators, linear wear U is taken — the height of the worn layer of material (the resource of the friction unit is determined

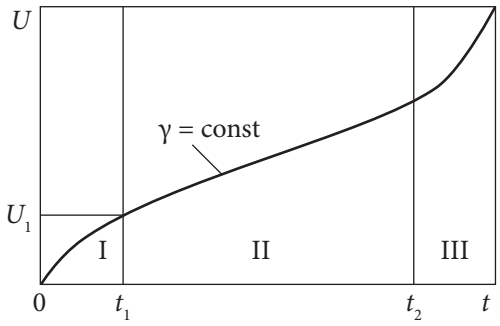

Fig. 1.5. Dependence of wear indicators on time

by the maximum allowable linear wear), wear intensity $i = U/L$ — the ratio of linear wear to the path on which wear occurred, wear rate $\gamma = U / t$ — the ratio of linear wear to wear time.

The process of wear of properly selected friction pairs usually has three stages (Fig. 1.5): I — stage of micro-running, during which the initial technological roughness changes into operational roughness, corresponding to the given conditions of friction and wear and having the ability to self-reproduce in the process of friction. Depending on the conditions, the parameters of the initial roughness at the stage of micro-running may decrease or increase. The closer the initial surface roughness is to the operational roughness, the shorter the stage of their running-in. When rubbing pre-deformed or inaccurately positioned (skewed) surfaces, there is also a period of macro-running, during which wear leads to a change in the nominal contact area of the friction surfaces.

The second stage (II) is the stage of normal, steady wear: $\gamma = \text{const}$, $U = U_1 + \gamma\left(t - t_1\right)$. In many cases, there is a stage of catastrophic wear (III) — the stage of an intensive increase in the wear rate due to an unfavorable change in external factors or a change in friction conditions due to the achievement of the maximum allowable wear.

The steady wear mode with boundary friction characteristic of mechanical seals is described almost completely by the molecular-mechanical (adhesion-deformation) theory of friction and fatigue wear developed by I.V. Kragelsky [8, 24]. In accordance with these theories, friction is caused, on the one hand, by the deformation of the material by embedded irregularities (elastic or plastic displacement) and, on the other hand, by overcoming molecular (adhesive) bonds in the contact zone. As a result of deformations that are constantly repeated during friction, associated both with pushing back and with the continuous formation and destruction of friction bonds, defects are accumulated in the deformed microvolumes of the surface layer, leading to fatigue failure.

To reduce the wear intensity, it is very important that the delamination of the material due to shear deformations is localized in a thin surface layer and does not capture the entire deformable microvolume. This is possible as long as there is a weakened layer with low shear resistance on the friction surface. This condition is formulated as a universal positive gradient rule [24]: $d\tau / dn > 0$, i.e., shear resistance should increase in the direction of the normal n to the friction surface (the normal is directed deep into the material).

Based on the above concepts of friction and wear processes, calculation formulas are proposed for estimating wear indicators, containing a number of coefficients that should be determined experimentally for specific materials and friction conditions. In the monographs of E. Mayer [42], A.I. Golubev [17], and L.A. Kondakov [23], a large amount of experimental material on friction and wear of mechanical seals is collected, which makes it possible to predict roughly the durability of seals at the stage of their design.

The main factor determining wear is the contact pressure, which, in turn, depends not only on the design and operational parameters but also on a number of internal processes that accompany the seal. In particular, the processes in a friction pair can be significantly affected by force and temperature deformations, which are determined by the geometric shape of the sealing rings, the power of friction losses, and heat removal conditions.

Due to the complexity of the processes of thermohydroelasticity, friction, and wear, the calculation of mechanical seals has to be limited to rough estimates and comparison of newly designed seals with proven in operation analogues. Even for the same materials, the wear intensity can vary by several orders of magnitude when the operating mode changes: pressure of the sealed liquid, peripheral speed, temperature, axial and angular vibrations. Currently, estimates of wear indicators are based on operating experience and cannot be expected to have a high degree of reliability. The most reasonable and acceptable formulas for engineering calculations for calculating the wear intensity are given in the fundamental reference book [24]. However, the special physical and mechanical characteristics included in these formulas (the parameter of the frictional fatigue curve, the correction factor for the number of cycles corresponding to the separation of the wear particle, the coefficient characterizing the stress state on the contact patch, etc.) are partially systematized only for some common structural materials under dry friction conditions. Yet there are no such characteristics for antifriction materials of friction pairs of mechanical seals in the presence of an intermediate film of the sealing liquid.

The literature provides both simple power-law [20] and linear [41, 42] dependences of the wear rate on the contact pressure and sliding speed. For example, in [54], the Archard formula is analyzed

$$\gamma = k_0 p_c \omega r_c / H,$$

where H is the surface hardness, which is determined by the indentation method; k_0 is the wear coefficient, which must be determined experimentally for each combination of friction pair materials and the fluid being sealed, as well as for specific operating conditions, including friction mode, temperature, vibrations, abrasive particles, etc. Thus, the outward simplicity of the formula is achieved at the cost of losing its generality: it is necessary to measure the wear rate experi-

mentally to determine the wear coefficient, and if the wear rate is determined, then the formula becomes unnecessary.

So far, the only way to predict the wear of designed seals is to use the results obtained for similarly designed prototypes operating under similar conditions. The task is facilitated by the fact that wear is an integral average statistical characteristic, relatively little sensitive to random changes in individual parameters, on the totality of which it depends. Due to this, in [42], based on extensive studies, the wear rate is given (Fig. 1.6) depending on the mode (coefficient) of friction of a carbon-graphite-metal pair for seals of the first two groups of Table 1. The monograph by A.I. Golubev [17] provides wear data for all four groups of seals. The wear rate of pairs of siliconized graphite for the fourth group of seals does not exceed 0.001 μm/h.

Fig. 1.7 shows the data of Williams [69], which illustrates the dependence of the friction coefficient and wear rate on the sealing pressure in the seals of the feed pumps of thermal and nuclear power plants.

Thus, if the maximum allowable wear of the contacting surfaces U^* is given, then the average wear rate can be used to estimate the sealing resource $T = U^*/\gamma$. For example, if $U^* = 2$ mm, and the average wear rate $\gamma = 0.1$ μm/h, then $T = 2 \cdot 10^4$ h, which means that even for a relatively high wear rate, the resource of the friction pair is so large that the reliability of the assembly is limited by the secondary seal, drivers, and pressure elements. The correct choice of materials for the

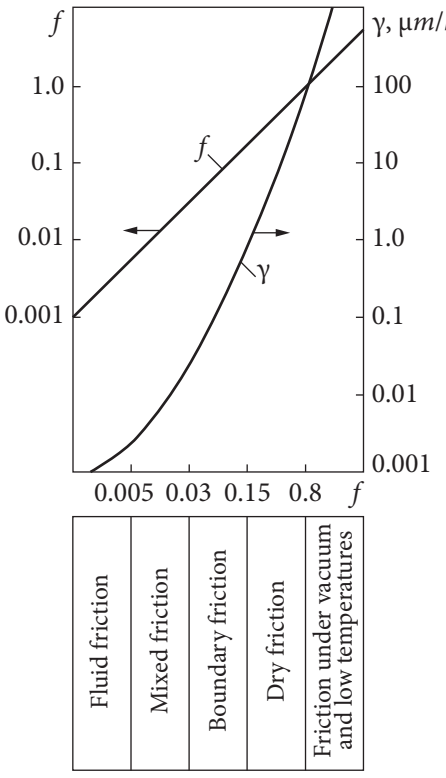

Fig. 1.6. Wear rate of carbon-graphite-metal friction pairs according to [42]

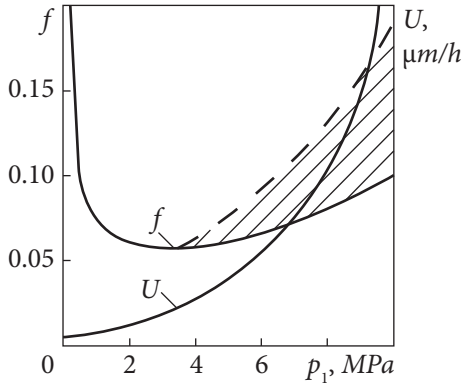

Fig. 1.7. The dependence of the coefficient of friction and wear rate on the pressure of the sealing liquid (steam carbon-graphite-metal, sealing liquid — water, circumferential speed 5 m/s) according to [69]

friction pair and the seal design ensures sufficient durability of its operation at a level of $p_1 v$ <100 MPa m/s. For large load parameters, it is recommended to use thermohydrodynamic seals or hydrostatic seals with a guaranteed self-adjusting end clearance. (See Chapter 3).

1.6. Development of a mechanical seal closed design model

Based on the analysis of the physical foundations of the operation of mechanical seals, a model of sealing and bearing capacity is proposed, which allows to solve the problems of designing mechanical seals.

Let us consider the general model of an ordinary mechanical seal in the contact joint of which, formed by the curved surfaces of the sealing rings, a confusor or diffuser form of the gap is formed in the radial direction.

While designing a conventional mechanical seal, the designer needs dependencies to estimate the expected leakage through the seal, the magnitude of the friction force, and the possible durability of the assembly. These calculated dependences and estimates can be obtained based on a closed working model containing a mathematical description of the processes occurring in the sealing gap and a given criterion for their optimality.

There are a several hypotheses about the mechanisms of the carrier force formation during the friction of lubricated surfaces:

- thermal wedge (change in lubricant density due to temperature increase along the length of the travel path);
- a viscous wedge (a change in the viscosity of the lubricant due to an increase in temperature along the length of the path of movement);
- representation of microroughnesses in the form of stepped microbearings;
- formation of a support force due to the impact action of microroughnesses;
- deviation of sliding surfaces from parallelism.

The most significant mechanism for the occurrence of a support force is the influence of the deviation of sliding surfaces from parallelism. The reason for such deviations, according to researchers [18, 33, 41, 43, 44], may be thermal and mechanical deformations of the sealing surfaces that occur during the operation of the mechanical seal, as well as the initial errors of these surfaces obtained during operation, finishing operations in the manufacture of rings or assembly of the sealing node.

The transition of a mechanical seal from the stage of rest to the stage of operation with a rotating shaft, up to reaching the nominal speed mode, is associated with several processes that usually remain outside the known models describing the operation of mechanical seals. So, in the known models of the

mechanical seal operation, only the stationary mode with certain loading parameters becomes the object of description and study without considering the influence of the processes preceding this stage [18, 42].

Let us examine the processes occurring in the sealing gap of a typical unloaded mechanical seal of the pump shaft. The working process in the mechanical seal from the moment the shaft begins to rotate until the establishment of a stationary mode of operation is associated with the development of several non-stationary phenomena in the sealing joint and the body of the seal rings with a gradual transition of the parameters to those established under the nominal mode of operation.

We take the following as initial conditions:

- liquid medium pressure p_1 in the seal chamber is equal to atmospheric pressure;
- differential pressure across the seal is 0;
- contact pressure $p_c = f(F_n, S_c)$ at the joint of the sealing surfaces of the rings is determined by the force of the elastic elements F_n and the nominal contact area S_c of the rings sealing surfaces;
- the temperature in the seal rings is equal to the temperature of the medium being sealed $T_k = T_c$.

After the drive is turned on and the rotating ring begins to move, the sealing work is associated with an increase in the sliding speed and with the non-stationary friction phenomena of the sealing surfaces. Between the surfaces of the rings, initially pressed to each other by the axial force created by the elastic spring elements, during their relative movement — under the conditions of contact interaction — phenomena associated with the rejection of the axially movable ring by a certain amount from the surface of the axially stationary ring arise (due to interaction of the circumferential moment and the braking forces of contact friction between the sealing surfaces of the rings). The initial moment of relative movement of the ring surfaces occurs in conditions of almost complete absence of lubrication between the sealing surfaces. However, frictional forces in the contact surfaces cause frequent axial movement of the axially movable ring, thereby ensuring the lubricant flow between the sealing surfaces. The friction of the surfaces in individual contact patches leads to heat generation and uneven heating of the rings along the height. The resulting temperature changes on the sealing surfaces of the rings depend on the value of the contact pressure at the junction of the surfaces and the sliding speed in the rubbing pair: $T_k = f(p_c, u_\phi^*)$, where u_ϕ^* is the peripheral sliding speed in the rubbing pair of rings (variable at the starting stage of the seal operation).

From the impact of a local axial temperature difference in the bodies of the rings, a deformation close to axisymmetric with a slightly pronounced wave-likeness in the circumferential direction occurs with an axial deformation

$\Delta_i = f(T_k)$ with dimensions of fractions of micrometers, associated with a local rotation of the sections of the rings relative to the longitudinal axis of symmetry in the direction of temperature drop. The appearance of a weakly pronounced wave-likeness of the sealing surfaces of the rings and the number of waves on their outer diameters are the results of the uneven action of forces from individual springs or a single elastic element (central spring, bellows, membrane), from the angle of intersection of the longitudinal axes of the rotating and non-rotating rings, the non-parallelism parameter of the rings sliding, and also on the relative sliding velocity in the friction pair.

There is also a temperature difference across the width of the rings, leading to a local (in fractions of micrometers) rise of the surface of each of the rings near the inner radius of the sealing shoulder. In the end gap, a conical shape with irregular waviness of the conjugation of the sealing surfaces is formed, with a gap size on the outer diameter of the rings in fractions of micrometers and local cavities of the same order of axial dimensions between the sealing surfaces, formed by the resulting unorganized bulges and depressions. The reasons for the appearance of the latter can also be local anisotropy of the materials of the rings, micro waviness obtained during finishing operations, stress relaxation in the bodies of the rings associated with a change in their thermal state, and non-axial symmetry of both the bodies of the sealing rings and the elements of their interface with adjacent parts.

The initial stationary regime of almost dry friction passes into the stage of boundary friction with a continuing increase in the sliding speed and with a gradual decrease in the contact interaction of the surfaces due to the lubricant entering the cavities formed between the sealing surfaces during their relative displacement.

The medium to be sealed fills and releases emerging and disappearing cavities, removes the generated heat from the sealing surfaces of the rings, and heats itself up. With a further increase in the sliding speed in the butt joint, the process of transition from the boundary regime to the regime of semi-fluid friction and the exit of the surfaces from the contact interaction proceeds. These processes are mainly associated with the effect of the shape changing of the sealing surfaces in the circumferential direction and with the phenomenon of throwing off the axially movable ring when the sealing surfaces come into contact. Here, the sources of the formation in a thin layer of lubricant of the carrier hydrodynamic force due to viscous phenomena during the relative movement of the surfaces are local deviations from the flatness of the surfaces in the pair.

A bearing force arises due to the wedge effect formed when a flat or convex section of the surface of one ring moves relative to the local convex part of the section formed on the surface of the other ring, which is simply described for

the circumferential flow in the end gap by a special case of the differential lubrication equation in the form of dependence:

$$-\frac{1}{r}\frac{\partial}{\partial\phi}\left(\frac{\rho h^3}{12\mu r}\frac{\partial p}{\partial\phi}\right)=\frac{1}{r}\frac{\partial}{\partial\phi}\left(\frac{\rho h}{2}\right).$$

In addition, processes associated with cavitation effects, as well as the influence of squeezing the lubricant layer from axial displacements of the end surfaces of the rings in the sealing gap, occur simultaneously in the lubrication layer, which is described for the radial flow by the dependence

$$\frac{1}{r}\frac{\partial}{\partial r}\left(r\rho\frac{h^3}{12\mu r}\frac{\partial p}{\partial r}\right)=\rho u_r \tag{1.1}$$

and for the circumferential flow by the dependence

$$-\frac{1}{r}\frac{\partial}{\partial r}\left(\frac{\rho h^3}{12\mu r}\frac{\partial p}{\partial\phi}\right)=\rho u_\phi . \tag{1.2}$$

Here, r is the radial coordinate of the gap being sealed, h is the current gap between the surfaces, p is the pressure in the lubrication layer, ρ is the density of the lubricating medium, μ is the viscosity of the lubricant layer, ϕ — angle in the circumferential direction, u_ϕ is the circumferential velocity of the lubricant flow, u_r is the radial velocity of the lubricant flow.

The flow of lubricant in a thin layer between the sealing surfaces occurs pretty much due to changes in the angle of intersection of the axes of the rotor and body parts of the seal assembly due to the compliance of the angular position of the axially movable block.

In the absence of pressure drop across the seal or its low level under conditions of low loading of the pair by the axial force created only by spring elements, the resulting bearing force in the gap between the end surfaces is sufficient to ensure non-contact operation of the mechanical seal without wear of the sealing surfaces.

For the hydrodynamic lubrication regime, the lifting force in the gap largely depends on the gap between the relatively moving surfaces (it is proportional to the 5th power of the wedge gap). Thus, a lifting force sufficient to separate the surfaces in the slot is formed even at very small gaps, which are characteristic of the boundary friction regime.

At small gaps and continuing up to reaching the stationary mode of operation, an increase in the relative velocity of sliding of the surfaces of the rings in the friction pair, significant heat generation is formed. This causes a noticeable increase in temperature in the medium that fills the end gap and further deformation of the surfaces forming this gap. The rate of temperature growth in the

gap and the rings is significant; the main part of this process takes the first few seconds of the operation of the sealing unit [44].

The temperature of the medium in the sealing gap depends on the circumferential speed of rotation of the shaft, the coefficients of thermal conductivity of the ring materials, the conditions of heat transfer to the medium to be sealed surrounding the seal assembly, and the thermophysical properties of the medium to be sealed.

Under the influence of thermal deformations of the rings, along with the waviness of the sealing surfaces, there is a process of active formation of a gap close to the axisymmetric wedge shape in the radial direction with a maximum opening of the gap from the side of the outer diameters of the rings.

With an increase in the shaft speed, the pressure behind the pump impeller increases, and the pressure drop increases across the seal. The axial load on the sealing joint of the pair and the hydrostatic component in the axial unloading force increase due to the growth of the pressure diagram in the radial direction along the end gap; the hydrodynamic component of the bearing force is reduced. The force deformations, growing in this case from loading the mechanical seal parts with the pressure of the medium being sealed in some seal designs, can be significant and even exceed the deformations from temperature phenomena. The direction of action of force deformations in the vast majority of cases (due to the design features of the execution of parts of mechanical seal units) is associated with the rotation of the cross-section of the rings in the direction opposite to that which was the result of temperature deformations from the axial temperature gradient.

In the entire time interval of the mechanical seal reaching the nominal operating mode, the friction surfaces are running in, associated with an increase in the supply of lubrication to the rubbing surfaces in accordance with the loading conditions of the end pair. The lubricating layer thickness grows between the sealing surfaces of the rings. With the formation of a sufficient supply of lubricant to the rubbing surfaces in the end pair, the stage of liquid friction begins.

The main influencing factors on the bearing force magnitude are the flow of lubricant in the radial direction and the radial shape of the gap between the end surfaces of the rings, as well as the non-parallelism of the sliding of their sealing surfaces. Local deviations in the circumferential irregularity of the shape of the surfaces of the rings cease to be a significant source of bearing force due to the radial spreading of the lubricating layer due to the narrow width of the sealing collar. The bearing force in the liquid layer becomes quasi-stable and is in equilibrium with the force loading the axially movable block. This balance is maintained by means of the current change in the minimum size of the gap in the approach of the surfaces, as well as by increasing or decreasing the current taper of the gap in the radial and circumferential directions due to the non-par-

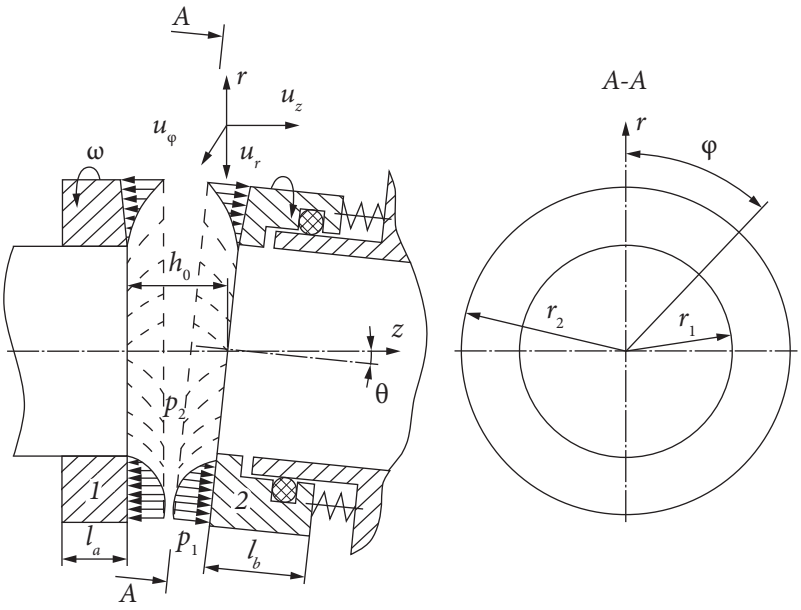

Fig. 1.8. Scheme of the end gap of the sealing unit after it enters the liquid friction mode with the determining influence of hydrostatic forces

allel sliding of the sealing surfaces. This is ensured mainly by compliance with the angular displacement of the axially movable block. The scheme of the end gap of the sealing unit after it enters the liquid friction mode with the decisive influence of hydrostatic forces is shown in Fig. 1.8 [45].

Let's introduce the following definitions: *r, z*, are radial, axial, and angular coordinates; u_r, u_z, u_ϕ are the radial, axial, and angular velocities of the medium flow; ω is the angular velocity of rotation of the ring; p_1, p_2 — pressure before and after the seal; F_n is the force of the elastic spring element; h_0 — the average gap between the sealing surfaces; l_a, l_b are the body heights of ring A and ring B, respectively; θ — the angle of non-parallelism of the sealing surfaces of the rings; r_1, r_2 — inner and outer radii of the sealing surfaces of the rings

Now, the greatest influence on the value of the bearing force between the end surfaces is exerted by the value of the average gap between the sealing surfaces.

Studies have shown that a change in the circumferential direction of the non-parallelism parameter of the sealing surfaces within the average gap size can affect the bearing force in sizes up to 40% of the loading force. Thus, the change in the non-parallelism of the sealing surfaces in the end joint of the rings is a potent factor influencing the bearing force.

With an already established fluid friction mode, current changes in loading modes (for example, pressure, coolant flow rate, etc.) can change the lubrication

conditions in the sealing gap. So, insufficient heat removal from the rings, the unfavorable nature of their force deformations, leading to the formation of a diffuser shape of the sealing gap, or insufficient angular compliance of the axially movable block of the seal assembly (due to a decrease in the elastic properties of the secondary sealing elements or insufficient gaps in the mating of parts) can cause a significant change in the nature of the lubrication of the sealing surfaces [52].

These changes are the result of the lubricant layer overheating in the sealing gap, a drop in the viscosity properties of this layer and the associated increasing convergence and contacts of the surfaces, and the occurrence of semi-dry and dry friction processes in the sealing gap.

Further development of processes in the sealing gap, even before reaching the stationary mode of operation or already in the stationary area of operation with changes in the parameters of the nominal operating mode, can proceed according to three schemes:

- the transition of the mechanical seal to the contact mode of operation with dry or mixed friction;
- operation of the mechanical seal in the non-contact liquid hydrostatic mode of friction in the lubricating layer between the sealing surfaces in the end gap;
- operation of the mechanical seal with cyclic transitions from non-contact to contact mode and vice versa.

The operation of an ordinary mechanical seal according to the first scheme is typical for cases with supercritical deviations of parameters from those already established and providing a favorable hydrodynamic lubrication regime. This may be due to a deterioration in the quality of the sealing unit cooling with a change in the dynamic properties of the "rotor-axially movable ring" system.

According to the second scheme, the mechanical seal operation makes it possible to obtain a long-term performance of the assembly, low leakage rates, and friction power costs when sealing medium and high-pressure drops. A well-developed section of the lubrication theory can be used to describe the mathematical model and obtain the necessarily calculated dependences in the stationary mode,.

According to the third scheme, the mechanical seal operation is one of the most frequently encountered in practice. Such a scheme of operation is common for low-loaded seal assemblies and medium-loaded seals, and it is associated with current changes in loading modes in terms of pressure, rotor speed, or assembly cooling. The existence of such a scheme of work is associated with frequently arising issues of wear of the sealing pair rings and low current working life of the mechanical seal assembly — in cases where there are no strict requirements for maintaining the routine parameters of the assembly during operation.

The cause of unstable deformation of the sealing gap can also be dynamic loads. For example, vibrations of a rotor can cause bending oscillations of its axis [60] and the corresponding evolution of the sealing surface of a rotating ring.

Let us examine in more detail the processes occurring in the second, most favorable, and economically feasible scheme of the mechanical seal.

It is possible to determine what the minimum gap will be in the end gap when the mechanical seal is operating in the design mode by the force loading of the end joint and the given leakage, as well as by the shape of the end sealing gap.

The determination of the calculated dependences for the end slot in the hydrodynamic theory of lubrication for narrow slots is based on the joint solution of the system of differential equations of motion of the working fluid, the continuity of the lubricant flow, the state, and energy that describes the hydro- and thermodynamic processes in the tract and changes in the parameters of the system motion.

Due to the complexity of the initial differential equations, some generally accepted assumptions are made, due both to the peculiarities of the operation of seals and to simplifications that do not significantly affect the accuracy of the results obtained but greatly facilitate computational work:

1. The flow of the working fluid in the slot is assumed to be isothermal — it is based on the fact that when the mechanical seal operates in the liquid friction mode, there is intense heat transfer from the lubricating layer to the rings and, therefore, the temperature of the lubricating layer over the slot can be averaged without much error. This approach is also supported by experimental data [44].

2. The pressure of the working fluid does not change along the layer thickness — it is based on the smallness of the contribution to the pressure change of inertial forces in the lubricating layer compared to the forces of viscosity when the mechanical seal operates in the liquid friction mode.

3. The laminar flow regime of the medium is realized in the sealing gap — it is based on the fact that when the mechanical seal operates in the liquid friction mode, with current operating clearances and the loading pressure drops, only the laminar flow regime of the medium being sealed.

4. Changes in the gap per revolution of the ring are averaged — based on the fact that after the mechanical seal reaches the design mode of operation, it is considered as steady with stable parameters.

Since the changes in the viscosity of the medium being sealed in the gap due to temperature are insignificant, the effect of changes in the temperatures of the medium along the gap on the pressure distribution can be neglected, and the energy equation cannot be introduced into the system of equations describing the processes in the end gap of the seal. The system of equations for the stationary case of a laminar flow of a medium through an end gap (formed by smooth

surfaces) as applied to mechanical seals can be written as a continuity equation:

$$\frac{\partial(\rho r u_r)}{\partial r}+\frac{\partial(\rho u_\phi)}{\partial \phi}+r\frac{\partial(\rho u_z)}{\partial z}=0\,, \tag{1.3}$$

and the equations of fluid motion — due to the assumption of constant pressure across the thickness of the lubricating layer — can be represented in the form of a system of Reynolds equations:

$$\begin{gathered}\frac{\partial p}{\partial r}=\frac{\partial}{\partial z}\left(\mu\frac{\partial u_r}{\partial z}\right)-\rho\frac{u_\phi^2}{r};\\ \frac{\partial p}{\partial z}=0;\\ \frac{\partial p}{r\partial \phi}=\frac{\partial}{\partial z}\left(\mu\frac{\partial u_\phi}{\partial z}\right);\end{gathered} \tag{1.4}$$

with boundary conditions:

$$z=0;\ u_r=0;\ u_\phi=0;\ u_z=0;\ z=h;\ u_r=0;\ u_\phi=\omega r;\ u_z=0; \tag{1.5}$$

which represent the kinematic conditions on the walls limiting the investigated flow for Newtonian fluids (here, ϕ is the displacement angle of the rotating ring along the angular coordinate, see Fig. 1.8).

Integrating the system of equations (1.4) concerning z under boundary conditions (1.5), we obtain the generalized Reynolds lubrication equation:

$$\begin{gathered}-\frac{1}{r}\frac{\partial}{\partial r}\left(r\rho\frac{h^3}{12\mu}\frac{\partial p}{\partial r}\right)-\frac{1}{r}\frac{\partial}{\partial r}\left(\frac{r^2\rho^2\omega^2h^3}{40\mu}\right)-\\ -\frac{1}{r}\frac{\partial}{\partial \phi}\left(\frac{\rho h^3}{12\mu r}\frac{\partial p}{\partial \phi}\right)-\frac{1}{r}\frac{\partial}{\partial \phi}\left(\frac{\rho\omega r h}{2}\right)+\rho u_z=0\,.\end{gathered} \tag{1.6}$$

Restricting ourselves to considering the axisymmetric problem only for radial flow in the end gap, according to the above-described picture of processes for the design mode in the sealing joint and neglecting the effect of compression of the medium film in the gap, we obtain expression (1.6) in the form:

$$-\frac{1}{r}\frac{\partial}{\partial r}\left(r\rho\frac{h^3}{12\mu}\frac{\partial p}{\partial r}+\frac{r^2\ \rho^2\omega^2h^3}{40\mu}\right)=0. \tag{1.7}$$

Here, the gap change and the current pressure change in the radial direction are the unknowns.

For isothermal flows of the medium, the necessary additional relations for solving the equations are the pressure dependences of the viscosity μ and density ρ of the medium. Restricting ourselves to the consideration of the mechanical seal operation for a liquid in the region of medium pressures, we set $\mu(p)$ = const and $\rho(p)$ = const.

The following design characteristics are required to evaluate the efficiency of the calculated mechanical seal: leakage Q through the seal, power consumption N for its operation, and long-term assembly performance, which can be guaranteed only by the non-contact operation of the sealing pair.

The optimization parameter (which, as a given basic criterion, the designer needs to focus on when designing the seal unit) can be the maximum rigidity of the liquid layer in the sealing gap, associated with the shape of the gap itself and the characteristics of the medium being sealed [30, 46].

Integrating (1.7) over r, using in the solution the substitution $Q = -2\pi r\int_0^h u_r dz$, an intermediate solution when integrating systems (1.3), (1.4), and introducing dimensionless quantities, we obtain the system of equations:

$$\begin{cases} \dfrac{d\overline{p}}{d\overline{r}} = \dfrac{\overline{\mu}}{\overline{h}^3}\dfrac{\overline{R}_B}{\overline{r}}\overline{Q} + \Omega_c\dfrac{\overline{\rho r}}{\overline{r}_1}; \\ \dfrac{d\left(\overline{\rho}\overline{Q}\right)}{d\overline{r}} = 0. \end{cases} \tag{1.8}$$

Here, $\Omega_c = \dfrac{0{,}3\omega^2 r_1\left(r_2 - r_1\right)\rho^*}{\Delta p}$ is the dimensionless centrifugal parameter of the gap; ρ^* is the base (initial) value of the density of the medium; $\Delta p = p_1 - p_2$ is the pressure drop across the seal.

Introducing a new variable $\overline{x} = \overline{r} - \overline{r}_1$, we integrate system (1.8) under boundary conditions:

$$\begin{cases} \overline{p}(\overline{r}_1) = 0; \\ \overline{p}(\overline{r}_1 + 1) = 1. \end{cases} \tag{1.9}$$

The solution to the problem can be represented as:

$$\overline{Q} = \frac{1 - \Omega_c\int_0^1 \overline{\rho}\left(1 + \dfrac{\overline{x}}{\overline{r}_1}\right)d\overline{x}}{\overline{\rho}\int_0^1 \dfrac{\overline{v}d\overline{x}}{\overline{h}^3\left(1 + \dfrac{\overline{x}}{\overline{r}_1}\right)}}; \tag{1.10}$$

$$\overline{p}(\overline{x}) = \overline{p}(0) + \overline{p}\overline{Q} = \int_0^{\overline{x}} \frac{\overline{v}d\overline{x}}{\overline{h}^3\left(1+\frac{\overline{x}}{\overline{r}_1}\right)} + \Omega_c \int_0^{\overline{x}} \overline{\rho}\left(1+\frac{\overline{x}}{\overline{r}_1}\right)d\overline{x}; \tag{1.11}$$

$$\overline{F} = \frac{\int_0^1 \overline{p}\left(1+\frac{\overline{x}}{\overline{R}_B}\right)d\overline{x}}{1+\frac{0.5}{\overline{r}_1}}, \tag{1.12}$$

where $\overline{F} = \frac{F}{F^*}$, $F = 2p\int_{r_1}^{r_2} prdr$ is the hydrostatic bearing force in the gap; F^* is the base value of the bearing force.

To determine the moment of friction $M = \pi \int \tau r\, dr$, it is necessary to integrate elementary moments from shear stresses over the area of the gap:

$$\tau = \mu \frac{du_\phi}{dz} = \frac{\mu\omega r}{h}.$$

After transformations in dimensionless form, we have

$$\overline{M}_F = \int_0^1 \frac{\overline{\mu}\left(1+\frac{\overline{x}}{\overline{r}_1}\right)^3 d\overline{x}}{\overline{h}}. \tag{1.13}$$

In dimensional form $M_F = \overline{M}_F M_F^*$, where

$$\begin{cases} \overline{M}_F = 2\pi\int_{r_1}^{r_2} \tau r^2 dr, \\ M^*_F = \dfrac{2\pi\mu^*\omega r^3(r_2 - r_1)}{h_m}. \end{cases} \tag{1.14}$$

The obtained dependences (1.6)—(1.10) allow us to determine the main characteristics of the mechanical seal: leakage, bearing force in the gap, friction moment, and pressure diagram.

Due to the fact that during the operation of a mechanical seal, the absence of axial symmetry of the annular gap is possible due to the non-parallelism of the rubbing surfaces of the rings (see Fig. 1.8), the use of formulas (1.10),

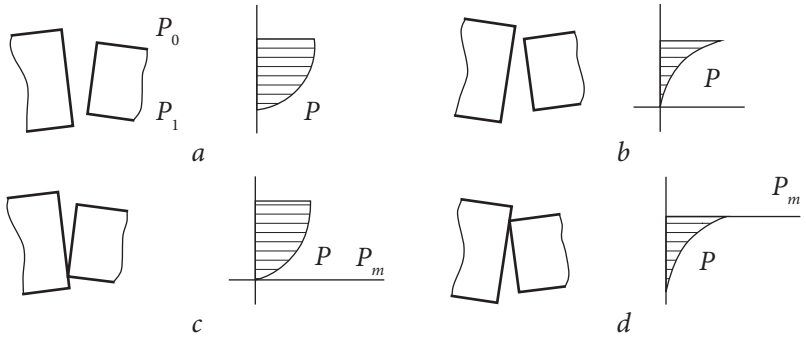

Fig. 1.9. The location of the sealing surfaces of the mechanical seal rings and the diagram of the pressure of the sealed liquid: *a* — confusor open joint, *b* — diffuser open joint, *c* — confusor joint with contact, *d* — diffuser joint with contact

(1.12) and (1.13), obtained under the assumption of axisymmetric flow, may be illegal, since for these conditions it becomes necessary to consider a three-dimensional problem.

However, with a small change in the gap in the circumferential direction, when the radial pressure gradient is much greater than the circumferential one, the effect of non-parallelism of the rings surfaces in the friction pair can be taken into account in the first approximation based on the fact that the values dM_F, dF, and dQ for each elementary annular sector with an angle $d\phi$ can be determined by the formulas (1.10), (1.12) and (1.13) for the current value of the radial gap. By integrating the obtained solutions for elementary ring sectors, one can obtain generalizing partial solutions of the characteristics M_F, F, and Q for several axisymmetric approaches of the surfaces of a sealing pair of rings.

When the pump drive is turned off, the end of the mechanical seal operation begins with a gradual decrease in the sliding speed and a drop in the pressure drop across the seal. In the gap, the fluid mode of friction is still preserved; however, the process of changing the radial profile of the shape of the slot, in the direction of decreasing confusion due to a decrease in temperature and force deformations, is underway the role of axial force from the elastic element of the compression of the rings increases; the convergence of the sealing surfaces of the rings increases.

There is a local contact of these surfaces along the tops of the waviness, and the number of contacts increases. The stage of liquid friction passes into semi-fluid and then into boundary friction. The deformation of the rings due to force factors disappears, and the nature of the deformation is determined by the temperature inhomogeneity in the bodies of the rings. There comes a stage of semi-dry sliding of surfaces with contact interaction of surfaces and with an

accelerated drop in the sliding speed. The rotating seal ring stops. This is the general picture of the working process of an ordinary mechanical seal.

Consider the options for the mutual arrangement of the sealing surfaces of the mechanical seal rings (Fig. 1.9).

In the first case (Fig. 1.9, *a*), there is no contact between the sealing surfaces, so the force that opens the joint is created due to fluid pressure in the gap. The average fluid pressure is somewhat greater than the average of the internal and external pressures, as the fluid pressure plot shows for this case. For the case of a diffuser open joint (Fig. 1.9, *b*), the pressure in the film is less than the average value of the internal and external pressures. This case is not stable and will result in contact between the rings, as shown in Fig. 1.9, *d*. Fluid pressure distribution diagrams in cases of contact between the rings, shown in Fig. 1.9, *c* and *d*, will take extreme forms as the minimum film thickness approaches zero. Thus, the total possible change in the magnitude of the load created by the pressure of the liquid when moving from a fully divergent (confusor) joint to a fully convergent (diffuser) joint ranges from zero to a pressure equal to the pressure being sealed. Since, in practical cases, the film thickness cannot be zero due to roughness, these limits cannot be reached.

In the last two cases shown in Fig. 1.9, contact occurs in the presence of a radial cone. For these cases, the concentrated contact load acts either inside or outside, depending on the direction of the radial cone.

1.7. Conclusion

The results of the physical foundations of the mechanical seals' operation analysis show that after the seal reaches the stationary mode, a stable lubricating layer is formed between the sealing surfaces in the end gap, i.e., the seal operates in liquid hydrostatic friction mode. Thus, mechanical seals can be classified as *conditionally contact seals*.

Mechanical shaft seals for centrifugal machines appeared a little over 100 years ago, and, during this time, they have come a long way in the evolution from primitive devices with a service life of several tens of hours in case of leakage, as in stuffing box seals, to high-tech multi-stage units that ensure reliable operation of equipment for tens of thousands of hours without repair or maintenance.

The classification of mechanical seals presented in the chapter allows us to judge visually the variety of designs that have emerged over the years. The mechanism of the appearance of a lubricating film between the rings of the end pair is complex and poorly understood; however, the presented calculation methods make it possible to obtain, with sufficient accuracy for practice, the connection between the geometric characteristics and operating conditions with the main operational characteristics of the seal.

The practice has shown that the shape of the end gap has a great influence on the characteristics of the lubricating film in a friction pair. In the area of hydrodynamic load support in the case of a convergent joint or a converging film, the slope of the pressure diagram is such that reducing the film thickness increases the hydrodynamic support. This is called positive stiffness and allows stable, non-contact seal operation.

If the joint is divergent (diffusor), then the pressure diagram has the so-called negative stiffness and provides unstable load support. In this case, the film collapses, and the seal operates in contact mode, i.e., a non-contacting diverging film is unstable.

Thus, when designing mechanical seals, it is necessary to calculate the deformations of the sealing rings caused by both the pressure of the sealed medium and thermal effects to predict the size and direction of the radial cone and avoid the unstable operation of the seal.

CHAPTER 2

FUNDAMENTALS OF MECHANICAL SEALS CALCULATION

2.1. Computing loads in the friction pair of mechanical seal

The condition for axial balance of the axially-movable ring of the mechanical seal (Fig. 2.1) is written as

$$F + F_n = F_c + F_s \pm F_m, \tag{2.1}$$

where F — axial pressure force, which presses the axially-movable ring to the seat, $F = p_1 S_1 + p_2 S_2$; F_n — the force of elastic element; $F_c = p_c S_c$ — the force of contact pressure; F_s — force driven by hydrostatic pressure P_s in the end clearance; F_m — friction force on secondary seal preventing displacement of the axially-movable ring in one direction or another.

Square signs S_1 and S_2 are considered positive if pressure forces acting on them increase contact pressure in the friction pair and negative if the corresponding pressure forces open the end joint. (Fig. 2.2)

Taking into account the accepted rule of signs $S_c = S_1 + S_2$, an expression for force F may be written as

$$F = \Delta p S_c (k + p_2 / \Delta p). \tag{2.2}$$

Here $\Delta p = p_1 - p_2$ — sealed surplus pressure; $k = S_1/S_c = b_1 r_1 / b_c r_c$; $b_1 = r_e - r_1, b_c = r_e - r_i$; $r_p = 0.5(r_e + r_1)$; $r_c = 0.5(r_e + r_i)$.

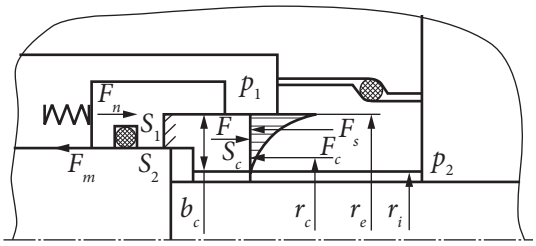

Fig. 2.1. Scheme of forces acting on the axially movable ring of a mechanical seal

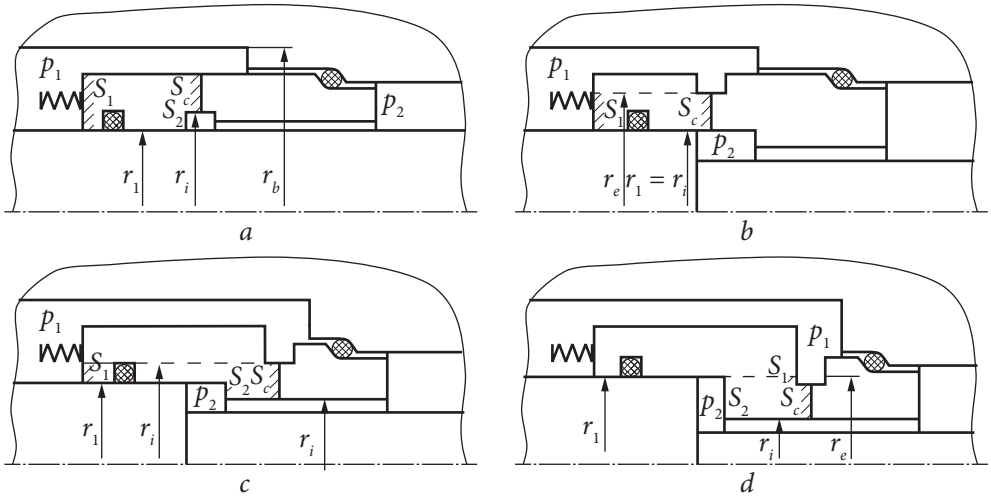

Fig. 2.2. To the definition of the load factor

If $S_2 > 0$, then $k < 1$ (balanced seal) if $S_2 < 0$, so $k > 1$ (loaded seal). If the pressure downstream is not zero ($p_2 > 0$), then $k_e = k + p_2 / \Delta p$ should be taken as an effective coefficient of load.

The force of hydrostatic pressure that opens the end joint is determined by the pressure distribution in the clearance gap and can be obtained by summing the elementary pressure forces throughout the entire contact area S_c:

$$F_S = \int\limits_{(S_c)} p_s ds = \overline{p}_s S_c, \tag{2.3}$$

where gap mean hydrostatic pressure

$$\overline{p}_s = \frac{1}{S_c} \int\limits_{(s_c)} p_s dS.$$

Since the end clearance corresponds to contact surface roughness, it has not yet been possible to determine theoretically the pressure distribution in the clearance gap. Only with relatively large clearance gaps $(h_0 / \overline{R} > 3-5)$, corresponding to the liquid lubrication regime and peculiar to hydrostatic seals, pressure in the end channel changes from the inlet area to the outlet area according to the law close to linear:

$$p_s = p_2 + \Delta p \frac{r - r_1}{r_2 - r_i}.$$

Herewith

$$\overline{p}_s = 0.5(p_1 + p_2). \tag{2.4}$$

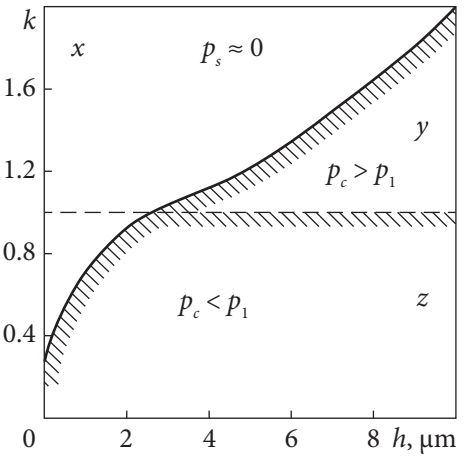

Fig. 2.3. Dependence of hydrostatic pressure on the end clearance and load factor: *x* — area of boundary friction; *y, z* — areas of mixed friction

Taking into account the hydraulic force, the balance equation may be written as $p_c S_c = \Delta p S_c k_e - \overline{p}_s S_c + F_n - F_m$, whereof

$$p_c = \Delta p k_e - \overline{p}_s + \frac{F_n - F_m}{S_c}. \qquad (2.5)$$

The sign of friction force depends on whether it prevents the contact surfaces from closing with each other under load. The force of an elastic element is usually assumed to be somewhat larger than the friction force; therefore, the last summand in balance (2.5) is small and can be neglected. For a liquid friction mode (2.4), it may be written as

$$p_c = \Delta p(k - 0.5) + (F_n + F_m)/S_c, \qquad (2.6)$$

meaning that the contact pressure is completely determined by load factor k and the sealed surplus pressure Δp . It can be seen from (2.6) that at k<0.5, there is a danger of opening the end joint. Therefore, take k = 0,55 ÷ 0,85 for balanced seals and for loaded seals k = 1,1÷1,2.

For seals with drip leaks, E. Mayer [42], based on a generalization of the results of experiments, gives a diagram (Fig. 2.3) that characterizes the dependence of the hydrostatic pressure on the average gap between the microroughnesses of the contact surfaces and on the load factor. Between the surfaces of friction pairs, there are contact spots, and the total deformations of the rings, which are measured by the angle ϕ of rotation of their sections, do not exceed the values $\phi b_c / r_e \le 1.2 \cdot 10^{-4}$. Due to the lack of accurate methods for estimating the pressure in the gap, in the future, we will use the diagram (Fig. 2.3). In the region *x* (the region of boundary friction) $\overline{p}_s \approx 0$ and

$$p_c = \Delta p k_e + (F_n - F_m)/S_c. \qquad (2.7)$$

In areas of mixed friction, *(y, z)* $\overline{p}_s$ will be determined by formula (2.4), and the contact pressure — by formula (2.6).

The mean clearance gap between the rough surfaces in the presence of contact markings (p_c> 0.15 MPa) can be evaluated by the formula [42]

$$h_0 = 0.5\left(\frac{R_{a1}}{K_1^2} + \frac{R_{a2}}{K_2^2}\right), \qquad (2.8)$$

where $K_{1,2}$ — coefficients of surface smoothness of axially-movable and base rings respectively, $K_{1,2}=\dfrac{R_{a_{1,2}}}{R_{\max 1,2}}$; for mechanical seals $1\geq K\geq 0.67$. At a high contact pressure, when unevenness interpenetration is observed, accurate values for clearance gaps are determined from the formula

$$h=\frac{1}{20}\left(\frac{R_{a_1}}{K_1}+\frac{R_{a_2}}{K_2}\right). \tag{2.9}$$

If the difference F_i-F_m is neglected, for boundary friction mode at p_2=0, it follows from the formula (2.5) that the coefficient of the load is equal to the ratio of average contact pressure to sealed pressure: $k=p_c/p_1$.

2.2. Determination of the mechanical seal hydrodynamic characteristics

The method for determining the hydrodynamic characteristics of a mechanical seal assembly with any slot shape requires a pretty complex software product, and it is advisable to use it at the final stage of developing a mechanical seal assembly. At the stage of a preliminary study of the design, the developer needs a quite simple tool for a simplified evaluation calculation of the selected variant of the design solution. Such a tool was developed [46] on the basis of a number of simplifications, including the model of the contact joint, by replacing the surfaces of complex shapes formed during the operation of a mechanical seal with surfaces of a simple wedge shape (Fig. 2.4). Below is a simplified solution technique.

When developing a sealing assembly, the designer must have certain guidelines in the form of optimality criteria in assessing the geometry of the sealing gap and the ratio of the sizes of the hydrostatic loading areas of the axially movable block and the sealing joint. Let us define these optimality criteria and calculated dependencies for a mechanical seal with a wedge-shaped gap.

The calculation algorithm under consideration is based on the model of a one-dimensional laminar flow of an incompressible medium through an end gap.

Restricting ourselves to the axisymmetric problem, the conditions of the isothermal flow of the medium and the short length of the sealing gap, and also neglecting the effects associated with the rotation of one of the rings, we write equation (1.7) in the form

$$\frac{d}{dx}\left(\frac{dp}{dx}h^3\right)=0 \tag{2.10}$$

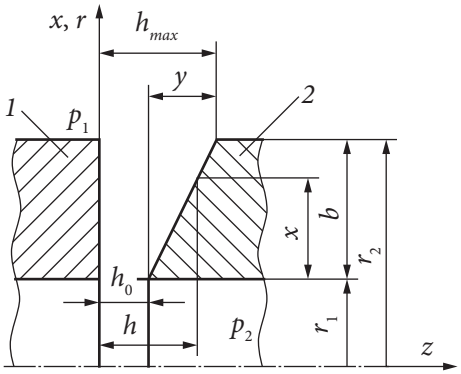

Fig. 2.4. Model of the contact joint of the end gap. Dimensional designations: *b, x* — full and current length of the sealing gap; *h*, h_0, h_{max} — current, minimum and maximum gaps in the seal gap; p_1, p_2 — pressure before and after the seal; r_1, r_2 are the outer and inner radii of the sealing surfaces of the rings; $y = h_{max} - h_0$; *r, x, z* — axes of the cylindrical coordinate system

with boundary conditions $p = 0$ at $x = 0$ and $p = p_1$ at $x = b$, in relation to the scheme of the end slot (see Fig. 1.8) between rings *1* and *2*, where the gap is $h(x) = h_0 + yx / b$. The shape of the slot can be either a diffuser ($y < 0$) or a confusor ($y > 0$).

Let us move on to dimensionless quantities: $h = \overline{h}(y + h_0)$, $x = \overline{x}b$, $y = \overline{y}b$, $h_0 = \overline{h}_0 b$. Then equation (2.10) can be written as:

$$\frac{d}{d\overline{x}}\left[\frac{d\overline{p}}{d\overline{x}}\left(\overline{yx} + \overline{h}_0^3\right)\right] = 0 . \tag{2.11}$$

Integrating over $\overline{x}$ twice and substituting the integration limits, we obtain an expression for the pressure distribution in the gap:

$$\overline{p_s}(\overline{x}) = \frac{\overline{x}(\overline{y} + \overline{h}_0)^2(\overline{yx} + 2\overline{h}_0)}{(\overline{yx} + \overline{h}_0)^2(\overline{y} + 2\overline{h}_0)} . \tag{2.12}$$

The dimensionless hydrostatic bearing force in the slot is found by integrating the equation

$$\overline{F} = \int_0^1 \overline{p}_s(\overline{x})d\overline{x} , \tag{2.13}$$

where

$$\overline{F} = \frac{F}{F^*} , \; F^* = \Delta p\pi(r_2^2 - r_1^2) .$$

Then, taking into account (2.12), we obtain:

$$\overline{F} = \frac{\overline{y} + \overline{h}_0}{\overline{y} + 2\overline{h}_0} . \tag{2.14}$$

Since the parameter $\overline{F}$, in fact, is the ratio of the average pressure drop $\overline{p}_s$ in the gap to the total pressure drop across it, then for contact mechanical seals, if we neglect the force from the elastic element, it follows from the balance of axial forces that the specific dimensionless value of the bearing force $\overline{F}$ in the gap must correspond to the specific dimensionless force loading the rings of the pair. The specific force loading the rings of the pair is expressed as the ratio of the area of axial hydraulic loading of the axially movable block to the radial area of the sealing joint and is called the seal load factor *k*.

Differentiating (2.14) with respect to , we obtain an expression for the axial stiffness $\overline{W} = \dfrac{d\overline{F}}{d\overline{h}_0}$ of the layer in the gap:

$$\overline{W} = \frac{\overline{y}}{(\overline{y} + 2\overline{h}_0)^2}. \tag{2.15}$$

Using relation (2.14) in the expression for the center of the pressure diagram

$$Z_c = \frac{\int_0^1 \overline{p}_s(\overline{x})\overline{x}d\overline{x}}{\int_0^1 \overline{p}_s(\overline{x})d\overline{x}}, \tag{2.16}$$

we get

$$Z_c = \frac{\overline{y} + \overline{h}_0}{\overline{y}^3}\left(\frac{\overline{y}^2 + 2\overline{h}_0^2}{2} - \frac{\overline{h}_0^3}{\overline{y} + \overline{h}_0} - \overline{h}_0^2 \ln\frac{\overline{y} + \overline{h}_0}{\overline{h}_0} \right). \tag{2.17}$$

Let's consider the qualitative side of the obtained dependencies using the examples presented in the illustrations for the solution. Fig. 2.5 shows the dependences of the bearing force $\overline{F}$ and stiffness $\overline{W}$ of the lubricating layer in the gap for a number of values h_0 of the convergence of the sealing surfaces on the gap shape parameter $C = y/h_0$.

It follows from them that positive values of the axial stiffness of the liquid layer in the slot, as well as the mode of liquid friction in the end pair, are provided only for the confusor shape of the gap, i.e., for $C > 0$.

A seal with a gap formed by parallel surfaces ($C = 0$) has zero hydrostatic stiffness. The friction mode in the end pair is in unstable equilibrium and can go

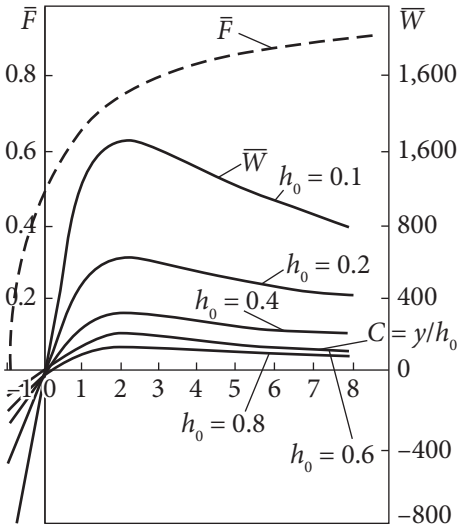

Fig. 2.5. Dependence of the bearing axial force $\bar{F}$ and axial stiffness $\bar{W}$ of the layer of the medium being sealed on the parameter C of the gap shape

either into a liquid or into a mixed friction mode. A seal with a diffuser slot shape has a negative axial rigidity of the liquid layer. The friction mode in the end pair can be either mixed (at $-1 < C < 0$) or dry (at $C < -1$). As follows from Fig. 2.5, the maximum axial stiffness of the fluid layer for a wedge-shaped slot exists at the slot shape parameter $C = 2$. In this case, the value of the hydrostatic bearing force in the gap $\bar{F} = 0.75$. The optimization parameter for a seal with a wedge-shaped gap is the axial stiffness $\bar{W}$ of the carrier fluid layer at the junction of the end surfaces of a pair of mechanical seal rings.

The controlled compaction parameters are the load factor k and the value y (see Fig. 2.4) on the high-pressure side. These parameters determine the closest approach between the working surfaces of the seal. From the condition of the optimum value $\bar{W}$, the load factor k of the compaction should be taken close to the value $k = 0.75$.

2.3. Computing leaks and friction power losses

The derivation of dependences for calculating the leakage through the seal and the power of friction losses in it can be performed taking into account the non-isothermal flow of the medium in the sealing gap and the "curvature" of the gap associated with differences in the circumference for a variable current radius of the gap.

The original Reynolds equation for the annular gap, taking into account the previously accepted assumptions, has the form:

$$\frac{d}{dr}\left(\frac{dp}{dr}\frac{\pi h^3 r\rho}{6\mu}\right) = 0 \qquad (2.18)$$

under boundary conditions

$$p = p_1 \text{ at, } r = r_2,\ p = 0 \text{ at } r = r_1. \qquad (2.19)$$

To solve the problem, we introduce a number of dimensionless and basic quantities: $\bar{r}$ — dimensionless current radius; $\bar{\rho}$, $\bar{\mu}$ are the dimensionless den-

sity and viscosity of the medium to be sealed; μ^* — the base value of viscosity; Q^* is the base value of the leakage.

$$Q^* = \frac{\pi \Delta p (y + h_0)^3}{6\mu^*}.$$

Now, the expression for the current gap in the gap

$$\overline{h} = \frac{\overline{y}(r - \overline{R}_H) + \overline{h}_0}{\overline{y} + \overline{h}_0}.$$

We integrate (2.18) concerning the boundary conditions (2.19) and obtain the dependence for calculating the leakage:

$$\overline{Q} = \frac{(\overline{yr}_1 - \overline{h}_0)^3}{\overline{\mu}(\overline{y} + \overline{h}_0)^3 \left[\ln \frac{\overline{y} + \overline{h}_0}{\overline{r}_2} + \frac{2\overline{yr}_2}{\overline{y} + \overline{h}_0} - \frac{\overline{y}^2 \overline{r}_2^2}{2(\overline{y} + \overline{h}_0)^2} - \ln \frac{\overline{h}_0}{\overline{r}_1} - \frac{2\overline{yr}_1}{\overline{h}_0} + \frac{\overline{y}^2 \overline{r}_1^2}{2\overline{h}_0^2} \right]}. \quad (2.20)$$

The expression for leakage through the seal in the case $y = 0$ has the form

$$Q = -\frac{\pi \Delta p h_0^3}{6\mu \ln \frac{r_1}{r_2}}, \quad (2.21)$$

known for calculating leaks through a plane-parallel gap [56].

For evaluation calculations, the value y as a characteristic of the gap can be obtained from dependence (2.14), given the load factor k, and also by determining the value of the gap h_0 from dependence (2.21), given the allowable leakage through the seal. The determination of the refined dimensions y and h_0 for the sealing gap can be performed by jointly solving equations (2.14) and (2.20) by the approximation method, where its value calculated from dependence (2.21) can be taken as the initial value of the gap h_0.

For seals operating in the optimal mode of boundary lubrication (region *X* in Fig. 2.3), formula [37] is proposed

$$Q = 2\pi r_e h^2 \frac{\Delta p}{p_c^2} q(v), \quad (2.22)$$

The coefficient $q(v)$ depends on the average circumferential speed $v = \omega r_c$ and is determined from the graph (Fig. 2.6). The gap between rough surfaces must be calculated using formulas (2.8) or (2.9).

Considering the friction losses in the sealing gap, as in the Couette flow $\left(\text{i.e., neglecting the losses in the radial flow due to the smallness of } \frac{du_r}{dz}\right)$, we

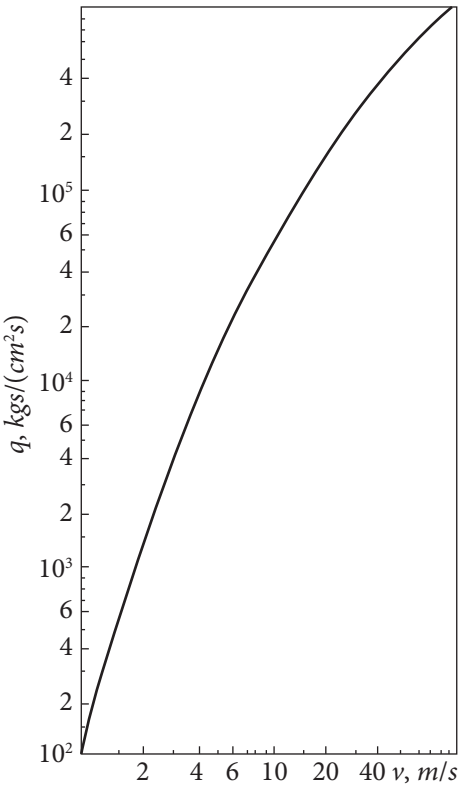

Fig. 2.6. Function *q(v)*

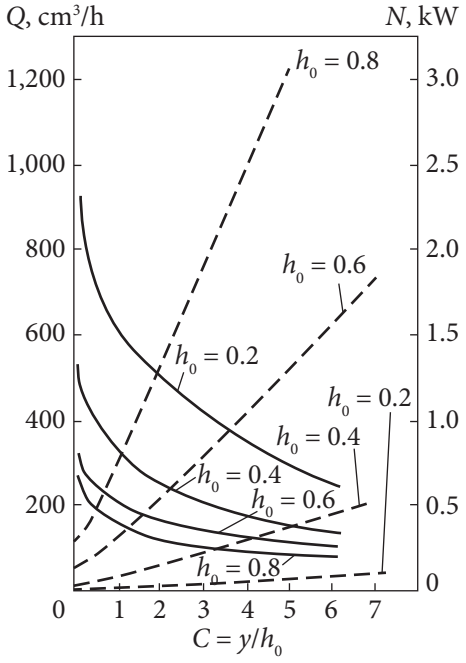

Fig. 2.7. Dependences of leakage *Q* and power loss *N* due to friction in the end gap on the parameter *C* of the shape of the end gap for a number of gaps

write the initial differential equation for the friction moment in the accepted form

$$dM_F = 2\pi r dr \tau \tag{2.23}$$

where $\tau = \mu du/dz$, $du/dz = \omega r/h$. Then

$$\tau = \mu\omega r/h \text{ and } dM_F = 2\pi\mu(\omega r^3/h)dr. \tag{2.24}$$

Reducing to a dimensionless form, integrating over $\overline{r}$, and carrying out some transformations, we obtain:

$$\overline{M}_F = \frac{\overline{\mu}(\overline{y}+\overline{h}_0)}{\overline{y}^4}\left[\overline{y}^3\left(3\overline{r}_c\overline{r}_1+\frac{1}{3}\right)-\overline{y}^2\overline{h}_0\left(3\overline{r}_1+\frac{1}{2}\right)+\overline{y}\overline{h}_0^2-c_1^3\ln\frac{\overline{y}+\overline{h}_0}{\overline{h}_0}\right], \tag{2.25}$$

where $c_1 = \overline{h}_0 - \overline{yr}_1$.

Then $M_F = M_F^* \bar{M}_F$, where $M_F^* = \dfrac{2\pi\mu\omega(r_2 - r_1)^4}{y + h_0}$.

Since the power loss due to friction in the gap $N_F = M_F\omega$, then

$$N_F = \bar{M}_F M_F^* \omega . \tag{2.26}$$

Fig. 2.7 illustrates the dependences of the leakage *Q* through the seal, along with the power loss *N* for a number of values h_0 of the minimum convergence of surfaces in the gap on the gap shape parameter.

According to the parameter *C* determined in this way, it is possible to approximately determine the power losses due to friction in the end pair according to dependences (2.25) and (2.26).

In the boundary lubrication mode, the friction coefficient can be determined for each pair of materials and operating conditions experimentally only. According to the data of paper [37], obtained as a result of testing several hundred friction pairs at the contact pressure of 0.15—20 MPa and sliding velocity 0.01 to 50 m/s, the friction coefficient sharply decreases with an increase in the contact pressure from 0.15 to 0.65 MPa. At p_c > 0.65 MPa, the friction coefficient of a given pair of materials becomes constant and does not depend on the peripheral velocity, pressure, or width of the contact surfaces, provided that the deformations of sealing rings are small $(\phi < 1.2 \cdot 10^{-4} \times r_e / b_c)$ and temperature in contact does not exceed vaporization temperature of the boundary film, i.e., conditions of boundary lubrication are preserved. At the same time, for different pairs of materials and properties of the fluid being sealed, the established value of the friction coefficient is in the range of 0.03—0.15.

The test results were also obtained for friction pairs made of siliconized graphite. With an increase in contact pressure to 0.9 MPa, the friction coefficient decreases and then stabilizes within. $f = 0.02 - 0.04$. These values are preserved not only for the siliconized graphite pair but also for the cermet hard alloy, mineral ceramics, and steel, working in tandem with siliconized graphite.

Unfortunately, currently, we have to confine ourselves to these general remarks about the friction coefficient and, in the absence of exact experimental data for each individual case, use approximate values from the indicated range or carry out estimated calculations of friction costs for limiting values $f_{\min} = 0.02$ and $f_{\max} = 0.15$ if boundary lubrication conditions are provided.

Friction force at the surface of ends $F_F = fp_cS_c$, and friction power losses

$$N_c = 2\pi f p_c \omega r_c^2 b_c = S_c f r_c \omega p_c . \tag{2.27}$$

Table 2.1. **Formulas for calculating the coefficients of disk friction**

Flow conditions	Flow regime	
	laminar	turbulent
Free disk $\mathrm{Re} = \dfrac{\omega R_2^2}{\nu}$ 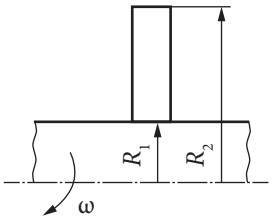	$c_1 = 3.87\mathrm{Re}^{-0,5}$ $\mathrm{Re} \le 3 \cdot 10^5$	1) Smooth disk: $c_1 = 0.982/(\lg\mathrm{Re})2.58$ $10^4 \le \mathrm{Re} \le 3.3 \cdot 10^9$ 2)Rough disc: $c_1 = 0.108(Ra/R_2)^{0.27}$ $125 \le Ra/R_2 \le 3 \cdot 10^3$
Disc in the casing $\mathrm{Re} = \dfrac{\omega R_2^2}{\nu}$ 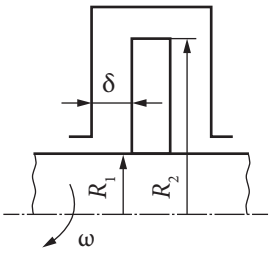	1) Narrow gap: $c_1 = 2\pi R_2 / s\,\mathrm{Re};$ $s / R_2 << 1;$ $\mathrm{Re} \le 10^5.$ 2) Wide gap: $c_1 = 2.67\,\mathrm{Re}^{-0.5};$ $s > 2\delta,$ δ — adjacent layer thickness	1) Narrow gap: $c_1 = 0.0277 / \left(\mathrm{Re}\dfrac{s}{R_2}\right)^{0.2};$ $10^4 \le \mathrm{Re} \le 10^6.$ 2) Wide gap: $c_1 = 0.0622 / \mathrm{Re}^{0.2}.$ 3) Rough disc: $c_1 = 0.051(Ra / R_2)^{0.27};$ $125 \le R_2 / Ra \le 3 \cdot 10^3;$ $0.02 \le s / R_2 \le 0.01$
Free cylinder $\mathrm{Re}_1 = \dfrac{\omega R_1^2}{\nu}$ 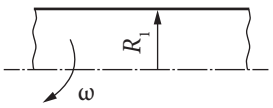	$c_2 = 4 / \mathrm{Re}_1;$ $\mathrm{Re}_1 < 10^3$	1) Smooth cylinder: $c_2 = 0.0153 / \mathrm{Re}_1^{0.125}.$ 2) Rough cylinder: $c_2 = \left[4.071g(R_1 / R_a) + 2.12\right]^{-2};$ $R_1 / Ra \langle 3 \cdot 10^3$

The end of Table 2.1

Flow conditions	Flow regime	
	laminar	turbulent
Cylinder that rotates in a fixed casing $\mathrm{Re}_2 = \dfrac{2h_0 R_1 \omega}{\nu}$ 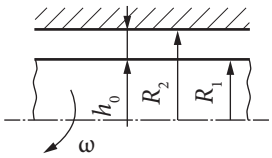	1) Big gap: $c_2 = \dfrac{4\nu R_2^2}{\omega R_1^2 (R_2^2 - R_1^2)}$; $\mathrm{Re}_2 < 2 \cdot 10^3$. 2) Small gap: $c_2 = 4 / \mathrm{Re}_2$; $h_0 / R_1 << 1$	1) Small gap: $c_2 = 0.0365 / \mathrm{Re}_2^{0.24}$; $h_0 / R_1 \langle\langle 1;\ \mathrm{Re}_2 \rangle 1.5 \cdot 10^3$. Additional axial flow at medium speed *w*: $c_2 = 0.0365 \mathrm{Re}_2^{-0.24} \times \times \left[1 + 5.22 (w / \omega R_1)^2\right]^{0.38}$

For the mode of liquid film lubrication

$$N_c = \frac{2\pi\mu\omega^2 r_c^3 b}{h_0}. \tag{2.28}$$

The total power supplied on the seal performance increases due to losses associated with liquid leakage $N_p = Q\Delta p$ and disk friction losses. If leakages take some heat away from the contact surfaces, then disc losses increase the liquid temperature in the seal chamber, thereby increasing the total thermal stress of the assembly. Liquid friction power of rotating end and cylindrical surfaces is expressed through coefficients of disk friction [55]

$$N_1 = 0.25 c_1 \rho\omega^3 (R_2^5 - R_1^5),\ N_2 = c_2 \pi\rho\omega^3 R_1^4 l, \tag{2.29}$$

where R_1 and l — cylinder radius and length; R_2 and R_1 — outside and inside disc radii; ρ — liquid density; c_1 and c_2 — coefficients of disk friction, the formulas for calculating which are given in Table 2.1.

The coefficients of friction for a disk in a casing are less than for a free disk since the fluid core between the disk and the casing rotates at a frequency about half that of the disk. Accordingly, the gradient of speed and friction force is less if there is a casing. With a small width of the end chamber, when the adjacent layers on the disk and casing are closed, friction losses increase with a decrease in the gap.

The friction loss coefficient of a cylinder coaxially rotating inside an immovable cylinder casing in laminar flow is determined by the formula of N.P. Petrov, from which, as a special case, one can obtain the corresponding formulas for a small radial clearance and for a free cylinder. The values of shear

stresses and friction loss coefficients for rapidly rotating cylinders accordingly when the fluid flow around them becomes turbulent can be obtained using the 1/7 power law or the universal law of velocity distribution in the nearby layer.

It should be noted that the power losses due to disk friction (2.29) are proportional to the cube of the rotor speed and, at low frequencies (up to 3,000 rpm), are measured in fractions of a kilowatt, so taking into account these losses is advisable only for high-speed machines.

2.4. Computing of the mechanical seal thermal state

Friction power in the sealing clearance is converted into heat, which spreads through the contact end surfaces along the sealing rings, creating an uneven temperature field. Contact surface heating significantly affects the friction mode: firstly, the mechanical and physical properties of the materials of the rubbing bodies and the separating layer of the sealed liquid change, and secondly, the rings are subject to thermal deformations, which violate the uniformity of contact in the friction pair. Excessive heating leads to the evaporation of the liquid layer. Herewith, the friction coefficient increases sharply, and temperature and wear rise, i.e., there is thermal cracking of the rings and loss of impermeability.

The main tasks of thermal calculation are to determine maximum temperatures in the friction pair and to assess temperature deformations of the rings to ensure such conditions in the structure under which temperatures and deformations do not exceed the allowable values.

Calculation of the thermal state is based on heat balance equations. The average liquid temperature in the seal chamber is determined from the equality of total heat flow released during the seal performance and convective removal from its case (Fig. 2.8).

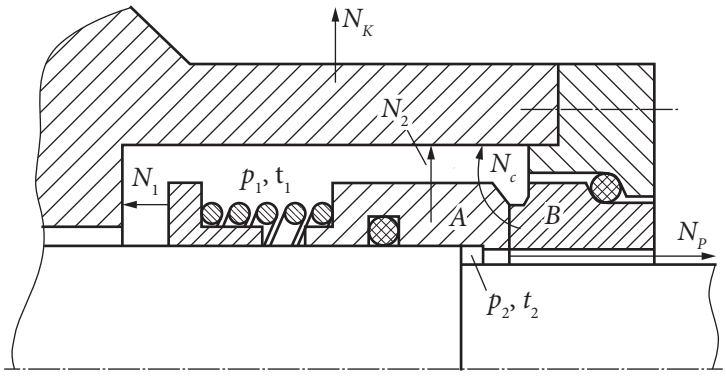

Fig. 2.8. Diagram of heat flows in mechanical seal

The heat balance equation is written as

$$N_c + N_1 + N_2 = N_k + N_p, \tag{2.30}$$

where heat removal from the case $N_k = S_k \alpha_k (t_1 - t_2)$, and heat removal via the seals as a result of leakage $N_p = Qc\Delta t$. Where S_k — the reduced area of the seal case, from which heat is released to the external environment; α_k — heat transfer coefficient; c — specific heat capacity of the sealed liquid; Δt —increase in its temperature, taking into account the removed heat; t_1 and t_2 — temperature of the liquid inside the seal case and temperature of the external environment.

If the seal is provided with forced cooling, then the corresponding heat flow rate must be added to the right side of the equation (2.30). During normal seal performance, when leakages are small (approx. 10 cm^3 / h), their influence on the thermal state can, as a rule, be neglected $(N_p \approx 0)$.

The temperature in the friction pair is determined based on the heat balance equation for the sealing rings, from surrounding them sealed leakage and external environment

$$N_c = N_a + N_b, \tag{2.31}$$

where N_a and N_b — heat flows released, respectively, from the rotating ring *A* and base *B* rings.

The temperature field of sealing rings is generally described by a second-order nonlinear differential equation for a parabolic derivative. If weak dependence of the heat conduction coefficient on temperature in a stable thermal process is not taken into account, then the temperature field can be described by Laplace's equation with complex boundary conditions. But at the same time, the numerical solution of the problem for rings of complex shapes is connected with significant difficulties. In this case, the methods of electronic modelling of the thermal state of the seal are effective.

For a rough estimate of temperature on the contact end surfaces, let us simplify the problem by taking hollow cylinders (Fig. 2.9, *a*) with a heat flow uniformly distributed on the contact surface $q = N_c / S_c$ and constant in length heat transfer coefficients of cylindrical surfaces washed by the sealed liquid or the external environment as a design model of the rings,

$$\frac{d^2\theta}{dx^2} - m^2\theta = 0, \tag{2.32}$$

under boundary conditions $x = 0 : \theta = \theta_0$, $x = l : \frac{d\theta}{dx} = -\frac{\alpha}{\lambda}\theta_1$, where $\theta = t(x) - t_2$; $m = (\alpha L / \lambda S)^{0.5}$; t_2 — ambient temperature; λ — thermal conductivity of the ring material; α — heat transfer coefficient from the ring surface to the external

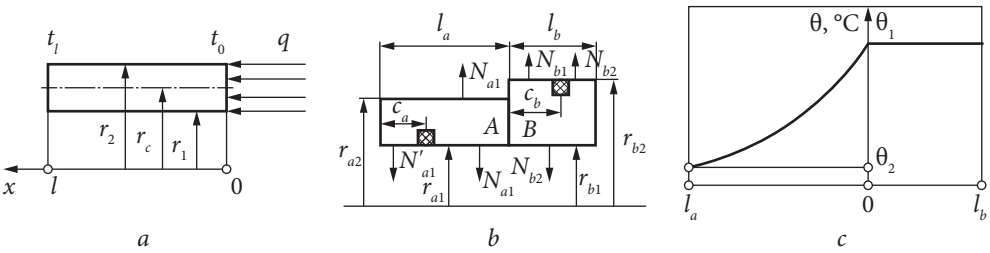

Fig. 2.9. Diagram of the thermal state of the seal: *a* — the model of the separate ring; *b* — calculating diagram of the axially-movable *A* and base *B* rings; *c* — temperature change along the rings; $\theta_1 = 94.4$, $\theta_2 = 42.7$

environment; $L = 2\pi r_2$ — perimeter of the ring surface on which heat is transferred; $S = \pi(r_2^2 - r_1^2)$ — area of the ring cross-section.

The equation is (2.32) solved according to the law of temperature change along the ring:

$$\theta(x) = \theta_0 \frac{\operatorname{ch}\left[m(l-x)\right]}{\operatorname{ch} ml}. \tag{2.33}$$

Meanwhile, a decrease in temperature along the length is caused by heat transfer to the external environment. Inserting (2.33) into the Fourier equation $N = \lambda \frac{d\theta}{dx} S$, we obtain the formula for the heat removed per unit of time:

$$N = \lambda S m \theta_0 \operatorname{th} ml. \tag{2.34}$$

In real seals, in different areas of the ring, its surfaces can be in contact with differeIn real seals, in different areas of the ring, its surfaces can be in contact with different media or can be made of materials with various thermal conductivity coefficients. Therefore, the calculation model can be represented by cylinders (Fig. 2.9, *b*) with different heat transfer coefficients and different ambient temperatures in certain areas of the surface.

Herewith, the total heat transfer of each ring consists of the sum of heat transfer from individual sections:

$$N_a = N_{a1} + N'_{a1} + N_{a2}; \; N_b = N_{b1} + N_{b2} + N'_{b2}. \tag{2.35}$$

Here, the first index is the ring number, and the second characterizes the external environment of the given section: 1 — the sealed liquid with temperature t_1; 2 — the external environment (air) with temperature t_2. Each term is calculated by the formula (2.34), taking into account the corresponding parameter values:

$$S_a = \pi(r_{a2}^2 - r_{a1}^2), \; S_b = \pi(r_{b2}^2 - r_{b1}^2),$$

$$r_{a1} = r_{b1} = r_1,$$

$$l_{a1} = l_a,\ l'_{a1} = c_a,\ l_{a2} = l_a - c_a,$$

$$l_{b2} = l_b,\ l'_{b2} = l_b - c_b,\ b_{b1} = c_b,$$

$$L_{a1} = 2\pi r_{a2},\ L'_{a1} = L_{a2} = L_{b2} = 2\pi r_1,$$

$$L_{b1} = L'_{b2} = 2\pi r_{b2}.$$

For the section of rings contacting with the sealed liquid $\theta_{01} = t_0 - t_1$, for areas contacting with the external environment, $\theta_{02} = t_0 - t_2$,; t_0 — the temperature at the contact of the rings.

Inserting (2.35) into the heat balance equation, we obtain

$$N_c = (A_{a1} + A'_{a1} + A_{b1})\theta_{01} + (A_{a2} + A_{b2} + A'_{b2})\theta_{02}, \tag{2.36}$$

whereof

$$t_0 = \left(\frac{N_c}{B_1} + t_1 + \frac{B_2}{B_1}t_2\right) / \left(1 + \frac{B_2}{B_1}\right), \tag{2.37}$$

where B_1 and B_2 — heat transfer coefficients into the sealed liquid and external environment, $B_1 = A_{a1} + A'_{a1} + A_{b1}$, $B_2 = A_{a2} + A_{b2} + A'$. Taking into account that heat transfer from the surfaces of the rings, which are shifted towards the external environment $(\alpha'_{a1}, \alpha_{a2}, \alpha_{b1}, \alpha'_{b2})$, is small compared to heat transfer of the rotating surfaces (α_{a1}) and (α_{b2}), it can be written as $B_1 \approx A_1$ $B_2 \approx A_{b2}$ or

$$\left.\begin{aligned} B_1 &= S_a\lambda_a m_1 \mathrm{th}(m_1 l_1), \\ B_2 &= S_b\lambda_b m_2 \mathrm{th}(m_2 l_2) \end{aligned}\right\},\ \begin{aligned} m_1 &= \left[\alpha_1 L_{a1} / \lambda_a S_a\right]^{0,5}, \\ m_2 &= (\alpha_2 L_{b2} / \lambda_b S_b)^{0,5}. \end{aligned} \tag{2.38}$$

Consequently, the change in the cross-section average temperature along the ring can be determined by the formula (2.33), and the average temperature on the contact surfaces of the mechanical seal can be determined by the formula (2.37). The more accurate calculation, taking into account the change in temperature along the ring radius, was carried out in papers [44, 50].

Based on the conditions of heat resistance of contact surfaces and preservation of the liquid film in the clearance gap at a given pressure, the temperature in the friction pair is a limited t_* value. Herewith, allowable friction power can be determined for the given conditions of heat removal using the formula (2.36)

$$N_* \le (B_1 + B_2)t_* - B_1 t_1 - B_2 t_2, \tag{2.39}$$

and the allowable value of operational load:

$$(\omega r_c \Delta p f)_* \le \frac{1}{k_e S_c}\left[(B_1 + B_2)t_* - B_1 t_1 - B_2 t_2\right]. \tag{2.40}$$

The heat transfer coefficients of cylindrical surfaces, necessary for assessing the thermal state, are expressed in terms of Nusselt numbers: for a free cylinder and a rotating cylinder inside a stationary cylindrical casing with a gap h_0, the corresponding coefficients are equal to

$$\alpha_1 = \frac{\lambda}{\hat{e}} Nu_1, \quad \alpha_2 = \frac{\lambda}{2h_0} Nu_2, \tag{2.41}$$

where, according to the semi-empirical formula of Dropkin and Carmi

$$Nu_1 = 0.095(2\,\mathrm{Re}_1 + Gr)^{0.35},$$

and for heat removal into the gap, when free convection can be neglected [18],

$$\mathrm{Nu}_1 = \mathrm{Pr}\,\mathrm{Re}_2\sqrt{2c_2}\left[5\ln\left(\frac{\mathrm{Re}_2\sqrt{2c_2}}{30} - 1\right) + 15\,\mathrm{Pr}\right]^{-1}. \tag{2.42}$$

Grashof and Prandtl criteria

$$\mathrm{Gr} = 8\beta g r^3 \nu^{-2}\overline{\theta}, \quad \mathrm{Pr} = \mu c_p / \lambda, \quad \overline{\theta} = \overline{t} - t_2$$

are expressed through the following characteristics of the medium: β — coefficient of thermal expansion, 1/°C; λ — coefficient of thermal conductivity, W/(m°C); c_p — specific heat capacity, J/(kg°C); ν — kinematic, m²/s, and μ — dynamic, N/(m²s), viscosity coefficients; g — acceleration of gravity, m/s²; $\overline{t}$ and t_2 are the average temperature of the heat-releasing surface and the average ambient temperature, °C. The friction loss coefficient of the cylindrical surface for $\mathrm{Re}_2 > 1{,}500$ is equal to

$$c_2 = 0.0365\,\mathrm{Re}_2^{-0.24}; \ \mathrm{Re}_1 = \omega r^2 / \nu, \ \mathrm{Re}_2 = 2\omega r h_0 / \nu, \tag{2.43}$$

where r is the radius of the rotating cylinder; h_0 — radial clearance between the cylinders (rotating and stationary).

The Grashof criterion characterizes convective heat transfer due to the Archimedean lift forces caused by the difference in densities at individual points of a no-isothermal flow through thermal expansion. The Prandtl criterion is the ratio of turbulent momentum transfer due to internal friction to turbulent heat transfer due to heat conduction. For air under normal conditions, Pr = 0.74; for water at t = 0 °C Pr = 13.0. As the water temperature rises to 250 °C (on the saturation line), the Prandtl number decreases to Pr = 0.84; with a further increase in temperature, the Prandtl number increases again [66].

If an axial flow with an average velocity w over the gap is superimposed on the circumferential flow in the annular gap, then the intensity of heat removal increases [67]: $c_2 = 0.0365\,\mathrm{Re}_2^{-0.24}\left[1+5.22(w/\omega r)^2\right]^{0.38}$.

The set of criteria $\mathrm{Re}_2\sqrt{2c_2}$, included in expression (2.42), taking into account formula (2.43), can be reduced to the form

$$\mathrm{Re}_2\sqrt{2c_2} = 0.27\,\mathrm{Re}_2^{0.88},$$

wherein

$$Nu_2 = \frac{0{,}27\,\mathrm{Pr}\,\mathrm{Re}_2^{0.88}}{5\ln(0.009\,\mathrm{Re}_2^{0.88}-1)+15\,\mathrm{Pr}}.$$

To make the influence of individual parameters on the thermal state of the rings clearer, we transform formulas (2.38), taking into account (2.41):

$$m_1 = \left(2\pi\frac{\lambda_1 Nu_1}{\lambda_a S_a}\right)^{0.5},\quad m_2 = \left(2\pi\frac{\lambda_2 \mathrm{Nu}_2}{\lambda_b S_b}\right)^{0.5},$$

$$\left.\begin{aligned} B_1 &= (2\pi S_a \mathrm{Nu}_1\lambda_1\lambda_a)^{0.5}\,\mathrm{th}(m_1 l_1),\\ B_2 &= (2\pi S_b \mathrm{Nu}_2\lambda_2\lambda_b)^{0.5}\,\mathrm{th}(m_2 l_2),\end{aligned}\right\}$$

where λ_1 and λ_2 are the thermal conductivity coefficients of the sealed liquid and the external environment (air). The ratio of heat transfer to air and liquid, which is included in the formula (2.37), taking into account that $S_a \approx S_b$, $\lambda_a \approx \lambda_b$ it takes the form

$$\frac{B_2}{B_1} = \left(\frac{\mathrm{Nu}_2\lambda_2}{\mathrm{Nu}_1\lambda_1}\right)^{0.5}\frac{\mathrm{th}(m_2 l_2)}{\mathrm{th}(m_1 l_1)}.$$

Since the thermal conductivity coefficient λ_2 and the Nusselt number Nu_2 for air are much smaller than for liquid, in many cases, the ratio B_2 / B_1 in formula (2.37) can be neglected compared to unity and to estimate the temperature in the friction pair, use the simplified formula

$$t_0 = t_1 + N_c/B_1. \qquad (2.44)$$

It can be seen from formulas (2.37) that in order to reduce the temperature in a friction pair, it is necessary to reduce the power losses due to friction and increase heat removal by intensifying heat transfer (increasing the Nusselt number), increasing heat transfer coefficients and cross sections of the rings. The length of the rings is included only in the argument of the hyperbolic tangent,

the limit value of which is one. Since for ml = 1.6 th(ml) = 0.9217, i.e., close to the limit value, further increase in the argument due to the length of the ring is inefficient. The feasibility of certain methods of reducing the temperature in the contact zone should be determined in relation to specific operating conditions.

To perform a thermal calculation of seals, coefficients that characterize the physical properties of liquids and gases that wash the surfaces of sealing rings are needed.

The dynamic coefficient of viscosity and the coefficient of thermal conductivity of gases can be estimated by the approximate Sutherland formulas if we neglect their slight increase with increasing pressure (at pressures up to 20 MPa):

$$\mu = \mu_0 \frac{T_0 + T_s}{T + T_s}\left(\frac{T}{T_0}\right)^{1.5}; \ \lambda = \lambda_0 \frac{T_0 + T_s}{T + T_s}\left(\frac{T}{T_0}\right)^{1.5},$$

where T is the absolute temperature, T_0 = 273K; μ_0, λ_0 — viscosity and thermal conductivity at atmospheric pressure and temperature; T_s is a constant.

The kinematic coefficient of viscosity $\nu = \mu / \rho$ and the density of the gas, depending on pressure and temperature, is determined by the Claperon formula

$$\rho = \rho_0 \frac{pT_0}{p_0 T}.$$

2.5. Thermal deformations of friction pair rings

The operating experience of mechanical seals shows that as a result of angular deformations of the rings, the wear of the contact surfaces along the radius is uneven. Deformations in the first approximation can be considered as a rotary movement of the ring cross-section without changing its shape and not taking into consideration interaction between the ring fibers, i.e., considering the stress state as uniaxial, which makes it relatively easy to calculate the rotational angle of the ring [47]:

$$\phi = \frac{M_t + M_p}{El_y} y_c, \tag{2.45}$$

where y_c — radius of the centroid of section; I_y — second area moment towards the axis Oy, passing through the centroid and perpendicular to the ring axis; E — elasticity modulus of the ring material; M_t, M_p — force moments towards the axis Oy, conditioned by unevenness of the temperature and pressure fields.

The moment conditioned by temperature change over the ring length is determined by integral [47]

$$M_t = \int_{(s)} E\beta\theta x dx, \tag{2.46}$$

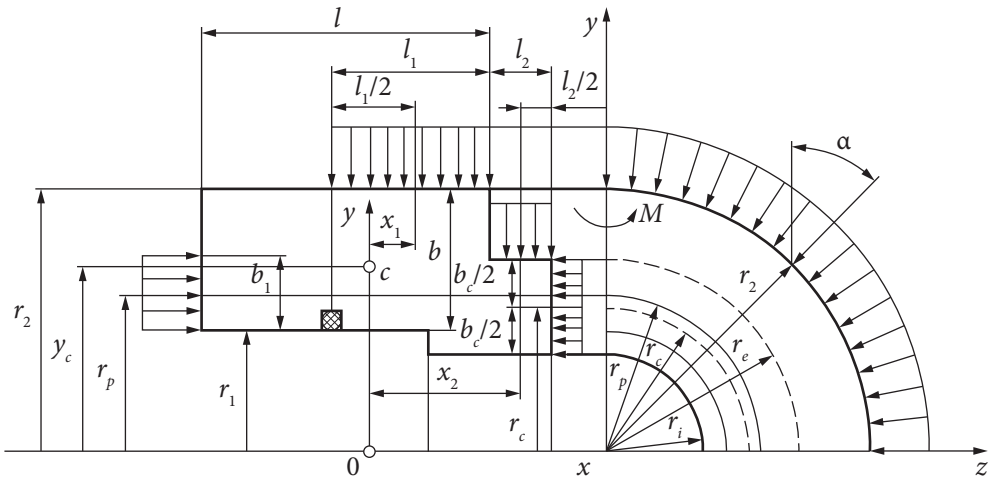

Fig. 2.10. Diagram of sealing ring deformation

i.e., a decrease in the temperature moment can be achieved using combined rings: a slip ring made of an antifriction material with a low elasticity modulus and linear expansion coefficient is fixed in the steel retaining ring. Herewith, the components of temperature moment decrease, which correspond to the intersection areas farthest from the O*y* axis, and are subject to the action of large temperature gradients $(\theta x)_{\max}$ (Fig. 2.9, *c*). For the ring shown schematically in Fig. 2.10, rotation of the section as a result of temperature deformations occurs counterclockwise; therefore, the temperature moment is positive $M_t > 0$.

If the ring section is close to a rectangular shape, then $I_y = bl^3/12$, $dS = bdx$, $y_c = 0.5\ (r_1 + r_2)$. With a constant-by-section elasticity modulus and linear expansion coefficient, the temperature component of the slope of the elastic curve is calculated by the formula

$$\phi_t = \frac{6\beta(r_1 + r_2)}{l_3}\int_0^l \theta(x)x dx, \tag{2.47}$$

and taking into account (2.33) to distribute temperature over the ring length

$$\phi_t = \frac{12\beta\theta_0(r_1 + r_2)}{m^2 l^3}\frac{\mathrm{sh}^2(ml/2)}{\mathrm{ch}(ml)}. \tag{2.48}$$

Formula (2.48) may be used for a rough estimation of temperature deformation. [42] gives the formula obtained from (2.47) on the assumption that the temperature over the ring length changes linearly. In this case, the deformations turn out to be significantly underestimated.

Moment M_r about an axis O*y* of radial pressure forces acting on a cylindrical surface with radius r_2 and length l_1 will be obtained if we sum up the mo-

ments of projections of elementary pressure forces (see Fig. 2.10) onto the plane $xOz: dM_r = -p_1 l_1 r_2 x_1 \sin\alpha d\alpha$.

The total moment over two cylindrical surfaces is

$$M_r = \int_0^{\pi/2} dM_r = -p_1(l_1 r_2 x_1 + l_2 r_e x_2). \tag{2.49}$$

If, when calculating the moments of radial forces, the projections of elementary pressure forces change, then when calculating the moment of axial forces, the arm of the elementary force is variable:

$$dM_a = p_1 b_1 r_p^2 \sin\alpha d\alpha - p_c b_c r_c^2 \sin\alpha d\alpha.$$

Taking into consideration that $p_c = kp_1$, $k = S/S_c = b1r_p/b_c r_c$, it should be written

$$M_a = p_1(b_1 r_p^2 - k b_c r_c^2) = p_1 b_1 r_p^2 (1 - r_c / r_p). \tag{2.50}$$

It follows from the formula (2.50) that the moment of axial forces depends on the load coefficient. For balanced seals $k < 1$, $r_p > r_c$, $M_a > 0$, for loaded seals — $k < 0$, $r_p < r_c$, $M_a < 0$. If $k = 1$, then $r_p = r_c$, $M_a = 0$. Consequently, the more the load coefficient differs from one, the module of the moment of axial forces is greater. it is necessary to select the ring so that the displacement x_1 of the center of radial load towards the centroid of the section is minimal to reduce the moment of radial forces [45].

The total slope of the elastic curve (2.45) is determined by the algebraic expression of moments or algebraic expression of the corresponding components of the slope of the elastic curve $(\phi = \phi_t + \phi_p)$. Herewith, the possibilities for reducing total ring deformations expand: temperature deformations can be compensated for by force deformations. Displacement of the outer points of the contact surface towards the inner ones can be determined on the basis of the total slope of the elastic curve: $\delta = \phi b_c$.

Based on the experience of many years in the development and operation of mechanical seals in various conditions [42], the acceptable limit value δ is determined from the ratio $\delta / r_e \le 1.2 \cdot 10^{-4}$. Positive displacements correspond to the opening of the end clearance from the side of a larger radius r_e of the contact surface.

Based on the results of experimental and computational studies [43, 47], it is possible to obtain a solution to the temperature problem that is quite acceptable for calculating the thermal deformations of the mechanical seal rings, limited to estimating heat generation in the sealing gap under conditions of liquid friction. In the research process, the dependences of the relative flow coefficients C_Q and power C_N were obtained (Fig. 2.11).

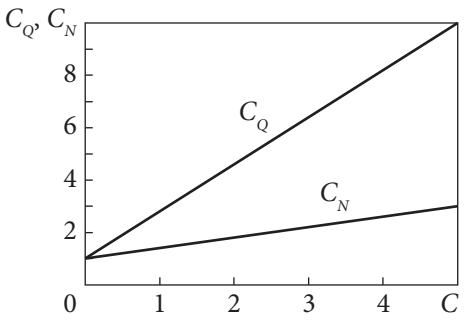

Fig. 2.11. Dependence of the relative flow coefficients C_Q and power C_N on the coefficient C of the shape of the mechanical seal gap

The calculation model is based on the following assumptions:

• only the stationary mode of operation of the seal unit is considered;

• sealing rings with a cross-section of a simple rectangular or close to it shape is used;

• in the seal chamber, a low (not higher than 10° C) temperature difference is maintained between the temperature on the side surface of the rings and the cooling medium in the chamber;

• temperature differences in the rings of the end pair are determined by their height (axial differences);

• the temperature of the non-working rear end of the ring is assumed to be equal to the temperature of the medium being sealed in the seal chamber;

• specific heat fluxes in the rings of the friction pair are distributed according to the thermal conductivity of the materials of the rings according to the dependence $\frac{q_1}{q_2} = \frac{\lambda_1}{\lambda_2}$;

• the heat flux supplied to the sealing surface of the rings is dissipated over the entire volume of each ring of the friction pair;

• when determining the temperature difference along the height of each of the rings (by solving the heat conduction equation), the Fourier law is used for the one-dimensional problem of temperature distribution in the body of the ring.

The results of works [41, 45] showed that the dominant role in the size of deformations of the mechanical seal rings from the temperature field is played by axial temperature drops in the rings. Below, Table 2.2 presents a detailed algorithm for calculating the axial temperature difference and temperature deformations in the mechanical seal rings developed in [43] in the calculation procedure form.

An analysis of the factors affecting the deformation of rings from heat releases shows that the deformation of each of them is expressed by the functional dependence

$$\phi = f(\alpha_t, \mu, \nu^2, b, B, l^{-1}, \lambda^{-1}),$$

where α is the coefficient of linear expansion of the material; μ is the viscosity of the medium to be sealed; b is the width of the sealing band of the friction pair; B is the width of the ring along the radial coordinate; H — ring thickness; λ is

Table 2.2. **Method for determining thermal deformations in mechanical seal rings**

Step	Order of definition
1	The design of the assembly and the geometric dimensions of the parts are selected: r_1, r_2 are the outer and inner radii of the sealing band of the rings; materials of friction pair rings (including thermal conductivity λ and linear expansion α coefficients); the area F_K of the sealing contact of the surfaces of a pair of rings; load factor k; slot shape parameter C; correction factors C_Q and C_N (to select the values of the correction factors you can use the graph in Fig. 2.11)
2	The operating parameters of the seal are assigned: differential pressure Δp across the seal, shaft angular frequency ω, allowable leakage through the seal Q, temperature t, and dynamic viscosity μ of the medium to be sealed in operating mode
3	A draft design of the mechanical seal unit is being developed. In the subsequent calculation of the sealing unit, the shape of the sealing joint obtained as a result of force and temperature deformations is considered to correspond to such a shape in which the specific value of the bearing force $\overline{F}$ in the sealing joint corresponds to magnitude to the load factor k.
4	The size of the minimum gap h_0 in the sealing slot is calculated, taking into account the correction factor C_Q, using dependence (2.21) for leakage through a mechanical seal with a flat slot. The size of the leak Q is specified by correcting for the shape of the gap according to the selected load factor k of the seal assembly
5	Since in the hydrodynamic lubrication regime, the load factor k is equal to the dimensionless bearing force $\overline{F}$, from the graph in Fig. 2.5, you can set the value of the slit shape parameter C
6	From the expression $C = y/h_0$, the height y of the wedge at the junction of the surfaces forming the sealing gap is determined, which occurs under the hydrodynamic friction regime as a result of force and temperature deformations of the rings
7	For a mechanical seal with a known minimum sealing gap, the friction power losses are determined, taking into account the correction factor C_N. $$N = \frac{\pi\mu\omega^2(r_2^4 - r_1^4)}{2C_N h_0}$$
8	The specific heat flux into the rings from heat generation in the sealing gap is determined: $q = \frac{N}{F_K}$
9	The relative distribution of heat flows into the mechanical seal rings of the friction pair is determined: $k_\lambda = \frac{\lambda_1}{\lambda_2}$ or $\frac{q_1}{q_2} = \frac{\lambda_1}{\lambda_2}$, where $q_1 + q_2 = q$

The end of Table 2.2

Step	Order of definition
10	The dissipations of the heat flux in the ring's coefficients are determined k_1 and k_2. In this case, the following simplifying assumptions are used: the heat flow brought to the sealing surface of the ring is distributed over the entire body of the ring; the temperature of the non-working rear end of the ring is assumed to be equal to the temperature of the medium being sealed in the seal chamber; $k_1 = \frac{r_{21} - r_{11}}{r_2 - r_1}$ — for ring 1; $k_2 = \frac{r_{22} - r_{12}}{r_2 - r_1}$ — for ring 2
11	The general axial temperature differences in the rings of the friction pair are determined: $t_1 - t_c = \frac{q_1 H_1}{\lambda_1 k_1}$ $t_2 - t_c = \frac{q_2 H_2}{\lambda_2 k_2}$
12	The temperature deformations of the sealing surfaces of each of the rings are determined due to the rotation of the section from the axial temperature gradient $\phi_1 = \frac{\alpha_1 (t_1 - t_c)(r_2^2 - r_1^2)}{2 l_a}$, $\phi_2 = \frac{\alpha_2 (t_2 - t_c)(r_2^2 - r_1^2)}{2 l_b}$
13	The total temperature deformation of the rings in the seal is determined: $\phi = \phi_1 + \phi_2$

the coefficient of thermal conductivity of the ring material; ν is the relative slip velocity in the friction pair.

The biggest influence on the deformation is exerted by the relative sliding speed of the rings in the sealing pair. When designing a seal assembly, it is desirable to select the materials of a pair of rings in such a way that the complexes $\alpha B/\lambda$ for them are close in size.

2.6. Force deformations of sealing rings

When designing mechanical seals, it is necessary to calculate the expected deformations of the sealing surfaces of the rings to determine their shape in the end joint. Let us consider a calculation method based on the provisions of the theory of axisymmetric deformations of annular parts and the possibility of its practical use in the example of calculating a typical mechanical seal.

The rings of mechanical seals experience the action of axisymmetric radial and axial forces, as well as bending moments when loaded with the pressure of the medium being sealed.

The theory of axisymmetric deformations of annular parts with small displacements based on the following assumptions is used to calculate the defor-

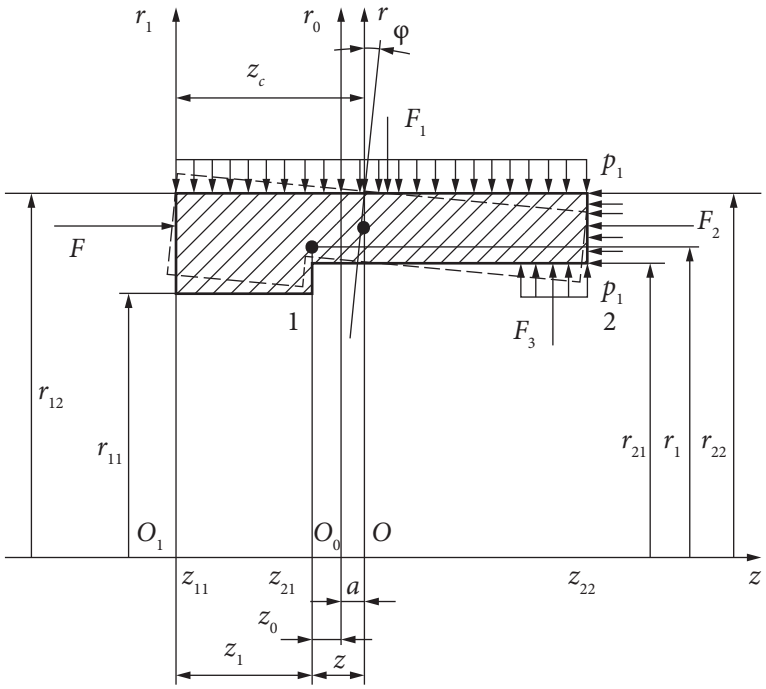

Fig. 2.12. Calculation scheme for the mechanical seal ring in the case of loading it with a pressure drop: p_1 is the pressure of the medium being sealed; F is the loading force; φ is the angle of rotation of the ring section; c is the center of mass of the ring section

mations in the body of the rings under the influence of the pressure of the medium being sealed:

• the shape of the cross-section of the ring remains unchanged, and when loaded, the section only rotates in its plane relative to the center of gravity;

• the stress state at any point of the ring is uniaxial, i.e., the annular fibers are deformed in the circumferential direction and do not exert force on each other.

Here, the main provisions of this theory are presented, which are used further in the calculation method. Let us consider a ring of a balanced mechanical seal, typical in shape, shown in Fig. 2.12

The deformation of the cross-section of the ring is represented as a rotation of the section through an angle relative to its center of mass c, the stresses in which are equal to 0. When searching for a solution to the problem, the following geometric characteristics for the cross-section of the ring are used:

$$I_1 = \iint_S \frac{dS}{r};\ I_2 = \iint_S \frac{zdS}{r};\ I_3 = \iint_S \frac{z^2 dS}{r},$$

where r and z are the radial and axial coordinates of an arbitrary point of the ring section; dS is the elementary cross-sectional area of the ring.

The quantities I_1 and I_3 are always positive, and the sign of I_2 depends on the choice of the coordinate axis position.

The axis Or is called the main axis of the ring section if the integral I_2 of the ring cross-section is equal to 0. To determine the position of the main axis, an arbitrary auxiliary axis O_1r_1 is chosen. The distance between the axes O_1r_1 and Or will be denoted by z_c. Then the distance to point *A* from the auxiliary axis will be z_1, from the main axis $z = z_1 - z_c$, and the geometric characteristic

$$I_3 = I_3^{O_1r_1} - I_1 z_c^2 .$$

The cross-section of the ring can be divided into a number of rectangles, in which z_{i1} and z_{i2} are the initial and final coordinates of the i^{th} rectangle on the *z* axis. In this case, the integrals I_1, I_2, I_3 with respect to the auxiliary axis O_1r_1 can be written in the form of expressions:

$$\begin{aligned} I_1 &= \sum_{i=1}^{n} (z_{i2} - z_{i1}) \ln \frac{r_{i2}}{r_{i1}}; \\ I_2 &= \sum_{i=1}^{n} \left(\frac{z_{i2}^2 - z^3{}_{i1}}{2} \right) \ln \frac{r_{i2}}{r_{i1}}; \\ I_3 &= \sum_{i=1}^{n} \left(\frac{z_{i2}^3 - z^3{}_{i1}}{3} \right) \ln \frac{r_{i2}}{r_{i1}} - \frac{I_2^2}{I_1}, \end{aligned} \tag{2.51}$$

where the index i is the number of the rectangle; r_{i1} and r_{i2} are the coordinates of the i^{th} rectangle on the *r* axis.

For a section of a ring consisting of a single rectangle of length *z*, the axis Or passes through its center of symmetry, and dependences (2.51) have the form:

$$I_1 = z \ln \frac{r_2}{r_1}; \; I_2 = 0; I_3 = \frac{z^3}{12} \ln \frac{r_2}{r_1}. \tag{2.52}$$

It is necessary to know the position of the neutral line O_0r_0, which depends on the nature and magnitude of the loading of the ring, to calculate the stresses in the body of the ring. The coordinates of points in the ring z_0 and the angle ϕ of rotation of its section are counted from this line when calculating the required values of the ring deformation. The position of the neutral line is determined by the stresses in the cross-section of the ring. The latter, in turn, are associated with an external load and can be found by solving the equilibrium equations for half the ring from the radial forces and moments of the loading forces.

Normal forces F_N and bending moments *M* for special cases of loading, reduced to the ring section in a form convenient for use in compiling equilibrium equations, are shown in Fig. 2.13 [43].

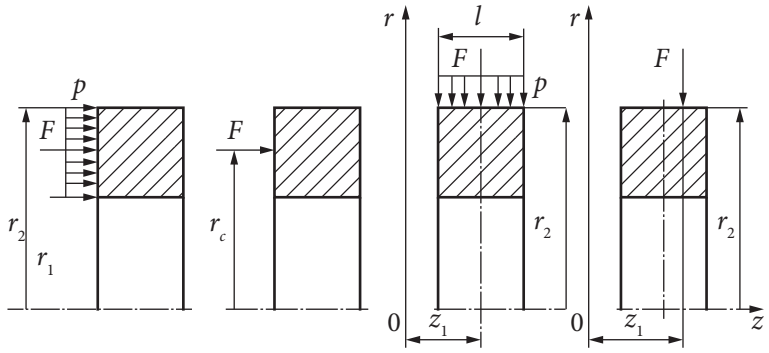

Fig. 2.13. Normal forces F_N and bending moments M in the cross-section of the ring for special cases of loading

For seals of high-speed shafts with a speed of more than 100 m/s, it is necessary to take into account the effect of inertial load on the deformation of the rotating ring of the end pair. This influence should be taken into account in the equation of radial forces by the term

$$N_i = \int_{r_{i1}}^{r_{i2}} \rho\omega^2 z_i r^2 dr$$

and in the equation of bending moments, the term

$$M_i = \int_{r_{i1}}^{r_{i2}} \rho\omega^2 z_i (z_{i2} - z_{i1}) r^2 dr\,,$$

where ρ is the density of the ring material; ω is the angular frequency of the shaft; r is the radial coordinate of the selected i^{th} rectangle of splitting the section of the ring.

Under the action of an axisymmetric load, only normal stresses arise in the cross sections of the ring. These voltages can be positive or negative; at the points of the neutral line, the voltages are 0. Relative deformation of the annular fiber in the body of the ring

$$\varepsilon_i = \frac{\Delta r}{r} = \frac{\phi z_0}{r}\,,$$

where z_0 is the distance from the considered point in the section of the ring to the neutral line; ϕ is the angle of rotation of the ring section. Accordingly, circumferential stress

$$\sigma_i = \varepsilon_i E = \frac{\phi z_0 E}{r}\,; \qquad (2.53)$$

where E is the modulus of elasticity of the material. Taking into account dependence (2.53), we obtain:

$$F_N = \phi E \int_S \frac{z_0 dS}{r};\ M = \phi E \int_S \frac{z_0 z dS}{r}. \tag{2.54}$$

We denote the distance between the main axis Or and the neutral line $O_0 r_0$ by a, then the known distances z from the main axis to any point in the section of the ring can be expressed in terms of its distances $z_0 = z - a$ from the neutral line $O_0 r_0$, and equations (2.54) take the form:

$$F_N = \phi E \left[\int_S \frac{dSz}{r} - a \int_S \frac{dS}{r} \right];\ M = \phi E \left[\int_S \frac{dSz^2}{r} - a \int_S \frac{dSz}{r} \right].$$

Using the introduced notation and setting $I_2 = 0$ since the axis Or is the main one, we obtain

$$F_N = -\phi E a I_1,\ M = \phi E I_3. \tag{2.55}$$

Hence, the angle of rotation of the ring section relative to the center of mass c:

$$\phi = \frac{M}{EI_3}, \tag{2.56}$$

and the distance to the neutral line

$$a = -\frac{F_N}{EI_1 \phi} = -\frac{F_N I_3}{M I_1}. \tag{2.57}$$

Using dependence (2.53), you can get the stress for any point of the section:

$$\sigma_i = \frac{M z_0}{r I_3} + \frac{F_N}{r I_1}. \tag{2.58}$$

If the normal force N in the section is equal to 0, then the ring experiences only bending, i.e., $a = 0$ and the neutral line $O_0 r_0$ coincides with the main axis Or of the section; if $M = 0$, the stress in the body of the ring does not depend on the coordinate z.

The above dependences are used to calculate the shape of the sealing gap of a balanced mechanical seal.

2.7. Conclusions. Basic recommendations for the calculation of mechanical seals

The given dependencies allow us to determine the main characteristics of the mechanical seal: leakage, bearing force in the gap, friction moment, and pressure diagram with a known shape of the radial gap.

For their calculation, when designing a mechanical seal, the following quantities must be specified or determinable:

- leaks Q through the seal;
- initial conditions of the nominal operating mode for the mechanical seal: pressure drop across the seal, shaft rotation frequency, characteristics, and properties of the medium being sealed (including thermophysical ones associated with the pressure and temperature of this medium being sealed at the gap), initial conditions for the temperature of the medium in the seal chamber;
- thermophysical characteristics of the materials of the rings and adjacent parts of the seal assembly (heat capacity, thermal conductivity, coefficient of thermal expansion);
- strength characteristics of ring materials;
- the nature of the deformation of the rings from power loads;
- the nature of deformations of the rings from the characteristics of the temperature distribution in them;
- gaps and shapes of the end gap in the radial direction;
- the relationship between the rigidity of the lubricating layer in the seal gap and the shape and dimensional parameters of this gap.

The temperature of the medium in the sealing gap, as well as in the rings of the mechanical seal, is the biggest ambiguity in the definition of all the listed values necessary for designing.

Based on the model of the mechanical seal described above and the proposed recommendations for calculating the unit, the task of the developer is to design the elements of the parts of the seal unit in such a way that the level and type of deformation of the rings from the pressure of the medium and temperature factors provide the necessary calculated optimal shape of the gap, in the end, sealing joint of the pair of rings. The shapes of the sealing surfaces in the end interface should provide the possibility of supplying the friction pair with a lubricant that meets the loading conditions and guarantees the liquid friction mode during operation at nominal mode, as well as acceptable values and high-performance stability.

For a mechanical seal with a hydrostatic loading mode and a liquid friction mode, temperature and force loads on the parts of the unit lead to the formation of radially curved shapes of the sealing surfaces of each of the rings with the closest approach of these surfaces in the end slot near the inner radius of the sealing ring. It is possible to simplify the calculation process, taking the form of a conical sealing gap. Such simplification gives of 10—15% deviations, as studies have shown.

CHAPTER 3

NON-CONTACT MECHANICAL SEALS

3.1. Classification and purpose

The main distinguishing feature of non-contact mechanical seals from mechanical seals is the presence of a guaranteed gap in the end pair during shaft rotation. The specified end clearance during operation is filled with a sealing medium (liquid, gas) or a medium from an external source, which provides lubrication and cooling of the sealing belts of the rings. The presence of a guaranteed clearance allows the rings of the sealing pair to operate practically without the slightest wear in liquid lubrication conditions, which significantly expands the range of non-contact seals in the direction of high sealing pressures and shaft rotation speeds. In this case, a significant increase in the life and reliability of the mechanical seal is achieved; however, due to the appearance of some, in most cases insignificant, leakage through the mechanical pair.

According to the principle of creating a gap, non-contact mechanical seals are divided into the following main types:

- hydrostatic;
- hydrodynamic;
- hydrostatic dynamic (hybrid, mixed);
- impulse.

Unlike contact mechanical seals, whose end pair rings are made with narrow, flat sealing bands, non-contact mechanical seals are designed with significantly wider sealing surfaces. Special pockets, steps, or another form of surface are made on the sealing surface, due to which it is possible to provide the required clearance in the end pair during sealing.

Considering the design features and principles of operation, non-contact mechanical seals are used mainly in high-speed centrifugal machines. Reliable sealing of the rotor, which rotates at a frequency of 10,000 rpm or more, is a com-

plex scientific and technical problem, the successful solution of which often determines the very possibility of creating and further operating such equipment.

Also, non-contact mechanical seals are used in cases where mechanical seals cannot provide the required reliability and service life under difficult operating conditions, whether it be high sliding speeds or high sealing pressures, for example, end seals of the main circulation pumps of nuclear power plants. It follows that efficient and reliable designs of non-contact mechanical seals are often unique and are created as a result of large-scale theoretical and experimental studies.

Also, one of the characteristic distinguishing features in the proposed classification of types and types of mechanical seals is the size of the expected gap in the gap between the sealing surfaces during the operation of the sealing device. According to A.I. Golubev [18], the gaps during the operation of conventional mechanical seals are 0.5—2 μm; for non-contact hydrodynamic seals — more than 2 μm, and for hydrostatic ones — more than 5 μm.

3.2. Hydrostatic mechanical seals

Hydrostatic non-contact mechanical seals include seals in which the static pressure of the fluid being sealed or supplied from an external source is used to create a gap in the friction pair.

The prototype for these seals was hydrostatic thrust bearings, which use the same principle of creating a lubricating film between the end surfaces.

A distinctive feature of hydrostatic thrust bearings from seals is the nominal clearance between the end surfaces and the purpose. Unlike seals, the bearing is designed to absorb loads acting on the machine shaft, while the amount of lubricant flow through the end gap is not critical, so the calculated gap is in the range of 20—40 μm. In hydrostatic mechanical seals, the size of the mechanical clearance is of decisive importance since it determines the amount of leakage through the seal; therefore, when designing the seal, they try to ensure the minimum possible mechanical clearance, which ensures the guaranteed absence of contact between the sealing bands during operation. As a rule, the optimal end clearance for hydrostatic seals is in the range of 5—10 μm.

Depending on the design, hydrostatic mechanical seals are divided into seals:

- with closed chambers;
- with a porous insert;
- with deformable insert;
- with confusor end clearance;
- with a step in the radial direction.

In designs of hydrostatic mechanical seals with chambers or a porous insert, the formation of a bearing force in the lubrication layer of the sealing gap

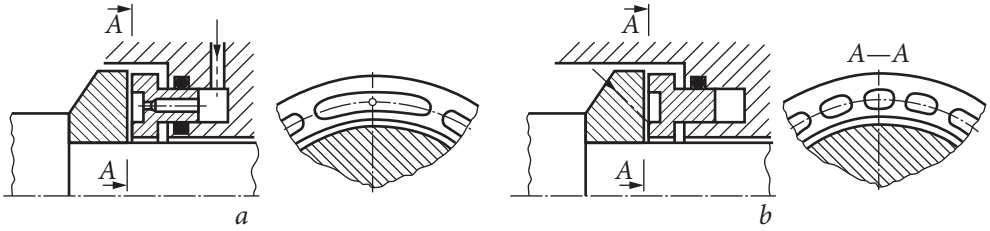

Fig. 3.1. Lubrication schemes for mechanical seals friction pairs: *a* — supply of lubricant from an external source; *b* — supply with lubricant from the sealed cavity

is achieved by supplying a medium from the sealed cavity or from a separate pressure source to the contact zone. The supply channels are throttling devices that determine both the rigidity of the lubricant layer in the gap and the damping properties of the system due to the resistance of the chokes to the flow of the medium through them when the size of the gaps in the sealing gap changes. In such seal designs, chokes are built into the supply channels; usually, these are capillaries (calibrated holes) or porous inserts.

When high-pressure fluid is supplied to the end slot, the gap between the end surfaces is maintained and self-regulated due to the continuity of the medium flow with a flow rate determined by the resistances of the flow path elements. The relationship between the pressure in the lubricant layer and the gap is characterized by the "stiffness" of the layer (changes in the force in the gap from a change in the size of the gap). The rigidity of the layer must increase with a decrease in the gap for stable operation of the seal [45].

In hydrostatic mechanical seals, the loading force that presses the axially movable ring against the counter ring is perceived by the reaction force that occurs in the lubrication layer of the sealing gap. The formation of this reaction is due to the properties inherent in such a layer with a viscous flow in a narrow gap in the radial direction between the walls that limit it from a high-pressure cavity to a low-pressure cavity, as well as the ratio between the resistance characteristics of the lubricant supply channels to the chambers and removal from them.

For hydrostatic mechanical seals with devices for supplying lubrication to the surfaces of a rubbing pair of rings, made in the form of simple chambers or chambers with inserts, lubrication can be supplied in a constant or pulsed supply mode. Mechanical seals with a constant supply mode are usually supplied with lubrication through channels located in the same ring where the chambers are located (Fig. 3.1, *a*).

In mechanical seals with a pulsed power supply, the channels for supplying lubrication to hydrostatic chambers are usually located in one ring, and the chambers themselves are located in another ring of the end pair (Fig. 3.1, *b*). Mechanical hydrostatic seals are used for pressure drops from 5 to 50 MPa.

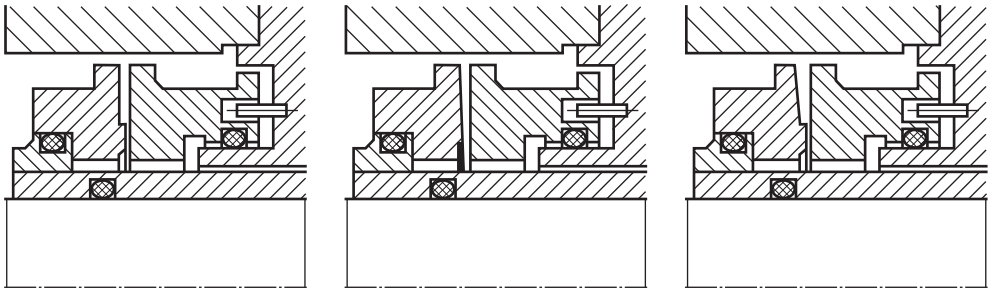

Fig. 3.2. Hydrostatic seals: *a* — with a microstep; *b* — with a bevel; *c* — with bevel and microstep

In hydrostatic mechanical seals with constant lubrication, the channels for supplying lubricant to the sealing surfaces of the rings are usually made in the body or on the surface of the same ring of the end pair in which the chambers or grooves are located.

In hydrostatic seals, the bearing force in the lubrication layer that occurs during seal operation, is practically independent of the shaft speed. This is because the bearing capacity of the lubricating layer is created only by hydrostatic pressure and is not affected by the hydrodynamic forces that occur during rotation. In this regard, the end clearance in such seals is also independent of the shaft speed.

Another feature of hydrostatic seals is that in the absence of shaft rotation (in the parking lot) but with liquid supply under pressure to the friction pair, it opens by the value of the calculated gap and the seal leaks, i.e., does not work as a parking lot.

Another disadvantage of hydrostatic mechanical seals, especially those with a porous insert or capillary, is that such seals are very sensitive to the presence of contaminants in the liquid that is supplied through the supply channels. Channels and porous inserts become clogged with dirt over time and lose their capacity, which leads to a loss of seal performance.

Hydrostatic seals, which have chambers on their working surface, grooves with inserts, steps in the radial direction, confusor, or their combination, are shown in Fig. 3.2.

In this case, the wedge gap is connected to the high-pressure space of the sealed or sealing medium by channels for supplying lubricant. Such designs make it possible to automatically maintain a certain gap between the working surfaces by changing the pressure diagram depending on the change in the value of the axial gap. The seals are simple in design and do not require additional systems. Their disadvantages are the absence of an equalizing moment and in-

creased sensitivity to wear since the step and bevel have dimensions of the order of several tens of micrometers.

For non-contact operation, hydrostatic seals require a certain pressure drop, which creates a guaranteed axial clearance; otherwise, the rings will be in contact and wear during operation.

Hydrostatic mechanical seals with a wedge-shaped sealing joint in the radial direction are effective when the ratio of the gap size at the inlet to the size of the gap between the sealing surfaces at the outlet is not more than 8:1 (the optimal ratio is within 3:1). Therefore, despite the apparent simplicity, the implementation of sealing surfaces of such a shape (with a wedge leg size of up to one or several micrometers) presents certain technological difficulties.

Hydrostatic mechanical seals with a step in the radial direction captivate with the simplicity of their design since technologically obtaining such steps is not difficult.

If in conventional (contact) mechanical seals, the initial phase of the operation of the seal assembly is carried out with direct contact between the sealing surfaces, then in hydrostatic mechanical seals with a constant lubrication regime, the initial phase of the operation of the mechanical seal is possible without contact between the sealing surfaces.

In hydrostatic mechanical seals, the loading force that presses the axially movable ring against the axially stationary one is perceived by the reaction force that occurs in the lubrication layer of the sealing gap. The formation of this reaction is due to the properties inherent in such a layer with a viscous flow in a narrow gap in the radial direction between the walls, limiting it from the cavity with high pressure to the cavity with low pressure, as well as the ratio between the resistance characteristics of the channels for supplying lubricant to the chambers and removing from them. The choke of the inlet and outlet channels is also the sealing gap itself with a flat, stepped, or confused shape.

A combination of two or more chokes is used as slot pressure distribution regulators. Examples of seals with two chokes are designs of mechanical seals with stepped and tapering gaps, where the chokes are the resistances of the inlet and outlet sections of the gap.

When high-pressure fluid is supplied to the end gap, the gap between the end surfaces is maintained and self-regulated due to the continuity of the medium flow with a flow rate determined by the throttle resistances. The relationship between the pressure in the lubricant layer and the gap is characterized by the "stiffness" of the layer (changes in the force in the gap due to a change in the gap size). For stable operation of the seal, it is necessary that the stiffness of the layer increases with a decrease in the gap [45]. Devices with pliable working surfaces deformable under pressure are characterized by high-performance properties:

- increased bearing capacity;
- significant rigidity at small gaps;
- the ability to resist blows;
- less sensitivity to the presence of foreign particles in the lubricant;
- do not demand careful processing of a working surface;
- allow small leaks even with significant deformations of the working surfaces.

Thanks to these advantages, pliable surfaces have also found application in mechanical seals.

The results of experiments on mechanical seals with segmented hydrodynamic grooves showed that the effect of temperature non-uniformity in rings with grooves on the formation of the waviness of the surfaces of rubbing pairs is negligible [44, 47], especially for seals loaded with high pressure. In such seals, part of the rubbing surfaces is washed by the environment and cooled much more intensively than in ordinary seals, which leads to a significant radial temperature unevenness in the body of the ring. This leads to the confusor shape formation of the end joint in a pair of sealing surfaces.

In mechanical seals, in which cooling grooves are made on the sealing surface, the resulting bearing force in the lubricant layer depends more significantly on the shaft speed. It is because, with an increase in the sliding speed in the friction pair and an increase in heat release in the gap, the heat removal from the periphery of the rings also increases due to the supply of lubricant to the sliding surfaces. It leads to an increase in thermal non-uniformity in the height and width of the rings, the confusor gap, and the thickness of the lubricating layer increase.

It should be noted that the characteristic of the grooves on the surfaces of the inner seals is good cooling of a part of the surfaces of the rings from the side of the outer diameter. This contributes to the formation of a confusor shape of the sealing gap in the radial direction and the manifestation of hydrostatic effects. Assumptions that significant differences in temperature characteristics are formed on the surface of the rings between the grooves, which can cause wave-like deformation of the surfaces and the occurrence of hydrodynamic effects, have not been experimentally confirmed [44, 47]. Therefore, such mechanical seals should be classified as hydrostatic.

Under high-pressure differential and rotational speed, when it is required to provide an extended service life and insignificant leaks are allowed seals with a continuous liquid film are used increasingly. They include hydrostatic seals consisting of the same components as conventional mechanical seals. To form a guaranteed gap between sealing surfaces (Fig. 3.3, *a*), closed chambers (*2)* are made on one of them, which are connected through throttles (*3)* to cavity (*1)*. Axial gap size depends on the size of throttles, chambers as well as the force of springs. The throttles are a correcting member and provide self-regulation of the

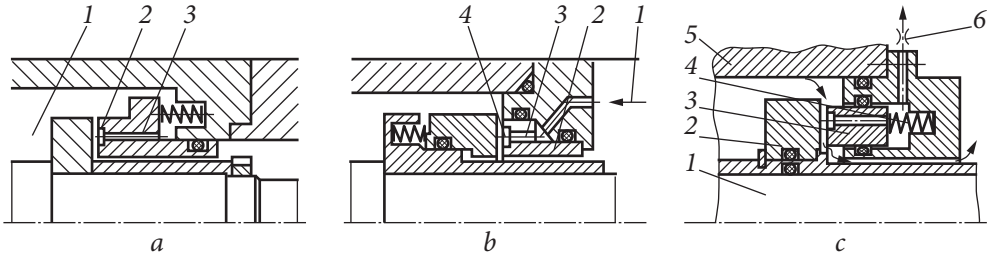

Fig. 3.3. Hydrostatic seals: *a* — with a fixed gap; *b* — with a regulated gap; *c* — with controlled leaks

axial gap. When the gap is reduced, the pressure profile in the opening increases, and when the gap increases, the pressure decreases. To limit leaks through seals and to ensure self-regulation of the axial gap between the sealing surfaces, the throttles should have high hydraulic resistance and, therefore, are made with a very small cross-section (capillary). A significant disadvantage of capillaries is their tendency to the clogging and erosion wear. In such cases, the normal operation of seals is disrupted.

Figure 3.3, *b* shows the design of a hydrostatic seal with a self-regulating axial gap [63], in which hydrostatic pressure from external source (*1)* is used to separate the operating surfaces. Water under high pressure is supplied through capillaries (*3*) to the cavities of chambers (*4)* made on fixed ring (*2)*. Axial gap size depends on the water flow rate through the capillaries. The seal allows separation of the operating surfaces before shaft rotation and also, if necessary, regulation of water supply to seal cavity, changing thereby the axial gap between the operating surfaces. Disadvantages of such a seal include possible damage to the external pressure support system, sensitivity to liquid contamination degree, thermal transients, and changes in the throttle characteristics due to clogging or erosion.

A hydrostatic seal with intermediate pressure extraction (Fig. 3.3, c) manufactured by Hayward Tyler (UK) is of interest. The main seal components are ring (*2)*, which rotates together with shaft (*1)*, and axial component (piston) (*3)*, installed in casing (*5)*. An annular groove connected by channels to the intermediate chamber is made on the operating end surface of the piston. Spring (*4)* ensures the primary contact between ring (*2)* and piston (*3)*. The seal operation principle is based on the fact that the controlled axial gap between the sealing surfaces is automatically maintained by external throttle (*6)*. If the gap increases, the pressure in the chamber behind the piston increases, which causes hydraulic downforce to increase. As the axial gap is reduced, the pressure behind the piston decreases, resulting in a seal opening. Depending on the parameters of the seal and throttle components, the piston is installed in a balanced position under a certain axial gap.

In hydrostatic seals, leaks through the axial gap are almost independent of the relative rotation of the sealing rings and are determined by pressure differential. Therefore, leaks remain the same during stoppage as during pump operation. Thus, it is necessary to install additional stop seals, which makes the design more expensive and complicates operation and repair.

3.3. Hydrodynamic mechanical seals

In hydrodynamic mechanical seals, the surfaces of the sealing joint of rings are designed in such a way that when they move relative to each other, a velocity head is generated in the lubricating layer. The transition of a part of this velocity head into static pressure is the source of the hydrodynamic component of the bearing force in the lubricant layer between the sealing surfaces of mechanical seal rings. Variants of grooves on the mechanical sealing surfaces of hydrodynamic seals are shown in Fig. 3.4.

The formation of a bearing force in the end gap of hydrodynamic mechanical seals due to squeezing the lubricating layer is caused by a change in the size of the gaps between the sealing surfaces in the circumferential direction due to the wedge, stepped or wavy shape of these surfaces under the influence of centrifugal forces.

It is necessary to know the exact values of the elements of the shape of the surfaces to calculate hydrodynamic mechanical seals. Therefore, in the practice of computational design, only those seal designs have found application, the dimensions of the contact surfaces of which can be accurately made and controlled.

For hydrodynamic seals, the contact interface of the sealing end surfaces is assumed only in the absence of rotation of the rotor and in the initial period of its rotation. With the relative displacement of the ring's surfaces of the hydrodynamic seal, rigid feedback is formed between the magnitude of the hydrodynamic force that occurs between the sealing surfaces of the end gap and the dimensions of the gap.

In hydrodynamic mechanical seals, the force that presses the axially movable ring to the axially stationary one is perceived by the reaction force that occurs in the lubricant layer separating these surfaces. The formation of this reaction force is due to the properties inherent in such a layer during viscous flow in a narrow gap between the bounding walls. The shape of the sealing gap due to thermal deformation can significantly depend on the sliding speed in the sealing pair of rings.

When calculating hydrodynamic mechanical seals, the goal is to find such shapes and size ratios of the sealing surfaces of the rings, in which the hydrodynamic rigidity of the liquid lubricant layer for normalized leakage would be maximum [4].

Fig. 3.4. Some typical seal face patterns

Besides the hydrodynamic rigidity of the lubricant layer, the absolute value of the hydrodynamic force is also important. It depends largely on the ratio of the sizes of the sealing surfaces of the rings, which determine the area of action of pressure in the lubricant layer and the leakage of the sealed medium in the radial direction.

For approximate calculations of hydrodynamic mechanical seals, the methods used in the development of hydrodynamic thrust bearings and based on rich experimental data on their research are used [45].

Mechanical hydrodynamic seals are used for pressure drops from 5 to 50 MPa.

Thus, hydrodynamic mechanical seals, according to the method of supply with lubricant, can be divided into the following: hydrodynamic constant supply (with devices for a constant supply of lubrication to chambers made on the surface of one of the rings of the end pair from the sealed space or from a separate source of high pressure); hydrodynamic impulse supply (with channels for the cyclic supply of cavities with lubrication, made on the surface of one of the rings of the end pair from the sealed space or from a separate source of high pressure).

3.3.1. Hydrodynamic mechanical seals with permanent grease supply

Hydrodynamic mechanical seals with a constant supply of lubricant, depending on the combination of the type of channels for supplying lubricant to the friction pair and the shape of the cavities on the surfaces of the contact joint of the pair of rings, can be divided as follows:

- with Rayleigh chambers (Fig. 3.5 — step a or wedge b shape in the circumferential direction);
- with scoop-type spiral grooves (Fig. 3.5, c);
- with discharge grooves (like an impeller);
- with circumferentially wavy sealing surfaces of the rings.

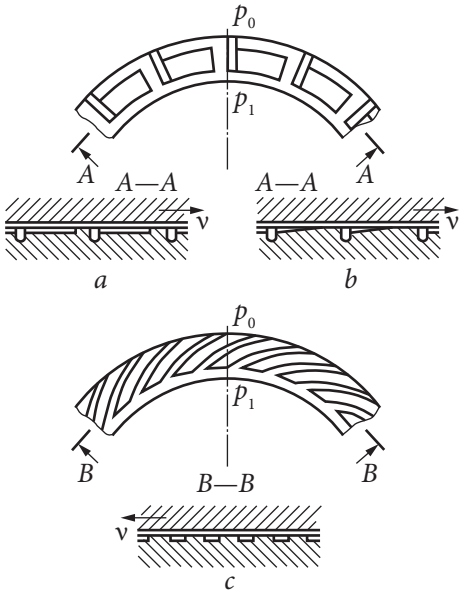

Fig. 3.5. Hydrodynamic type devices for supplying lubrication to the surfaces of a rubbing pair of rings: *a* — supply of lubricant to the flat Rayleigh chambers; *b* — supply of lubricant to the Rayleigh wedge chambers; *c* — lubrication supply by scoop-type spiral grooves; p_0 is the pressure in the seal chamber; p_1 — pressure behind the seal

Consider the designs of hydrodynamic mechanical seals and some information related to their characteristics. A number of Rayleigh chambers stepped in the circumferential direction, made on the surface of one of the mechanical seal rings, contain feeding radial grooves tenths of a millimeter deep, which supply the medium to be sealed, usually into rectangular-shaped cavities several micrometers deep. Rayleigh chambers can be made both with a flat bottom (Fig. 3.5, *a*) and with a wedge-shaped bottom (Fig. 3.5, *b*), while the dimensions of the wedge-shaped and flat bottom steps must be comparable to the working gap between the surfaces formed during the dynamic operation of the seal unit.

The available experience in the development of seals with Rayleigh chambers has shown that the seal works most efficiently with a groove depth that is 22.5 times the end gap [18, 25, 30].

The magnitude of the additional bearing force in the layer of the medium to be sealed from hydrodynamic effects depends largely on the length of the hydrodynamic pockets between the sealing surfaces of the rings, the ratio of the radial extent of the hydrodynamic pockets, and the width of the seal face. In mechanical seals, the width of the seal face of the rings is usually about 0.1 of the average ring diameters. During normal seal operation, the pressure in the pockets exceeds the sealing pressure. However, with an increase in pressure in the hydrodynamic pockets, the medium flows ("lateral" leakage) from the pockets in the radial direction towards the cavities with sealing pressure and low pressure. The nature of this process is determined by the hydraulic resistance of the bridges between the hydrodynamic pockets and these cavities, the values of which depend on the gap between the sealing surfaces of the rings.

The characteristics of mechanical seals with Rayleigh chambers are determined both for support of infinite width by introducing a coefficient that takes into account lateral leakage or by numerical methods [4].

Spiral grooves on the sealing surface of one of the rings (Fig. 3.5, *c*) are made with a constant depth of several micrometers and with such a direction of the inlet part of the grooves that the grooves are scoops. Due to this, the compacted medium enters the groove under the action of pressure drop and rotation, accelerates, and slows down at the end of the groove, creating zones with high hydrodynamic pressure in it [4].

Based on calculations and experimental data obtained during the operation of mechanical seals with spiral grooves, there is an assumption that the maximum rigidity of the medium film in the gap is formed at a depth of the spiral groove equal to three thicknesses of the gap that occurs during the dynamic operation of the seal [25]. Usually, the height of the spiral groove is selected in the range h = 7—10 μm with the load factor of the end pair k = 0.8—0.85. The edges of the grooves must be sharp.

According to A.I. Golubev [18], a mechanical seal with spiral grooves can operate stably in a non-contact mode, even at low shaft speeds. For this, a depth of 3 μm spiral grooves is sufficient.

Leading foreign companies specializing in the production of such seals have developed several technical solutions: John Crane branched spiral grooves, EagleBurgmann opposite grooves, and Pacific double-sided Rayleigh chambers.

A comparison of the efficiency of helical, double-sided wedge-shaped grooves and Rayleigh chambers showed that the largest load-bearing force is generated in the helical grooves. Bilateral wedge-shaped grooves generate a bearing force of 30—50% less than spiral grooves, but they are operable in any direction of rotor rotation. At the same time, double-sided wedge-shaped grooves have a higher bearing capacity than seals with double-sided constant-depth grooves [11].

The waviness of the sealing surfaces can also be the cause of the occurrence of hydrodynamic forces in the friction pair. However, when operating seals with this type of sealing surface, a significant increase in leakage is observed.

To evaluate the hydrodynamic effect in friction pairs with wavy surfaces, some works [11, 25] proposed calculation dependencies that make it possible to determine the bearing force and leakage in the seal with known characteristics of the surface shapes. These dependencies are based on the condition of liquid layer discontinuity due to cavitation in the expanding parts of the gap. This approach is not implemented for seals where cavitation on the high-pressure side is suppressed [18].

3.3.2. Thermohydrodynamic mechanical seals

As mentioned above, a feature of such seals (Fig. 3.6, *a*) is crescent-shaped grooves on one of the contact surfaces. These seals are characterized by the fact

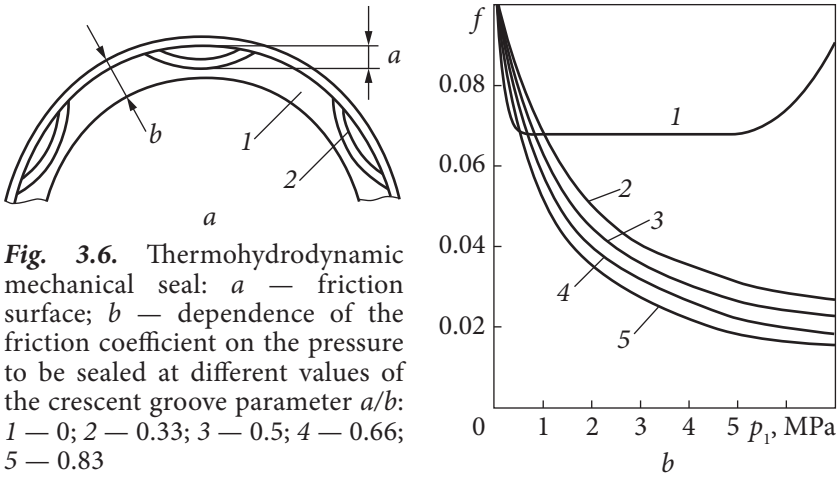

Fig. 3.6. Thermohydrodynamic mechanical seal: *a* — friction surface; *b* — dependence of the friction coefficient on the pressure to be sealed at different values of the crescent groove parameter *a*/*b*: *1* — 0; *2* — 0.33; *3* — 0.5; *4* — 0.66; *5* — 0.83

that the coefficient of friction in them decreases with increasing sealing pressure (Fig. 3.6, *b*) and circumferential speed. This is explained by the fact that in the zone of the grooves, the cooling conditions are better than in the areas of the contact surface remote from them [53].

The advantage of these seals is that as the sliding speed and pressure differential increase, the temperature difference between certain sections of the operating surface increases. Under the impact of high thermal stress and deformations it causes, the zones with micro-wedges expand, lifting forces increase, and the friction coefficient in the operating gap decreases. During a stoppage, a thermohydrodynamic seal provides full tightness, as there are no surface deformations caused by additional thermal stress.

Thermohydrodynamic seals have the ability to self-regulate frictional power losses: an increase in contact pressure leads to an increase in temperature effects, which reduce the steady value of power losses. Unfortunately, the feedback on the temperature of the friction pair is relatively weak and cannot be predicted. Therefore, the successes achieved in the field of thermohydrodynamic seals are based on practical experience and engineering searches for optimal designs [32].

3.3.3. Hydrodynamic mechanical seals with microwaviness in circumferential direction

The waviness of the sealing surfaces can also be the cause of the occurrence of hydrodynamic forces in the friction pair. However, when operating seals with this type of sealing surfaces, a significant increase in leakage is observed.

To assess the hydrodynamic effect in friction pairs with wavy surfaces, several works [1, 3] proposed calculation dependencies that make it possible to

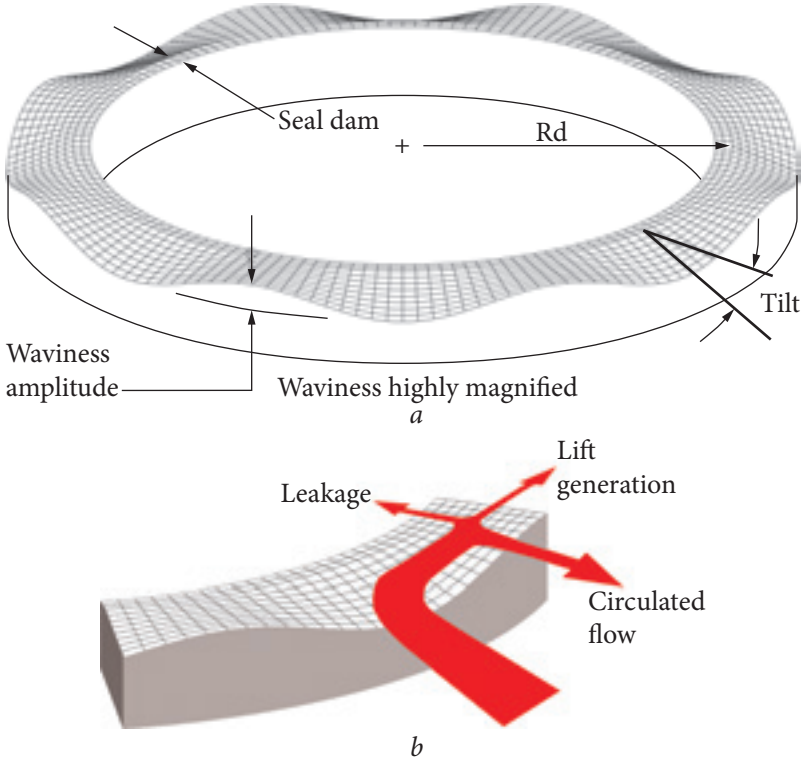

Fig. 3.7. Wavy shape of the sealing band surface: [31] *a* — wavy face geometry, *b* — recirculation effect of Wavy Technology

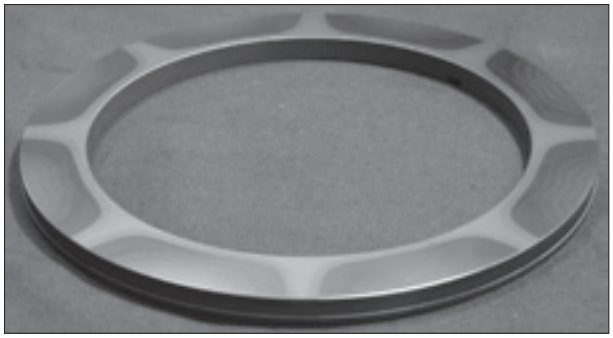

Fig. 3.8. Laser processing of the sealing surface [31]

determine the bearing force and leakage in the seal with known characteristics of the surface shapes. These dependencies are based on the condition of liquid layer discontinuity due to cavitation in the expanding parts of the gap. This approach is not implemented for seals where cavitation on the high-pressure side is suppressed [1].

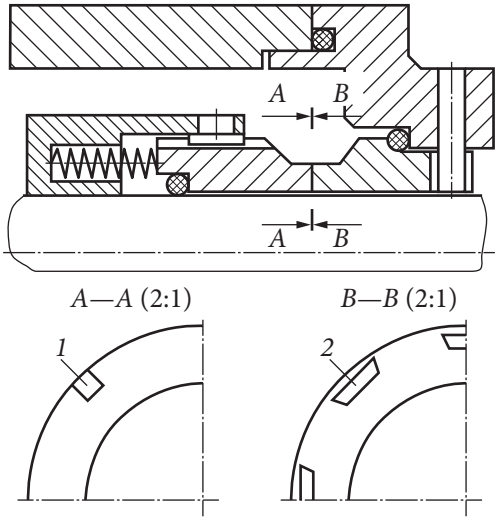

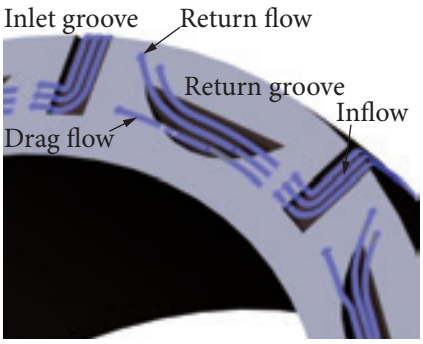

Fig. 3.10. LaserFace™ grooves with assumed flux vectors [22].

◀ ***Fig. 3.9.*** Forms of lubrication grooves on the sealing surfaces of the rings: *1* — rectangular; *2* — segmented

Flowserve manufactures mechanical seals with rings that have a wavy surface on the sealing collar, which is created using laser heating of certain areas [31] (Fig. 3.7).

As a result of residual deformations after laser processing, "hills" and "hollows" remain on the outer surface of the end girdle, evenly distributed along the circumference, and the inner part of the girdle remains flat (Fig. 3.8).

The experience of research and application of such seals shows that the specified technology of creating hydrodynamic wedges, due to the waviness, ensures reliable operation of seals in difficult operating conditions with minimal wear and leakage.

3.3.4. Hydrodynamic mechanical seals with LaserFace backflow structures

LaserFace seals were first proposed in 1997 by Mueller H. [49]. Grooves are made up to several micrometers deep. The shape of the grooves can be very diverse (Fig. 3.9) [49].

With the help of grooves open from the high-pressure side, the medium to be sealed is brought to a part of the surface of the friction pair [22] (Fig. 3.10).

This medium, entered into the grooves, when sliding one surface over another, enters the gap between these sealing surfaces and (due to the constant renewal of the volumes of the medium in the grooves) cools the sealing surfaces of the rings.

Fig. 3.11 shows the comparative characteristics of mechanical seals with traditional surface technology, with hydrodynamic grooves, and with LaserFace™ surface technology obtained as a result of experimental studies [22].

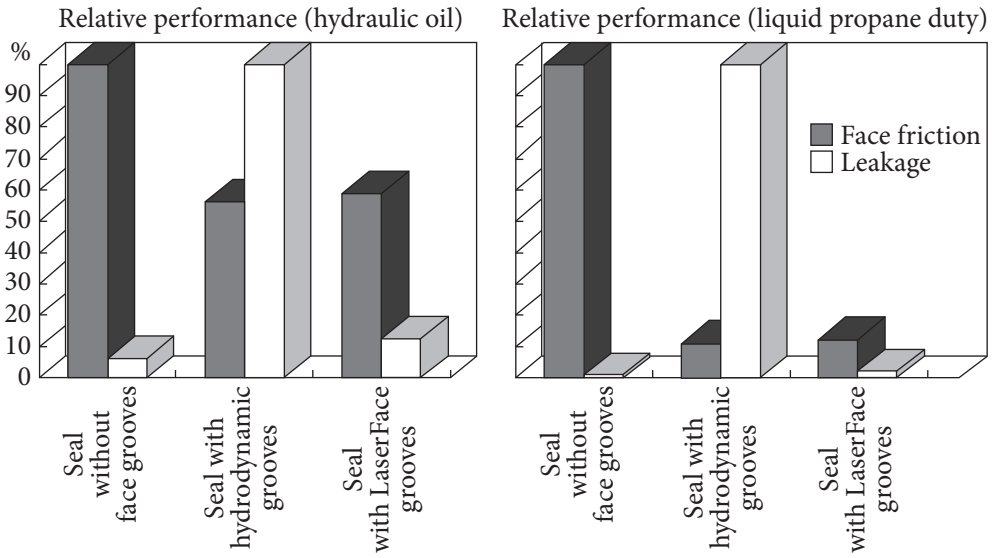

Fig. 3.11. Comparison of mechanical seals performance with different types of surfaces [22]

The shape of the grooves' influence on the quality of cooling is insignificant; rather, this effect is significant for power losses due to fluid friction associated with the nature of the flow around the grooves involved in the process of medium flows.

Since the beginning of the 21st century, John Crane has been widely using LaserFace rings in feed pump seals, which has extended their range of application towards high temperatures and sliding speeds and significantly reduced power losses [22].

3.4. Impulse mechanical seals

An impulse mechanical seal belongs to non-contact seals with self-adjusting clearance; as an alternative to hydrostatic and hydrodynamic non-contact mechanical seals, it was invented during the creation of rotor seals of the main circulation pumps for nuclear power plants [37]. Comprehensive experimental studies and full-scale tests have shown that impulse seals meet the stringent requirements for reliability, tightness, and resource life required for the main equipment of nuclear power plants [63]. Due to their high-performance characteristics, impulse mechanical seals have attracted the attention of developers of high-speed centrifugal machines for other industries and for fuel pumps of liquid-propellant rocket engines (LREs) in particular [39, 40]. Impulse seals were also the prototype of promising gate mechanical seals with a coaxial arrangement of steps.

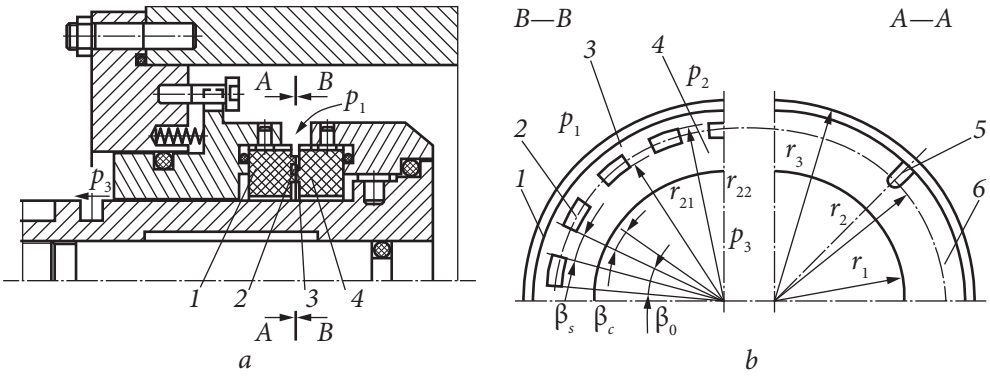

Fig. 3.12. The diagram of an impulse mechanical seal

Impulse mechanical seals with self-adjusting clearance have a number of undeniable advantages compared to conventional mechanical seals and non-contact mechanical seals of hydrostatic and hydrodynamic types. In conventional mechanical seals, the friction power is proportional to the sealing pressure and the peripheral speed; therefore, their operability is preserved only in a narrow, calculated range of operating parameters — the sealing pressure and the rotation speed. In impulse seals, an increase in the rotation frequency results in a larger end clearance, and the friction power losses practically do not increase, thus making their use especially effective for high-speed machines. Low friction power losses and good heat dissipation with leakage from the friction pair make it sometimes possible to do without additional cooling systems even in pumps running on hot liquids, for example, in feed pumps of nuclear and thermal power plants.

With the proper choice of the basic geometric parameters of the friction pair of an impulse seal, it is possible to ensure the optimal value of the end clearance, the required leakage, and power loss in the friction pair in a wide range of sealing pressures and rotor speeds. Therefore, the development of methods for calculating impulse mechanical seals based on a study of their working processes is relevant.

The simplest design of a single-stage impulse compaction unit is shown in Fig. 3.12. An impulse seal differs from a mechanical seal in the following design features. Closed chambers (*2)* are located on the end surface of the axial-movable ring (*1)*, and several radial feed channels (*5)* are made on the rotating support ring (*6)* and are open towards the cavity to be sealed.

Through these channels, the medium to be sealed is injected into the chambers under a sealing pressure p_1 for those short periods of time $t_c = \beta_c / \omega$, during which the rotating channels (*5)* pass by chambers (*2)*. At these moments, the pressure p_2 in the chambers increases abruptly to $p_{2\max} = p_1$ minus the inertial pres-

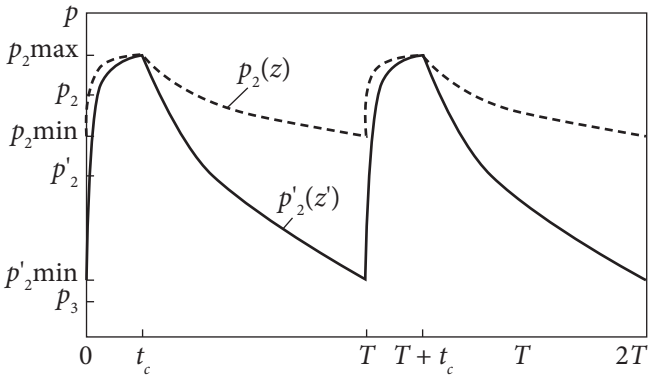

Fig. 3.13. The change in pressure in the chamber during the period T between injections

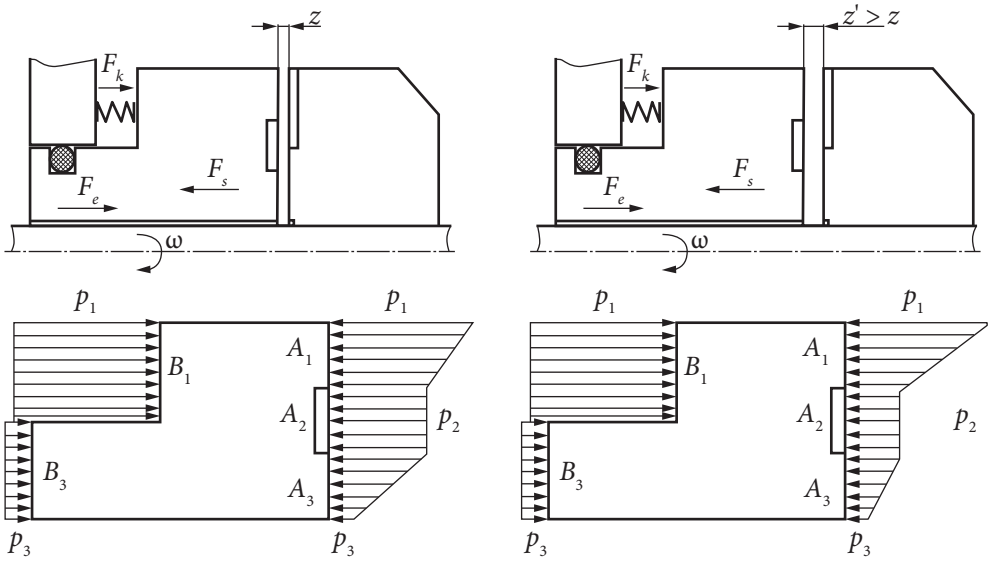

Fig. 3.14. The change in pressure on the end surfaces of the axially movable ring, depending on the end clearance: z` > z

sure $p_* = 0.5\rho\left(r_3^2 - r_2^2\right)\omega^2$ that occurs in the rotating radial feeding channels. By changing the shape of the feeders, it is possible to slightly change the value of p^* and, thereby, the value of $p_{2\max} = p_1 - p_*$. The inertial pressure can be eliminated completely by placing the feeders on a non-rotating ring and the chambers on a rotating ring. The inertial pressure influence on the seal characteristics will be ignored.

Let us consider the nature of the change in pressure in the chamber over a period of $T = 2\pi/\omega n_i$ (n_i is the number of feeders) between two subsequent injections. The change in pressure depends on the hydraulic resistance g_1 of the

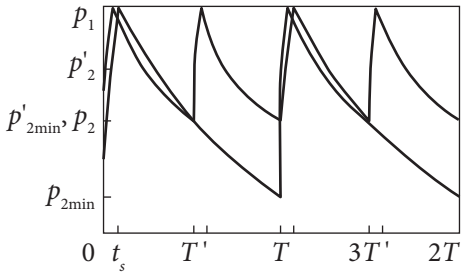

Fig. 3.15. The influence of the period T on the average pressure in the chambers: $T^* = 0.5T$

feeders and the conductivities of the internal (from the side of the pressurized pressure) (*3)* and the external (*4)* end clearance throttles $g_1(z)$ and $g_3(z)$.

Fig. 3.13 [71] shows approximate graphs of pressure changes in a separate chamber. The larger the gap, the smaller the $p_{2\min}$.

A similar picture takes place during the expansion process when the feeder is located outside sector β_c at the time interval $T - t_c$.

After the feeder leaves sector β_c occupied by the chamber, the pressure p_2 in the chamber begins to decrease due to leakage of the compressed medium through the external flat gap *(4)*; A_1, A_3 are the wall areas of the flat annular gaps (Fig. 3.14).

The pressure drop continues until the next injection (Fig. 3.13), and the drop depth, i.e., the value of $p_{2\min}$, depends on the size of the end clearance: the larger the gap, the smaller the $p_{2\min}$. Another possible combination of parameters is when the pressure reaches the minimum of p_3 in the time of $t < T = 2\pi/\omega n_i$. With a decrease in the gap, the amplitude of the pressure changes in the chamber decreases, and the average pressure increases.

Sometimes, a radial purge channel is made on the outer belt A_3. It increases leakage, so it can be used if there are no strict restrictions on the amount of leakage and the medium to be sealed contains solids. At the moment the purge channel passes through the chamber, the pressure in it abruptly decreases, and the outflowing jet carries away the solid particles that have entered the chamber through the internal feeder.

The shorter the time between injections, the smaller the depth of the pressure drop $p_{2\min}$ in the chambers (Fig. 3.15), the greater the averaged pressure p_2 in the chambers, and the greater the force F_s that opens the butt joint.

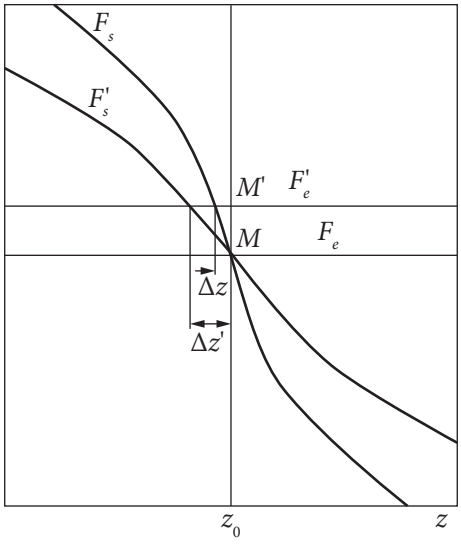

Fig. 3.16. Effect of curve steepness on static deflection under external load

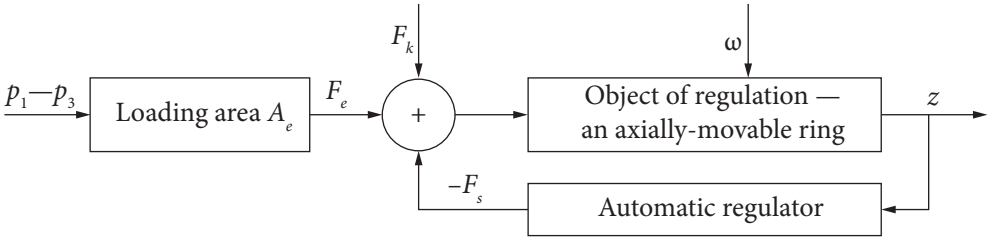

Fig. 3.17. The model of impulse seal as the automatic control system: z — end gap (adjustable); F_s — pressure force opening the butt joint; F_e — external force (regulating influence); F_k — the force of elastic elements; p_1— sealing pressure; p_3 — back pressure; ω — rotor speed

The pressure force $F_s(z)$ revealing the end joint depends on the pressure $\overline{p}_2(z)$ and, accordingly, on the gap. As the gap decreases, the pressure force increases and its balance with the external force F_e independent of the gap is violated (Fig. 3.16).

Under the action on an axially movable ring of the positive difference $F_s - F_e > 0$, the gap decreases (Δz) so that the equality $F_s = F_e$ is restored. The steeper the dependence falls, the less the new equilibrium position M' deviates from the initial position M.

Thus, there is negative feedback between the end clearance z (adjustable value) and the force F_s (regulatory effect), which ensures self-regulation of the end clearance. The seal operation is based on the creation of high-frequency pressure pulses in the discharge chambers; therefore, it is called an impulse seal.

The model of a non-contact mechanical seal, as a system for automatic control of the mechanical clearance and leakage, on the example of impulse compaction [60] is shown in Fig. 3.17.

3.4.1. Research on the influence of pulse compaction parameters on static characteristics

To estimate the pressure in the chambers, we will consider the radial flow of a viscous compressible fluid in a flat channel having the form of a sector with a central angle β_c and a radial size of r_3–r_1 formed by elements of the sealing surfaces and separated by a flow chamber (Fig. 3.12). The right wall of the gap on which the feeders are located rotates; the left wall has freedom of axial movement within the micron-size mechanical gap. The circumferential component of the flow is not taken into account. The flow in the channels is unsteady. The feeder, passing over time t_c=β_c/ω through the chamber filled with liquid, spasmodically brings pressure p_1 to it. As a result, the pressure rises to the maximum value of p_1, compressing the liquid in the chamber. After the feeder leaves the

sector β_c, the volume of the liquid compressed in the chamber flows out, and the pressure decreases to the initial minimum value. The expansion process takes place during the time $T–t_c$. After this, compression begins again, and the process repeats (Fig. 3.15). During compression, the difference in the volumes of the liquid flowing in through the feeder and the internal end throttle $\left(Q_i + Q_1\right)dt$ and flowing out $\left(Q_3 dt\right)$ through the outer throttle is compensated by the volume filling the volume $-dV$ freed up as a result of the compression of the liquid in the chamber:

$$\left(Q_i + Q_1\right)dt - Q_3 dt = -dV. \tag{3.1}$$

In the process of expansion, the volume of the outflowing fluid $\left(Q_3 dt\right)$ is greater than the volume of the inflowing fluid $\left(Q_1 dt\right)$ by the amount of dV with the opposite sign:

$$Q_3 dt - Q_1 dt = dV. \tag{3.2}$$

Equation (3.1) differs from (3.2) only in the flow rate through the feeder and in the initial condition: the compression starts from the minimum pressure, and the expansion starts from the maximum.

The bulk modulus of the fluid is

$$E = -V_0 \frac{dp}{dV},$$

where $dV = V - V_0$ is the difference between the final V and initial V_0 volumes of the fluid, V_0 is the unchanged volume of the chamber, E is the isothermal volumetric modulus of elasticity of the fluid, Q_i is the flow rate through the feeder, and Q_1, Q_3 are the flow rates through the internal and external end throttles of the sector β_c.

For a laminar flow, the costs linearly depend on the pressure drops:

$$Q_i = g_i\left(p_1 - p\right),\ Q_1 = g_1\left(p_1 - p\right),\ Q_3 = g_3\left(p - p_3\right). \tag{3.3}$$

The conductivities of the mechanical throttles for laminar flows are proportional to the cube of the gap z [32] and are expressed by the formulas:

$$g_1 = g_{1n}u^3,\ g_3 = g_{3n}u^3,\ \ u = z/z_n,$$

$$g_{1n} = \frac{\beta_{\tilde{n}} z_n^3}{12\mu \ln\left(r_3/r_{22}\right)} \approx \frac{\beta_{\tilde{n}} z_n^3 r_3}{12\mu l_1},\ \ l_1 = r_3 - r_{22},$$

$$g_{3n} = \frac{\beta_{\tilde{n}} z_{\tilde{n}\ n}^3}{12\mu \ln\left(r_{21}/r_1\right)} \approx \frac{\beta\ z^3 r_{21}}{12\mu l_3},\ \ l_3 = r_{21} - r_1,$$

z_n =(2…6) μm is the nominal end clearance adopted for this design, $u = z/z_n$ is the dimensionless current gap, and μ is the dynamic viscosity of the fluid being compacted.

Substituting the expressions of expenditures in (3.1) and (3.2) and dividing both sides of the equalities by *dt*, we obtain the equations of volume expenditures balance. On the time intervals of compression $\left(0 \le t \le t_c\right)$ and expansion $\left(t_c \le t_* \le T - t_c\right)$ relative to the current pressure p_c, p_p in the chamber, we obtain inhomogeneous first-order differential equations

$$\frac{V_0}{E}\frac{dp_c}{dt} = g_i\left(p_1 - p_c\right) + g_1\left(p_1 - p_c\right) - g_3\left(p_c - p_3\right),$$

$$\frac{V_0}{E}\frac{dp_p}{dt_*} = g_1\left(p_1 - p_p\right) - g_3\left(p_p - p_3\right), \tag{3.4}$$

$$\left(t_* = t - t_c\right).$$

After some transformations, the equations of pressure growth during compression and pressure drop during expansion in the chamber take the following form:

$$T_c\frac{dp_c}{dt} + p_c = \frac{1}{G}\left[\left(1 + \alpha_{1i}u^3\right)p_1 + \alpha_{3i}u^3 p_3\right] = G_c,$$

$$T_p\frac{dp_p}{dt_*} + p_p = \alpha_{e3}p_1 + \alpha_{e1}p_3 = G_p, \tag{3.5}$$

where the constants of the time of filling and emptying the chamber, weight coefficients, dimensionless pressure, and conductivity are expressed by the formulas:

$$T_c = \frac{\overline{T}_c}{G\left(u\right)},\ \overline{T}_c = \frac{V_0}{Eg_i},\ G\left(u\right) = 1 + \left(\alpha_{1i} + \alpha_{3i}\right)u^3;\ T_p = \frac{\overline{T}_p}{u^3},\ \overline{T}_p = \frac{V_0\alpha_{e3}}{Eg_{1n}},$$

$$G_c = \frac{1}{G}\left[\left(1 + \alpha_{1i}u^3\right)p_1 + \alpha_{3i}u^3 p_3\right],\ G_p = \alpha_{e3}p_1 + \alpha_{e1}p_3,$$

$$\alpha_{e3} = \frac{g_{en}}{g_{3n}},\ \alpha_{e1} = \frac{g_{en}}{g_{1n}} = 1 - \alpha_{e3},$$

$$\alpha_{1i} = \frac{g_{1n}}{g_i},\ \alpha_{3i} = \frac{g_{3n}}{g_i},\ \alpha_{31} = \frac{g_{3n}}{g_{1n}};\ g_{en} = \frac{g_{1n}g_{3n}}{g_{1n} + g_{3n}},\ g_e = g_{en}u^3.$$

The sealing pressure p_1 and the back pressure p_3 are constant in time; therefore, introducing substitutions

$$p_c = p'_c + G_c,\ p_p = p'_p + G_p \tag{3.6}$$

we arrive at the homogeneous equations

$$T_c \frac{dp'_c}{dt} + p'_c = 0,\ T_p \frac{dp'_p}{dt} + p'_p = 0. \tag{3.7}$$

The initial conditions necessary for solving equations (3.5) are determined based on the approximate graphs of the pressure change in the chamber during the periods of compression and expansion (Fig. 3.13). The end of compression means that $p_c \approx G_c$ and at the end of expansion means that $p_p \approx G_p$. Using these limit values, we obtain

$$p_c(0) \approx G_p,\ \ p_p(0) = p_c(t_c) \approx G_c.$$

To find a solution to the equations of (3.7), we will use the operational method. Let us denote the Laplace image of the desired pressure as $p'_c(t) \doteqdot P'_c(s)$ and the image of the derivative will be $\frac{dp'_c}{dt} \doteqdot P'_c(s) - p'_c(0)$. Substituting these expressions in the first equation of (3.7), we arrive at an algebraic equation for the image

$$(T_c s + 1)P'_c(s) - T_c p'_c(0) = 0,$$

where the pressure image is

$$P'_c(s) = \frac{T_c p'_c(0)}{T_c s + 1}.$$

Using the tables of inverse Laplace transforms, we obtain the original pressure as

$$p'_c = p'_c(0) e^{-\frac{t}{T_c}}. \tag{3.8}$$

Taking into account (3.6) and the initial conditions, we finally have

$$p_c = G_c - (G_c - G_p) e^{-\frac{t}{T_c}}. \tag{3.9}$$

In Fig. 3.18, the transient response of the compression is represented by the exponent in the time interval of $t \le t_c$. The characteristic asymptotically approaches the horizontal line of G_c = const, and the time constant T_c is numerically equal to the length of the tangent at the asymptote G_c = const. If we do not take into account the compressibility of the medium being compressed ($E \to \infty$), then $T_c = 0$, $p_c = G_c$, the pressure remains constant, and its value is determined

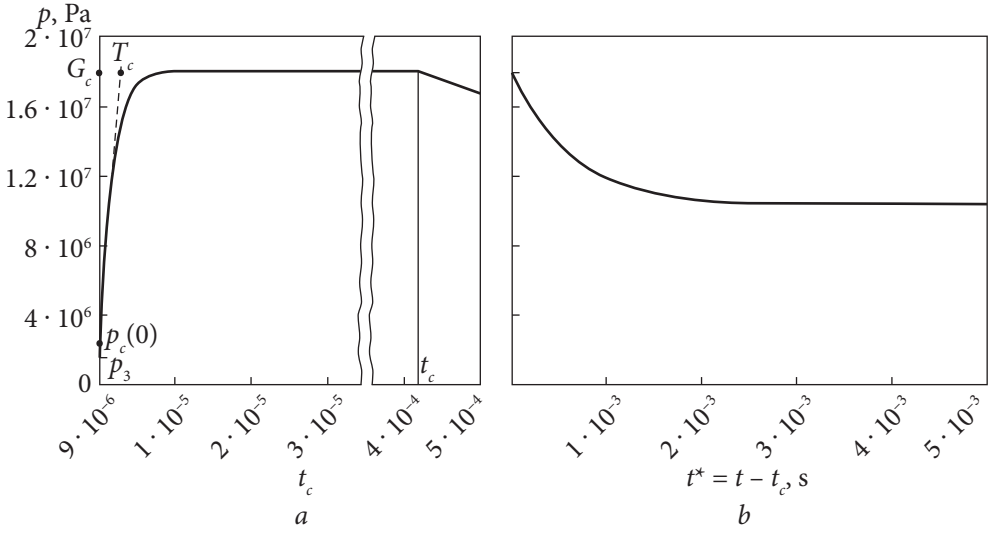

Fig. 3.18. The change in pressure in the chamber on the segments: *a* — compression ($0 \le t \le t_c$); *b* — extensions ($t_c < t \le T$)

by the ratio of the conductivities of the end throttles g_1, g_3 and feeders g_i with unlimited growth of g_i, $\alpha_{1i} \approx \alpha_{3i} \approx 0$, $p_c \approx p_1$.

Static characteristics are the dependencies of the steady-state values of the end clearance on the steady-state pressures p_1, p_3 and the rotor speed ω. The current values of the compression and expansion pressures must be replaced by the values averaged over a period T to determine them.

The average pressure p_{2c} in the chamber over the compression time t_c is

$$p_{2c} = \frac{1}{t_c}\int_0^{t_c} p_c dt = G_c - \left(G_c - G_p\right)\frac{T_c}{t_c}\left(1 - e^{-\frac{t_c}{T_c}}\right).$$

The curve $p_c(t)$ in section $0 < t < T_c$ practically merges with the ordinate axis, and in section $T_c < t < t_c$, the same happens with the horizontal line $G_c \approx p_1$. Thus, as a first approximation, the average pressure in the chamber during the compression period can be taken as equal to the compaction pressure of $p_{2c} \approx p_1$.

The expansion process is described by the second equation (3.5), the solution of which is similar to (3.8):

$$p'_p = p'_p\left(0_*\right)e^{-\frac{t_*}{T_p}}. \qquad (3.10)$$

The expansion begins at the moment the feeder leaves the sector in which the chamber is located, i.e., at the moment t_c when $t_* = 0$. The current time in

the expansion section is $t_* = t - t_c$. According to the formulae, (3.6) and (3.10) are similar to (3.9):

$$p_p(t_*) = G_p - (G_p - G_c)e^{-\frac{t_*}{T_p}}.$$

For incompressible fluids, $T_c = T_p = 0$ $p_p = G_p$ = const.

The average pressure p_{2p} over the expansion time $T - t_c$ in the chamber is

$$p_{2p} = \frac{1}{T - t_c}\int_0^{T-t_c} p_p dt_* = G_p - (G_p - G_c)\frac{T_p}{(T - t_c)}\left[1 - \exp\left(-\frac{T - t_c}{T_p}\right)\right].$$

As seen in Fig. 3.18, the expansion pressure curve $p_p(t)$ asymptotically approaches the horizontal line o $G_p = \alpha_{e3}p_1 + \alpha_{e1}p_3$ and differs little from the averaged pressure p_{2c}.

Based on the found expressions of the average pressure on the temporary segments of compression and expansion, we will determine the total average pressure over the entire period T between successive injections:

$$p_2 = \frac{1}{T}\left[p_{2c}t_c + p_{2p}(T - t_c)\right]. \tag{3.11}$$

The compression pressure distributed over the entire period is included in (11) with a small factor of t_c/T; the expansion pressure has a factor of $(T - t_c)/T$ close to one. Thus, the main contribution to the averaged pressure is made by the expansion process. Therefore, the existing calculation methods [3, 4] do not take into account the pressure p_{2c}.

After a number of simplifications [60], we will obtain the following formula for calculating the dimensionless value of the averaged pressure in the chambers:

$$\psi_2(u) \approx \alpha_{e3}\psi_1 + \alpha_{e1}\psi_3 + \alpha_{e1} \cdot \frac{t_{cn}/\Omega - \overline{T}_c + \overline{T}_p/u^3}{T_n}\Omega\Delta\psi, \tag{3.12}$$

where the first two summands represent the pressure in the gap without feeders, the last two summands with the factors T_p, T_c are the average pressures during expansion and contraction of the liquid in the chamber. The main contribution to the value of $\psi_2(u)$ is made by the addendum $\alpha_{e3}\psi_1$.

Using the linear pressure plots shown in Fig. 3.14, let us calculate the forces included in the equations of axial equilibrium. The regulatory action is the pressure force F_s on the contact surface, revealing the mechanical gap. The pressure force F_c pressing the ring against the support disk is an external load, and the driving force is the force F_k of the elastic elements.

$$F_s = 0.5\left(p_1 + p_2\right)A_1 + p_2A_2 + 0.5\left(p_2 + p_3\right)A_3 = F_{s0} + Ap_2\left(u\right),$$

$$F_{s0} = 0.5\left(A_1p_1 + A_3p_3\right), \tag{3.13}$$

$$A_1 = \pi\left(r_3^2 - r_{22}^2\right),\ A_2 = \pi\left(r_{22}^2 - r_{21}^2\right),\ A_3 = \pi\left(r_{21}^2 - r_1^2\right),$$

$A = 0.5\left(A_1 + 2A_2 + A_3\right)$ is the contact area effective with respect to the average pressure in the chamber p_2.

$$F_e = B_1p_1 + B_3p_3,\ F_k = k\left(\Delta + z\right),$$

$$B_1 = \pi\left(r_3^2 - r_4^2\right),\ B_3 = \pi\left(r_4^2 - r_1^2\right). \tag{3.14}$$

The pressure force component F_{s0} in the gap and the pressing pressure force F_e do not depend on the size of the mechanical gap. The equation of axial equilibrium $F_s = F_e + F_k$, taking into account the fact that the end clearance is negligible in comparison with the preliminary deformation of elastic elements $z << \Delta$, after substituting forces in (3.13) and (3.14), it is reduced to

$$Ap_2 = -0.5\left(A_1p_1 + A_3p_3\right) + B_1p_1 + B_3p_3 + k\Delta, \tag{3.15}$$

where k is the reduced coefficient of axial stiffness of the elastic elements. We will divide this equality term by Ap_n and move on to dimensionless forces by introducing the following notation:

$$\chi = F_k/Ap_n = k\left(\Delta + z\right)/Ap \ \approx k\Delta/Ap\ ,$$

$$\phi_e = F_e/Ap_n = \frac{1}{A}\left(B_1\psi_1 + B_3\psi_3\right), \tag{3.16}$$

$$\phi_s = \frac{F_s}{Ap_n} = \phi_{s0} + \psi_2\left(u\right),\ \phi_{s0} = \frac{F_{s0}}{Ap_n} = \frac{1}{2A}\left(A_1\psi_1 + A_3\psi_3\right),$$

where p_n is the nominal pressure of the liquid being sealed at the inlet. As a result, from (3.15) we obtain the equilibrium equation of a dimensionless form:

$$\phi_s = \phi_{s0} + \psi_2 = \phi_e + \chi$$

or

$$\psi_2\left(u\right) = -\phi_{s0} + \phi_e + \chi. \tag{3.17}$$

Given (3.16), we will represent the latter equality in the form of

$$\psi_2(u) = \frac{B_1 - 0{,}5A_1}{A}\psi_1 + \frac{B_3 - 0{,}5A_3}{A}\psi_3 + \chi.$$

We will introduce the notation of the dimensionless areas K and σ and reveal the difference of $\phi_e - \phi_{s0}$:

$$K = \left(B_1 - 0.5A_1\right)/A,\ \sigma = \left(B_3 - 0.5A_3\right)/A = 1 - K,$$
$$\phi_e - \phi_{s0} = K\psi_1 + \left(1 - K\right)\psi_3. \tag{3.18}$$

In this case, equation (3.17) of the axial equilibrium of the axially movable ring takes the form

$$\psi_2(u) = K\psi_1 + \left(1 - K\right)\psi_3 + \chi,$$

where $\psi_2(u)$ is also determined by formula (3.12). From the joint solution of the equations of the balance of expenses and the equation of axial equilibrium of the axially movable ring, we will express the dependence of the gap on external perturbations ψ_1, ψ_3, Ω and the driving action χ as

$$K\Delta\psi + \psi_3 + \chi = \alpha_{e3}\psi_1 + \alpha_{e1}\psi_3 + \alpha_{e1} \cdot \frac{t_{cn}/\Omega - \overline{T}_c + \overline{T}_p/u^3}{T_n}\Omega\Delta\psi.$$

After grouping the terms, we will find the dependence of the end clearance on the compacting pressure drop, on the rotor speed, and on the pre-compression force of the elastic elements, i.e., we will find the desired static characteristic:

$$u = \left\{ \frac{\alpha_{e1}\dfrac{\overline{T}_p}{T_n}\Omega}{\dfrac{\chi}{\Delta\psi} + K - \alpha_{e3} - \alpha_{e1}\dfrac{t_{cn} - \overline{T}\Omega_c}{T_n}} \right\}^{1/3}. \tag{3.19}$$

The analysis of the static characteristics revealed the influence of the pulse compaction design parameters on the size of the end clearance. It can be seen from formula (3.19) that an increase in the parameters of $\Delta\psi, \Omega, \overline{T}_p, n_i$, as well as a decrease in $K, \chi, \overline{T}_c, z_n$, leads to an increase in the steady-state value of the end gap.

3.4.2. Identification of factors affecting the dynamic characteristics of the seal

Let us consider the axial vibrations of the ring, excited by harmonically changing external influences ψ_1, ψ_3, relative to the equilibrium position. In centrifugal machines, as a rule, the sealing pressure and the back pressure change with

a frequency equal to or a multiple of the rotational speed. The maximum amplitudes have fundamental harmonics with the frequency ω; therefore, the forced oscillations of the ring relative to the position of static equilibrium u_0 will be considered under the influence of dimensionless pressures:

$$u = u_0 + u_a e^{i\omega t},\ \psi_1 = \psi_{10} + \psi_{1a} e^{i\omega t},\ \psi_3 = \psi_{30} + \psi_{3a} e^{i\omega t}, \tag{3.20}$$

where ψ_{10}, ψ_{30} are the constant components of the pressures; ψ_{1a}, ψ_{3a} are the amplitudes of their oscillations; u_a is the amplitude of the axial oscillations of the ring. The rotation frequency and the setting action change quasi-statically, so they only affect the steady-state position of the ring.

In dynamics, the axial vibrations of the ring lead to the appearance of additional flow components. The period of change of these terms is $2\pi/\omega$, and it differs from the periods t_c and $T - t_c$ of the compression and expansion rates caused by pressure pulses supplied to the chamber by the feeders. To facilitate further consideration of these terms in the generalized equation of the balance of expenses, we will consider in more detail the transformation of equations (3.4):

$$Q_i + Q_1 - Q_3 = \frac{V_0}{E}\left(\frac{dp}{dt}\right)_c,\quad Q_1 - Q_3 = \frac{V_0}{E}\left(\frac{dp}{dt}\right)_p.$$

Having multiplied these equations by $(dt)_c$ and $(dt)_p$, respectively, we turn to the volume balance equations

$$(Q_i + Q_1 - Q_3)(dt)_c = \frac{V_0}{E}(dp)_c,\quad (Q_1 - Q_3)(dt)_p = \frac{V_0}{E}(dp)_p,$$

which do not contain time derivatives and can be added summand by summand:

$$Q_i (dt)_c + (Q_1 - Q_3)\left[(dt)_c + (dt)_p\right] = \frac{V_0}{E}\left[(dp)_c + (dp)_p\right].$$

The sums of the increments of time and pressure cover the entire period T between successive injections; they can thus be denoted as $(dt)_c + (dt)_p = dt$, $(dp)_c + (dp)_p = dp$:

$$Q_i (dt)_c + (Q_1 - Q_3)dt = \frac{V_0}{E}dp.$$

Dividing this equality by *dt*, we go to the complete equation of the expense balance

$$Q_i \frac{(dt)_c}{dt} + Q_1 - Q_3 = \frac{V_0}{E}\dot{p}.$$

We replace the infinitesimal time increments on the left side of the last equation with the corresponding finite increments $(dt)_c \approx \Delta t_c = t_c - 0 = t_c = \beta_c/\omega$,

$dt \approx \Delta T = T - 0 = T$. As a result, the flow balance equation in the absence of forced axial vibrations takes the form

$$Q_i \frac{t_c}{T} + Q_1 - Q_3 = \frac{V_0}{E} \dot{p}. \tag{3.21}$$

The equation obtained with axial vibrations of the axially movable ring excited by harmonic oscillations of external pressures contains two additional terms. They take into account the flow rate of compression-expansion of the fluid in the chambers Q_p and the flow rate of displacement Q_v from the end clearance (sector β_c) with a periodic change in pressure caused by fluctuations in the gap with frequency ω under the influence of external pressures (3.20) [16]:

$$Q_p = \frac{V_0}{E} p_n \frac{d\psi}{(dt)_\omega}, \; Q_v = A_s z_n \frac{du}{(dt)_\omega}, \tag{3.22}$$

where $A_s = \frac{\beta_c}{2\pi}(A_1 + A_2 + A_3)$ is the butt surface area of the sector β_c.

The lower index ω indicates that the increment $(dt)_\omega$ changes in an interval equal to the period $T_0 = 2\pi/\omega = n_i T$ of axial oscillations. In contrast to the static analysis where the averaged, time-independent pressure $\psi_2 = p_2/p_n$ (3.11) was used, here we are dealing with a time-varying pressure, which we will denote by p without an index but in the dimensionless form $\psi = p/p_n$.

As in the derivation of equation (3.21), we will replace the differentials with finite increments, i.e., we will use approximate expressions:

$$\frac{d\psi}{(dt)_\omega} = \frac{d\psi}{dt}\frac{dt}{(dt)_\omega} \approx \dot{\psi}\frac{\Delta t}{(\Delta t)_\omega} = \dot{\psi}\frac{T}{T_0} = \frac{1}{n_i}\dot{\psi},$$

$$\frac{du}{(dt)_\omega} = \frac{du}{dt}\frac{dt}{(dt)_\omega} \approx \dot{u}\frac{\Delta t}{(\Delta t)_\omega} = \dot{u}\frac{T}{T_0} = \frac{1}{n_i}\dot{u}.$$

Let us substitute them in (3.22) and add the resulting expressions to the right side of (3.21)

$$Q_i \frac{t_c}{T} + Q_1 - Q_3 = \frac{V_0}{E}\dot{\psi}\left(1 + \frac{1}{n_i}\right) + \dot{A}_s \frac{z_n}{n_i p_n} \cdot \dot{u}.$$

Having expressed the spending through the pressure drops (3.3), we arrive at a first-order nonlinear differential equation concerning the desired dimensionless pressure ψ in the chamber:

$$\left(g_i \frac{t_c}{T} + g_{1n} u^3\right)(\psi_1 - \psi) - g_{3n} u^3 (\psi - \psi_3) = \frac{V_0}{E}\left(1 + \frac{1}{n_i}\right)\dot{\psi} + A_s \frac{z_n}{n_i p_n}\dot{u}. \tag{3.23}$$

In the future, we will consider the linearized system without taking into account the inertia of the liquid during its unsteady motion. We will linearize the area of the position of static equilibrium, passing to the deviations of the variables on both sides of the equation (3.23). We will also introduce the notations $g_i' = g_i t_c / T$; $g_{1n} u_0^3 = g_{10}, g_{3n} u_0^3 = g_{30}$, where g_{10}, g_{30} are the conductivities of the corresponding end throttles for the steady-state gap value of z_0. After a series of transformations, the normalized equation of the balance of expenses in deviations takes the form

$$T_2 \dot{\psi} + \psi = -\left(\tau_2 \dot{u} + \kappa_s' u\right) + k_1 \psi_1 + k_3 \psi_3,$$

where

$$T_2 = \frac{V_0}{E g_{s0}} \left(1 + \frac{1}{n_i}\right), \tau_2 = \frac{A_s z_n}{n_i p_n g_{s0}},$$

$$k'_s = \frac{3}{g_{s0} u_0} \left[g_{30} \left(\psi_0 - \psi_{30}\right) - g_{10} \left(\psi_{10} - \psi_0\right) \right] = \frac{3}{g_{s0} u_0} \left(k_1 g_{30} - k_3 g_{10}\right) \left(\psi_{10} - \psi_{30}\right), \tag{3.24}$$

$$k_1 = \frac{g_i' + g_{10}}{g_{s0}}, k_3 = \frac{g_{30}}{g_{s0}}, g_{s0} = g_i + g_{10} + g_{30} = g_{sn} u_0^3.$$

If we introduce the time differentiation operator $s = d/dt$ and denote

$$T_2 s + 1 = D_2(s), \ \tau_2 s + k'_s = M_2(s),$$

then we will come to the equation in the operator form with respect to the pressure in the chamber:

$$D_2(s) \psi(t;u) = -M_2(s) u + k_1 \psi_1 + k_3 \psi_3. \tag{3.25}$$

We will obtain the dynamic equation of the automatic controller by substituting the pressure $\psi(t;u)$, determined by the differential equation (3.25), in the linear expression (3.16) for the dimensionless force ϕ_s:

$$\psi(t;u) = -\frac{M_2}{D_2} u + \frac{k_1 \psi_1 + k_3 \psi_3}{D_2}.$$

At the same time, the regulatory impact is

$$\phi_s = \psi(t;u) + \phi_{s0} = -\frac{M_2}{D_2} u + \frac{k_1 \psi_1 + k_3 \psi_3}{D_2} + \phi_{s0},$$

and we obtain the controller equation by multiplying both sides of this equality by the differential operator $D_2 = T_2 s + 1$

$$D_2(s) \phi_s = -M_2(s) u + k_1 \psi_1 + k_3 \psi_3 + D_2(s) \phi_{s0}. \tag{3.26}$$

From equation (3.26), the dimensionless dynamic stiffness of the system, which is the transfer function of the controller by mistake, is expressed by the formula

$$W_2(s) = \frac{\phi_s}{u} = -\frac{\tau_2 s + k'_s}{T_2 s + 1}.$$

The ring is considered a single-mass system that performs one-dimensional axial vibrations described by the equation

$$m\ddot{z} = F_s - F_e - F_k - c\dot{z},$$

where the term $c\dot{z}$ represents the external (outside the end clearance) linear viscous friction force. The remaining forces are described by formulae (3.14) and (3.16) when replacing the averaged pressure in chamber $\psi_2(u)$ with a pressure of $\psi(t; u)$ that depends on both the gap and time. Using these formulae, we will write

$$m\ddot{z} + c\dot{z} + kz = F_s - F_e - k\Delta = Ap + 0.5\left(A_1 p_1 + A_3 p_3\right) - \left(B_1 p_1 + B_3 p_3\right) - k\Delta,$$

and after going over to deviations under the condition that $k\Delta$= const, $\delta\left(k\Delta\right) = 0$ and after dividing each term by Ap_i, we will get

$$\frac{mz_n}{Ap_n}\ddot{u} + \frac{cz_n}{Ap_n}\dot{u} + \frac{kz_n}{Ap_n}u = \phi_s - \phi_e = \psi + \frac{1}{2A}\left(A_1\psi_1 + A_3\psi_3\right) - \frac{1}{A}\left(B_1\psi_1 + B_3\psi_3\right).$$

Let us denote the coefficients of the left side of this equation

$$T_1^2 = \frac{mz_n}{\grave{A}p_n},\ 2\xi = \sqrt{\frac{c^2 z_n}{mAp_n}},\ \chi_n = \frac{kz_n}{{}_n}$$

and use the load factor K (3.18):

$$\phi_{s0} - \phi_e = -\left[K\psi_1 + \left(1-K\right)\psi_3\right].$$

In the operator form, we will obtain the final form of the equation of axial oscillations of the ring:

$$\begin{aligned} D_1(s)u = \phi_s - \phi_e &= \psi - K\psi_1 - \left(1-K\right)\psi_3, \\ D_1(s) &= T_1^2 s^2 + 2\xi T_1 s + \chi_i. \end{aligned} \tag{3.27}$$

The coefficients have the following physical meaning: T_1 is the period of free vibrations of the axially movable ring; ξ is the damping coefficient of free vibrations due to external linear friction; and χ_n is the dimensionless coefficient of rigidity of the elastic elements.

If the right-hand side of (3.27) is equal to zero, then the equation

$$D_1(s)u = T_1^2\ddot{u} + 2\xi T_1\dot{u} + \chi_n u = 0$$

becomes the equation of free axial vibrations of the ring suspended on elastic elements with equivalent rigidity *k* without taking into account pressure forces. In this case, $\chi_n / T_1^2 = k/m = \omega_0^2$ is the natural frequency of the axial vibrations of the ring without a regulatory action.

We obtain the equation of dynamics of pulse compaction as an automatic control system by eliminating the force ϕ_s from equations (3.26) and (3.27):

$$D_1 u = -\frac{M_2}{D_2}u + \frac{k_1\psi_1 + k_3\psi_3}{D_2} + \phi_{s0} - \phi_e.$$

Let us multiply both sides of the equality by the operator D_2

$$(D_1 D_2 + M_2)u = k_1\psi_1 + k_3\psi_3 + D_2(\phi_{s0} - \phi_e)$$

and group the terms in powers of *s*, taking into account (3.18):

$$\left[T_1^2 T_2 s^3 + (T_1^2 + 2\xi T_1 T_2)s^2 + (2\xi T_1 + \chi_n T_2 + \tau_2)s + \chi_n + k'_s\right]u =$$
$$= -\left[KT_2 s + K - k_1\right]\psi_1 - \left[(1-k_s)T_2 s + 1 - k_s - k_3\right]\psi_3.$$

The expressions in the square brackets represent the operator of the system $D(s)$ and the operators $N_1(s), N_3(s)$ of external influences:

$$D(s)u = -N_1(s)\psi_1 - N_3(s)\psi_3, \tag{3.28}$$

where $D(s) = a_0 s^3 + a_1 s^2 + a_2 s + a_3$,

$$N_1(s) = b_0 s + b_1, \quad N_3(s) = c_0 s + c_1,$$
$$a_0 = T_1^2 T_2,\ a_1 = T_1^2 + 2\xi T_1 T_2,\ a_2 = 2\xi T_1 + \chi_n T_2 + \tau_2,\ a_3 = k'_s + \chi_n, \tag{3.29}$$

$$b_0 = KT_2,\ b_1 = K - k_1;\ c_0 = (1-K)T_2,\ c_1 = 1 - K - k_3. \tag{3.30}$$

An axially movable ring in the axial direction is affected by a number of perturbations, among which harmonic perturbations with frequencies equal to the rotor speed prevail (3.20). In the dimensionless form, the pressure deviations are

$$\delta\psi_1 \to \psi_1 = \psi_{1a}e^{i\omega t}, \delta\psi_1 \to \psi_3 = \psi_{3a}e^{i\omega t}, \delta\psi \to \Delta\psi = (\psi_{1a} - \psi_{3a})e^{i\omega t}.$$

Within the framework of the linear compression model under consideration, the superposition principle is valid, i.e., the resulting ring reaction is the

sum of harmonic reactions to individual elementary harmonic perturbations. Therefore, the analysis of harmonic axial vibrations of the ring caused by each of the harmonic perturbations is of practical importance. The rotation frequency, as a rule, has the form of a stepwise or linear function of time, and the reaction to it is characterized by time characteristics. Forced oscillations are characterized by amplitude and phase frequency characteristics, which are the amplitudes and phases of the frequency transfer functions. For equation (3.28) with two harmonic effects, the frequency transfer functions are written as follows:

$$W_1(i\omega)=\frac{u_{1a}e^{i(\omega t+\gamma_1)}}{\psi_{1a}e^{i\omega t}}=-\frac{N_1(i\omega)}{D(i\omega)}=A_1(\omega)e^{i\gamma_1},$$

$$W_3(i\omega)=\frac{u_{3a}e^{i(\omega t+\gamma_3)}}{\psi_{3a}e^{i\omega t}}=-\frac{N_3(i\omega)}{D(i\omega)}=A_3(\omega)e^{i\gamma_3},$$

where A_1, A_3 are the amplitude characteristics while γ_1,γ_3 are the phase frequency characteristics for perturbations ψ_1 and ψ_3, respectively. It can be seen from the above formulae that when the natural operator is equal to zero, the amplitudes increase indefinitely. The corresponding speeds are the natural frequencies of the ring-regulator system. It is necessary to represent the transfer functions as complex numbers in the algebraic form to express the amplitudes and phases in terms of the coefficients (3.30). To do this, in the operators of (3.29), we will introduce the following changes in $d/dt = s = i\omega$:

$$D(i\omega)=-ia_0\omega^3-a_1\omega^2+ia_2\omega+a_3=U+i\omega V;$$

$$U=a_3-a_1\omega^2,\ V=a_2-a_0\omega^2;$$

$$N_1(i\omega)=ib_0\omega+b_1,\ \ N_3(i\omega)=ic_0\omega+c_1.$$

Now, the transfer functions take the form

$$W_1(i\omega)=-\frac{b_1+i\omega b_0}{U+i\omega V},\ W_3(i\omega)=-\frac{c_1+ic_0\omega}{U+i\omega V}.$$

We will divide the real and imaginary parts of these expressions by multiplying the numerators and denominators by the complex number conjugate to the denominator:

$$W_1(i\omega)=-\frac{(b_1+i\omega b_0)(U-i\omega V)}{U^2+\omega^2V^2}=-(U_1-i\omega V_1)=-A_1(\omega)e^{i\gamma_1},$$

$$W_3(i\omega)=-\frac{(c_1+i\omega c_0)(U-i\omega V)}{U^2+\omega^2V^2}=-(U_3-i\omega V_3)=-A_3(\omega)e^{i\gamma_3},$$

$$U_1 = -\frac{b_1 U + \omega^2 b_0 V}{U^2 + \omega^2 V^2},\ \ V_1 = \frac{b_1 V - b_0 U}{U^2 + \omega^2 V^2}, \tag{3.31}$$

$$U_3 = -\frac{c_1 U + \omega^2 c_0 V}{U^2 + \omega^2 V^2},\ \ V_3 = \frac{c_1 V - c_0 U}{U^2 + \omega^2 V^2}.$$

The amplitudes and phases of (3.31) are expressed by the formulae:

$$A_1(\omega) = \frac{u_{1a}}{\psi_{1a}} = \sqrt{U_1^2 + \omega^2 V_1^2} = \sqrt{\frac{b_1^2 + \omega^2 b_0^2}{U^2 + \omega^2 V^2}},$$

$$\gamma_1 = -\operatorname{arctg}\omega\frac{c_0 U - c_1 V}{c_1 U + \omega^2 c_0 V}, \tag{3.32}$$

$$A_3(\omega) = \frac{u_{3a}}{\psi_{3a}} = \sqrt{U_3^2 + \omega^2 V_3^2} = \sqrt{\frac{c_1^2 + \omega^2 c_0^2}{U^2 + \omega^2 V^2}},$$

$$\gamma_3 = -\operatorname{arctg}\omega\frac{c_0 U - c_1 V}{c_1 U + \omega^2 c_0 V}.$$

According to the amplitude frequency characteristics, it is possible to estimate the dimensional values of the amplitudes of the forced axial vibrations of the ring at any speed if the magnitude of the amplitudes of the oscillations of the pressure deviations p_{1a}, p_{3a} is set as follows:

$$z_{1a} = A_1(\omega) z_n\, p_{1a}/p_n,\ z_{3a} = A_3(\omega) z_n\, p_{3a}/p_n.$$

The Routh-Hurwitz stability criterion can be used for the dynamic stability analysis. According to this criterion, the third-order system is stable if all the coefficients (3.30) of its own operator are positive (the coefficients satisfy this condition). In addition, the inequality $a_1\, a_2 > a_0 a$ must be satisfied, which, after substituting the values of the coefficients, is reduced to

$$2\xi\left[T_1^2 + T_2\left(2\xi T_1 + \chi_i T_2\right)\right] > T_1\left(k'_s T_2 - \tau_2 - 2\xi\frac{T_2}{T_1}\tau_2\right).$$

If external damping ($c = \xi = 0$) is not taken into account, then the stability condition reduces to the inequality

$$\tau_2 > T_2 k'_s, \tag{3.33}$$

from which there is a stability margin with some tolerance.

After substituting the values of (3.24) in (3.33), it is possible to determine the chamber volume admissible in stability:

$$V_0 < \frac{A_s E z_0 g_{s0}}{3(1+n_i)(k_1 g_{30} - k_3 g_{10})(p_{10} - p_{30})}. \quad (3.34)$$

Since $k'_s \sim \Delta\psi$ (3.24), the dynamic stability condition must be satisfied for the maximum possible working differential pressure of the liquid being sealed, i.e., for the value of the stiffness coefficient corresponding to $\Delta\psi_{max}$.

3.4.3. An example of engineering calculations for the impulse mechanical seal

We will consider the engineering calculation procedure using an example of an impulse mechanical seal similar to one stage of the main circulation pump seal for a nuclear power plant. The initial data are $r_0 = 0.115$ m, $p_1 = (4 \div 16)$ MPa, $p_3 = 0$, $p_n = p_{1n} = 10$ MPa, and $\omega = \omega_n = 150$ s^{-1}.

The sealed medium is water, $\mu = 10^{-3}$ Pa · s, $E = 2.2 \cdot 10^3$ MPa.

For the design purposes, the dimensions of the contact surface are the following: $r_1 = r_0 + 0.005 = 0.12$ m, $r_3 = 0.14$ m, $r_2 = 0.5(r_1 + r_3) = 0.13$ m, $r_{21} = 0.128$ m, $r_{22} = 0.132$ m, $l_1 = l_3 = 0.08$ m, as well as the size and number of chambers and feeders: $n_i = 4$, $n_c = 32$, $V_0 \approx 1.8 \cdot 10^{-7}$ m^3, $d_i = 0.4 \cdot 10^{-3}$ m, $l_i = 8 \cdot 10^{-3}$ m, $\beta_s = 2\pi/n_c = 0.196 \approx 1.6\beta_c$ and $\beta_c = b_c/r_2 = 0.123$ rad.

We will calculate the area of the end sections: $A_1 = \pi(r_3^2 - r_{22}^2) = 6.84 \cdot 10^{-3}$ m^2; $A_2 = \pi(r_{22}^2 - r_{21}^2) = 3.27 \cdot 10^{-3}$ m^2; $A_3 = \pi(r_{21}^2 - r_1^2) = 6.23 \cdot 10^{-3}$ m^2; $A_c = 64 \cdot 10^{-6}$ m^2; $A = 0.5(A_1 + 2A_2 + A_3) = 9.8 \cdot 10^{-3}$ m^2.

The determined parameters are the conductivity of the end throttles and their dimensionless values, the time constants of filling and emptying of the chambers, and weight coefficients. The calculation results are given in Tables 3.1—3.3 for 5 values of the nominal clearance. This will allow us to evaluate the effect of z_n on the static characteristics.

Let us calculate the coefficient of hydrostatic stiffness (Table 3.4).

Table 3.1. **Butt throttle conductivity**

z_n, μm	g_i	g_{1n}	g_{3n}	g_{en}
3	$7.854 \cdot 10^{-11}$	$4.843 \cdot 10^{-15}$	$4.428 \cdot 10^{-15}$	$2.313 \cdot 10^{-15}$
4		$1.148 \cdot 10^{-14}$	$1.05 \cdot 10^{-14}$	$5.483 \cdot 10^{-15}$
6		$3.875 \cdot 10^{-14}$	$3.542 \cdot 10^{-14}$	$1.851 \cdot 10^{-14}$
8		$9.184 \cdot 10^{-14}$	$8.397 \cdot 10^{-14}$	$4.386 \cdot 10^{-14}$
10		$1.794 \cdot 10^{-13}$	$1.64 \cdot 10^{-13}$	$8.567 \cdot 10^{-14}$

Table 3.2. **Dimensionless conductivities**

z_n, μm	α_{1i}	α_{3i}	α_{e1}	α_{e3}
3	$6.166 \cdot 10^{-5}$	$5.638 \cdot 10^{-5}$		
4	$1.462 \cdot 10^{-4}$	$1.336 \cdot 10^{-4}$		
6	$4.933 \cdot 10^{-4}$	$4.51 \cdot 10^{-4}$	0.48	0.52
8	$1.169 \cdot 10^{-3}$	$1.069 \cdot 10^{-3}$		
10	$2.284 \cdot 10^{-3}$	$2.088 \cdot 10^{-3}$		

Table 3.3. T**ime constants of filling and emptying chambers as well as weighting factors**

z_n, μm	G_c	G_p	T_c	T_p	T_n	t_c
3	10^7		$1.736 \cdot 10^{-6}$	0.015		
4	10^7		$1.736 \cdot 10^{-6}$	$6.205 \cdot 10^{-3}$		
6	$9.995 \cdot 10^6$	$5.224 \cdot 10^6$	$1.735 \cdot 10^{-6}$	$1.839 \cdot 10^{-3}$	0.01	$8.2 \cdot 10^{-4}$
8	$9.989 \cdot 10^6$		$1.732 \cdot 10^{-6}$	$7.756 \cdot 10^{-4}$		
10	$9.979 \cdot 10^6$		$1.729 \cdot 10^{-6}$	$3.971 \cdot 10^{-4}$		

Table 3.4. **Coefficients of hydrostatic stiffness**

z_n, μm	3	4	6	8	10
k_s	–0.5	–0.21	–0.06	–0.03	–0.014

Table 3.5. **Values of compaction parameters**

z_n, μm	K_n	B_1, m^2	r_4, m
3	1.231	0.015	0.121
4	0.843	0.012	0.126
6	0.644	$9.726 \cdot 10^{-3}$	0.128
8	0.595	$9.251 \cdot 10^{-3}$	0.129
10	0.578	$9.082 \cdot 10^{-3}$	0.129

As a result, $\kappa_s < 0$, i.e., the equilibrium stability condition, is satisfied for 5 values of z_n.

We will calculate the load factor K_n, which provides the nominal clearance in the nominal mode of $\Delta\psi \approx \Omega \approx 1$, as well as the load area B_1 and the inner radius r_4 corresponding to this value (Table 3.5).

The numerical evaluation of the pre-compression force of elastic elements effect will be performed for its three values: χ = 0.004, 0.01, and 0.03.

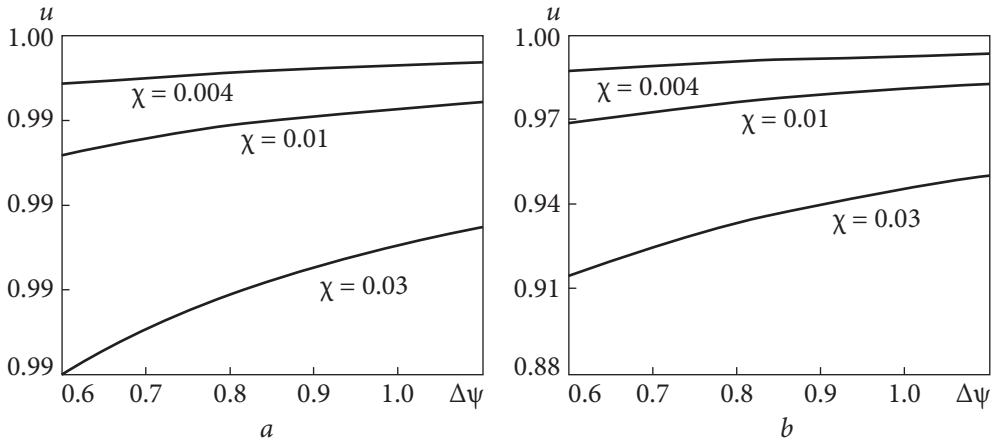

▲

Fig. 3.19. Static characteristics for various nominal gaps z_n: *a* — z_n = 3 μm; *b* — z_n = 4 μm

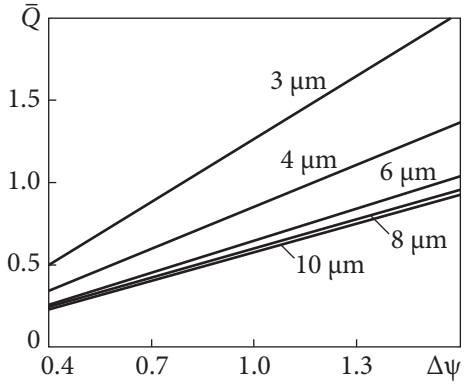

Fig. 3.20. Consumption characteristics for various values of the nominal clearance z_n

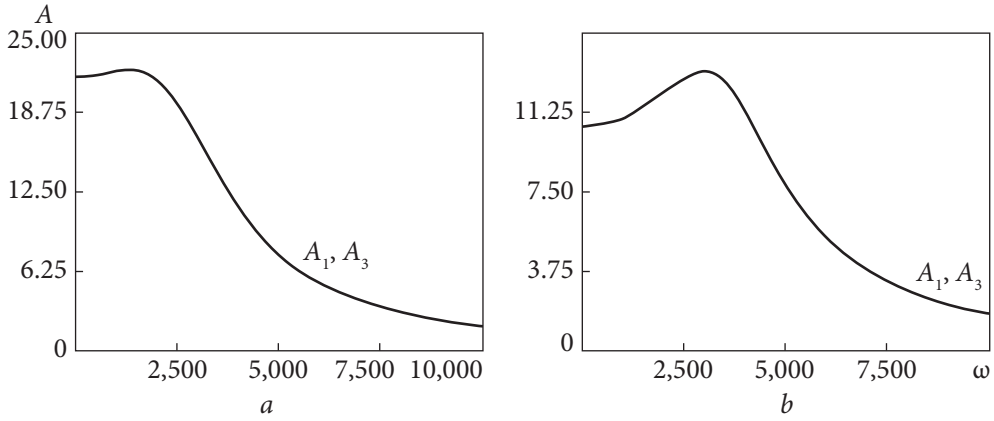

Fig. 3.21. Amplitude-frequency characteristics for various nominal gaps z_n: *a* — z_n = 6 μm; *b* — z_n = 8 μm

We will construct static (Fig. 3.19) and consumption (Fig. 3.20) characteristics. The dynamic calculation consists of constructing the amplitude and phase frequency characteristics for external influences ψ1 and ψ3. Of practical interest are, first of all, the amplitude frequency characteristics. The results of their calculation for various values of the nominal gap are shown in Fig. 3.21.

The characteristics obtained during the engineering calculations show that in the given pressure range of the liquid being sealed, the end clearance differs little from the base value, which ensures optimal working conditions. An increase in the dimensionless compressive force of the elastic elements χ leads to a decrease in the gap.

The obtained expressions of the amplitude and phase frequency characteristics (3.32) make it possible to identify dangerous regions of rotational frequencies and select the sealing parameters so that the amplitudes of the forced axial vibrations of the ring cannot go beyond the permissible limits.

Factors affecting the dynamic stability of pulse compaction were identified. The resulting expression (3.33) shows that stabilization is facilitated by an increase in the displacement time constant τ2, a decrease in the compression time constant T2, and the hydrostatic coefficient of rigidity k′s. It follows from formula (3.34) for determining the chamber volume that is acceptable for stability that the stability region expands, first of all, due to a decrease in the chamber volume and a decrease in the hydrostatic stiffness coefficient. The obtained expressions allow to provide a stability boundary with a certain margin due to the selection of the geometric parameters of compaction.

The restrictions adopted during the development of the methodology for calculating impulse seals were that the pressure change in the end clearance section with a constant gap is linear in its radius, and the inertia forces of the liquid in the mechanical gaps are small. The authors believe that the assumptions made do not distort the qualitative picture of the ongoing processes, and taking into account calculations with a certain margin, they are quite acceptable for practical use. This is confirmed by the successful experience in the industrial operation of impulse seals developed and designed using the developed calculation methodology.

It should be noted that the operation of impulse seals is accompanied by complex non-stationary high-frequency hydrodynamic processes in the friction pair. This opens up a wide field for study since a rather large number of questions remain regarding the features of the operation of seals of this type under various conditions that require further research.

3.5. Designs of non-contact mechanical seals

A unified impulse mechanical seal assembly for high-speed pumps is shown in Fig. 3.22 [33]. The pumps are used in the primary circuit of water-cooled reactors to supply shut-off water with boron to the seals of the main circulation pump (MCP), as well as to inject the necessary additives that reduce the coolant's corrosive activity. The pumped water contains up to 30 g/kg of boric acid, up to 30 mg/l of ammonia, and some other chemical compounds. The temperature does not exceed 70 °C. The pressure of the sealed liquid is 0.6—1.0 MPa, the rotor speed is 8,900 rpm, the diameter of the shaft under the seal is 0.07 m, and the average peripheral speed of the contact surface of the mechanical seal is 50 m/s.

Due to the high circumferential speed, the pumps originally had gap seals, leakage through which was about 10 m^3/h. The preparation of leaks for reuse was expensive, so the design of an impulse mechanical seal was developed, which was recommended after detailed bench tests [36].

The optimal end clearance is 2 μm, which provides stable boundary lubrication with a low coefficient of friction so that the seals do not require external cooling systems. The heat removal from the friction pair is carried out by

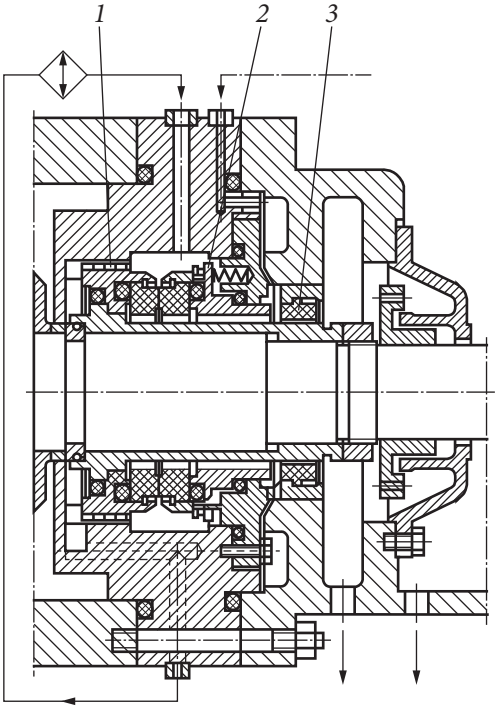

Fig. 3.22. Impulse seal for high-speed booster pump

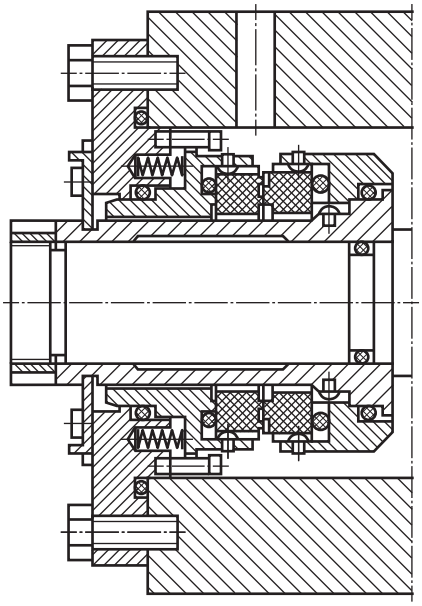

Fig. 3.23. Impulse mechanical seal assembly of a high-speed pump

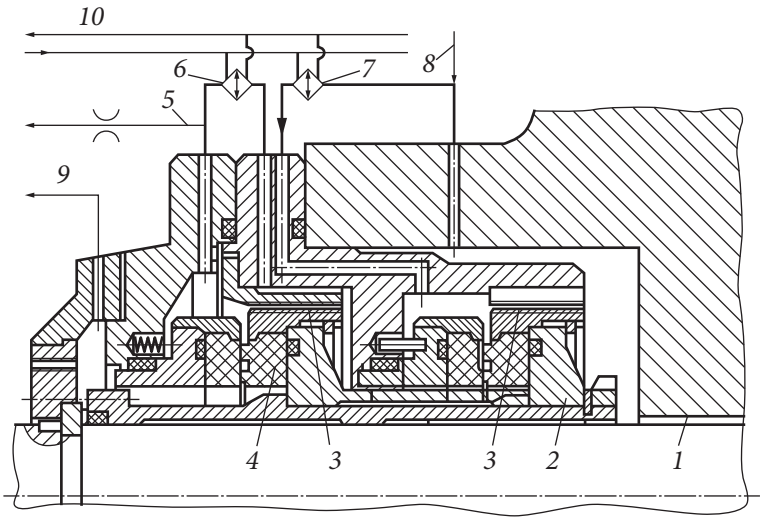

Fig. 3.24. Two-Stage Impulse Seal: *1* — gap seal; *2*, *4* — the first and second stages of the impulse mechanical seal; *3* — labyrinth seal; *5* — organized leakage line; *6*, *7* — refrigerators; *8* — buffer water supply line; *9* — leakage line; *10* — cooling water inlet and outlet lines

pumped water, the circulation of which through the seal chamber is provided by the axial impeller (*1)*. In the stagnant zones, the surfaces become covered with boron crystals over time, so periodic flushing of these surfaces is required. To reduce the consumption of condensate for flushing, the cavity behind the axially movable ring (*2)* is sealed with a locking slotted seal (*3)*, which is also an emergency in case of failure of the main seal.

Fig. 3.23 shows an end mechanical shaft seal designed for feed pumps of thermal power plants [33]. Such an impulse-type seal is used in pumps with pressure loading parameters not exceeding 18 MPa and peripheral speeds up to 100 m/s.

Mechanical seals with two or three stages are used to prevent the liquid pumped by the pump from entering the environment and also when the sealing pressure increases above 15 MPa. An example of such a solution for an impulse mechanical seal assembly is shown in Fig. 3.24 [30].

The seal assembly operates at high temperatures (up to 285 °C) of the pumped medium. To prevent leakage of hot water into the surrounding space, cooling and sealing water are supplied to the sealing unit with a pressure of 0.05—0.1 MPa higher than the pressure in the sealed cavity of the pump. The main elements of the sealing system are an internal gap seal (*1)*, two stages of an impulse mechanical seal (*2)* and (*4)*, cooling circuits (*6)* and (*7)*, a barrier water supply (*8)*, and an organized leakage outlet (*5)*. During normal operation, the end stage of the mechanical seal assumes the full pressure drop, and the other

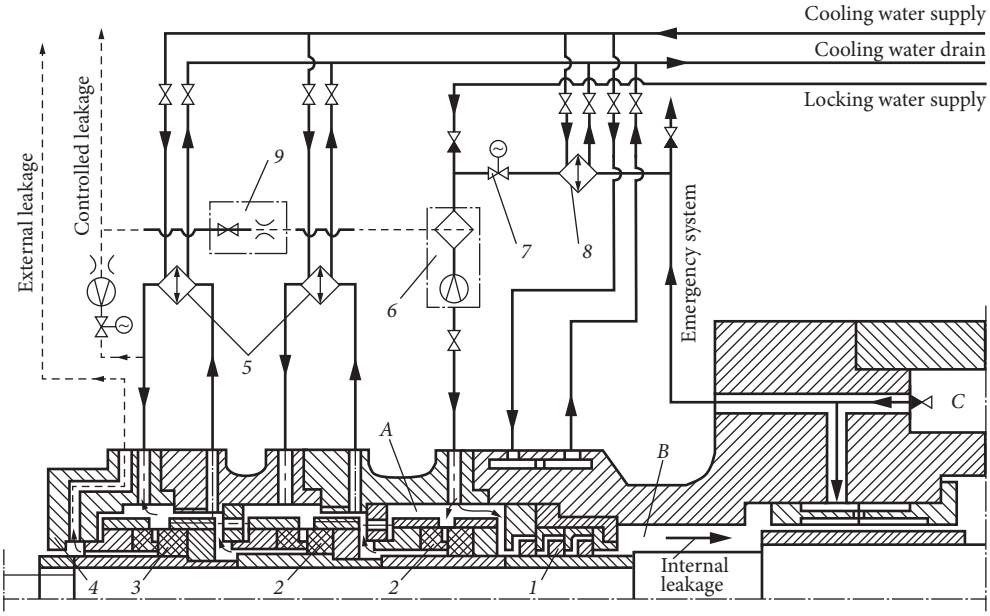

Fig. 3.25. Diagram of the sealing system of the NPP main circulation pump rotor

performs the function of a backup (emergency). Silicified graphite is used as a material for both rings of friction pairs. External barrier fluid leakage is no more than 1 l/h, which is ten times less than for similar seal assemblies with floating rings.

Rotor sealing is one of the most complex and critical components of the MCP that determines the reliability of the entire unit. This is explained by the difficult operating conditions of the seals in combination with high requirements for tightness at nominal, transient, and emergency operations of the pump. The seal assembly (Fig. 3.25) consists of seals such as inner (*1)*, main (*2)*, closing (*3)*, and end (*4)*.

The inner seal (*1)*, which is a set of three floating rings, separates chamber *A*, where cold water is supplied, from the sealing cavity *B* of the pump. On the floating rings, the end contact belts are made on both sides. In the event of an emergency drop in the pressure of the locking water, the rings operate on a pressure difference that is changed in the direction, and the entire assembly provides the required tightness for 40 seconds. The pressure drop across the inner seal is maintained within 0.1—0.5 MPa; the inner and outer diameters of the rings are 200 mm and 210 mm. The main seal (*2)* is two series-connected stages of the impulse end seal. The same stage (*3)* serves as a closing seal, which should briefly perform the functions of the main in case of failure of the latter. The end seal (*4)* is a simple ring throttle. The sealing system includes a line for supplying

shut-off water to chamber *A* by high-pressure feed pumps through a hydrocyclone (*6)*. Water throttled on the main seals (*2)* is cooled in heat exchangers (*5)*. In case of failure of the shut-off water supply system, the alarm system is activated: valve (*7)* opens through cooler (*8)* and hydrocyclone (*6)* enters chamber B, ensuring the normal long-term operation of the seal. Part of the controlled leakage through the throttle device (*9)* can be returned to the supply line of the locking water if necessary.

The accumulated experience in industrial operation shows that impulse mechanical seals meet the stringent requirements for reliability, durability, and tightness, which are imposed on the seals of the rotors of NPP pumping equipment [33].

3.6. Conclusions

This chapter examined hydrostatic, hydrodynamic, and impulse non-contact mechanical seals, the main difference of which is the principle of creating and maintaining a lubricant layer in the end gap.

Hydrostatic mechanical seals have not found widespread use in power-generating machines due to several disadvantages that are inherent in them, namely, large leakage during operation caused by large gaps in the mechanical pair, low hydrostatic rigidity of the liquid film in the gap, leakage when parked, and instability performance characteristics, due to the tendency to clog calibrated supply holes (nozzles).

Hydrodynamic mechanical seals are quite widely used by foreign manufacturers in feed turbopumps in the operating conditions of the seals, which cannot be called comfortable — a low-viscosity, low-boiling liquid being sealed at high sliding speeds in a friction pair does not contribute to the formation of a stable lubricating film, the presence of which is an indispensable condition for long-term operation of the seal. These seals differ in the shape and size of the grooves on the end surface, but the common thing is that micron gaps in the friction pair are formed due to the interaction of the liquid with micron grooves, a slight change in the size of which, due to inevitable erosive wear, leads to a significant deterioration in performance characteristics.

Due to their high-performance qualities, impulse-type mechanical seals have been used in domestic energy pumps for quite a long time; they have the following advantages:

- the optimal value of the end gap is in the range of 2...3 microns, which allows for reliable lubrication and heat removal from the sealing surfaces while leaks remain at an acceptable level;
- the size of the end gap depends on the pressure being sealed and the shaft rotation speed, with an increase in which the end gap also increases, which provides a wide range of seal operations both in pressure and speed. It can be

argued that impulse seals have virtually no restrictions on rotation speed, so their use is especially effective for high-speed machines;

• impulse seals are reversible, i.e., their performance does not depend on the direction of shaft rotation;

• they reliably perform the role of parking lots because in the absence of shaft rotation, liquid under pressure does not enter most of the chambers, and the pressure force of the sealed medium far exceeds the force opening the end gap.

Forty years of experience in research and successful operation of impulse mechanical seals have shown that they are insensitive to the physical properties of the sealed medium and are able to operate reliably in various liquids, including cryogenic ones, gases, and even gas-liquid mixtures.

The foregoing allows us to make an unambiguous conclusion that impulse mechanical seals have significant advantages over other types of non-contact mechanical seals and are the most promising for severe operating conditions.

CHAPTER 4

BASIC MATERIALS OF MECHANICAL SEAL PARTS

The correct choice of materials from which the mechanical seal parts are made is crucial for the long-lasting and reliable operation of the seal under certain operating conditions.

4.1. Designations of the main materials of mechanical seals

According to the EN 12756 standard, the following designations of the main materials from which mechanical seals are made are accepted.

4.1.1. Basic materials of friction pair rings

Synthetic carbon graphite: A — carbon graphite impregnated with antimony; *B* — carbon graphite impregnated with synthetic resin.

Carbides: U — tungsten carbide; U_1 — tungsten carbide with cobalt binder (*WC-Co*); U_2 — tungsten carbide with a nickel binder (*WC-Ni*); U_3 — tungsten carbide with a nickel-chromium-molybdenum binder (*WC-NiCrMo*); *Q* — silicon carbide: Q_1 — hot-pressed silicon carbide (*SiC*); Q_2 — reaction-sintered silicon carbide (*SiC-Si*); Q_3 — graphite impregnated with silicon (*SiC-C-Si*), in other words — siliconized graphite.

Metal oxides: V — aluminum oxide (Al_2O_3 — 99.5%); *YSZ* — zirconium dioxide, partially stabilized with yttria (ZrO_2 — Y_2O_3).

4.1.2. Auxiliary seal materials

Rubber O-rings, rubber compounds based on: *B* — butyl rubber; *E* — ethylene propylene diene (*EPDM*) rubber (*Nordel*); *K* — perfluoro rubber (*Karez, Chemraz*); *N* — chloroprene rubber (*Neoprene*); *P* — nitrile butadiene rubber (*Perbunan*); *S* — silicone rubber (*Silopren*); *V* — fluorine rubber (*Viton*).

Wedge-sphere rings, *U*-shaped cuffs: *T* — fluoroplastic (*PTFE*).

4.1.3. Spring materials

F — chromium-nickel steel, AISI 304 (1.4301); *G* — chromium-nickel-molybdenum steel (1.4571); *M* — Hastelloy C-4 (2.4610).

4.1.4. Construction materials of seal parts

E — chromium steel, AISI 420 (1.4021, 1.4028); *F* — chromium-nickel steel, AISI 304 (1.4301); F_1 — chromium-nickel steel, AISI 431 (1.4057); *G* — chromium-nickel-molybdenum steel, AISI 316 (1.4401); *L* — chromium-nickel-molybdenum steel, AISI 316L (1.4404); *D* — duplex chromium-nickel-molybdenum steel, (1.4404); *M* — Hastelloy C276; G_4 — 316 Ti (1.4571).

4.2. Materials of friction pair rings

The history of the creation and development of mechanical seals is described in sufficient detail in Chapter 1, and it is inextricably linked with the evolution of friction pair materials [13]. The choice of certain materials for the friction pair of the mechanical seal depends on the operating conditions of the seals and the operating requirements regarding their reliability, durability, and tightness, as well as the manufacturability and economic indicators of manufacturing the sealing rings.

Figuratively speaking, the friction pair is the "heart" of the mechanical seal, so the "success" of the design is often determined by the correct choice of appropriate materials. They are subject to very high and often contradictory requirements:

- high wear resistance;
- low coefficient of friction on the mating ring;
- corrosion resistance in the working environment;
- high mechanical properties: compressive, tensile and bending strength;
- high modulus of elasticity, on which the resistance of the rings to force and thermal deformations largely depends;
- high thermal conductivity;
- resistance to impacts, i.e., impact strength;
- resistance to thermal cracking under "thermal shock" conditions, etc.

Currently, hard ceramic materials based on silicon carbide, various compositions of silicon carbide with graphite, and carbon graphite are widely used in friction pairs of seals. Much less commonly used are hard alloys based on tungsten carbide, as well as oxide ceramics — aluminum oxide, titanium (chromium) oxide, and zirconium dioxide, partially stabilized with yttrium oxide.

Let's take a closer look at the materials used for the sealing rings of mechanical seals.

4.2.1. Soft carbon-graphite materials

Carbon-graphite materials have been used in mechanical seals since the 40s of the 20th century in combination with solid materials. Initially, counter rings were made from various types of tool steel with preliminary heat treatment; later, metal rings with hard wear-resistant coatings began to be used as a counter body, then various types of hard alloys and silicon carbide.

The main features of carbon-graphite materials are:

- excellent anti-friction qualities;
- high heat and electrical conductivity;
- low hardness;
- low mechanical strength;
- fragility;
- low modulus of elasticity.

Carbon-graphite materials for mechanical seal rings are divided into fired and graphitized. The composition of both is approximately the same, and they differ only in the degree of heat treatment. Petroleum coke, soot, graphite, and pitch are used as starting materials in the production of carbon graphite. After final pressing, the blanks are fired in a furnace to produce fired carbon-graphite materials.

If, after firing, they are also kept in a furnace at a temperature of 2,400—2,600 °C, at which part of the amorphous coal turns into graphite, then such materials are called graphitized. At the same time, the thermal conductivity of carbon graphite increases (approximately 2 times), their antifriction properties improve, oxidation resistance increases, but strength decreases. After firing and graphitization, carbon-graphite materials have a porosity of 6—30%. To eliminate it and improve the antifriction and mechanical properties of carbon graphite, they are impregnated with resins, salts, metals, etc. In general, impregnation reduces porosity and increases the elastic modulus, hardness, temperature coefficient of linear expansion, and thermal conductivity of the material.

Antifriction materials based on carbon are divided into the following main types: carbon burnt with impregnation, graphite with impregnation, and graphite fluoroplastic. The wide range of physical and mechanical properties of carbon materials is due to the variety of compositions of components and production methods (Table 4.1).

In domestic designs of mechanical seals, graphite of the KHIMANIT, KHIMANIT-T brands, graphites AO-1500, and AG-1500 impregnated with lead or babbitt are used widely.

Impregnation of porous graphite with resins, salts, and metals, including lead, tin, copper, and antimony, is usually carried out in autoclaves, where at a temperature above the melting point of the impregnation material, pressure,

and vacuum are created alternately to fill the voids in the graphite body with the impregnation material.

One of the disadvantages of carbon-based antifriction materials is low impact strength, but this only manifests itself at the stage of processing the part and installing the seal. During the operation of the mechanical seal, impact axial loads are damped by an elastic pressing element. All carbon materials have a lower thermal coefficient of linear expansion than metals, and this must be considered when choosing fits in the joints of carbon-graphite and metal parts.

Table 4.1. **Characteristics of common carbon-graphite materials**

Properties of material	Carbon graphite — A (Impregnation with antimony)	Carbon graphite — B (Impregnated with synthetic resin)	Himanite	AO-1500 CO5	AO-1500 B83
Density, g/cm^3	2.15—2.5	1.75—1.83	1.85—1.89	2.7—3.0	2.4—2.8
Tensile strength at compression, N/mm^2	276—350	207—205	130—170	260—280	140—150
Tensile strength at tensile strength, N/mm^2	41—49	35—49	—		
Tensile strength at bending, N/mm^2	83—89	60—79	32—38		
Elastic modulus, 10^3 N/mm^2	26—33	18.5—2.4	—	17	13.5—14
Shore hardness	80	83—95	—	70—75	70—72
Coefficient of thermal linear expansion, 10^{-6} 1/K	4—4.7	2.4—4.9	10—15	6.5—8.5	6.5
Thermal conductivity coefficient, W/m*K	12	8—13	50	30	80—90
Maximum application temperature, °C			200	300	230

4.2.2. Silicon carbide

A silicon carbide (*SiC*) molecule consists of one silicon atom bonded to one carbon atom. This results in a strong bond that is extremely stable over a wide range of temperatures and chemical environments.

Silicon carbide practically does not occur in nature. It was first discovered in 1824 but remained a kind of a rarity until 1892, when C. E. Acheson developed a manufacturing process using an electric arc furnace, making SiC commercially available. This method is still one of the most common technological processes for producing large SiC crystals, which are crushed to the required particle size then. The resulting silicon carbide crystal powder is used then to sinter O-ring blanks. It also has other very important properties, such as a very high hardness and high modulus of elasticity.

Silicon carbide rings have been used in sealing technology since the mid-70s of the last century. This has led to a significant increase in the service life and reliability of mechanical seals, thanks to the exceptional hardness, chemical resistance, and rigidity of this material.

The modern range of silicon carbide materials, depending on manufacturing technology and chemical composition, can be divided into three groups:

- hot-pressed silicon carbide — Q_1 (*SSiC*);
- reaction sintered silicon carbide — Q_2 (*SiC-Si*);
- hot-pressed silicon carbide containing graphite — *SSiC-C*.

Most often, reaction-sintered silicon carbide Q_2 (*SiC-Si*) is used in sealing technology; its other designation is *RbSiC*. This is because the technology for sintering blanks is quite simple and well-developed. This material is formed by bonding silicon carbide particles to each other through a reaction process. Silicon carbide particles and carbon are mixed with a binder and pressed into the desired shape. The compressed workpiece is placed in a furnace with an inert atmosphere and exposed to molten silicon metal. Metallic silicon penetrates the pores of the workpiece and, reacting with free carbon forms new *SiC* grains. This reaction literally bonds the original *SiC* particles together, forming additional SiC particles that bind the entire workpiece material together like glue. As a result of silicon impregnation, all voids and pores in the workpiece material are filled with metallic silicon. In modern grades of silicon carbide, the content of free silicon ranges from 8 to 12%. The properties of silicon carbide materials are given in Table 4.2.

Although silicon metal does not significantly affect most of the physical and thermal properties of the resulting material, it limits its chemical resistance. All chemicals that can react with elemental silicon can cause corrosion of the free silicon in the *RbSiC* ring, which leads eventually to partial or complete destruction of the O-ring made of this material and, as a result, failure of the me-

chanical seal. The most common chemicals that destroy *RbSiC* are alkalis and other high-pH chemicals, as well as strong acids. Therefore, reaction-sintered silicon carbide is not used in alkalis and strong acids.

Silicon carbide is characterized by high chemical stability, thermal conductivity, and wear resistance. The disadvantage is the low tensile strength and fragility, which has a significant impact on the reliability of mechanical seals in conditions of increased equipment vibration.

Hot-pressed (self-sintered, self-bonded) silicon carbide. In 1979, a technology for sintering *SiC* particles directly to each other was patented. This process is based on the use of non-oxide binders such as carbon, boron, or aluminum, which are then burned off when the workpiece is heated in an inert environ-

Table 4.2. **Properties of silicon carbide materials**

Properties of material	Silicon carbide — Q_1 (*SSiC*)	Silicon carbide — Q_2 (*SiC-Si*)	Silicon carbide (*SSiC-C*) (*SiC*-95%, *C* — 5%)	Siliconized graphite — Q_3 (*SiC-Si-C*) (*SiC* — 62%, *C* — 35%, *Si* — 3%)
Density, g/cm^3	3.1—3.2	3.05—3.1	3.0—3.02	2.65
Tensile strength at compression, N/mm^2	3,500	3,500	2,000	>600
Tensile strength at tensile strength, N/mm^2	175—250	180—240	—	70
Tensile strength at bending, N/mm^2	410	340	240	140
Modulus of elasticity, 10^3 N/mm^2	430	380	360	140
Microhardness	2,300	1,400—3,500	2,100	—
Thermal coefficient linear expansion, 10^{-6} 1/K (from 20 to 100 °C)	3	3.4	4.1	3
Thermal conduc-tivity coefficient, W/m K	115	115	104	125
Maximum temperature applications, °C	1,500	1,350	1,500	600

ment at temperatures above 2,000 °C. The material resulting from this process has come to be called self-sintered (*SSiC*), hot-pressed, direct-sintered silicon carbide (*DSSiC*), or alpha-sintered silicon carbide (α*SiC*). It is the same material, and the names are used interchangeably.

This material consists almost entirely of *SiC* with very little unconnected pore volume. Due to the absence of free silicon and other impurities, the silicon carbide ring produced by this technology is chemically stable in virtually any fluid under operating conditions that might be encountered in a centrifugal pump.

Some of the initial research on self-sintering silicon carbides (*SSSiC*) was done with beta-phase *SiC*. Later studies used alpha-phase *SiC*. These new materials and production methods were patented, significantly limiting their availability and slowing their adoption into industry.

Parts made from hot-pressed silicon carbide differ from reaction-sintered silicon carbide (*RbSiC*) in greater hardness, wear resistance, rigidity, and strength but also are more fragile and prone to chipping. In addition, the absence of free silicon significantly reduces the already low antifriction characteristics of silicon carbide.

Controlled Silicon Carbide. The vast majority of *SiC* material grades are a solid, homogeneous material that does not have a significant volume of pores and voids. The result is very flat and smooth seal surfaces. Under certain conditions, completely flat and smooth surfaces can prevent lubricating fluid from being forced through the seal, which can prevent the seal surfaces from being properly lubricated. Over the past decade, silicon carbide manufacturers have been creating silicon carbide materials whose properties are controlled throughout the materials' structure. When the seal surface is lapped, these features create small surface anomalies that can provide improved sealing performance.

The most common varieties of these materials include loose graphite particles dispersed throughout the *SiC* material. On a lapped surface, this results in small areas of graphite surrounded by a hard *SiC* surface. Graphite does not provide additional lubrication due to its supply to the sliding surface. Instead, the soft graphite material creates small indentations on the surface that improve lubrication by process fluids. As an alternative, silicon carbide is available with small, controlled voids throughout the material, which also create small indentations on the lapped surfaces. It is even possible to create a material with both free graphite and controlled porosity.

4.2.3. Siliconized graphite

One of the most widely used materials in mechanical seals of energy pumps is siliconized graphite. It consists of hard grains of silicon carbide interspersed with softer inclusions of silicon and carbon.

The high wear resistance and durability of siliconized graphite is due to the special structure of the material, which is a rigid frame made of high-hardness silicon carbide and free graphite included in it, which provides high antifriction properties and thermal conductivity (see Table 4.2).

Siliconized graphite is produced by impregnating the entire volume of the original graphite with liquid silicon at temperatures above 2,000 °C. In this case, a reaction occurs with the formation of silicon carbide. However, during a chemical reaction, not all silicon is combined with carbon-free silicon in siliconized graphite, limiting the chemical resistance of these materials. In particular, siliconized graphites *SG-T* and *SG-P* are unstable in alkalis. Siliconized graphite *GAKK 55/40* is more resistant under these conditions and is currently the most universal antifriction material with high chemical resistance.

Table 4.3. **Properties of siliconized graphites**

Properties of material	*SG-P*	*SG-P 0.5*	*SG-P 0.5P*	*GAKK 55/40*
Density, g/cm^3, not less	2.2	2.2	2.2	2.43
Tensile strength at compression, N/mm^2	411.9	235.3		118—246
Tensile strength at tensile strength, N/mm^2			—	226—492
Bending strength, N/mm^2	98.1	76.5		443—787
Elastic modulus, 10^9 N/mm^2				—
Hardness, HRC				—
Linear coefficient thermal expansion, 10^{-6} 1/K (from 20 °C to 1,000 °C)	4.2	4.0		5.0
Coefficient of thermal conductivity, W/m K	112	73		90
Application temperature, °C	–70 + 300		1,500	Up to 450
Composition, % mass:				
graphite				55
silicon carbide				45 (35—55)
free silicon (impurities)				3

Table 4.3 shows the properties of siliconized graphites. Friction units made of siliconized graphite are operational at temperatures up to 350 °C. Products made of siliconized graphite are resistant to aggressive environments: hydrochloric, acetic, phosphoric, sulfuric, nitric, formic, hydrofluoric acids, melted caprolactam, methyl chloride, ethyl acetate, and acetic anhydride [14].

4.2.4. Metal carbides (hard alloys)

In friction pairs of mechanical seals, alloys based on tungsten carbide are often used with various metal binders, which impart a certain ductility and impact strength to the hard alloy. Cobalt or nickel are most often used as metal binders, and nickel-cobalt binders are much less commonly used. In addition to tungsten carbide, in the mechanical seal assemblies of some manufacturers you can also find rings made of chromium carbide with a nickel binder or titanium carbide.

Table 4.4. **Properties of tungsten carbide and oxide ceramics**

Properties of material	Wolfram carbide — 92%, cobalt — 8% — U_1	Wolfram carbide — 92%, nickel — 8% — U_2	Wolfram carbide — 92%, nickel-chrome-cobalt — 8% — U_3	Oxide aluminum 99,5% — V	Dioxide zirconium 97%
Density, g/cm^3	14.3—14.9	14.8—14.9	12.5—14.6	3.8—3.9	5.7
Tensile strength at compression, N/mm^2	3,200—6,200	4,000—5,500	4,500—5,600	3,000—3,500	
Tensile strength at tensile strength, N/mm^2	>600	500—900	—	150—300	—
Tensile strength at bending, N/mm^2	1,500—2,150	1,200—1,900	1,300—3,500	250—400	650
Elastic modulus, 10^9 N/mm^2	550—620	600—630	570—590	350—380	200
Microhardness, HV	1,230—1,600	1,400—1,500	1,400—1,700	1,500	1,000
Linear coefficient thermal expansion, 10^{-6} 1/K	4.6—7	4.8—5.6	5.0—5.6	8.5	11
Thermal conductivity coefficient, W/m K	80—115	36—80	35—120	30	3
Maximum application temperature, °C	1,500	1,350	1,500	1,700	

Tungsten carbide gives the alloy rigidity, compressive strength, hardness, wear resistance, and the binder metal give impact strength and bending strength.

Tungsten carbide with cobalt as a binder has limited use, mainly for abrasive-containing media. Cobalt has low chemical resistance — it dissolves even in distilled water, and the cobalt bond of tungsten carbide rings is subject to severe corrosion in sea water. In addition, materials containing cobalt, which has a long half-life, cannot be used in seals for pumps in nuclear power plants [5]. If nickel is used instead of a cobalt binder, such phenomena do not occur [37].

Due to the low temperature coefficient of linear expansion of hard alloys (2—3 times less than that of corrosion-resistant steel), the deformation of friction surfaces is insignificant. The high thermal conductivity of hard alloys (only siliconized graphites and graphitized carbon graphites have higher thermal conductivity) makes them possible to use under conditions of high thermal loads.

In centrifugal energy pumps, mechanical seals with rings made of hard alloy are practically not used, possibly with the exception of pumps pumping liquids with a large inclusion of abrasive particles, for example, slurry pumps transporting coal pulp.

4.2.5. Oxide ceramics

The exclusivity of Al_2O_3 oxide ceramics is determined by its chemical resistance in environments with strong oxidizing properties, in which other materials are unstable, for example, in oleum.

Mineral ceramics are made on the basis of aluminum oxide. Thus, mineral ceramics *TsM-332*, containing 99% aluminum oxide (corundum), has high resistance in environments with strong oxidizing properties. Due to their fragility and relatively low thermal conductivity, ceramics are prone to thermal cracking during sudden cooling and rapid heating, so the "lubricant starvation" mode for ceramics is undesirable.

In the designs of mechanical seals, *TsM-332* mineral ceramics are used in combination with soft carbon-graphite materials. Aluminum oxide rings have not been used in pump seals.

Table 4.4 shows the properties of tungsten carbide and oxide ceramics.

4.2.6. Wear-resistant coatings and sprayings

One ring of the end pair is made of a relatively cheap material, usually stainless steel, with a hard wear-resistant coating applied to the end surface to reduce the cost of seals. This coating can be performed by plasma (gas plasma) or detonation method using aluminum or chromium oxide powders, tungsten, or chromium carbides. The thickness of these coatings does not exceed tenths of a millimeter. An important condition for the good performance of such rings

is the closeness of the coefficients of thermal expansion of the base material of the ring and the coating material. In addition to spraying, ring coatings are performed using galvanic methods: chrome plating, nickel plating, or oxidation. Also, the hardness of metal rings can be increased through heat treatment, nitriding, cementation, carbonitration, etc.

4.3. Auxiliary and secondary seal materials

Secondary sealing devices are a necessary component of the mechanical seal assembly. They serve to seal the places of radial and axial interfaces of rotating and non-rotating rings and sealing blocks with the shaft and housing parts and also provide the ability to elastically, at the level of micro-movements, monitor angular and axial influences in the sealing joint during the relative movement of the rings of a friction pair. The designs of secondary sealing devices are divided into two types: those formed on the basis of elastomeric ring and lip seals and those formed on the basis of elastomeric or metal bellows units (Fig. 4.1) [43].

Rubber rings of various cross-sections are the most common in the designs of secondary sealing devices, which is explained by the simplicity and low cost of such devices and their high tightness. Most often, O-rings, manufactured following standards, are used in mechanical seal assemblies.

The cross-sectional diameter of the rubber ring in the device is chosen to be as large as possible, which ensures when the ring is mated with adjacent parts of the device, its higher damping qualities in terms of response to angular micro-movements specified by the sealing joint during operation of the sealing unit.

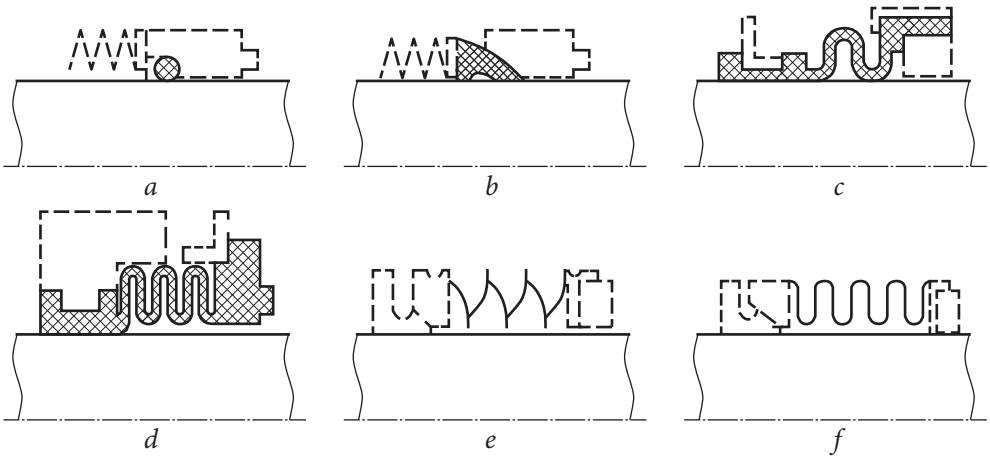

Fig. 4.1. Designs of auxiliary sealing devices for mechanical seals: *a* — rubber rings; *b* — fluoroplastic rings; *c, d* — bellows made of elastomers (rubber, fluoroplastic); *e* — welded metal bellows; *f* — seamless metal bellows

Table 4.5. **Recommended values of compressive deformation of the section of O-shaped rubber rings in sealing devices**

Shaft diameter d, mm	Ring diameter d_o, mm	Compression strain of the ring section, mm
15—30	4—5	0.5—0.7
30—100	5—6	0.7—1.3
100—200	6—8	1.3—2.0

Table 4.6. **Characteristics of elastomers used for the manufacture of sealing rings**

Elastomer name, rubber type	Suitability for use in environments	Unsuitable for use in environments
Nitrile, NBR, Butadiene nitrile	Hydrocarbons, oils, lubricants, fuels, weak solutions of acids and alkalis up to 20%	Ozone, ketones, ethers, aldehydes, chlorinated hydrocarbons, nitro compounds
Neoprene, CR Chloroprene	Weak solutions of acids and alkalis, ozone, fats, lubricants, fuels and solvents	Strong acids, ketones, esters, chlorinated, aromatic hydrocarbons, nitro compounds
EPDM Ethylene propylene	Water, steam, brake fluids, weak solutions of acids and alkalis	Mineral oils, solvents, aromatic hydrocarbons
Silicone, VMQ	Dilute acids and bases, ozone, sodium hydroxide, water and steam, some mineral oils	Solvents, oil, concentrated acids, sudden changes in environmental pressure
Polyacrylate	Ozone, high pressure, lubricants, hot oil, fats	Water, alcohols, glycols, alkali, ethers, aromatic hydrocarbons
Butyl, HR, Butyl rubber	Hot water and steam, gaseous media, acids and alkalis, oils, alcohols, ketones, ethers	Solvents, aromatic hydrocarbons
HNBR Hydrogenated butadiene-nitrile	Same as Nitrile, but improved chemical resistance, increased temperature resistance, and light ozone resistance	Ozone, ketones, ethers, aldehydes, chlorinated hydrocarbons, nitro compounds
Fluor silicone	Ozone, chlorinated solvents, oils, hydrocarbons and fuels	Brake fluids, ketones
Fluorocarbon, FKM	Aliphatic, aromatic hydrocarbons, acids, fats, various chemically aggressive media	Ketones, low molecular weight ethers and alcohols, nitro compounds, sudden changes in environmental pressure
Atlas, FFKM	Acids and alkalis, fuels, oils, sudden pressure changes	Freon, acetone, methyl butyl ethane, butyl acetate, tetrachloride carbons

Based on practical experience, the recommended values of compressive deformation of the ring cross-section in the sealing device should be of the order of 10—15%. Table 4.5 shows the compression values of rubber rings of various sections depending on the diameter of the shaft under the seal.

The long-term performance of rubber rings is achieved through their correct selection in relation to operating conditions.

In practice, such types of rubbers as ethylene propylene (temperature range of applicability from +40 to +150 °C), neoprene (from –40 to +150 °C), nitrile butadiene or *Buna N* (from –40 to +150 °C), fluor silicone (from –60 to +177 °C), fluor elastomer or *Viton* (from –18 to +200 °C) are widely used.

Recently, a number of new brands of rubber have appeared, such as *SB-26*, *26M, 26F, 26TF, PSB-26*, and *IE 06-02*. For the production of sealing parts for oil and gas production and petrochemical industries, rubber series *N-180*, *260*, and *400* were created based on nitrile-butadiene rubbers of different polarities (respectively *SKN -18, -26*, and *-40*). These rubbers are intended for the manufacture of rubber rings and cuffs. They differ from serial analogues by an extended temperature range, increased resistance to the accumulation of residual deformation, and anti-friction options by greater wear resistance [51]. Below are the characteristics of elastomers used for the manufacture of rings, with general recommendations for their applicability in sealed environments (Table 4.6).

4.4. Design and materials of axial clamping devices

A necessary element of any mechanical seal is a device that ensures that the sealing belts of the rings of the mechanical pair are pressed against each other. This device must create a certain initial contact pressure in the friction pair when parked, and when the machine enters operating mode, the contact pressure in the friction pair increases under the influence of the pressure of the product being compacted, i.e., hydraulic load. Various types of compression springs are used most often as devices for axial prestressing of the rings of the end pair, less often metal bellows or spring membranes, and even less often, rather exotic devices of magnetic clamping and hydraulic pressing.

Axial compression also acts as an elastic compensator for all possible axial and angular displacements of the axially movable element of the mechanical seal (ring or cage with a ring).

Cylindrical helical springs are used most widely as a device for constant axial preloading of the end pair rings. Central helical springs are used widely in mechanical seals for shafts with a diameter of up to 70 mm with a shaft rotation frequency of no more than 60 Hz. Typically, these springs are made with a small number of working turns (from one to three) in order to reduce the axial size of the seal as much as possible. The design of the seal is relatively simple. The use

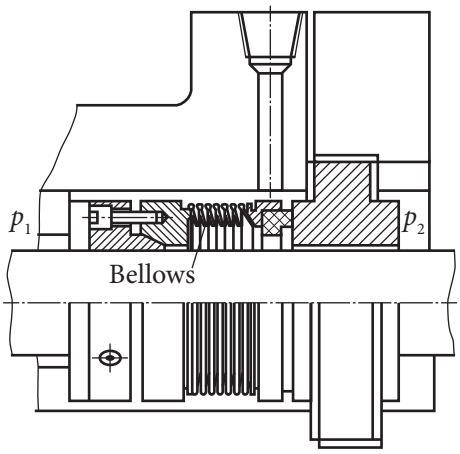

Fig. 4.2. Mechanical seal with fluoroplastic bellows

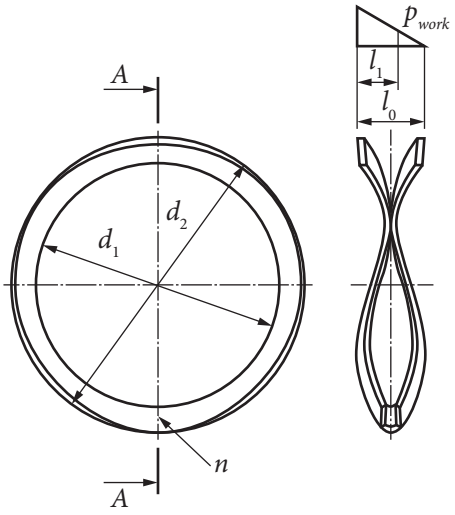

Fig. 4.3. Wavy spring

of large-diameter wire for the springs ensures their long-term performance in corrosive environments.

The disadvantages of the central spring are the uneven distribution of the load in the rubbing friction pair and the associated one-sided wear of the rings, the relatively large spring size in the axial direction, which entails increased axial dimensions of the mechanical seal.

Mechanical seals with multiple coil springs have a smaller axial dimension than units with a central spring. The use of a set of small springs allows them to be unified for some designs of mechanical seals — the same spring can be used for seals of different diameters. The compacting force can be adjusted by changing the number of springs and keeping the axial stroke of the elastic element constant. The disadvantage of elastic elements of this type is their low operating life in corrosive environments. Solid-drawn or welded bellows are widely used as a pressing device (Fig. 4.2).

Spring devices operate under high-frequency loads, often in very severe conditions associated with significant amplitudes of movement and often in a corrosive environment. The reliable operation of the device for axial preloading of the end pair rings is an important part of the overall reliability of the seal assembly.

Contact pressures in friction pairs from the spring force are selected within 0.1—0.5 MPa (the lower limit is for small fluid pressure differences; the upper limit is for large ones). The contact pressure from the conditions of seal reliability is taken to be higher than for loaded ones for hydraulically unloaded seals.

Wavy springs (Fig. 4.3) have become quite widespread due to the restrictions imposed by the international standard ISO 3069-2000 on the dimensions of seal chambers.

Springs are made from thin-sheet tape 0.3—0.8 mm thick from cold-worked steel or materials that acquire high elastic properties after heat treatment (for example, *Elinvar alloy* N 09902). The spring elements are connected by spot welding. The spring has a low height and is particularly attractive for double mechanical seals.

Cylindrical springs are made from steel carbon wire of class II, 251H60 , corrosion-resistant steel 420S45 (applicable up to a temperature of 400 °C) and steel AISI 316Ti , cold-worked wire made of steel 321S31, 321S51, 321S59, LW18, LW24, X6CrNiTi18-10 Springs can be made of *BrB2* bronze (applicable up to an ambient temperature of 150 °C) or from *Elinvar alloy* N09902 to operate in seawater conditions. *Elinvar alloy* N09902 is applicable for operating conditions at ambient temperatures up to 300 °C.

Springs made of alloys of the Ni-Cr-Nb system, such as 70NKHBMYu and 52NKHBMYu, as well as based on alloys of the Ni-Cr-Ti-Al system (alloys KhN77TYUR (EI437B), KhN68VKTYu (EP578), KhN67VMTYu (EP202)) are used to operate at high temperatures (up to 500 °C and above). In EU countries, the alloys *Inconel X*, *Inconel 718*, *Rene 41*, and *Nimonic 90* are used for this purpose.

It has been established that even slightly aggressive environments significantly affect the durability of springs. Thus, the durability of springs made of 40X13 steel, tested in industrial water, is 30% lower than the durability of springs tested in air. The durability of springs made of *Elinvar alloy* N09902 in industrial water is an order of magnitude greater than the durability of springs made of 420S45 steel.

Uncoated carbon spring wire can only be used in seals operating in oil and other petroleum products [45]. When seals operate on industrial water, copper and nickel plating are used as a protective coating for the wire. Zinc coatings protect against corrosion only in air and fresh water with temperatures up to +70 °C.

If it is necessary to manufacture springs from titanium materials, titanium alloys of the VT-16 and VT-23 grades are used for this.

4.5. Materials of main parts of mechanical seals

Housings, rotor bushings, axial movable races, and other metal parts of mechanical seals are made of steels and alloys that have good corrosion resistance in the pumped media at specified operating temperatures.

First of all, these are steels 420S37 , 321S31 , AISI 316Ti , AISI 904L , etc. As a rule, the corrosion resistance of mechanical seal parts should be higher than the resistance of the materials from which the pump flow parts are made.

In pump construction, low-carbon steels such as Steel M1020 , chromium steels such as 420S37 , AISI 420S, and much less frequently 321S31 and its analogs are widely used. Parts of the flow parts of pumps used in the energy sector are made of carbon unalloyed Steel 20L.

4.6. Design and materials of driving elements

It is necessary for the mechanical seal assembly to transmit torque from the rotating shaft to the rotating block and also fix a number of parts against angular displacement in both the rotating and stationary blocks to function. Several typical devices and connections are used for this purpose. Such devices and connections can be distinguished concerning the rotor parts of the seal, the stator parts, and the rings of the friction pair. Let's consider design solutions used to transmit torque or to protect against relative angular displacement of parts with regard to blocks and rings of mechanical seals.

Rotating blocks. To transmit torque from the shaft to the rotating seal block, screws, keys, springs, permanent connections, and threaded connections are used to fix the rotating ring of the pair.

Pin, key, spline connections, stamping bends, drivers, and bellows are used to transmit torque between adjacent parts inside the block.

Fixed blocks. Pins, screws, membranes, and bellows are used to secure the angular displacement of parts in a stationary block from the torque associated with the interaction of the rotating and non-rotating rings of the mechanical seal. Fixation of the rings included in the blocks from angular displacement relative to the adjacent part of the block is carried out using detachable connections: pin, key and spline connections, stamping bends, and leads.

4.7. Selection of friction pair materials

Based on the above, using the generalized experience and recommendations of world-famous manufacturers of mechanical seals, we can set out recommendations for the selection of materials for friction pairs of mechanical seals for energy pumps. First, one must proceed from the fact that, in most cases, it is necessary to compact feed water, steam condensate, and other water-based liquids containing acids and alkalis, which form crystalline deposits upon contact with the atmosphere.

The mechanical seals of feed, network, and condensate pumps often use a friction pair of siliconized graphite on siliconized graphite (*SG-P* on *SG-P*) or silicon carbide reaction sintered on siliconized graphite. This combination of materials is used due to the fact that water, especially at temperatures above 60 °C, has poor lubricity and cannot form a stable lubricating film on the end flanges of the rings, and therefore, to ensure the required service life and wear resistance, it is necessary to use solid materials in the friction pair containing graphite.

In the Western school of mechanical seals for water, a combination of hard and soft silicon carbide and carbon graphite usually impregnated with antimony, is used traditionally. Such a friction pair of a contact seal has the maximum possible range of application in terms of *PV* factor due to the antifriction properties of graphite and the thermal resistance of its impregnation. Unfortunately, antimony does not have chemical resistance in solutions of acids and alkalis, so graphite with such impregnation is used only in neutral liquids that do not contain solid abrasive inclusions. In chemically active liquids, graphite should be used impregnated with resins, which gives it greater chemical resistance, but this reduces the limit of use in terms of the *PV* factor.

Materials with high chemical and abrasive resistance are used in mechanical seals for chemical energy pumps, which are used in water treatment systems and supply of boron-containing water. Preeminently, these are ceramic materials, the content of free silicon in which does not exceed 1—2%. These include hot-pressed silicon carbide Q_2, siliconized graphite *GAKK 55/40*, composite materials based on pure silicon carbide, and graphite (*SiC-C*), which have been actively used since the beginning of the 21st century.

Mechanical seals for fuel oil pumps mainly use friction pairs made of reaction-sintered silicon carbide (*Si-SiC*) or tungsten carbide-based hard alloy. The hard-on-hard combination provides high wear resistance in abrasive fluids, while the long hydrocarbon molecules form a stable lubricating film separating hard, wear-resistant surfaces.

4.8. Conclusion

The history of the development and improvement of mechanical seals is connected closely with progress in the field of materials science. The creation of new chemically resistant and wear-resistant materials with antifriction capabilities is a decisive factor for increasing the time of normal trouble-free operation between scheduled repairs, expanding the range of their use towards higher sliding speeds, compacted pressure, and temperature differences.

It should be noted that in modern mechanical seals, friction pairs made of hardened steel X102CrMo17 on soft graphite impregnated with babbitt or an alloy of tin and lead (AG-1500 B83 and AG-1500CO5) are no longer used practically. Heat-strengthened bronze tool steel is used only in seals of gear pumps in oil supply systems for sliding bearings of large centrifugal pumps and electric motors. This is only because the designs of these pumps, together with the seals, were developed at least 50 years ago, when the design of the seal and pump was developed by pump specialists, and the issues of manufacturability and low cost of products that were mass-produced were at the forefront.

At the same time, siliconized graphites, invented in the USSR in the 70s of the last century, turned out to be such a successful solution for seals of pumps

pumping clean water that mechanical seals with friction pairs made of siliconized graphites of the *SG-P*, *SG-P 0.5*, and their modern analogues are successfully used in energy pumps at present and will be used for many decades to come.

Over the past decades, some new promising ceramic materials have been created, which will soon find their application in mechanical seals. These include silicon nitride (SiN_4), which has very high resistance to cracking; superhard boron carbide (*BC*), whose wear resistance and hardness exceed those of hot-pressed silicon carbide; and zirconium dioxide ZrO_2, which has a linear coefficient of thermal expansion, the same as steel and many other.

Also, a characteristic feature of the modern level of development of sealing technology is the use of diamond-like coatings (Diamond Like Coating — *DLC*) on silicon carbide rings, which significantly increase the service life of the friction pair and allow stable operation in conditions of insufficient lubrication and poor cooling. As a result, *DLC* ring seals are increasingly being used in feed pumps and other hot water pumping equipment.

CHAPTER 5

MANUFACTURING TECHNOLOGY OF MECHANICAL SEALS

Mechanical seals are high-precision units. The requirements for the manufacture of sealing parts and the assembly of components are very high; therefore, their implementation in pumps instead of stuffing box seals was quite difficult (due to high requirements for installation and maintenance). First, end assemblies were made by pump manufacturers, but the manufacture, assembly, and maintenance of this type of seal required a different, higher level of technology and personnel training than was required when using gland seals in pumps. The transition to mechanical seals became an important stage not only in the development of pump engineering but also largely determined the level of development of centrifugal compressors.

The service life of a seal is determined not only by its design and materials used but also by the quality of manufacture of the pump or compressor (degree of alignment, radial and axial runout of the shaft surface in relation to the housing, quality of bearings, etc.). In addition, the operation of the sealing unit is influenced by the temperature and pressure of the sealed medium, the nature of the start-stop mode, the quantity and quality of the supplied barrier liquid (gas), as well as some other factors related to the operation. Therefore, installing an expensive seal in a conventional water supply pump, for example, intended for a nuclear power plant pump, may not justify the resource declared for it due to low requirements for the manufacturing accuracy of the pump itself and its operation [15].

When producing mechanical seals, the manufacturer faces several specific questions regarding the technology of manufacturing the rings of the mechanical seal, the connection of the rings of the friction pair with the enclosing races or adjacent parts, the requirements for the rubbing end sur-

face of the rings in terms of the accuracy of manufacturing linear dimensions, roughness, and flatness, the technology of manufacturing specific spring seals, elements, requirements for assembling mechanical seals in the product.

The nature of the problems listed and the solutions proposed by practice are quite specific. This led to the need to separate the production of mechanical seals into a separate industry, which, along with bearings, became one of the strategic branches of industrial production. There are always companies in industrialized countries engaged in the mechanical seal assembly production and their supply to the world market as a high-tech product.

Let's look at some issues related to the manufacture of mechanical seals.

5.1. Manufacturing of mechanical seal rings

The production of mechanical seal rings involves a number of technological processes:

- mechanical restoration;
- connection of rings with reinforcing clips;
- fine-tuning the working surfaces of friction pairs;
- quality control of lapped ring surfaces.

5.1.1. Processing of friction pair rings

Rings of friction pairs made of carbon and some other materials (except for *SG-P*, *SG-T*, as well as tungsten, silicon, and aluminum carbides) are made by processing with a blade tool on screw-cutting lathes. Processing is carried out with cutters with plates made of hard alloy *HG30, HG40* with the following geometry of the cutting part:

- front angle of cutter sharpening — 10°;
- rear angle — 8—10°;
- main plan angle — 45—60°;
- radius at the apex — 1.0—1.5 mm.

Cutting modes: speed — 1.5—1.83 m/s; feed per revolution — 0.1—0.15 mm/rev; cutting depth — 1—3 mm [26].

Rings of friction pairs made of siliconized graphites *SG-P, SG-T*, as well as tungsten, silicon, and aluminum carbides, are processed by grinding on universal grinding machines. Grinding is carried out using diamond wheels of the *ACP* brand, grain size 100/63. An emulsion containing 2—3% soda is used as a cutting fluid [26].

Rings of friction pairs made of aluminum carbide-silicon (siliconized) graphite *GAKK 55/40* are processed with diamond cutters or cutters with plates made of hard alloy *HG30, HG40* on lathes. When using diamond cutters, cutting mode: speed — 1 m/s, feed — 0.5 mm/rev, cutting depth — 1.5 mm.

GAKK 55/40 graphite rings can be threaded. For example, for cutting M60x1.5 threads, carbide plates are used under the following modes: spindle speed 50—60 min–1, cutting depth — 0.25 mm [18].

When developing a technology for machining carbon parts, you can also use the recommendations of the German company Schunk, which produces carbon-graphite materials for friction rings.

Cutting and Sawing. It is recommended to cut (saw) carbon materials in a dry environment, i.e., without additional lubricants or coolants, using a continuous band saw with carbide or diamond teeth.

Turning. As a rule, preliminary processing is carried out with cutters made of hard alloy *VK10* with a rake angle of 0—3° and a rear angle of 16—20°. The average depth of cut during roughing is 3—5 mm with a feed of 0.2—0.4 mm/rev and a cutting speed of 0.7—1.2 m/s.

The cutting depth during finishing is 0.20—0.25 mm, with a feed of 0.2—0.5 mm/rev and a speed of 1—1.8 m/s. The geometry of the cutting edges of the finishing cutter is similar to that described above. Typically, the processing is carried out without coolant with good exhaust ventilation.

Milling. Performed using cutters with hard alloy inserts. The cutter geometry, feed, and rotation speeds are recommended to be the same as when turning with a cutter. If necessary, tools with diamond coatings also can be used. Typically, milling is done in a dry environment. When diamond tools are used, water cooling is used without additional additives.

Drilling. The usual drill material is carbide. The drill tip angle is in the range of 80—85°, and the clearance angle is 16—20°. Large diameter holes are drilled with diamond-coated tubular drills.

Grinding. Coarse grinding is carried out using a wet method on two-circle through grinding machines with a uniform feed. Wheels made of silicon carbide or diamond coated are used. Grinding accuracy — 0.02 mm with a surface roughness Ra = 1.8 μm.

In surface grinding machines, grinding is carried out using the dry method and only with silicon carbide wheels. In this case, the surface roughness reaches Ra = 0.8 μm, and the accuracy is 0.02 mm.

Eccentric grinding is carried out with a cooling medium with achievable accuracy of IT6 quality. With high-speed grinding of outer diameters, tolerances of IT7 quality are achieved. The wheels can be ceramic or diamond with a bronze bond. Internal grinding is carried out using grinding rods of appropriate grit.

In the manufacture of rings and associated parts, the accuracy of the rubbing and supporting end surfaces in terms of their deviations from perpendicularity is important. The axial runout of such surfaces when making a friction belt should be within 0.02 mm.

The width of the friction surface of rings made of siliconized graphite and silicon carbide must be greater than the width of the mating ring made of soft antifriction material. When using both elements of a friction pair made of siliconized graphite or silicon carbide, the width of the friction surface can be the same.

It is advisable to subject parts made of siliconized graphite and silicon carbide to natural aging (about 10—15 days) after machining and before final finishing to relieve internal stresses. Grinding provides a surface roughness [18] of the order of Ra = 0.8 μm.

Hydrodynamic grooves and chambers are made by etching, milling, ion milling, and laser. It is also possible to "build up" the contacting surface with a hard, wear-resistant coating made using plasma spraying using the "mask" method.

Friction pair rings for operating conditions at low pressures are made without reinforcement. This design of the rings is especially effective in conditions where high temperatures occur during the operation of the friction unit.

At elevated pressures, taking into account the low strength of graphite or for economic reasons, graphite rings are installed in metal cages. A strong connection to the holders is ensured by an interference fit or an adhesive connection. Issues related to such a connection are discussed below.

5.1.2. Connection of rings with reinforcing clips

When designing friction units using rings made of ceramics, siliconized, and other graphites, it is necessary to take into account that their linear expansion coefficients are much lower than for steels and alloys. A rigid fit of graphite rings on a metal shaft or installation in a cage can cause the destruction of the rings during operation under the influence of the unit heating, for example, from heat generated by friction. Due to lower tensile strength than compressive strength, graphite rings should be fixed (pressed and glued) along the outer diameter.

A hot fit, in which the metal holder is heated 100—150 °C above the operating temperature, and then graphite parts are inserted into it, is used to secure parts from turning during the operation of the seal assembly. When cooled, the metal clip tightly compresses the inserted ring.

The latter is performed using adhesives or resins (phenol-formaldehyde, epoxy, etc.), which are applied to a part made of ceramic or graphite in order to reliably seal the place where the ring fits into the cage. With such a fit of the mechanical seal rings, the adhesive is applied only to the cylindrical part of the ring. O-rings are sometimes secured using a union nut design.

The given methods for fastening the sealing rings of mechanical seals made of graphite or ceramic require final processing (finishing) of the friction surfaces of the rings after they are fixed into the cage.

Loose fit into the cage (without tension) eliminates the need to adjust the rings during operation. In this case, anti-rotation fixation is ensured by making in the ring's flats, grooves, and corresponding locking elements in adjacent parts or by using pin connections in conjunction with adjacent parts.

5.2. Grinding in and checking the flatness of sealing bands

Lapping (abrasive processing) is a quick and effective way to remove stock. The term "lapping" still conjures up images of ultra-fine, mirror-like finishes, and slow, labor-intensive material removal. In many cases, especially when machining complex shapes, lapping is much faster, better, and less expensive than traditional stock removal methods.

Lapping is not limited to obtaining only flat surfaces. It is often used to produce convex as well as concave surfaces with the highest degree of precision and finish. Super-machined ball bearings are an example of the precision lapping process for spherical shapes. Internal and external cylindrical surfaces are also easily produced using this abrasive finishing method. It is necessary to use the correct abrasive media and lapping material to remove stock quickly and efficiently using the lapping method. Course abrasives provide quick material removal but leave rough scratches; therefore, three or more abrasive grains are usually used. Regular grit is for quick stock removal, medium grit is for removing rough marks left by regular grit, and fine grit is for finishing lapped surfaces.

The following describes various ring-sealing surface lapping methods, equipment, and inspection methods.

5.2.1. Finishing the working surfaces of friction pairs

Many years of experience in operating mechanical seals have shown that the quality of the surfaces forming the sealing pair is ensured by meeting certain requirements for the roughness and non-flatness of these surfaces.

Because Mechanical seal ring surfaces are used to relieve high pressure on a very narrow surface, they must be lapped flat to within a few microns and have reflective, scratch-free sealing surfaces. Failure to do this usually will result in either excessive leakage or premature seal failure. Fig. 5.1 shows convex (*a*) and concave (*b*) working surfaces, which, since they are not flat, greatly change the seal balance as well as the contact surface area.

In the dry lapping process, the lapping abrasive is rolled or pressed into a lapping plate (lap), after which the lap is thoroughly washed and blow-dried. Although there are several lapping abrasives, such as aluminum oxide, silicon carbide, or boron carbide, that can be used, the most widely accepted recommendation is diamond paste. The dry lapping process is where the lapping abra-

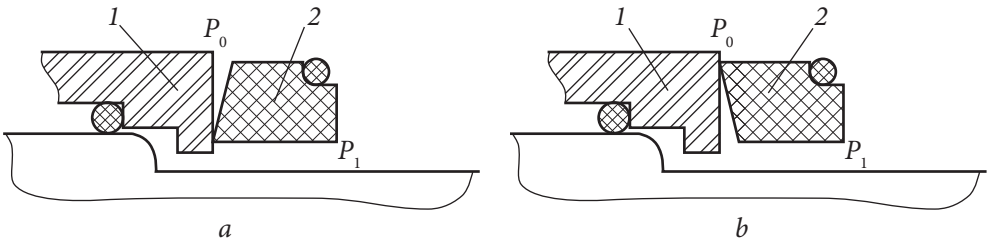

Fig. 5.1. Shapes of the working surfaces of the mechanical seal rings: *1* — rotating ring; *2* — fixed ring

sive is introduced into the lap, rather than the parts being dry lapped without lubrication. Theoretically, during this process, the lap does not wear out since the part being lapped comes into contact only with the sharp ends of the embedded abrasive. Dry lapping can be done using hand-lapping plates or a machine.

The friction surface of the rings is processed with a roughness of Ra = = 0.015—0.2 microns and with deviations from flatness of no more than 0.6 microns, which is achieved by finishing operations on lapping plates. The finishing technological process comes down to smoothing out surface irregularities using abrasive powders in the presence of lubricants. The lubricating fluid forms a layer between the surfaces of the lapping plate and the ring that is saturated with abrasive material. The thickness of the layer should not exceed the size of the abrasive (otherwise, the finishing performance is low); therefore, low-viscosity liquids such as water and kerosene are used for finishing.

In mass production conditions, machine finishing is used on lapping machines. Manual finishing is used on lapping plates for single production and repair work. Various abrasive powders can be used to refine the sealing surfaces of the friction pair rings: white electrocorundum, carborundum (black silicon carbide), boron carbide, and synthetic diamond.

Electrocorundum grains have the lowest microhardness ($2 \cdot 10^{10}$ Pa). White electrocorundum has the best cutting ability (finishing with this material is highly productive and provides good surface quality). Carborundum has high hardness, but its grains are brittle and fragile, making it difficult to achieve high productivity when working with this material.

Boron carbide is a durable and hard ($4 \cdot 10^{10}$ Pa) material. When finishing with boron carbide powders, high productivity is achieved, but the surface quality is lower than when finishing with electrocorundum, so boron carbide powders are recommended mainly for preliminary finishing.

Selecting diamond powders with a specific combination of hardness and grain size ensures low surface roughness and significantly reduces finishing time. Diamond pastes are produced based on synthetic diamond powders and are used for finishing friction pair rings made of hard materials.

Diamond pastes consist of diamond grinding powders of the *AC4* and *AC6* brands and micro powders of the *ASN* and *ACM* brands, as well as a special filler and dye. Pastes with *AC4* and *AC6* powders are intended for grinding and rough finishing of various materials. Pastes with *ASN* and *ACM* micro powders are intended for polishing, finishing, and fine polishing products made from alloys of ferrous and non-ferrous metals, as well as non-metallic materials.

Diamond pastes are produced from micro powders of the *ACM* and *ASN* brands with a grain size of (60/40)—(0.1/0) microns and from grinding powders of the AC4 brand with a grain size of (125/100)—(50/40) microns.

Diamond pastes can be:

- with normal (N), increased (P) and high (H) concentration of diamond powder;
- ointment-like (M), solid (T) consistency;
- with organic (O) and universal (VO) solvents.

An example of a symbol for a paste made from synthetic diamond powders:

Diamond paste *ACM 7/5 NVM*. Here, *ACM* is the powder brand, 7/5 is the grain size, N is the normal mass fraction of diamonds, V is washable with water, and M is a paste-like consistency.

When choosing an abrasive material, the hardness of the abrasive must be higher than the hardness of the surface of the friction pair element being ground (Na/Nm = 1.3—1.7).

The main purpose of preliminary finishing is to eliminate the waviness of the treated surface and bring it to the required flatness. Since this involves removing a thin layer of material from most of the surface of the processed ring, coarse abrasives are used, which increases finishing productivity, but the surface resulting from this operation is rough.

Cast iron and glass laps are used as the main tool for manual finishing. The hardness of laps made of gray cast iron of a homogeneous structure with a pearlite base is 140—150 HB. To increase wear resistance, fine-grained pearlitic cast iron with the addition of chromium or molybdenum (150—200 HB) can be used.

Cast iron laps are usually made in the form of a circular disk (for more uniform wear and to avoid deformation) with dimensions:

- Ø 350 × 30 mm for finishing rings with a diameter of up to 180 mm;
- Ø 430 × 40 mm for finishing rings with a diameter of up to 300 mm.

Glass laps are made from annealed glass of the *MKR-1* brand (*Pyrex* or *LK*). The lapping set includes six plates: three — a set for preliminary finishing of rings, three — a set for final finishing. The working surfaces of the plates are ground on a surface grinding machine to Ra = 0.8 μm and a non-flatness of 0.01—0.02 mm.

Preparing slabs for work. After grinding, the plates of the set are ground one after another using the "three plates" method in the sequence:

- the first slab on the second, then on the third;
- the third plate on the second, then on the first;
- the second slab on the first, then on the third.

5—10 g of electrocorundum (M28, M20 — for preliminary finishing, M10, M7 — for final finishing) are evenly poured onto the plate to be ground, and the plate is moistened with kerosene (5—10 g). Then, apply the second plate and grind in a circular motion in the form of the number "8", and the edge of the movable lap should periodically extend beyond the edge of the fixed one by 30—50 mm.

The straightening of glass laps is similar to the straightening of cast iron laps, with the only difference being that powder of grain size M28 is used as an abrasive, and clean water is used as a lubricant [17].

After straightening, the laps are coated with electrocorundum abrasive powder of grain size M14 — M28, for which 1.5—2 g of powder and 5—10 drops of water are applied to the glass lap. Then, grinding is performed with light movements of the upper circle along the lower one in the form of the number "8". The duration of the pattern is 3—4 minutes. The duration of patterning is 3—4 minutes. After grinding, the laps are thoroughly wiped with a stiff hair brush under running water [17].

Lapping is considered suitable for use if their surface has a non-flatness of no more than 1.5—2 μm. Finishing of sealing rings made of graphite materials. The friction surfaces of the mechanical seal rings made of siliconized graphite *SG-T* and *SG-P* are fine-tuned after their final processing to the size of pressing or gluing into the cages; then, no mechanical work with the rings and their cages is advisable.

When pre-finishing rings made of siliconized graphite, use diamond pastes *ACM 40/28, ACM 28/20, ACM 20/14*, diamond powder, or boron carbide, grain size M40, M28, M20; for final finishing — diamond pastes *ACM 14/10, ACM 10/7, ACM 7/5,* diamond powders or boron carbide powder with grain sizes Ml4, M10, M7, M5.

The final finishing, aimed at obtaining the required surface roughness, is carried out with fine-grained powder with a gradual reduction in the size of the abrasive grains as the quality of the surface of the part being ground improves.

Contact pressure on the ground surface is 0.03—0.06 MPa for preliminary lapping and 0.01—0.03 MPa for final finishing. Part movement speed — 0.1—0.5 m/s; An increase in speed and contact pressure is undesirable due to heating of the part, plate, and distortion of the shape of their surfaces.

Finishing is done by moving the ring in the form of the number "8", sometimes alternating with circular movements. During the finishing process, the ring must be periodically rotated around its axis by 60—90°. The average paste consumption per ring with a working belt diameter of 50—70 mm is 0.05 g.

Rings of friction pairs made of carbon materials of grades *2P-1000*, *Khimanit*, *AO-1500-S05*, etc., are pre-finished on glass laps using electrocorundum M5, M3, and finally — on cast iron laps. Pure kerosene is used as a lubricant.

Finishing is carried out until a smooth matte surface is obtained with a roughness of no more than Ra 0.16 μm. After finishing the friction pairs and holding them for a certain time, in some cases, deformations of the lapped surfaces in the form of waviness are observed.

When using press fits to connect rings to races, stresses are created in the rings; relaxation effects last for a long time. Due to various types of deviations in the size of the joints during the manufacture of parts, the exact distribution function of the contact pressure in the connection of the ring and the holder is unknown. The analysis of such connections showed [25] that the distortions in the flatness of the rubbing surface of the ring have a pronounced, mostly two-wave character in the shape of the ring bending.

To eliminate residual deformations, artificial aging of rings with cages can be carried out by heating or alternating heating and cooling [17]. After final processing, the part is cleaned of abrasives, washed with gasoline, and degreased with acetone.

The controlled surface must be shiny to ensure flatness control with PI glass plates. Shine is achieved by finishing on a carved lap in the following order: 1—2 g of ACM 10/7 diamond paste is applied to the cast iron lap, and 8—10 drops of kerosene are added and rubbed with a swab over the lap. Grinding of the lap is carried out with a second lap, superimposed on the first, by moving the upper lap in the form of the number "8". Sharging is completed with a sharp increase in the sheer force of the lap; then, the lap is cleaned of free abrasive with a gauze swab, washed with gasoline, and degreased with acetone.

The shine on the treated surface is obtained by moving the part along a curved lap in the form of a number "8" with a pressure of 500—1,000 Pa and a movement speed of 0.3—0.5 m/s.

Finishing of sealing rings made of steel and alloys. O-rings made of steel and alloys must be heat-treated to relieve internal stress; otherwise, the rings may warp during operation, causing increased leakage. Finishing of the sealing rings is the final operation, after which machining, metalworking, welding and soldering of solid, glued and pressed sealing rings and clips into the cages are not allowed.

Sealing rings made of steel and alloys are finished using cast iron laps. When finishing sealing rings made of steel and alloys with a hardness of less than 40 HRC, abrasive powder made of corundum, white electrocorundum, normal electrocorundum with a grain size of M20-M5, and *GOI* paste are used. Apply 1.5—2 g of abrasive powder and 8—10 drops of lubricant (kerosene with the addition of 2% stearin and 5% spindle oil) to the lap. The mixture of powder and lubricant is rubbed evenly over the lap. The finishing of the sealing rings is carried

out by moving (in the form of the number "8") the workpiece along the lap surface. Powders with a grain size of M20-Ml0 are used for preliminary finishing, for final finishing — M7-M5 and *GOI* paste. During processing, it is necessary to periodically rotate the ring being processed through an angle of 90°. Finishing is completed when a uniform matte color is obtained on the treated surface with a roughness of Ra = 0.1—0.2 microns. A shine is obtained on the surface being processed to make it easier to control the flatness of the PI glass plates. Paper coated with a thin layer of *GOI* paste is used as a rubbing surface to do this.

When finishing sealing rings made of steels and alloys with a hardness above 40 HRC, abrasive powder from boron carbide, silicon carbide, white electrocorundum, iron oxide, and *GOI* paste are used. Abrasive powders with a grain size of M28-M10 are used for preliminary finishing and for final finishing — M7-M3, iron oxide, and GOI paste. Diamond pastes and powders are used during preliminary finishing to polish rings with a hardness greater than 60 HRC.

5.2.2. Finishing of sealing rings made of polymer-based materials

O-rings made of polymer-based materials are polished on glass laps made of annealed glass, MKR-1 (Pyrex), or LK, coated with abrasive. Before finishing, glass laps must be straightened using the three-lap method using abrasive electrocorundum powder with a grain size of M14-M20 and lubricated with water. After straightening, the laps are coated with electrocorundum powder with a grain size of M14-M28; for this purpose, 1.5—2 g of powder and 5—10 drops of water are applied to the lap. Then, another glass lap is placed on the lap with abrasive and the grinding is carried out by moving the upper lap over the lower one (in the form of the number "8") with light pressure.

The friction surface of sealing rings made of polymer-based materials is fine-tuned on the surface of a glass lap, thoroughly washed with water, with a continuous supply of water. The load on the ring to be ground should be in the range of 50—1,000 Pa; the ring movement speed should be 0.1—0.2 m/s.

Friction pair rings made of fluoroplastic and *F4K20*-type materials are finished on glass laps without the use of abrasive. The role of the abrasive, in this case, is played by the marks on the laps formed during the finishing process of the laps. Pure water is used as a lubricant. When finishing, you should periodically monitor the laps and prevent the finishing of the sealing rings without supplying a lubricant [17].

5.2.3. Quality control of lapped ring surfaces

The cleanliness of the surface treatment of parts can be controlled by the results of processing measurements of their roughness obtained using a profilometer

Fig. 5.2. Scheme for measuring the flatness of the surface of rings using a glass plate PI

or by reference samples (cleanliness standards) made of the same material as the part being tested. Cracks, chips, cavities, and other defects on the contact surface of a pair of rings are not allowed.

A generally accepted method for monitoring the flatness of the friction surfaces of seal rings is the interference method. It consists of visually assessing the pattern of interference light fringes on the controlled surface by placing a flat glass plate on it for interference measurements. When checking flatness, both daylight and artificial monochromatic light are used (for this, devices with "helium" and "sodium" lamps are used).

When testing flatness using the interference method, the tested surface roughness should be no more than Ra 0.16 μm; otherwise, interference fringes are visible with great difficulty or are not visible at all. To improve their visibility, after finishing, the working surfaces of the rings are lightly polished by hand on clean coated or thick drawing paper placed on a lapping plate. In this case, the surface roughness changes little, but the surface acquires some shine.

Before checking the flatness, the glass plate and the tested surface are wiped with a clean soft cloth soaked in alcohol. When using natural light, the glass plate is applied to the controlled surface with slight pressure and shift, achieving contact that produces the smallest number of interference bands in the light spectrum.

Fig. 5.2 shows a diagram for measuring the flatness of the surfaces of mechanical seal rings using a glass plate PI using natural light. Each formed strip indicates a deviation of the tested surface from flatness by 0.3 μm. The number of interference fringes intersected by a straight-line segment in the direction perpendicular to these fringes, and multiplied by 0.3 μm, is the non-flatness of the surface on this segment. Curved stripes indicate that there are deviations from flatness in the form of bulges or depressions on the working surface of the ring. Deviation from flatness is determined by counting stripes of the same color.

In case if the glass plate is displaced in the vertical plane relative to the sample by a small angle, rectilinear parallel stripes are detected; then, the controlled surface has deviations from flatness of less than 0.3 μm.

With a decrease in deviations from flatness of less than 0.3 μm, the light stripes disappear, and when illuminated by daylight, the surface of the test sample, in the case of pressing the plate to the surface, is painted first green, pink,

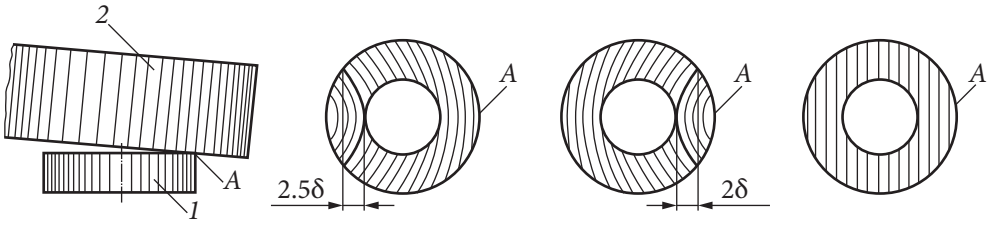

Fig. 5.3. Illustration for determining the flatness of ring surfaces using the interference method

then blue and, finally, light yellow ("straw") color. In the latter case, deviations from the flatness of the sample surface do not exceed 0.2 μm. This picture can be observed on metal and dark (for example, carbon-graphite, etc.) surfaces.

Under monochromatic illumination, the plate is placed on the controlled surface without pressing, forming contact with the surface of the ring, for example, at point *A* (Fig. 5.3). In this case, an air wedge is obtained as a result of loose contact of plate (*2)* with the surface of the controlled ring (*1)* (Fig. 5.3, *a*). The refraction of light in this gap leads to the appearance of dark-colored interference fringes on the surface of the plate. A series of parallel and evenly spaced straight stripes indicates that the part is optically flat and the deviation from flatness is less than 0.3 μm (Fig. 5.3, *d*). Curved stripes show that the surface is optically non-flat: concave (Fig. 5.3, *b*) or convex (Fig. 5.3, *c*).

Determination of non-flatness is carried out in the following sequence:

• determine the base interference line and the points of its intersection with the outer diameter of the sealing ring (the base interference line — the line touching the top of the inner diameter of the sealing ring, is shown thickened in Fig. 5.3);

• mentally connect with a straight line the points of intersection of the base line with the outer diameter of the ring and determine the number of interference fringes visible on the plane of the ring, cut off by a straight line from the inner diameter of the ring when connecting it with the points of the base line on the outer diameter of the ring (see Fig. 5.3);

• calculate the non-flatness as the number of cut-off light bands multiplied by the light wavelength of the source (for a helium illumination source, 5 = 0.29 μm).

Control of the flatness of a surface having a diameter greater than the diameter of the PI plate is carried out in separate sections, overlapping one section with another by sequentially rearranging the PI plate [18]. Based on experimental studies and experience in the production and operation of mechanical seals, the maximum deviations from the flatness of their friction pairs should not exceed 0.9 μm (three interference fringes). In this case, the circular interference fringes must be closed.

Fig. 5.4. Interference fringe patterns when measuring the flatness of ring surfaces using PI glass plates: *a* — normal plane; *b* — fine-tuning is needed

Fig. 5.4 shows the types of interference fringes encountered when monitoring flatness in rings. Of these, the group of rings in Fig. 5.4, *a* is suitable for assembly into a mechanical seal assembly; the group in Fig. 5.4, *b* — is unsuitable for use in a mechanical seal assembly and needs to be fine-tuned.

5.3. Manufacturing of main parts of mechanical seals

5.3.1. Manufacturing of spring elements

Cylindrical coil springs. Winding of helical springs is carried out on screw-cutting lathes using a special device. Small springs are made on automatic machines. After coiling, the springs undergo special heat treatment [18].

Springs made from wire II (GOST 9389-75) are tempered to relieve stress. The springs are laid in one row on a steel sheet and loaded into an electric oven or a special cabinet at 240—280 °C. After holding for 30—40 minutes, the springs are cooled in air.

Springs made of steel 420S45 are subjected to hardening and subsequent tempering. The springs are placed in an oven heated to 1,000 °C, and after the temperature has equalized, they are kept for 15—20 minutes. Springs are covered with carburizer or clean dry charcoal to protect them from decarburization when heated. After exposure to the oven, the springs are immersed in a bath with oil heated to 60—80 °C (machine, spindle, or industrial). Cooled springs are washed in a hot 10% soda solution and tempered at 250—350 °C for 1.5 hours. The hardness of the springs should be 43—48 HRC.

Springs made of steels 321S59 and AISI 316T are wound from the cold-worked wire as delivered. After winding and grinding the ends, tempering is performed at 420 °C with a holding time of 20—30 minutes. Then, the springs are cooled in the air.

Helical springs made of *Elinvar alloy* N09902 are wound from the cold-drawn wire as delivered, tempered at 600—700 °C. Electropolishing is recommended to increase the corrosion-fatigue properties of springs made *Elinvar alloy* N09902 (the following composition is used as an electrolyte: 86—88% orthophosphoric acid; 10—12% chromic anhydride; 2% distilled water).

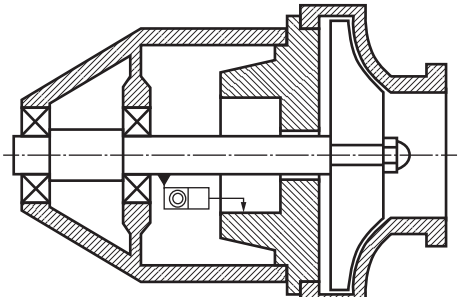

Fig. 5.5. Shaft misalignment with respect to seal chamber

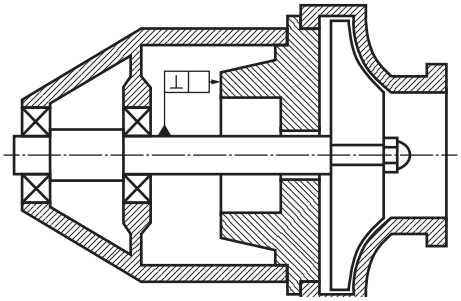

Fig. 5.6. Deviation from perpendicularity

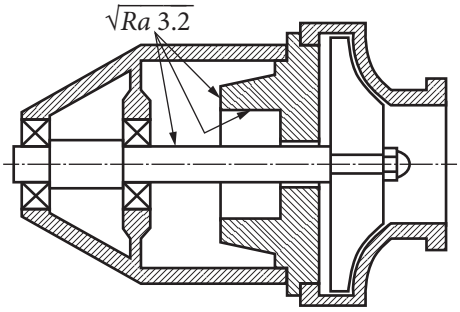

Fig. 5.7. Roughness of seating surfaces

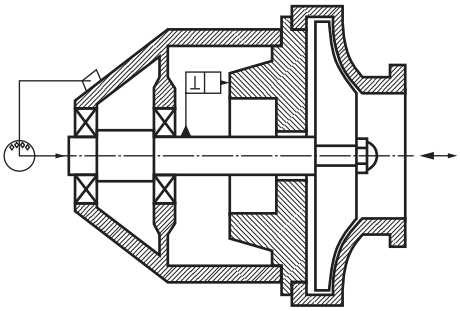

Fig. 5.8. Axial movement of the pump shaft relative to the housing

All helical springs are subjected to "bonding" (compression springs are compressed until the coils touch each other for 6 hours).

Wavy springs. Billets of wavy springs from *Elinvar alloy* N09902 are made from cold-worked tape with a thickness of 2.0 mm. When a wave is formed on the surface of the ring, the outer and inner diameters of the workpiece decrease. When designing tooling, it is usually assumed that 70% of the wave height is formed as a result of reducing the diameters of the workpiece and 30% as a result of its drawing. The spring elements are fastened by spot welding along all wave troughs or at two diametrically opposite points. The welding mode is selected depending on the thickness of the tape. The welded spring is subjected to hardening at a temperature of 920—950 °C and subsequent dispersion hardening at 650—700 °C with exposure for 2—4 hours.

5.3.2. Basic requirements for pump parts

Shaft misalignment. The shaft misalignment against the seal chamber (Fig. 5.5) should be no more than 0.2 mm.

Deviation from perpendicularity of the end surface of the seal chamber. The deviation from the perpendicularity of the end surface of the seal chamber relative to the shaft (Fig. 5.6) should be no more than 0.1 mm.

Roughness of seating surfaces. The roughness of the seating surfaces of the seal chamber and shaft at the installation site of the mechanical seal (Fig. 5.7) should be no more than Ra 3.2.

Axial movement. The axial movement of the pump shaft relative to the housing (Fig. 5.8) is no more than 2 mm.

Lead-in chamfers on the shaft and seal chamber. To avoid damage to secondary seals (rubber rings with a circular cross-section) during installation, the lead-in chamfers on the shaft and seal chamber must be at an angle of 15—30 degrees and at least 2.5 mm long.

5.4. Leak testing of mechanical seals

The final stage in the manufacture of cartridge-type mechanical seals is leak testing. There are static tests (at a stop) without shaft rotation and dynamic tests with shaft rotation. Static tests are mandatory after partial or complete disassembly of the sealing assembly, regardless of whether the mechanical seal parts were simply inspected or repairs were performed, during which the rubber rings of the secondary seals were replaced, springs were replaced, the mechanical rings were ground, or ground in, or metal parts were restored or replaced.

Tests of the mechanical seal during shaft rotation are carried out only after the seal has successfully passed the static test.

Typically, the following parameters are monitored when testing seals:

- working environment;
- temperature;
- sealing pressure;
- time and procedure for loading the seal with sealing pressure.

The controlled parameters depend on the operating characteristics of the seal in real conditions and are recorded in the technical specifications for a given type of seal and (or) in the technical requirements on the assembly drawing of the seal.

The procedure and methodology for testing single, double, and tandem mechanical seals are significantly different because a special fixture or test bench is required to test single mechanical seals. A universal fixture for static testing of single mechanical seals is shown in Fig. 5.9.

The device consists of a housing, which imitates the sealing chamber of the pump, a false shaft, on which the mechanical seal is installed and a transition cover, into which the studs are screwed, with the help of which the seal housing is fixed during testing. The testing device is installed vertically on a bench or a specially-made frame. The seal to be tested is mounted on top of the shaft, the body of which is secured using nuts and studs to the device; the rotor bushing of

the seal is securely fixed to the false shaft of the device. The mounting brackets are removed, and the seal is ready for testing.

The working medium is supplied into the sealed cavity through a threaded hole made in the body of the device. Typically, this is process water, diesel fuel, industrial oil, or air.

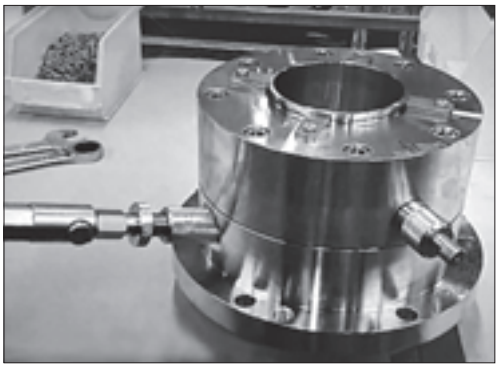

Fig. 5.9. Device for static testing of mechanical seals

It is convenient to use a manual plunger pump, with which you can quite easily create a pressure of up to 5.0 MPa in the sealed chamber to create the required pressure of the working medium. If air is used as the working medium, then pressure up to 0.8 MPa can be obtained from a piston compressor or 0.2—0.4 MPa from the pneumatic network of the enterprise. It is necessary to install a pressure gauge on the supply line of the working medium in the shut-off and control valves to control the pressure.

The tests are carried out as follows. The working medium is supplied into the cavity to be sealed under the required pressure, then the cavity of the device body is cut off from the pressure source using shut-off valves, and the seal is observed for 10—20 minutes.

If during testing, the pressure in the sealed cavity remains unchanged or decreases slightly, no more than 2—3% of the nominal value, while there is no leakage of liquid from the seal and there are no signs of sweating on the body parts of the seal, then such a seal is considered tight and has passed the test for parking. Otherwise, the mechanical seal is dismantled and sent for inspection and then for re-testing.

Parking tests on double mechanical seals can be carried out without test fixtures. In this case, it is sufficient to supply the working medium under pressure into the seal through the hole in the housing intended for supplying the barrier liquid. In this case, the hole for draining the barrier liquid must be plugged. Leak tests of tandem-type mechanical seals are performed in the same way, but the test pressure should not exceed 0.3 MPa. This is because during such tests, the mechanical seal of the first stage (internal) is loaded with pressure from the inside to the outside, which is an abnormal case and does not correspond to the load when the mechanical seal operates in the pump.

The procedure for testing the tightness of double and tandem mechanical seals is no different from testing single seals.

Rotation tests of mechanical seals are carried out on a special test bench, the typical design of which is shown in Fig. 5.10.

Typically, test stands for dynamic tests have a cantilever layout and include a support bracket with a test head, an electric motor, a tank with the working fluid, and a pump that creates the required pressure of the working fluid and circulates it through the test head, a pipeline system, shut-off and control valves, means of measuring operating parameters.

Tests with a rotating shaft are carried out only after the mechanical seal has been parked and has demonstrated the required tightness. Often, parking tests are carried out on the same bench as dynamic tests.

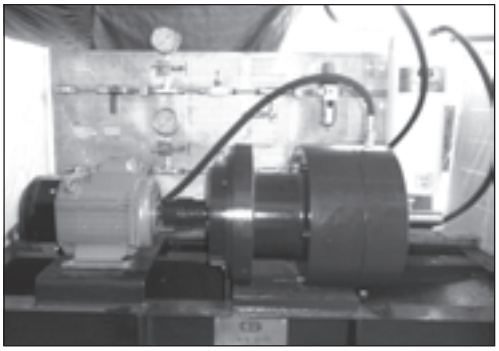

a

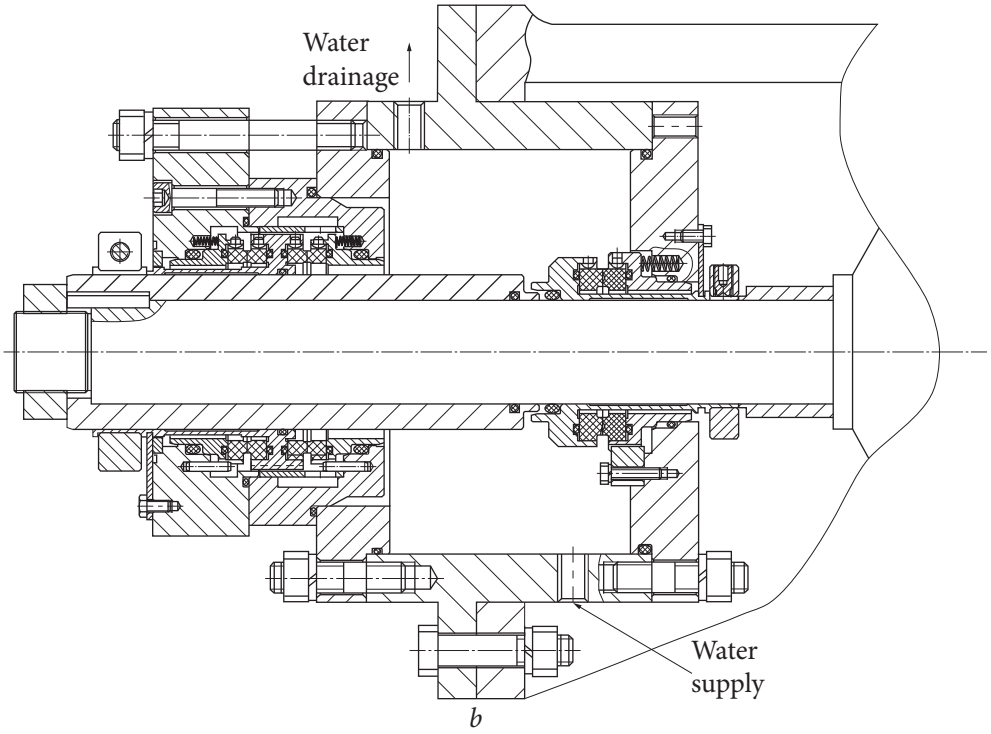

b

Fig. 5.10. Device for dynamic testing of mechanical seals: *a* — general view of the stand; *b* — section of the stand head

During dynamic testing of seals, the following is recorded:
- the pressure of the liquid being sealed;
- barrier fluid pressure (if it is a double mechanical seal);
- temperatures of these liquids;
- rotor speed;
- the amount of leakage through the seal, if any.

Liquid leakage is measured with a volumetric flask over a specified period of time, such as 10—15 minutes.

Mechanical seals with well-ground friction pairs often do not demonstrate visible leakage when tested at 3,000 rpm at pressures up to 1.0 MPa. This indicates a correctly chosen layout and well-thought-out design of the mechanical seal, as well as the high quality of manufacturing of its parts.

During dynamic tests of mechanical seals with non-contact friction pairs, as a rule, leakage is higher than that of contact-type seals. However, careful profiling of sealing ring geometry can virtually avoid leakage at relatively low sealing pressures.

5.5. Conclusion

Mechanical seals are high-tech, precision pump components, and the requirements for accuracy and quality of parts manufacturing are significantly higher than for other parts and components of the pump. Therefore, mechanical seals are manufactured at enterprises that specialize in such products and have the appropriate technological equipment and specially trained, highly qualified personnel.

The "heart" of the mechanical seal is the rings of the mechanical seal, which are made of super-hard and anti-friction materials. Their mechanical processing has significant differences from the manufacture of parts made of steel and alloys. One of the main technological processes in the manufacture of sealing rings is the lapping (finishing) of their sealing belts to ensure a non-flatness of no more than 0.0003 mm. Without stable production of rings that have a deviation from flatness no greater than that indicated above, there is no need to talk about the quality of manufactured or repaired mechanical seals.

The assembly quality of mechanical seals is no less important than the accuracy of manufacturing parts and lapping of the rings of the mechanical seal. Only specially trained personnel who have the required qualifications and permission from the enterprise management to perform this type of work are allowed to assemble seals.

The final stage of the process of manufacturing mechanical seals is the mandatory conduct of hydraulic tests for tightness, with recording in the test report of the operating parameters and conditions under which the tests were carried out, as well as the amount of leakage.

CHAPTER 6

DESIGNS AND OPERATING FEATURES OF MECHANICAL SEALS OF ENERGY PUMPS

As examples, let us consider the designs of mechanical seals of energy pumps, which, as a rule, pump hot media and operate under difficult operating conditions.

6.1. Mechanical seals for feed pumps

Feed pumps for thermal and nuclear power plants are designed to supply feed water with a temperature of 165 °C from the deaerator to high-pressure heaters. Depending on the type of drive, there are electric feed pumps (FEP) with a shaft rotation speed of up to 3,000 rpm or turbocharger feed pumps (TFP) with a shaft rotation speed of over 4,000 rpm.

To ensure the required service life of a mechanical seal in hot water, the temperature of the sealed liquid in the chamber in front of the mechanical seal must not exceed 80 °C. In this regard, it becomes necessary to cool the chamber in which the seals are installed. There are three ways to cool the fluid before sealing the shaft:

1) injection of cold condensate into the seal chamber with a temperature not exceeding 40 °C under pressure exceeding that being sealed by 0.05—0.01 MPa (Plan 42, according to API 682);

2) taking feed water from the first stage of the pump, cooling it in a remote heat exchanger, and supplying it to the mechanical seal;

3) circulation of the sealed liquid from the seal chamber through an external heat exchanger using a pump ring built into the mechanical seal (Plan 23, according to API 682).

Considering that the efficiency of remote heat exchangers is not very high, the designs of hot pumps, which include feed pumps, include a thermal barrier, i.e., covered with a cooling jacket through which condensate circulates at a temperature of 25—35 °C. The presence of a vibration barrier

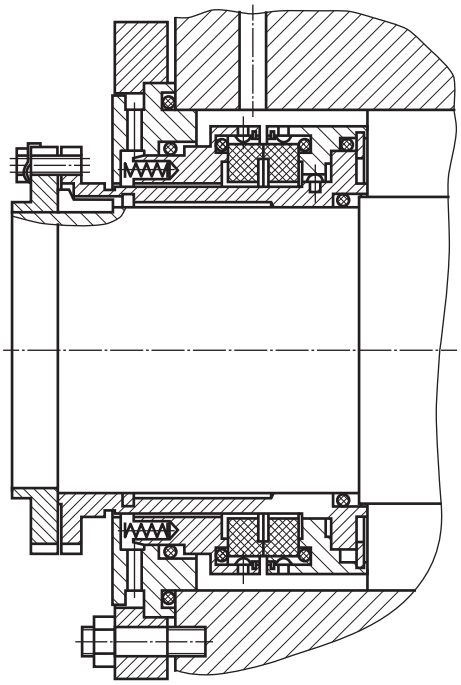

Fig. 6.1. Mechanical seal of the feed pump PE 380

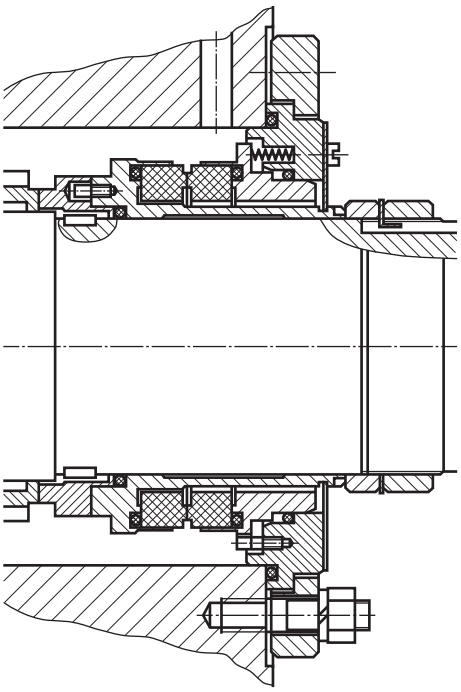

Fig. 6.2. Mechanical seal of booster feed pump PE 500-180-3

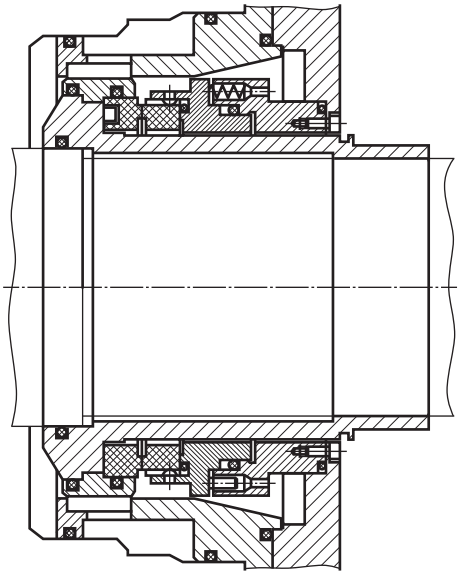

Fig. 6.3. Mechanical seal of the feed-water turbopump TPN 1150-340-2 after modernization

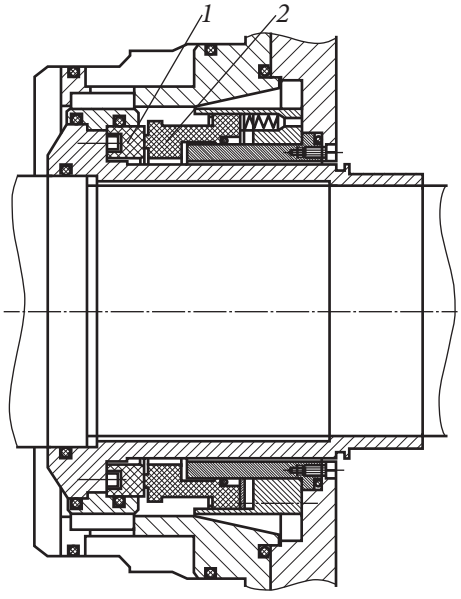

Fig. 6.4. The next type of mechanical seal of the turbo-feed pump PTN 1150-340-2: *1* — Rotating ring; *2* — Fixed ring

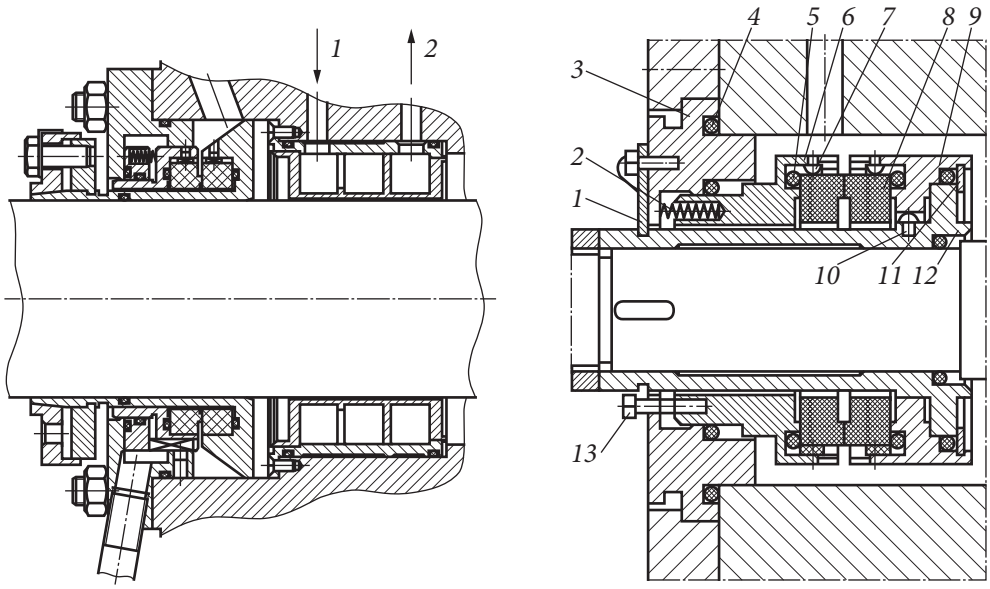

Fig. 6.5. Mechanical seal with cooling jacket of the starting-backup high-speed feed pump PE 650-320-4. *1* — Coolant inlet; *2* — Coolant outlet

Fig. 6.6. Mechanical seal type T-85

can significantly reduce the water temperature in front of the mechanical seal. Cooling efficiency depends on the design of the seal cover, the flow rate, and the temperature of the cooling condensate or chemically demineralized water.

Fig. 6.1—6.5 show examples of mechanical seal designs for feed pumps of various brands. Fig. 6.1 shows the mechanical seal of feed pumps of brands PE 380, PE 580, PE 720-185/200.

The block design of the T-type mechanical seal (Fig. 6.6) was developed by VNIIAEN.

The friction pair is formed by two identical rings (*8)* made of siliconized graphite SG-P, freely installed in an axially movable (*6)* and rotating (*9)* cages. The rings are held against rotation by driver (*7)* and sealed by rubber rings (*5)*. An axially movable ring with springs (*2)* is installed in seal housing (*3)* and secured against rotation by screws (*13)*. The rotating ring is secured with a spring washer (*11)* on the adapter sleeve (*12)* and is held against relative rotation by driver (*10)*. Mounting bracket (*1)* together with the adapter sleeve ensures a block-like design of the seal assembly. Rubber O-rings are used as secondary seals (*4)*.

The design of the cage (load factor of the axially movable cage is 0.7) and the method of installing the rings ensure their minimal deformation. The average diameter of the sealing belts is from 75 to 120 mm, the pressure of the sealed liquid is up to 6 MPa, and the peripheral speed is up to 25 m/s.

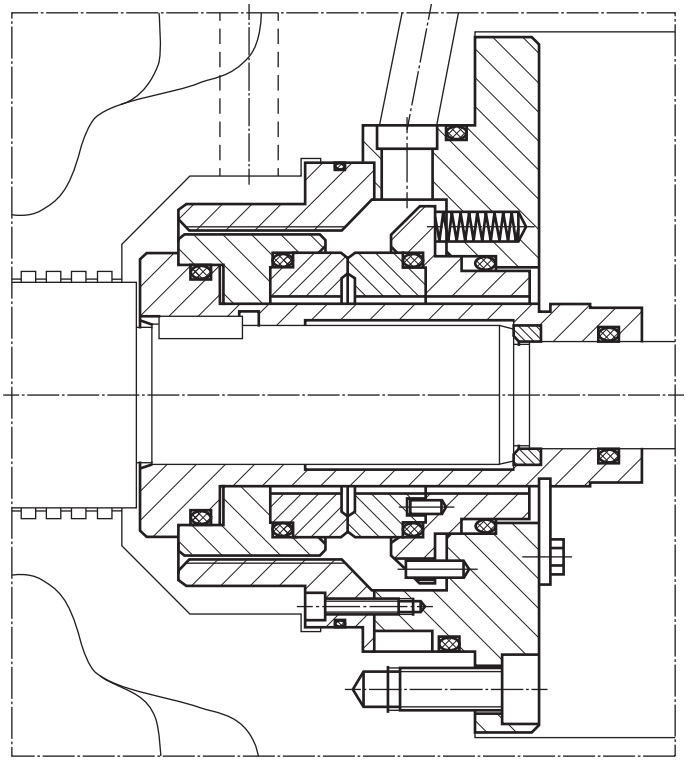

Fig. 6.7. Mechanical seal for feed pump from Eagle Burgmann

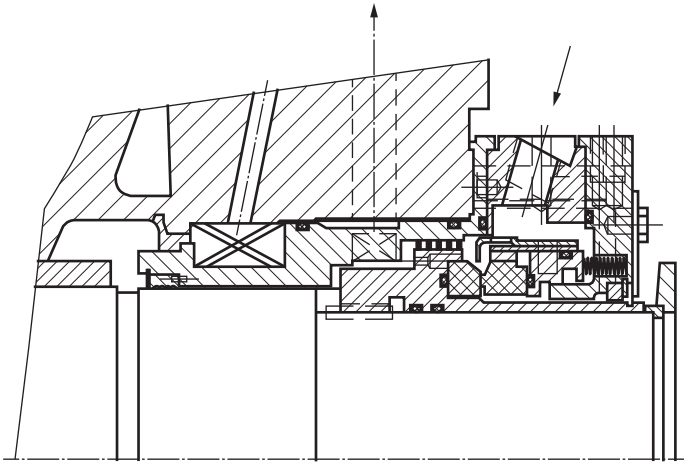

Fig. 6.8. Mechanical seal for Flowserve feed pump

The seals are used in the main (PEA 1650-80) and backup (PEA 250-80) feed pumps of nuclear power units, in condensate pumps KsVA 700-180 and KsVA 650-135, in cooling pumps, sprinkler and other pumps with rotor speeds up to 3000 rpm.

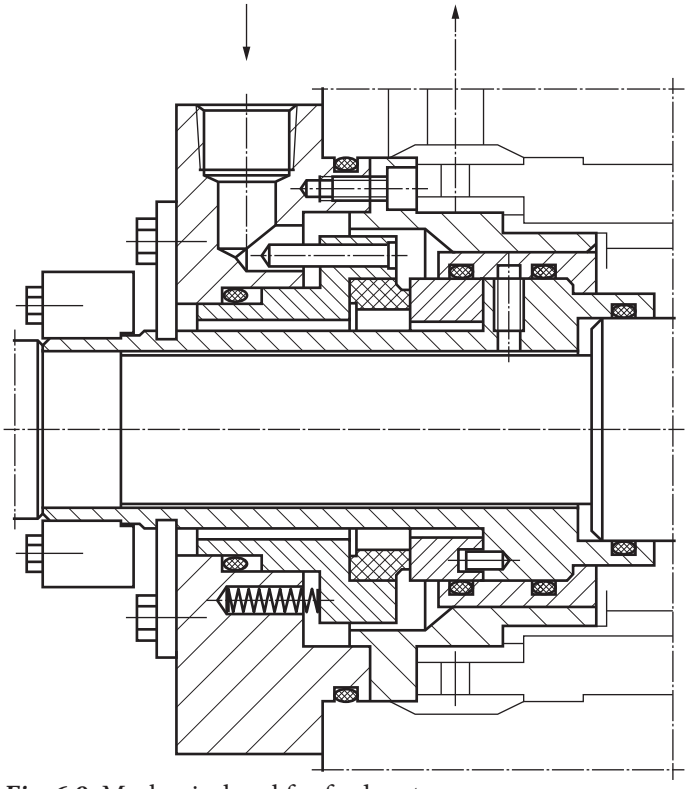

Fig. 6.9. Mechanical seal for feed-water pump

An analysis of the designs of mechanical seals of energy pumps from the world's leading manufacturers revealed the main trends in the directions of their design:

• the company EagleBurgmann, in the units produced (Fig. 6.7), uses silicon carbide with a diamond-like coating on the working surfaces in friction pairs instead of the previously used thermohydrodynamic friction pair rings;

• the Flowserve company, in its designs, (Fig. 6.8) uses friction pairs with a wavy surface;

• John Crane company, the design of the seal assembly is shown in Fig. 6.9, — friction pairs made of silicon carbide on graphite impregnated with antimony.

6.2. Mechanical seals for condensate pumps

The main purpose of condensate pumps is to supply water vapor condensate from the condenser through low-pressure heaters to the deaerator.

Structurally, condensate pumps are divided into vertical grades KsV and horizontal grades Ks. Vertical condensate pumps are usually multi-stage with an

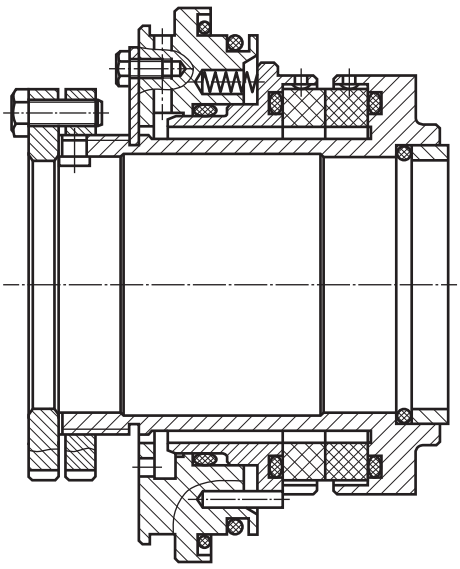

Fig. 6.10. Mechanical seal of the horizontal condensate pump Ks 1500-240

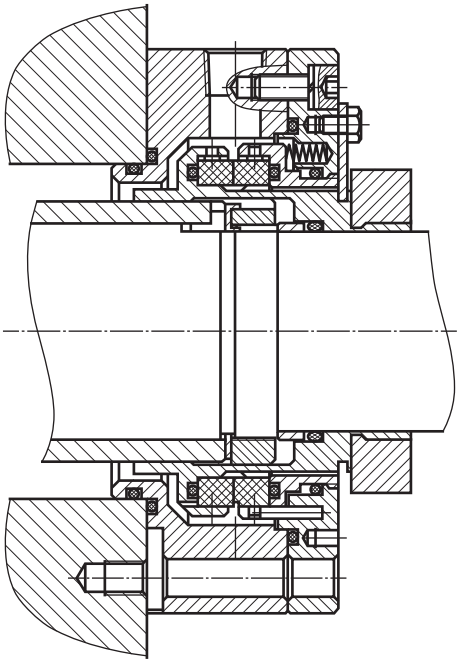

Fig. 6.11. Mechanical seal (replaces stuffing box seals) of horizontal condensate pump KsD 125-140

upstream impeller to provide the required cavitation characteristics. Horizontal pumps Ks can be single-stage with a double-entry impeller and a horizontal housing split, for example, Ks 1500-240, and multi-stage sectional, for example, Ks 800-100. Still very common are condensate horizontal multistage pumps of the KsD 125-140 and KsD140-140 brands with a horizontal housing split and a first-stage double inlet wheel.

Two types of mechanical seals are used in condensate pumps:

1) single mechanical seals;

2) double mechanical seals.

Fig. 6.10 shows the mechanical seal of the horizontal condensate pump Ks 1500-240 and Fig. 6.11 — pump KsD 125-140.

In vertical condensate pumps, double mechanical seals are widely used, which use a supply of cold condensate with a pressure exceeding the pressure of the sealed liquid in front of the mechanical seal (Plan 54, according to API 682). The use of double mechanical seals is due to the fact that when the pump is stopped and during operation; a negative pressure zone can form in the sealing area, which leads to air leakage from the environment through the end shaft seal. The most commonly used is the system diagram with the supply of barrier

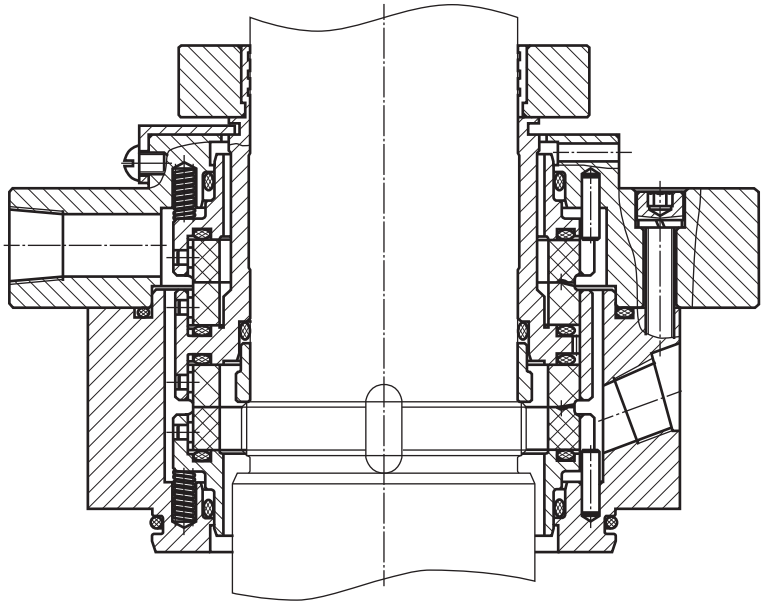

Fig. 6.12. Double mechanical seal brand 2TM 75-130

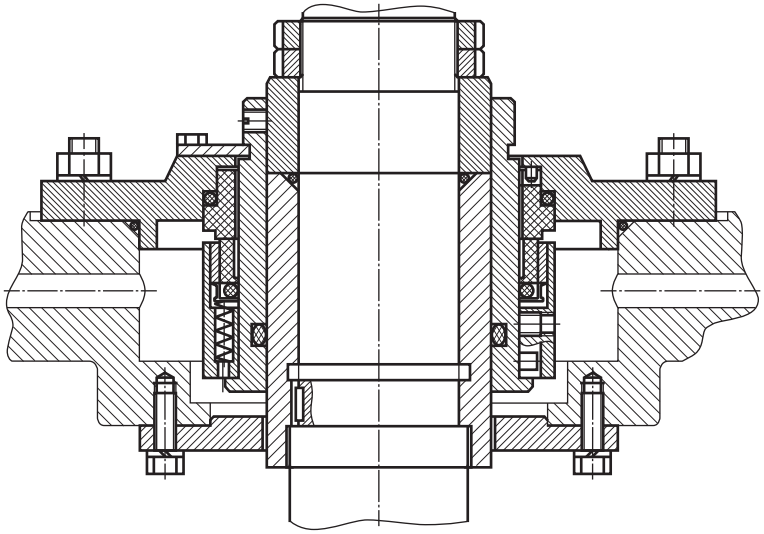

Fig. 6.13. Mechanical seal TUKsV320-02

fluid from a separate pipeline with excess pressure through a seal to the duct. At temperatures of the pump operating medium up to 150 °C, seals without a cooler are used at temperatures of the pumped medium 150—400 °C — with a cooler. Fig. 6.12 shows a double mechanical seal type 2TM 75-130 for pumps KsV 320 and KsV 500.

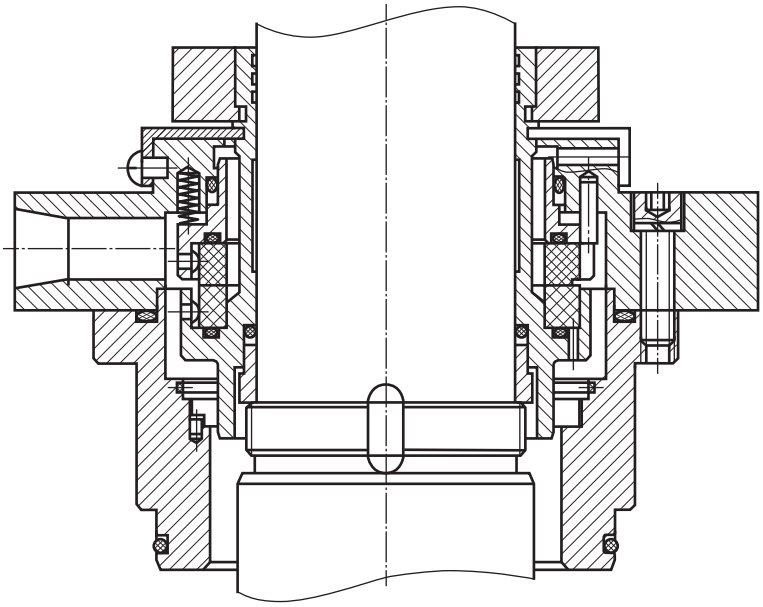

Fig. 6.14. Mechanical seal TMD 75-130

Also, one of the promising technical solutions is the use of single mechanical seals in vertical pumps with a supply of cold condensate from an external source, which enters the pump cavity through the gap seal. Fig. 6.13 shows a single mechanical seal of the TUKsV320-02 for KsV320.

A cartridge mechanical seal TMD 75-130 with a floating ring on the side of the sealed liquid is shown in Fig. 6.14.

6.3. Mechanical seals of network and circulation pumps

6.3.1. Mechanical seals for network pumps

Network pumps (NE) are designed to supply coolant (network water) to heat supply systems of populated areas. These are single-stage or two-stage pumps with double-entry impellers and a horizontally split casing in most cases. The pumps pump hot water with temperatures up to 120 °C, and in some cases, the water temperature can reach 170 °C.

Until recently, shaft seals were used widely in these pumps, but in recent decades, cases of installing mechanical seals in SE pumps have become more frequent. Basically, these are single mechanical seals with or without a remote heat exchanger and a cooling supply to the thermal barrier (a refrigerator built into the seal chamber), which is provided in the pump design to cool the shaft seal.

Fig. 6.15 shows a mechanical seal of the TUSE-1250, which is used widely in network pumps in the domestic energy sector.

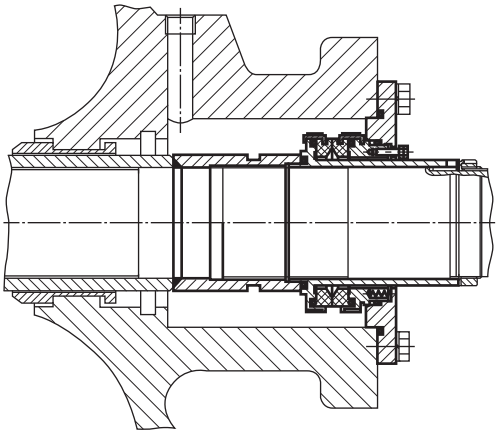

Fig. 6.15. Mechanical seal TUSE-1250

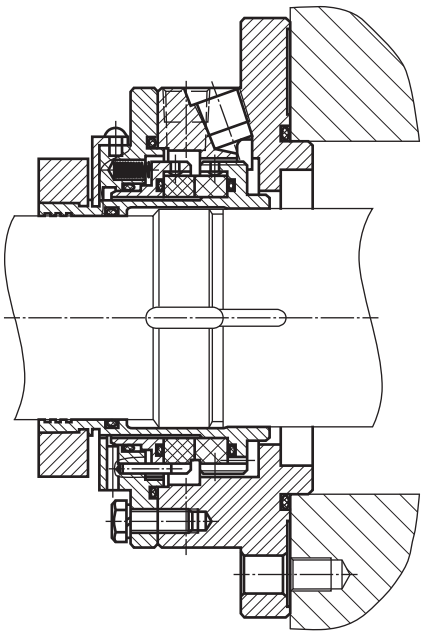

Fig. 6.16. Mechanical seal TM 100-160

Fig. 6.16 shows the mechanical seal TM 100-160 for the SE 5000-180-6 pump. Seals of this design have been used quite often in network pumps in recent years.

There are also a large number of flattened mechanical seals that are installed instead of stuffing box seals.

6.3.2. Mechanical seals for circulation pumps

The rotor seal is one of the most complex and critical components of the main circulation pump of a nuclear power plant (MCP), which determines the reliability of the entire unit. This is explained by the difficult operating conditions of the seals in combination with high requirements for tightness in nominal, transient, and emergency operating modes of the pump.

Fig. 6.17 shows a three-stage mechanical seal of the main circulation pump, in which uniform pressure distribution between stages is achieved using choke (*1)* installed on the external line [28]. Pressure separation is accompanied by constant leaks through the external line, amounting to several hundred liters per hour. The heat generated from the friction of contacting surfaces is removed through a special closed circuit with a heat exchanger (*2)* and a filter (*3)* to capture wear products. Circulation in the cooling circuit is created by an axial labyrinth pump (impeller) (*4)* built inside the seal.

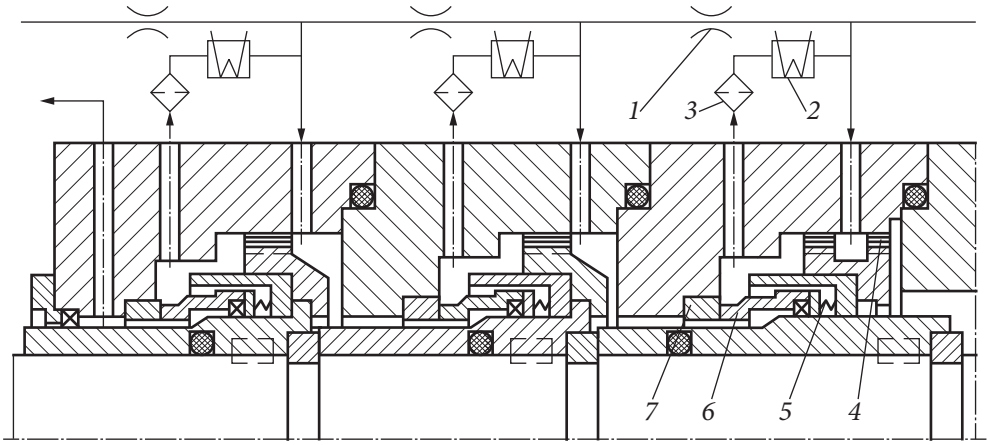

Fig. 6.17. Three-stage mechanical seal: *1* — throttle; *2* — heat exchanger; *3* — filter; *4* — impeller; *5* — spring; *6* — axially movable bushing; *7* — support ring

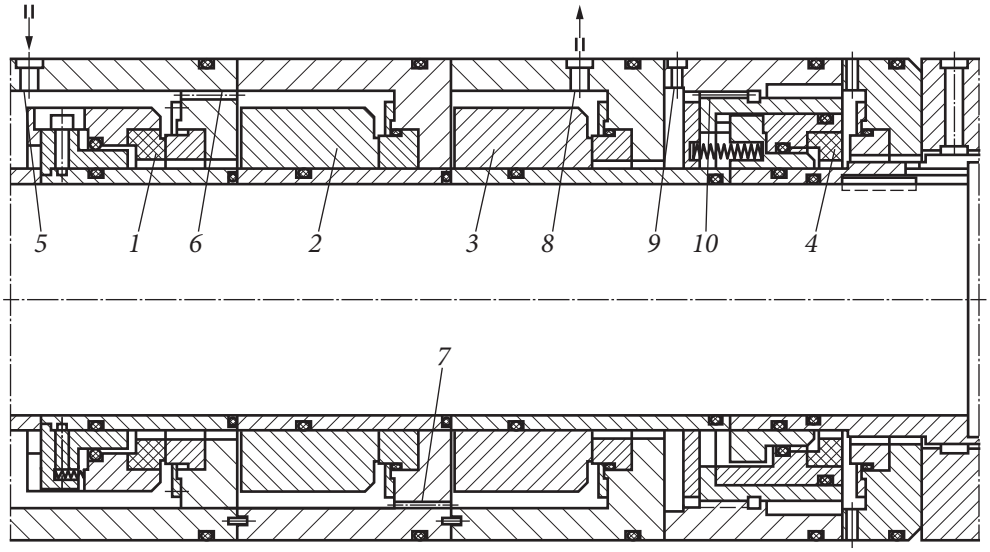

Fig. 6.18. NPP MCP sealing system with hydrostatic seal

Each of them is designed for the full pressure drop to ensure sufficient seal tightness in emergencies when one of the stages fails. The main elements of the seal are the axial movable sleeve (6) and the fixed support ring (*7*), which are constantly pressed against each other by medium pressure and springs.

Recently, MCP designs have appeared for nuclear power plant reactors, in which the full pressure drop is actuated at one stage of the hydrostatic seal, and external tightness is ensured by a mechanical seal of the end type (Fig. 6.18) [27]. At the same time, the shut-off water supply system is simplified, and the reliability of pumping units is increased.

At high-pressure drops and shaft speeds, when long service life is required and minor leaks are tolerated, continuous liquid film seals are being used increasingly. These include hydrostatic seals consisting of the same elements as conventional mechanical seals.

A hydrostatic seal has been proposed for circulation pumps, in which the throttles are capillary grooves made directly on the working surface and connected to the sealing cavity [58]. Such a seal makes it possible to slightly increase the cross-section of the chokes due to their elongation, as well as to create favorable conditions for cleaning the chokes from mechanical particles due to the relative rotation of the sealing surfaces. Since these surfaces, as a rule, are made of very hard and wear-resistant materials, this seal complicates the process of manufacturing supply capillary channels, which must also have the same flow characteristics.

Fig. 6.19 shows the sealing system of the main circulation pump of a nuclear power plant. The operating pressure and water temperature in the primary circuit are 12.5 MPa and 270 °C, respectively. The seal operates on sealing water, which is taken from the primary circuit, cooled to 40 °C, and cleaned by passing through a refrigerator and an ion exchange filter. Automatic regulators maintain a given (0.5—0.6 MPa) excess of the barrier water pressure over the pressure in the pump cavity, as a result of which about 50% of the supplied water (0.3—0.5 m^3/h) enters the pump, excluding release of hot radioactive coolant from it.

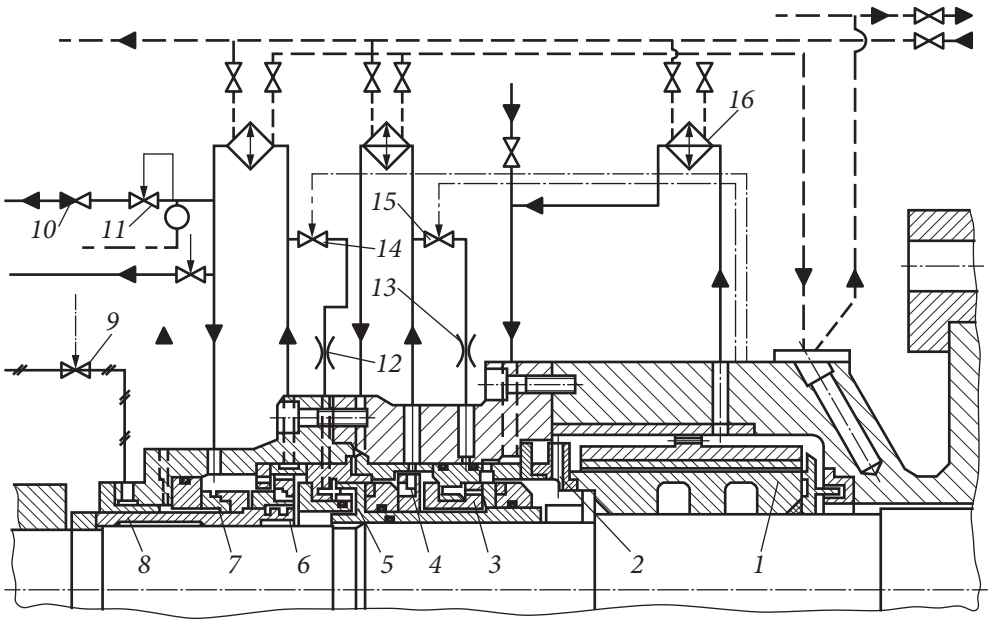

Fig. 6.19. NPP MCP sealing system

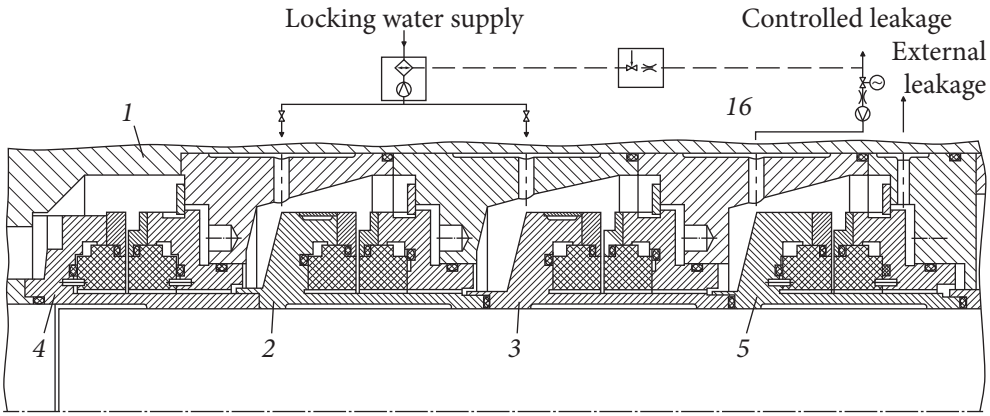

Fig. 6.20. Block of mechanical shaft seals of the main circulation pump

Together with sliding bearing (*1)*, operating on water, the sealing unit is separated from the pump body by a special thermal barrier — a neck cooled by water. Impeller (*2)* pumps shut off water through the bearing chamber and cooler (*16)* to eliminate cases of local boiling. The same function is performed by impellers (*4)* and (*6)*, located in the first (*3)* and second (*5)* stages of the hydrostatic seal. Before the closing mechanical seal (*7)*, the bypass valve (*10)* maintains a pressure of 0.42—0.45 MPa. External leaks through seal (*7)* are about 300 cm^3/h, and organized leaks are 0.3 m^3/h. Leaks through hydrostatic seals (*3)* and (*5)*, and therefore the end clearance, are kept constant by changing the conductivity of the external chokes (*13)* and (*12)* by control valves (*15)* and (*14)*.

If the supply of shut-off water stops or its leakage through a damaged seal increases, the temperature in the bearing chamber increases, and when 65 °C is reached, magnetic valve (*15)* begins to close, reducing the end gap in seal *(3)*. With a further increase in temperature to 70 °C, seal (*3)* closes completely and operates as a contact mechanical seal with minimal leakage. Isolation water is supplied to the cavity in front of the seal from an automatically switched-on backup system, and reduces the temperature in the bearing chamber. If the required effect is not achieved, then when the temperature rises to 80 °C, the second seal stage (*5)* is closed.

In the event of failure of both seal stages (*3)* and (*5)*, the pressure in front of the closing mechanical seal (*7)* and valve (*10)* becomes greater than permissible and leads to the closing of valve (*1)* and the opening of valve (*9)*, through which compressed air is supplied to the labyrinth seal chamber (*8)*. In this case, seal (*7)* must briefly stop the pump to perceive the full pressure drop. If it also fails, the role of a seal is performed by the labyrinth sleeve (*8)* with compressed air supplied to it under a pressure of 0.7 MPa. All of the above measures should prevent the release of radioactive water during the 3—10 minutes required for normal shutdown of the unit.

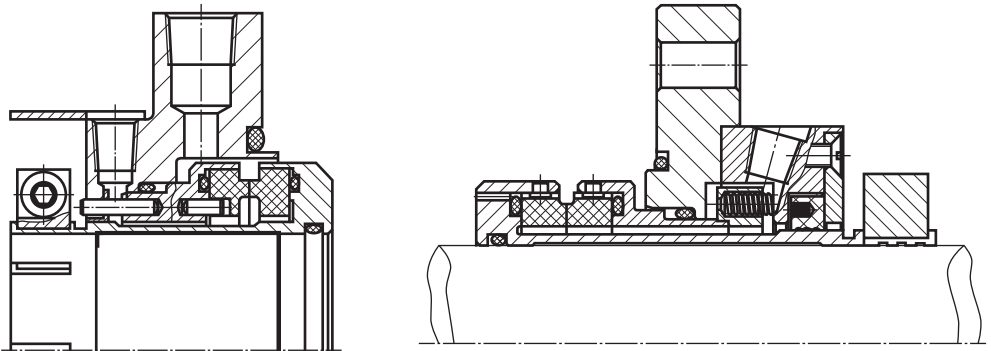

Fig. 6.22. Mechanical seal TMP 52-94

◄ ***Fig. 6.21.*** Mechanical seal BO-80

The disadvantage of the design under consideration is that in the stages of hydrostatic sealing, the axial movable pistons are centered on two rubber sealing rings, so the misalignments of the contact surfaces are not sufficiently compensated, and in the end gap, there are no conditions for the occurrence of a restoring moment. In addition, the circuit contains many automatic control devices that reduce the reliability of the sealing system.

Let's consider the shaft seal unit of the main circulation pump GCN-317, which serves to prevent water leaks from the primary circuit of a nuclear power plant with a VVER-440 reactor [70] (Fig. 6.20). The seal assembly consists of a housing (*1)*, in which two main stages of the mechanical seal (*2)* and (*3)*, a separating stage (*4)* and an end seal stage (*5)* are installed. The designs of the main throttling stages of the seals are the same and consist of stator and rotor parts.

The stator element can move in the axial direction and is pressed against the rotor element by springs. The sealing elements in the stator and rotor elements are rings made of siliconized graphite. On the end part of the rotor element ring, there are four grooves along the circumference with holes opening onto the outer cylindrical surface of the ring. Throttle jets are glued into the holes of the grooves. The locking water enters the grooves on the end surface of the ring through the jets and creates a hydrostatic lift force, pressing the stator seal

element to a gap of up to 10 microns. A lubricating film thickness of about 10 microns ensures guaranteed fluid friction and minimal water leakage through the seal. The stator element is pressed out at a pressure of 1.5—2 MPa.

During normal operation, the pressure is distributed approximately equally between the main stages. If one of the main stages fails, the remaining stage will throttle the pressure drop, maintaining the functionality of the seal, while the flow rate of organized leaks will increase approximately by 2 times. The separation and end stages also consist of stator and rotor elements with siliconized graphite O-rings and springs. In both stages, unlike the main stages, in all operating modes, the sealing surfaces of the sealing rings of the stator and rotor elements are in direct contact. The working parts of the sealing rings of the stator elements are made in the form of an ellipse to ensure water wetting of the rubbing surfaces.With a pressure drop of 2 MPa, the leakage of shut-off water into the primary circuit is about 200 l/h. During normal operation, leakage through the end stage does not exceed 50 l/h.In hydrostatic seals, leakage through the axial gap is almost independent of the relative rotation of the sealing rings but is determined by the pressure drop. Therefore, during a standstill, leakage remains the same as when the pump is running. It is necessary to install additional parking seals in series with the main one, which complicates and increases the cost of the design, its operation, and repair to seal the shaft when stopped. For example, the Champlain company for a hydrostatic seal allows startup at a pressure drop of at least 2 MPa. Only with such a difference the non-contact operation of the seal guaranteed. Mechanical seals are made with one-stage or multi-stage.

The mechanical seal stages can alternate in the axial direction, radial direction, and in both directions. The number of stages dictates the level of pressure being sealed. Typically, a pressure differential of no more than 20 MPa is allowed to operate at one stage.

6.4. Mechanical seals for fuel oil, chemical, and auxiliary pumps

6.4.1. Mechanical seals for fuel oil and oil pumps

In the fuel oil industry of thermal power plants, two main types of centrifugal pumps, 5N5 × 4 and NK 200/370 are used widely. The first pump with a horizontally split casing is a multistage pump with a transfer pipeline of an inter-support design. The NK 200/370 two-stage cantilever pump, with a shaft diameter at the seal installation site of 80 mm, is designed taking into account the use of mechanical seals of various designs (single, double, tandem) as end shaft seals. Fig. 6.21 shows a single mechanical seal type BO-80 for the NK 200/370 pump.

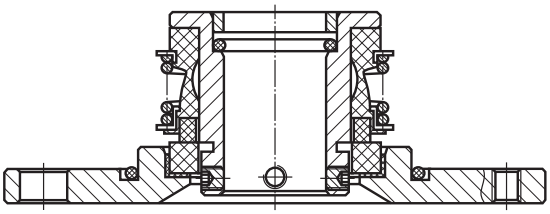

Fig. 6.24. Cartridge design mechanical seal

◄ ***Fig. 6.23.*** Typical single mechanical seal for the oil pumps

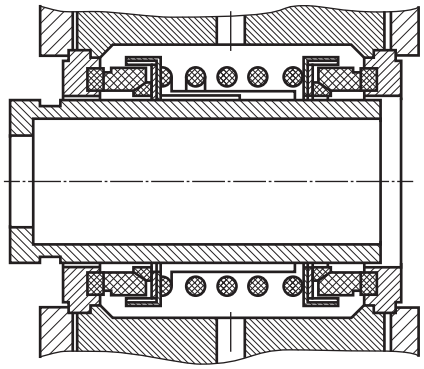

Fig. 6.25. Design of double mechanical seal brand 2G50

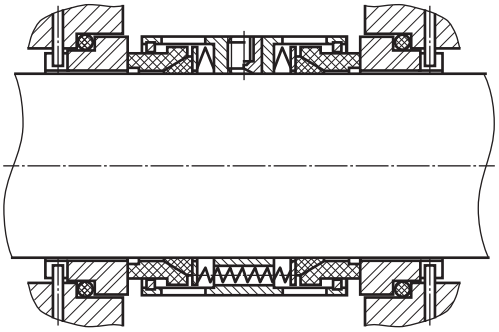

Fig. 6.26. Design of double mechanical seal 153D

In double-bearing pumps 5N5 × 4, the dimensions of the sealing chamber allow the installation of only a single mechanical seal with an auxiliary (safety) seal in the form of a floating ring or throttle bushing. Fig. 6.22 shows the TMP 52-94 mechanical seal for the 5N5 × 4 fuel oil pump.

Taking into account the increased requirements for ensuring the safety of pumping equipment pumping flammable, fire-hazardous liquids, tandem-type mechanical seals with piping according to API 52 are being increasingly used. Creating excess pressure in the tank after filling it is not required. Installation of a safety valve on the tank pipelines is not required when the pressure in the pump stuffing box is less than the tank design pressure (4 MPa). Tandem-type mechanical seals can be used both with a refrigerator at a pump operating temperature of up to 400 °C and without it at an operating temperature of up to 150 °C. Oil pumps in thermal and nuclear power plants are used to circulate oil

through the generator rotor end seal system and supply oil to the plain bearings of the turbine unit and centrifugal pumps. As a rule, to supply oil to sliding bearings, gear pumps of the NSh brand are used, which traditionally use the simplest mechanical seals with a friction pair made of hardened steel on bronze and a central spring. The softer bronze ring wears out, and the seal begins to leak during operation. A typical single mechanical seal for oil pumps is shown in Fig. 6.23.

Reliable sealing of NSh oil pump shafts can only be achieved using high-quality mechanical seals, the sealing rings of which are made of modern materials.

Fig. 6.24 shows a mechanical seal of a cartridge design, which is installed in the oil pump of the electric motor of the PE 500-180 pumping unit at the Kremenchuk CHPP.

6.4.2. Mechanical seals for chemical pumps

Chemical cantilever pumps X and AX are used in chemical water desalination plants and traditionally, they use non-cartridge-type double mechanical seals. Fig. 6.25 shows the design of a double mechanical seal type 2G50 for a centrifugal chemical pump AX 50/49.

A more modern design of a double mechanical seal type 153D for chemical pumps is shown in Fig. 6.26.

6.5. Conclusions

The mechanical seal designs of modern energy pumps are constantly being improved and differ significantly from the seals of the late 20th century. Cartridge-type mechanical seals have become widespread and are widely replacing non-cartridge seals, even on small, cheap general-purpose pumps.This is because despite the higher cost, complexity, and labor-intensive manufacturing, cartridge-type seals are much more convenient and safer to use, especially when installing (dismantling) equipment, and allow you to avoid most installation errors. Manufacturing the seal in the form of a cartridge allows you to perform hydraulic tests for the tightness of the seal on a special device and then mount it on the pump with full confidence that the seal will not "leak" when filling the pump with liquid before putting it into operation. The tightness of the seal of a non-cartridge design is checked only as part of the pump, and if it is not tight, then you have to disassemble the pump and eliminate the cause of the leak, and sometimes this can be repeated more than once.In recent years, several manufacturers of mechanical seals for pumps pumping hot liquids have been practicing the production of combined designs of mechanical seals, into which

a device containing a “cooling jacket” (refrigerator) is integrated. This design solution makes it possible to provide additional cooling of the mechanical seal and reduce the temperature of the liquid in the seal chamber to a quite comfortable 40—60 °C.

There is a pronounced tendency of leading foreign manufacturers to abandon the use of remote heat exchangers in the cooling circuits of the mechanical seals of feed pumps. This is due to saving energy resources and is achieved using modern materials and specially profiled rings of the end pair, which ensure the operation of the seal with the minimum possible heat losses.It also should be noted that the creation of reliable and hermetic mechanical seal assemblies for energy pumps operating in difficult operating conditions must be carried out in close cooperation between the pump designer and a specialist in the design of seal assemblies.

CHAPTER 7

ANALYSIS OF THE MAIN CAUSES OF FAILURE AND REPAIR OF MECHANICAL SEALS

7.1. Basic provisions

The main signs of abnormal operation of a mechanical seal are an excess of the permissible amount of liquid leakage, in other words, loss of tightness and/or increased temperature of the metal parts of the seal. This indicates that processes occurring in the seal will soon lead to its failure.

A characteristic difference between mechanical seals and seals of other types is that during abnormal operation, their depressurization occurs suddenly, and the leak reaches such a magnitude that an emergency shutdown of the unit is required with subsequent repair of the shaft seals. There are frequent cases of a gradual increase in leakage during operation, but they do not lead to emergency equipment shutdowns and, therefore, do not cause serious consequences.

As a rule, the reasons for seal failure are divided into:

• *related to the mechanical seal itself* (the design of the seal does not meet the operating conditions, incorrect choice of materials for the main parts, low-quality materials, manufacturing errors, violation of the requirements for assembly, transportation, and storage of the seal, etc.);

• *related to the installation, startup, and operating conditions of the equipment* (errors during installation of the seal (damage to seal parts, violation of the forces and tightening order of fasteners, the axial run of the rotor was not taken into account, etc.), incorrect startup of the equipment ("dry" start, "steaming" or "airing" of the pump, mounting brackets not removed before starting, supply of barrier or cooling liquid is shut off), equipment malfunction (cavitation, increased vibration, excessive radial or axial runout of the shaft, misalignment of the shaft with the seal chamber, destruction of bearings, unacceptable axial displacement of the rotor, etc.).

These are just a few of the many possible causes of seal failure, and they rarely occur on their own. Very often, two or more reasons occur simultaneously.

Seal-related causes, provided they occur within a predictable period of time, can be easily corrected, such as by installing new parts or performing routine seal maintenance. Hardware-related causes can be more difficult to determine, but in most cases, symptoms indicating a failure mode can help identify the problem and take corrective action. According to statistics from the Grundfos company, up to 39% of stops of centrifugal pumps are caused by abnormal operation of mechanical seals, and the cost of repair (replacement) of mechanical seals is up to 44% of the cost of all pump repairs [19].

According to EagleBurgmann statistics published in 2006 [9], the main causes of mechanical seal failures are:

- the so-called "dry running" or the absence of liquid in the friction pair during pump operation — 55%,
- increased wear of friction pair rings due to long service life — 8%;
- corrosion of seal parts — 7%;
- installation errors — 5%;
- other reasons — 25%.

According to Borg Warner [12], 60—70% of all seal problems are caused by other problems that have nothing to do with the design or workmanship of the mechanical seal.

7.2. The procedure for inspecting a mechanical seal to identify the cause of failure

Fig. 7.1 shows a single mechanical seal and the main paths through which the sealed liquid can leak out.

It is necessary to consider two modes — normal and abnormal for double mechanical seals (Fig. 7.2). Normal mode is when the pressure of the barrier liquid exceeds the pressure of the sealed liquid; abnormal mode is a situation when the pressure of the sealed liquid is higher than the pressure of the barrier liquid.

Let's consider a typical situation during operation — the mechanical seal has failed due to depressurization. It is necessary to inspect the seal in order to identify the reason that caused the damage based on the nature of the damage to the seal parts to establish the reason that caused the depressurization. Only after this is it possible to carry out repairs, restore functionality, and test the mechanical seal.

The cartridge-type mechanical seal must be removed from the pump with the mounting brackets installed (if it is still possible). The mechanical seal is delivered then to a repair shop that has the appropriate facilities and equip-

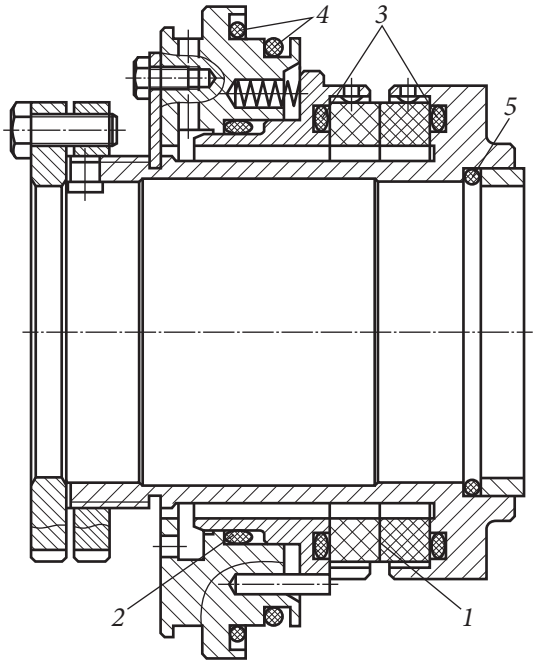

Fig. 7.1. Single mechanical seal and main possible leakage paths: *1* — contact of the sealing belts of the end pair; *2* — secondary seal of the axial movable element; *3* — secondary seals of static connections; *4* — static seal between the seal housing and the pump housing; *5* — static seal between the seal sleeve and the shaft

ment to repair, recondition, and hydraulically test the mechanical seal, as well as suitably trained personnel. If the enterprise does not have the conditions for repair and restoration of such complex and precision pump components, it is recommended to send the seals to the manufacturer in packaging that prevents damage to the seal parts.

CAUTION. Only personnel who have undergone special training in repairing mechanical seals and are authorized to carry out such work are allowed to work with mechanical seals.

Before disassembly, a visual inspection of the mechanical seal is carried out with the photographic recording of external damage to the parts, with special attention paid to the presence of a complete set of seal parts and mounting brackets.

Then, under the requirements of the operating manual, the mechanical seal is disassembled, with the photographic recording of damage to individual parts. Particular attention is paid (in order of importance) to damage to friction pair rings, rubber O-rings, springs, drive elements, metal parts, the presence of corrosion traces, salt deposits, abrasives, etc.

Based on the results of the audit, a short report is drawn up, which necessarily records the date of the audit, the brand of the mechanical seal, the manufacturer, the drawing number, the serial number of the seal, the date the

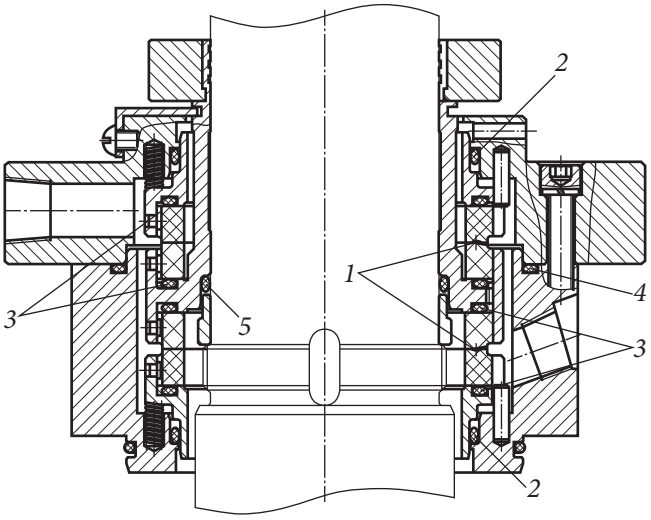

Fig. 7.2. Double mechanical seal and main possible leakage paths (Notations are the same as in Fig. 7.1)

equipment with the mechanical seal was put into operation, and the number of hours actually worked. This report is signed by the foreman or foreman of the repairmen who performed the audit.

7.3. Wear or destruction of the end rings

The friction pair is the main element of the mechanical seal, in which all the main sealing processes take place. The most important parts of a mechanical seal are the sealing surfaces of the rotating and stationary rings. Having examined them, we can draw the following conclusions.

1. If the surfaces are installed correctly, i.e., perpendicular and concentric to the shaft, even wear will be observed on both rings.

2. If the stationary surface is at right angles to the shaft, but the shaft is not concentric in the pump bore, the stationary surface will have a smooth circular shape, the center of which will not coincide with the center of the surface itself. The rotating surface will have a uniform circular wear pattern, the overall width of which will be slightly greater than that of the stationary surface.

3. Provided the offset is not too large, it will only appear as described above. In this case, the heat will be slightly increased.

However, if the misalignment is outside the acceptable limits, the wear pattern will be different. Due to high shaft misalignment, the rotating surface may tend to "wobble" — resulting in uneven wear on both the rotating and stationary surfaces.

The two examples above are based on the assumption that the centerlines of the shaft and housing are the same or parallel.

4. Consider the case where the shaft does not run parallel to the centerline of the pump. This results in the rotating surface not being straight. Assuming that the shaft itself is straight, the additional force generated by the indirect shape will act on only a portion of the total contact area with the stationary surface.

Because the spring load and hydraulic forces attempt to bring the rotating surface into full contact with the stationary surface, a uniform, indirect wear pattern will form on the stationary surface.

Depending on the duration of the operation, a more or less deep groove will form towards the outer diameter of the rotating surface. If the displacement is not too big, the seal can be allowed to "break in" to provide an acceptable service life.

Fig. 7.3 shows fragments of sealing rings with wear.

5. If the shaft is concentric with the pump, but the stationary surface is not perpendicular, then it will take time to break in the surfaces, as indicated in point 4.

In both cases, it is the degree of displacement that determines whether the seal will last. Too much misalignment will cause the face to oscillate, resulting in intermittent leakage and subsequent rapid seal failure.

The examples above can be corrected by inspecting the equipment in which the seal is installed and taking appropriate action to correct the discrepancies.

6. One of the most common causes of seal failure is dirt and abrasives, which can be sand, pipe scale, etc., that travel through pipelines. Fig. 7.4 demonstrates the wear of the sealing belts of the end pair.

Fig. 7.3. Fragments of sealing rings with wear

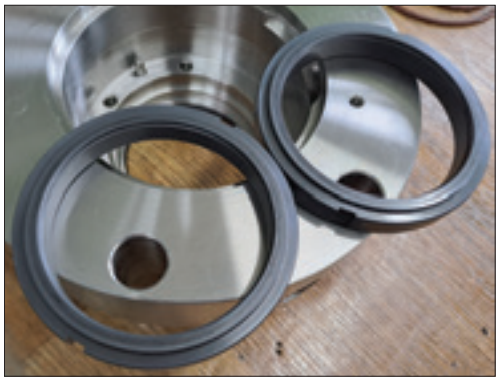

Fig. 7.4. Wear of the sealing strips of the end pair

Fig. 7.5. Results of thermal effects on the rotor hub and cage

Fig. 7.6. Clip with a destroyed ring

When the pump is operating under normal conditions, in practice, abrasives cannot get between the sealing surfaces since they adhere to each other within a few microns while they remain in contact.

However, seals fail because abrasives penetrate between the surfaces. This can occur because the hydraulics can cause mechanical overload if the union nuts and/or set screws are not tightened correctly. Hydraulic force forces the bushing against the support, resulting in a mechanical overload of the seal.

7. Deformation of surfaces (under the influence of temperature and/or pressure)

Temperature and/or pressure can have additional effects on the seal faces.

Often, under the influence of high temperatures, the races and rotor bushings in which the rings of the end pair are located are deformed (Fig. 7.5)

Under the influence of temperature and pressure, the rings of the end pair are also deformed. This usually appears as uniform wear in the radial direction, but the wear pattern may be deeper toward the outer or inner diameter of the surfaces, depending on the deformation mode.

In these cases, it is easier to detect the result than the cause, and it is necessary to check the coefficients of thermal expansion of materials or combinations of materials if thermal deformation is involved.

Violation of the flatness of the sealing belts due to force or temperature deformations of the rings of the end pair also can lead to the sealing rings' destruction (Fig. 7.6).

8. Cracks and chips in the surface. Cracks and/or chips on the surface (usually on a carbon surface) can be caused by:

- improper handling during transportation and/or installation;
- vibration.

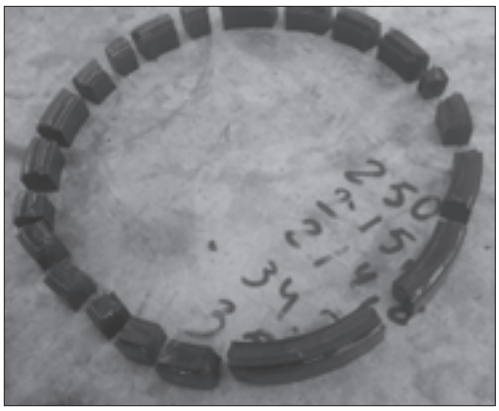

Fig. 7.7. Destruction of ceramic rings

In the second case, it is necessary to balance the rotating element of the pump. Sometimes, vibration can be caused by cavitation. In this case, the operating pressures of the equipment must be checked and adjusted to prevent cavitation. The destruction of ceramic rings due to increased axial vibration is shown in Fig. 7.7.

Cracking of hard ceramics may have other causes. For example, rings may be clamped unevenly or due to cold shock. Cold shock of tungsten carbide, for example, occurs due to steam breakthrough on a seal that is already at or near operating temperature.

9. Thermal cracks. Thermal cracks are radial cracks that appear across the entire surface of a metal or part of it (such as stellite or tungsten).

This may occur due to thermal deformation caused by differences in expansion rates between the base material and the stellite coating. In these cases, the solution may be to switch to a loose tungsten plate. When the stationary ring deforms under pressure, radial cracks may be found in a smaller portion of the contact area of the rotating ring.

The deformation of carbon rings under the influence of a sealing pressure that exceeds the design pressure, as well as under the influence of high temperatures, may exceed permissible values (see sections 2.5 and 2.6). This can lead to seal failure and is one of the reasons for the need to modernize mechanical seal designs.

10. Increased wear of end surfaces. Increased wear of rubbing surfaces is observed, as a rule, as a result of prolonged operation of the seal (Fig. 7.8).

In addition, cracks caused by cold shock, uneven compression, and heat generation can also cause increased wear due to the following phenomena.

The raised areas of the material can act as a cutting tool, quickly removing carbon. When the sealing lip becomes severely worn, the seal balance is completely disrupted, causing the sealing surfaces to deteriorate even more rapidly due to overheating.

High wear on sealing surfaces can also be caused by too much stress on the surface. In these cases, the adjustment should be checked and the seal balance should be adjusted.

12. Dry running. Seals operate under conditions of complete absence of liquid in the friction pair or insufficient quantity. In this case, a network of radial

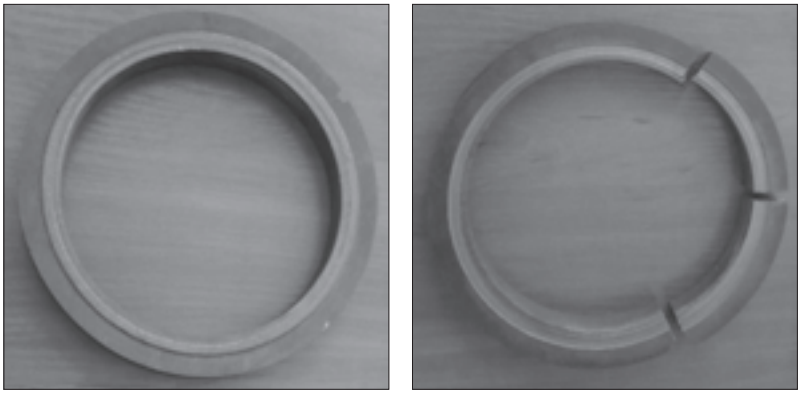

Fig. 7.8. Wear and destruction of rings as a result of long-term operation

Fig. 7.9. Destruction of friction pair rings

microcracks is formed on the working surfaces of the sealing belts. A typical picture of the destruction of rubbing surfaces under "dry running" conditions is shown in Fig. 7.9.

Slipping is another rare cause of seal failure and also is not easy to predict. However, this usually occurs when working with products that do not lubricate well. This can also occur if the surfaces are pressed together excessively (mechanically or hydraulically), causing the lubricant film to break down.

Slippage is easier to understand if we assume that the spinning ring continuously "stops" for a split second as it spins. This will cause random dark and shiny spots on the metal surface. It may also cause side effects such as clogging of drive pins, drivers, etc. When poor lubrication is the cause, the solution is to either use a double seal (thus trapping the poor lubrication between the surfaces) or flush the seal with a compatible fluid that has better lubrication properties. If the cause is overloading of the surfaces and if the pumped liquid

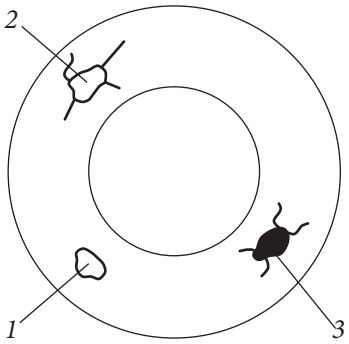

Fig. 7.10. Types of graphite ring damage: *1* — glossy spots; *2* — glossy spots with radial cracks; *3* — pit-type holes with cracks

Fig. 7.11. Damage to friction surfaces made of carbon graphite

has good lubricating properties, the only option is to check the installation procedure carefully.

13. Bonding surfaces. Broken locking pins, bent drivers, etc., can also be caused by sticking surfaces. Some fluids "glue" the seal surfaces on the atmospheric side. As long as the equipment is in working order, this is not an immediate problem, although, in the long term, it may cause the rings to become stuck. However, if a pump that pumps liquids with such peculiar properties sits for some time without moving, the product can "glue" the rings together. A subsequent launch may have disastrous results.

14. Formation of bubbles. Blistering (or crater) is a phenomenon sometimes encountered on graphite surfaces, sealing oil, or petroleum products. Since the formation of bubbles disrupts the flatness of the graphite ring, it will result in leakage, the amount of which depends on the number and type of bubbles.

We can define three types of blistering of increasing severity (Fig. 7.10).

Type *3* is often accompanied by a "comet-like trail" starting from the pit and extending toward the outer diameter of the surface. Because carbon is a porous material, the product can get trapped in cavities in the carbon.

This can happen under two circumstances:

- the material is not impregnated properly.
- the impregnation is washed away by the product.

The product in these cavities heats up and expands. However, the product cannot leave the cavities quickly enough, so the expanding liquid pushes the surface of the carbon upward. This raised part of the surface is subject to higher stress, causing increased friction and a sharp temperature rise. The raised part is polished by a rotating surface, and we have a type *1* blister (see Fig. 7.10).

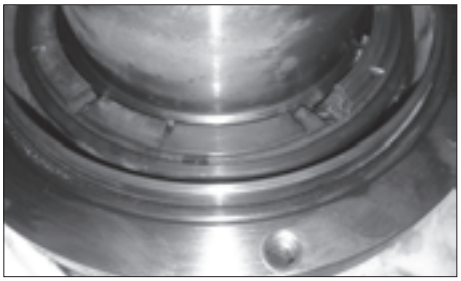

Fig. 7.12. Ring crushed by axial force

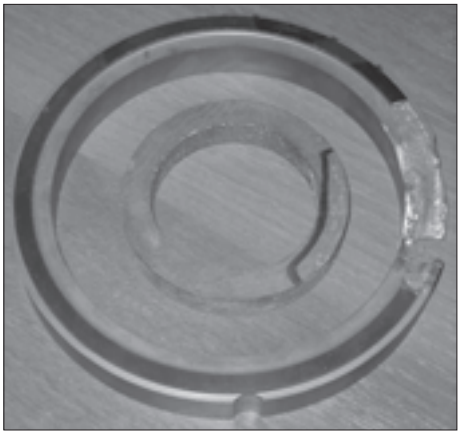

Fig. 7.13. Ring failure due to axial shear

Due to the above-mentioned increase in temperature, the pressure in the cavity increases, which leads to the formation of radial cracks (type *2*). Finally, stage *3* is reached when the liquid is heated above its boiling point and expands greatly, causing a crater to form on the surface of the carbon.

The main cause of blistering is temperature cycling, which is determined by the end load (seal setting and/or hydraulic load) and product type.

This type of damage to friction surfaces made of carbon graphite is called "blistering". As a result of large heat losses in the friction pair, the carbon graphite is heated, and the material with which it is impregnated is partially melted; as a result of this, large pores are formed on the friction surface (Fig. 7.11).

15. Inadmissible axial shift. Destruction of the rings of the end pair due to unacceptable axial movement of the rotor, caused, for example, by large wear of the hydraulic foot (over 2...3 mm) or destruction of the bearing that receives the residual axial force of the rotor is shown in Fig. 7.12.

Also, similar destruction of the rings occurs due to axial shear under the action of the sealing pressure of the rotor sleeve of the mechanical seal if it is not securely fixed on the pump shaft (Fig. 7.13).

7.4. Damage to secondary seals

Another reason for mechanical seal failure can be damage to the secondary seals. Currently, secondary seals are one of the shortest-lived elements of mechanical seals. The most widely used in modern mechanical seals are rubber rings with a circular cross-section (O-ring). PTFE rings, metal, and rubber bellows are used much less frequently.

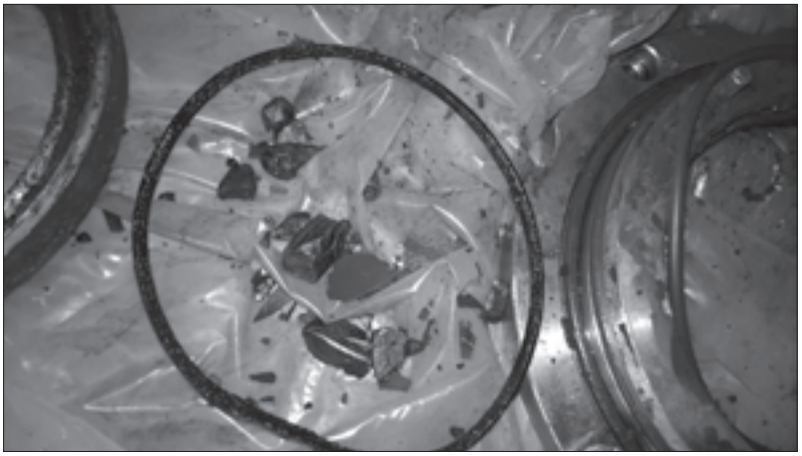

Fig. 7.14. Destruction of rubber rings

Rubber rings limit the use of mechanical seals by medium and temperature, fluoroplastic rings by pressure and rotation speed, and metal bellows by the differential pressure being sealed.

Most mechanical seals have a movable secondary seal between the rotating element and the shaft or sleeve (except for all metal bellows seals). There is also a non-dynamic gasket between the stationary surface of the housing and the sealing flange and a series of non-dynamic gaskets between the pump housing and the cooling inserts or seal chambers.

Generalization of experience in operating mechanical seals with auxiliary sealing devices based on elastomer rings allows us to identify the following typical cases of their damage.

7.4.1. Curing

When the secondary seal elastomer is exposed to heat outside its temperature range, it hardens and eventually cracks. This, of course, has a negative impact on seal performance, especially when it comes to a moving secondary seal.

Hardening, cracking, loss of shape, embrittlementare consequences of thermal exposure and occur when the permissible temperature for a given brand of rubber compound is exceeded (Fig. 7.14).

To avoid this problem, it is necessary to use better materials or, if this is not possible and the temperature is beyond the capabilities of all known elastomers, to apply water jacket cooling of the seal. An alternative solution is to use bellows seals.

7.4.2. Compression effect

As the secondary seal elastomer approaches its upper-temperature limit, it tends to lose its "memory" and harden into the form it is currently in. In practice, when disassembling the seal, it looks like "square O-rings", i.e., the O-ring takes the shape of the groove in which it was installed.

7.4.3. Cuts and nicks

If shafts with steps, keyways, threads, etc., are not properly "prepared" before secondary seals installation, the ring's transit through these "obstacles" may result in cuts and/or nicks, which will inevitably result in leakage. Visually, the leak will appear as liquid splashing at the outer end of the bushing.

7.4.4. Bloating

Typically, swelling occurs due to the chemical action of the sealing fluid on the secondary seal material. Swelling can lead to seal failure. It should be noted that the design or location of the secondary seal plays an important role. If the seal is completely closed (such as a U-cup), bulging will be less of a problem than with a more or less open O-ring.

The concentration of the liquid being compacted also plays an important role. It is well known that an environment in one percentage of components can be aggressive, but in other concentrations, it cannot be. The same applies to temperature.

Swelling is an increase in the volume and mass of the rings as a result of absorption of the compacted medium. It is characterized by the ratio of the increase in the ring's volume and mass to the initial volume or mass of the ring. Rings with swelling in the sealed medium at operating pressure and temperature above 3—5% are considered unsuitable for further use because, in this case, the mobility of the axially movable element is limited; as a result of this, the seal quickly fails.

In mechanical seals of energy pumps, rings made of ethylene-propylene rubber compounds (EPDM) are used widely, which swell and change their geometric dimensions even when contacted with a small amount of mineral oil or other lubricants. Quite often, this occurs as a result of lubricant leakage from the pump bearing assembly or if oil, petroleum-containing liquid, or solid lubricant is used when installing the seal in the pump.

To solve the swelling problem, you can use an alternative secondary seal material or change the seal fluid concentration to an acceptable level by injecting a compatible fluid into the seal cavity from an external source.

7.4.5. Extrusion

If the tolerances on the secondary seal grooves are too large and/or the Shore hardness of the seal material is too low, they may be extruded under pressure. Tighter tolerances must be adopted, or stiffer secondary seal elastomers must be used to avoid extrusion.

Sometimes, additional clamps or backup devices made, for example, of Teflon, are used for this purpose. The retainer must have smaller seating clearances than the main seal. Extrusion does not necessarily happen instantly. Depending on the combination of pressure and gaps, it may take days or even weeks for the effect to become apparent.

Generally speaking, any secondary seal that is placed between parts with gaps, such as an O-ring used as a runner seal, tends to extrude. As soon as a gap appears between two moving parts, the seal body tends to penetrate it towards the low-pressure area.

The tendency to extrude can be detected as "ridges" on the secondary seal in the above area.

However, extrusion is ever unlikely to occur at pressures below 5 MPa unless the gaps are excessive.

Shrinkage, loss of shape and elasticity occur due to the accumulation of residual deformation and lead to a decrease in contact pressure in the secondary seal. This phenomenon accelerates with increasing temperature.

Cuts, tears, and twisting occur as a result of the violation of the assembly order of the mechanical seal, especially often if the personnel have not received appropriate training.

Sticking of rubber rings to the shaft (some brands of rubber have good adhesion to metal and stick to the shaft with prolonged contact). Scratches and cuts on rubber rings (usually caused by sharp edges on the shaft, grooves, and keyways). Below are typical cases of damage to elastomer rings in seal assemblies, causes of damage, and methods for dealing with them.

7.4.6. Abrasive wear

Parallel or equidistant to the direction of movement or rotation of the contact surface, traces of wear are visible on the surface of the ring; foreign material pressed into the seal cross-section and tears may be found on the surfaces of the rings.

The causes of abrasive wear can be low cleanliness of the contact surfaces of parts in the assembly, the presence of abrasive inclusions in the sealed medium, heating of the rings to an unacceptably high temperature, and unacceptably large movements of the surfaces of the sealed parts. It is recommended to reduce the roughness of the surfaces of the grooves and the contact surface of the

rings, use elastomers with antifriction volumetric modification, and eliminate or limit the entry of abrasives and contaminants into the seal assembly during assembly and operation of the seal assembly to reduce abrasive wear of rings.

7.4.7. Residual compression deformation

The ring appears flattened in cross-section, with the flattened sides conforming to the shape of the seal's contact surfaces.

The causes of permanent compression deformation can be incompatibility with the chemical environment (excessive volumetric swelling of the elastomer in an aggressive chemical environment), abnormal thermal conditions of use, high compressive stresses, and incomplete vulcanization of the elastomer ring. It is recommended to use the correct geometric dimensions of the groove or seat and carefully select elastomers depending on the sealed medium, operating temperature conditions, and pressure loads of the medium to reduce significant compression deformations of the ring.

7.4.8. Chemical degradation

The ring surfaces show multiple signs of elastomer degradation, including blistering, cracking, blistering, and discoloration.

The causes of chemical degradation are incompatibility with the chemical environment and/or thermal conditions of use. It is recommended to choose for the rings an elastomer that is chemically resistant in the sealed environment (taking into account temperature conditions) to reduce the chemical degradation of the rings.

7.4.9. Caisson failure

Bubbles, cracks, and tears are found on the surfaces of the ring due to the adsorption of gas in the pores of the elastomer at high pressure and rapid release when the pressure decreases. The adsorbed gas creates bubbles and loosens the elastomer surface when the ambient pressure rapidly drops.

The cause of caisson failure is rapid changes in pressure, most often in rings made of low-hardness elastomers. Elastomers with higher hardness should be used for rings, and if possible, the variable pressure release rate should be reduced in the seal assembly to reduce caisson damage.

7.4.10. Squeezing ring material into the gap

The seal or seal elements develop fringed edges (usually on the low-pressure side) that appear flattened. Reasons for squeezing ring material into the gap

include excessively sized gaps in the seal assembly, excessive pressure, the use of low-hardness elastomers for rings, small dimensions of the ring groove, and sharp edges or corners on mounting parts or grooves. It is recommended to reduce the gaps between the sealing parts in the assembly, use an elastomer with a higher hardness, eliminate all sharp edges or corners on mounting parts or grooves, and use seals in the assembly that support anti-extrusion rings to prevent the extrusion of the ring material into the gaps.

7.4.11. Damage during installation

Small cuts, tears, and cuts are found on the surfaces of the rings. They may be caused by sharp edges or corners on mounting parts or grooves, the use of low-hardness elastomers for rings, contamination of the seal surface, or chips. It is recommended to eliminate all sharp edges or corners on mounting parts or grooves, use elastomers with higher hardness for rings, use elastomers with anti-friction volumetric modification, and make a groove for the ring of a more rational design to prevent damage during installation.

7.4.12. Outgassing of ingredients from the elastomer

The O-ring after operation may look simply like a seal with insufficient cross-section. Diagnosis of this type of seal failure is often difficult.

Causes may include improperly selected elastomer or seal vulcanization technology, high vacuum in the seal assembly, low elastomer hardness, or the use of a low molecular weight plasticizer. To reduce the loss of ingredients during the operation of elastomer rings, if such a phenomenon is detected, it is recommended to exclude the presence of a plasticizer in the rubber mixture. In addition, the rings must be put to an appropriate second stage of curing to minimize gas evolution.

7.4.13. Unacceptable compression deformation

The rings show depressed surfaces (corresponding to contact areas), and circular cracks may be observed on the depressed surfaces.

The reasons may be suboptimal groove design — an error in calculating the thermal expansion of the elastomer or its volumetric chemical swelling or unacceptable compressive deformation. It is recommended to double-check the design dimensions of the grooves, taking into account the properties of the material for the chemical properties and thermal parameters of the sealed medium to reduce compressive deformation.

7.4.14. Spiral twist

The O-ring seal shows spiral-shaped indentations or valleys. The cause of the phenomenon may be technological difficulties in installation or significant deformation of the rings during assembly (in the case of static seals), the use of elastomers with low hardness, unstable surface roughness of the O-ring (including excessive protrusion of the flash line), excessive width of the ring groove, unstable roughness or rough surface treatment of parts forming the groove, inappropriate lubrication. It is recommended to clarify the technology for installing the elastomer seal, use elastomers with higher hardness and with a volumetric antifriction modification for the rings, and make a groove for the ring of a more rational design and with lower surface roughness to reduce the spiral twisting of the rings.

7.4.15. Thermal degradation of the elastomer

The impact of excessive temperatures on secondary seals in the form of rubber rings can lead to their complete destruction (Fig. 7.15).

In some cases, radial cracks are visible on the surface of the rings, located in areas with maximum temperature exposure. Also, as a result of exposure to excess temperatures, softening zones can form on the surface of the rings — in the form of shiny surfaces (Fig. 7.16).

The cause of the phenomenon may be the temperature properties of elastomers, cyclic increases in temperature in the sealing unit exceeding permissible values. It is recommended to replace the elastomer with another material with higher thermal stability or consider cooling the sealing surfaces to reduce the impact of thermal degradation of the elastomer on seal assembly performance.

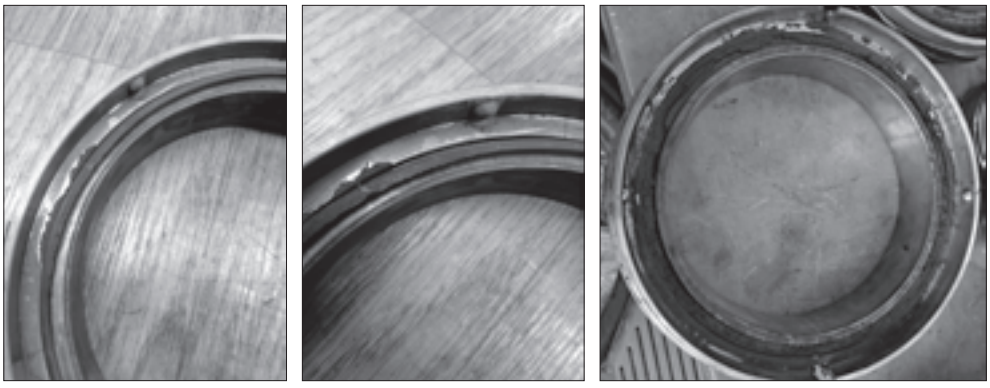

Fig. 7.15. Rubber rings burned in the sealing rings

7.4.16. Features of Teflon secondary seals

When Teflon came on the market, which was chemically inert and had acceptable temperature characteristics, it seemed like a solution to many problems.

However, over time, the enthusiasm has waned somewhat, especially in the field of mechanical seals. Teflon is still a great material, but it does have its drawbacks. Most materials have a linear expansion rate, but Teflon has a variable expansion rate at temperatures below 40° C. This makes it virtually impossible to manufacture Teflon seals to the tight tolerances that can be maintained for other materials.

PTFE rings are used only in mechanical seals of chemical pumps in case of insufficient chemical resistance of rubber compounds in a given liquid at a given temperature. PTFE rings are less reliable compared to rubber rings since they have practically no elasticity and are characterized by cold flow, i.e., rings are deformed at constant temperature and have low strength.

Modern mechanical seals for chemical pumps often use CLIN spherical fluoroplastic rings to seal axial movable rings. Experience in operating such seals shows that sometime after the start of operation, depressurization of the mechanical seal occurs due to wear of the metal part with which the fluoroplastic ring is in contact. In this case, the amount of metal wear sometimes can reach several millimeters.

Pure Teflon, at temperatures close to its operating limit combined with pressure tends to "cold flow". This also occurs at lower temperatures combined with relatively higher pressures. This tendency can be reduced by adding other materials, such as glass, to Teflon.

Teflon is also a non-memory material. In other words, once it is compressed into a certain shape, it does not return to its original configuration when the pressure is released.

Fig. 7.16. Thermal destruction of rubber rings

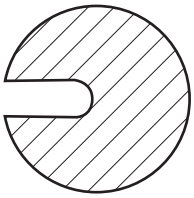

Fig. 7.17. Section of unidirectional secondary seal

Fig. 7.18. Sections of Borg-Warner ▶ secondary seals

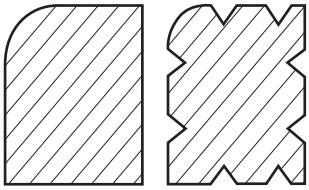

Whenever possible, the use of Teflon as a secondary seal (U-seal) or moving cage seal should be avoided unless there is no other alternative.

7.4.17. Direction of pressure

There are some secondary seals that, due to their configuration, make it nearly impossible to install the "wrong side" to the pressure being sealed, even if you are not familiar with that particular seal. Examples are the Borg-Warner U-cup and Durametallic V-cup or chevron gasket.

The O-ring is not a problem at all since it is "unidirectional" regarding pressure and vacuum and simply cannot be installed "back to front". However, in some cases, secondary movable cage seals are used, as shown in Fig. 7.17.

Obviously, they must be installed with the groove facing toward the pressure to function properly.

Borg-Warner seals use seberal secondary cage seals that can only be installed one way. We are talking about Teflon, Viton, asbestos, and graphoil seals of graphite rings in the cage. As can be seen from Fig. 7.18, they can only be installed with the rounded side facing the graphite.

7.5. Damage to leash products

Drive elements, despite their miniature and simplicity, are important parts of mechanical seals and perform the function of transmitting rotation to the rotor elements of mechanical seals or, on the contrary, securing the stator elements from rotation.

7.5.1. Causes of damage to driving elements

Local corrosion (pitting) are defects in the surfaces of metal parts in the form of cavities. It is caused by an electrochemical process in which the compacted liquid acts as an electrolyte, and defective areas are exposed to anodic action. To avoid pitting, it is necessary to correctly select the materials of the mating parts of the seal.

Fretting corrosion is corrosion-mechanical wear of the movable joint in the contact area of the secondary seal, as well as drive devices and springs. One of the main causes of intense fretting corrosion is unacceptable mechanical runout of the sealing ring, which is most often caused by:

Fig. 7.19. Drive element wear

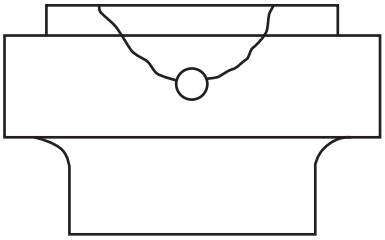

Fig. 7.20. Destruction of the ring at the location of the locking pin

• misalignment of the end of the seal chamber relative to the shaft axis;
• non-parallelism of the end surfaces of the fixed ring of the end pair;
• uneven thickness, un-removed flash or swelling of rubber rings sealing the back surface of the end-pair ring;
• abrasive deposits, salts, etc., on the back surfaces of the sealing rings.

With increasing shaft rotation speed, the intensity of fretting corrosion increases as the frequency of oscillatory movements in the moving joints of the seal increases. Fig. 7.19 shows an example of lead wear. It is also necessary, if possible, to exclude erosion and abrasive damage to the metal parts of the seal.

Erosive wear of seal parts is a consequence of exposure to a fluid flow that moves at a certain speed. Wear manifests in the form of local "potholes" (erosions) in both rotating and body parts. The wear rate increases with the increase in the flow rate of the liquid washing the seal parts and with the increase in the concentration of abrasive particles in it.

The most common cause of erosive wear is excessive fluid flow through the seal chamber and, as a result, high velocity of the fluid jet at the entrance to the sealed cavity.

7.5.2. Destruction of locking pins

Breaking out the locking pin can happen in two ways:
• in the radial direction;
• in the axial direction.

Breakout in the radial direction usually occurs when, for one reason or another, the torque transmitted to the pin from the friction of rotating and stationary surfaces becomes excessively large. This can occur due to excessive contact pressure in the seal or, for example, due to sticking or freezing of the O-ring surfaces. This can usually be corrected by adjusting the compression force or seal setting to a higher sealing pressure rating.

The reason for breakout in the axial direction can be twofold.

1. The groove that the locking pin fits into is too shallow. In this case, the crack will become visible, as shown in Fig. 7.20, which will ultimately lead to an impulse. Repeated processing to greater depth solves this problem.

2. Axial rupture due to overpressure may occur, but this is extremely rare. If there is excess pressure at any time during the service life of the seal, it can cause the seal's movable race to over-compress.

In this case, the locking pin may fail, and a crack may appear in the graphite ring. Seals are designed typically in such a way that this will not occur under normal pressure. Even slight excess pressure will not have a negative effect on the seal.

7.6. Other factors affecting the performance of mechanical seals

7.6.1. Corrosion

With the correct selection of materials, corrosion of metal surfaces does not exceed acceptable limits; otherwise, a change in materials is necessary. Another solution, in the case of a corrosive liquid seal, is to flush with a compatible non-corrosive liquid if corrosion occurs inside the seal.

Corrosion can also occur on the outside of the seal because some fluids only become corrosive when exposed to the atmosphere. As stated earlier, the mechanical seal must leak, so this relatively small amount of fluid can cause corrosion of the external parts. In this case, it can be prevented by hardening the surfaces of the parts.

Another form of corrosion is known as fretting corrosion. Some metals corrode when exposed to the atmosphere (oxygen). The best-known such metal is aluminum. Stainless steel is another one of these materials, and since stainless steel is a material commonly used in seal manufacturing, its corrosion sometimes causes seal failure. The most common location is on the bushing under the secondary or dynamic seal (e.g., U-ring, O-ring, chevron, wedge, etc.).

When the pump operates, friction occurs between the secondary seal and the bushing, which, combined with the aggressive atmosphere, destroys the chromium oxide layer that forms the protective shield of the stainless steel. Since the protective layer is being destroyed constantly, the chromium content of the alloy is depleted over a short period, leading to accelerated corrosion.

Fretting corrosion appears as a rough streak under the secondary seal and, depending on operating time, can create a deep groove in the area. The problem of fretting corrosion can be solved by proper maintenance or applying a hard coating to the bushing.

When equipment is regularly and properly maintained, i.e., shaft runout is within specified tolerances, no vibration, proper hydraulics, etc., fretting corrosion

is a problem. In terms of secondary seal material, fretting corrosion will be more evident when using Teflon than when using more flexible materials such as Viton.

7.6.2. Vibration

Methods for measuring vibration and interpreting the resulting readings have improved significantly over the past 10—15 years. Most power plants, oil refineries, and chemical plants now include vibration analysis in their preventive maintenance schemes.

Periodic measurements of equipment vibration usually allow maintenance personnel to stay one step ahead of sudden equipment failures. Nowadays, the techniques are so advanced that a skilled analyst can basically tell where to look for the problem.

Of course, vibration also affects the performance of mechanical seals. This is indicated by chipped and broken O-rings and uneven forms of contact between the parts of the bushing and the secondary seal.

In general, it can be said that when vibration becomes too high for the equipment containing the seal, the seal will also have problems.

7.6.3. Cavitation

Cavitation typically occurs at or near the suction port of a pump wheel because the pressure in that area may become (temporarily) lower than the vapor pressure of the product being pumped at the existing temperature.

When pressure increases, gas bubbles or cavities explode with great force. These forces can become so high that pieces of metal are actually pulled out of the volute or impeller.

Insufficient positive suction head can be the cause of all this, and therefore, steps must be taken to prevent serious damage to the pump. Cavitation also causes vibration and hydraulic disturbances in the pump, which can affect the mechanical seal.

7.7. Repair and restoration of mechanical seals

Mechanical seals can be repaired. The feasibility of repairs is determined in each specific case mainly by considerations of economy. All metal parts, bushings, flanges, spring holders, etc., as a rule, just require stripping. Secondary seals always should be replaced with new ones. The working surfaces of the sealing rings can be re-grounded, but before doing this, it is necessary to examine carefully the condition of the surfaces. If there are grooves, cracks, pitting, etc., replacement of the rings is recommended.

The above analysis of the reasons for the failure of mechanical seals allows us to give recommendations on methods for eliminating their malfunctions, which are summarized in Appendix for ease of use.

Malfunctions in the operation of mechanical seals, their causes and methods of elimination

Malfunction	External manifestation	Damaged parts	Side effects	Probable Cause	Recommended solutions
The elements of the drive system are damaged	Hardening on the surfaces of drive pins, keys, and drivers	Drive pins, keys, drivers	Damage to the elements of the drive system is possible Uneven drive	High viscosity liquid to be sealed	Increase the temperature of the liquid. Inject compatible low viscosity fluid
	As mentioned above	As mentioned above	Carbon spalling	Vibration. Cavitation	Check the equipment. Check flow and pressure and equipment piping
Thermal cracks	Radial cracks in a solid surface	Hard metal surfaces	Wear of softer mating surface due to raised particles. The seal becomes unbalanced when the sealing lip is completely worn out	Overheating caused by: excessive compression of the O-rings. Difference in thermal expansion between shaft and housing	Adjust the setting. Take into account the differences in materials and temperatures between the shaft and housing
				Thrust bearing failure	Repair the thrust bearing.
			O-ring slippage.	The sealed medium is too close to the steam pressure	Increase seal chamber pressure and/or cool it or use a sealing fluid with a higher vaporization limit

High wear	Excessive wea	Rubbing surfaces of sealing rings. Usually, the softer ring wears more	The seal becomes unbalanced when the sealing lip is completely worn out	Over compression	Adjust the setting. If only on the drive side, check for differences in expansion between the shaft and housing. If there is a difference, adjust accordingly	
	As mentioned above	As mentioned above	Possible slipping/ sticking. The seal becomes unbalanced when the sealing lip is completely worn out	Poor lubrication	Provide a compatible medium with good lubrication	
	As mentioned above	As mentioned above	Grooving on both sides. The seal becomes unbalanced when the sealing lip is completely worn out.	Abrasives	Install the cyclone(s). Provide a supply of locking fluid from a clean external source	
	As mentioned above	As mentioned above	Gumming on the atmospheric side of the edges. The seal becomes unbalanced when the sealing lip is completely worn out	Adhesion	Organize the supply of locking fluid from an external source. Change temperature and/or pressure if necessary	

Table continued

Malfunction	External manifestation	Damaged parts	Side effects	Probable Cause	Recommended solutions
High wear	As mentioned above	As mentioned above	Cracking of a metal surface causes surface particles to rise and become softer. The seal becomes unbalanced	Thermal shock on a metal surface	Replace damaged parts. Make sure the seals are maintained at the same temperature. Avoid large temperature fluctuations
Bloating	Pieces "torn out" from the mating surface	Graphite ring	Short seal life. Heavy leakage after a short period	Material is too low quality	Check with the supplier. Updating the material. Administer compatible fluid from an external source
The locking pin breaks	Immediate severe leakage	Graphite ring		High torque	Increase the number of pins or replace them with anti-rotation dowels
Vibration	Uneven operation of equipment	Graphite ring surfaces, bushings, drive pins, keys or drivers	Heavy leak. Short seal life	Imbalance (mechanical). Misalignment. Cavitation	Balance the rotor and clutch. Ensure alignment. Check the operating order

Corrosion	The bushings and/or shafts under the secondary seals are corroded. (Fretting corr.) Impact on metal parts, bushings, springs, etc	Shafts and/or bushings	Increased leakage	Insufficient corrosion resistance	Change material. Ensure that the fluid to be sealed is diluted from an external source with a compatible fluid. Use double or tandem seals. Use secondary seals where metal does not come into contact with the fluid being pumped
Insufficient axial compression of the rings	Bridge effect between the rotating ring and the cage in bellows seals	Rotating ring and bellows	Axial movement is stopped	No or insufficient cooling. Products that easily coke or crystallize on the atmospheric side	Check hardening. Dilute with washing liquid
	Clogged secondary seal between bushing and rotor	Rotating ring and bellows	Axial movement is stopped fretting corrosion,	As mentioned above.	As mentioned above. Rigid cover sleeve under the secondary seal
Insufficient or incorrect connections of piping and auxiliary devices	Thermal cracks	Metal surfaces	Increased leakage. Heavy wear	The water jacket is clogged. Cooler is blocked. Insufficient flow	Clean the water jacket and/or cooler. Increase the flow

Table continued

Malfunction	External manifestation	Damaged parts	Side effects	Probable Cause	Recommended solutions
Insufficient or incorrect connections of piping and auxiliary devices	Abrasives	Sealing surfaces of rings. Sometimes a rotating seal element	Corrugated surfaces. Mechanical wear of metal parts	Locking fluid supply is in the wrong place. No cyclones. The streams are incorrect. Suction pressure is lower than seal chamber pressure	Move feed. Install cyclones. Check pressure and openings. Set the reverse throttle to suction
	Various: Thermal cracks, severe wear, secondary seal hardening, melting	Graphite ring surfaces, secondary seals	Increased leakage	Blocked supply of locking fluid	Check the holes. If blocked, use a larger size
	Erosion	Usually a fixed ring	Destruction of the leash system. Destruction of the sealing surface	Jet effect of discharge flow. The hole is too big, so the flow is too big. The injection hole in the flange is too small. Incorrect injection flow angle	Install a smaller hole. Install away from the flange. Enlarge the hole. Change angle
Pipeline and auxiliary equipment	The inner ring has moved inside the chamber	Inner stationary ring with double seals	Contamination of the barrier flui	Pressure drops too low. Failure of the pressure compensator. The battery is broken. Excessive	Adjust settings. Check the battery. Replace outer seal

					leakage. The outer seal is leaking (the injection pump cannot cope)	
		Water in bearings	Bearings	Pump and seal failure	Closing pressure too high	Adjust the closing pressure. Install the lip seal onto the bearing
		The fixed ring moves	Fixed graphite ring	Heavy leak	Closing pressure too high. (typically, at low seal pressure)	Reduce closing pressure
		Uneven and severe wear (heat cracks)	Rotating and stationary rings	Short seal life	There is no ventilation hole provided. The seal works partly in pairs	Use a ventilation system according to API 02
		Thermal cracks	Metal surfaces and graphite rings (heavy wear)	Short seal life	No ventilation. The pipelines are long and there are many turns. there is no heat barrier. Baseplate cooler without thermosyphon and startup failure	Provide and use ventilation. Lay the pipeline as short as possible. Move the cooler above the shaft centerline
	Incorrect materials selected	Corrosion, wear, chemical attack	Any detail	Short seal life	Insufficient data for selection (mainly on basic seals). Materials do not meet standard	Check the selection table

The end of Table

Malfunction	External manifestation	Damaged parts	Side effects	Probable Cause	Recommended solutions
Deformations	Uneven wear. Pattern on surfaces	Surfaces of graphite rings	High leakage	Deformed clip. Uneven pressure. Secondary cage seal compressed	Adjust flange bolts. Measure the distance from the flange to the sealing surface. Check the thermal properties of materials. Increase the diameter of the seat
Secondary seals	Chemical damage. Destruction. Compression damage	Secondary seals	Swelling or shrinking. Heavy leak. Square rings	Medium concentration. The operating temperature is close to the limit of the materials	Dilute the medium. Change the temperature of the environment. Change the hardness or type of material
Secondary seals	Extrusion	Secondary seals	Sudden heavy leak	The material is too soft	Change the hardness or type of material
Secondary seals	Cuts, nicks	Secondary seals	Sudden heavy leak	Sharp edges on grooves, threads, steps, etc	Smooth out sharp edges
	Secondary seals are "sandwiched" between the parts	Secondary seals	Leak	The *O*-ring groove is too small or shallow. The *O*-ring is not positioned correctly	Check the groove size. Check that the *O*-ring is seated correctly
	O-ring is too big or small	Secondary seals	Leakage and/or installation difficulties	Wrong size selected	Check the dimensions using the *O*-ring chart

Incorrect installation	Different	All details	A leak. Increased wear. Uneven wear. Short seal life	Incorrect setting. The seal is pinched	Check the assembly setup according to the drawing. Check the shaft expansion relative to the pump housing expansion
	Different	All details	A leak. Increased wear. Uneven wear. Short seal life	Shaft offset too large. Shaft runout is too large	Check the end clearance and adjust according to the manufacturer's instructions. It is necessary to align or replace the shaft
				The radial clearance in the bearing is too large	Replace the bearing or check the fit of the bearing on the shaft and in the housing and adjust
				The shaft is not aligned with the body	Adjust the bearing(s)
				The cross section of the graphite rings is non-square	Treat the surfaces of the rings
	Heavy leak	Surfaces of graphite rings	A leak. Increased wear. Uneven wear. Short seal life	Excessive runout of the rotating ring race (inverted seals)	Check and correct

CONCLUSIONS

Modern mechanical seals of energy pumps are high-tech precision units that ensure the reliable operation of equipment for tens of thousands of hours without repair or maintenance.

The history of the emergence and development of mechanical seals presented in the book shows that their improvement is closely related to the use of new materials and modern technical solutions, the implementation of which requires a large number of diverse theoretical and experimental studies. In this regard, mechanical seals, as a rule, are developed and manufactured at specialized enterprises by highly qualified personnel using appropriate technological equipment.

The operating diagram of the mechanical seal described in the book made it possible to offer recommendations for calculating the unit. The resulting calculation methods make it possible to obtain, with sufficient accuracy for practice, a connection between the geometric parameters and operating conditions and the main operational characteristics of the seal. The importance of calculating the deformations of the sealing rings caused by both the pressure of the sealing medium and thermal effects is shown to predict the size and direction of the radial cone and avoid the unstable operation of the seal.

The given classification of mechanical seals allows us to judge the variety of their designs clearly. An analysis of directions for improving the designs of mechanical seals has shown stable trends towards the widespread use of cartridge-type mechanical seals and for pumps pumping hot liquids — designs of mechanical seals with non-contact friction pairs combined with coolers along the shaft.

Many years of operating experience and extensive results of theoretical and experimental studies of promising mechanical seal designs have shown that impulse seals have

significant advantages over other non-contact mechanical seals types and are the most promising for use in harsh operating conditions, which are typical for energy pumps. A modern method for calculating the main characteristics of impulse mechanical seals is presented, which allows to obtain with high accuracy the geometric dimensions of the friction pair rings that best correspond to the required operating conditions.

The book also pays attention to the features of manufacturing, assembly, and hydraulic testing of mechanical seals and examines the requirements for the accuracy and quality of manufacturing of their parts, which are significantly higher than for other parts and components of the pump.

A large number of the most common designs of mechanical seals used in feed, condensate, network, and other energy pumps are considered.

In the final part, an analysis of the reasons for the failure of mechanical seals is carried out, and recommendations on methods for eliminating their malfunctions are given.

REFERENCES

1. Adamczak, S., Kundera, C., Swiderski, J. (2017). Assessment of the state of the geometrical surface texture of seal rings by various measuring methods. *IOP Conference Series: Materials Science and Engineering*, *233*(1), 12—31.
2. Birger, I., Shorr, B., Iosilevich, G. (1993). *Calculation of machine parts strength*. Moscow, Mashinostroenie [in Russian].
3. Błasiak, S., Kundera, C. (2012). A numerical analysis of the grooved surface effects on the thermal behavior of a non-contacting face seal. *Procedia Engineering*, *39*, 315—326. https://doi.org/10.1016/j.proeng.2012.07.037
4. Błasiak, S., Zahorulko, A. (2016). A parametric and dynamic analysis of non-contacting gas face seals with modified surfaces. *Tribology International*, *94*, 126—137. https://doi.org/10.1016/j.triboint.2015.08.014
5. Bo, D., Suping, Y., Qingkai, Z., Xuzhou, C., Jiying, W., Xuan, Z. (2019). The speciation analysis of colloids in the primary coolant in nuclear power plant. *Radiation Physics and Chemistry*, *159*, 81—88. https://doi.org/10.1016/j.radphyschem.2019.02.023
6. Christensen, N. (1939). U. S. Patent 2180795.
7. Cooke, G.J. (1923). U. S. Patent 1545080.
8. *Dictionary-reference book on friction, wear and lubrication of machine parts*. (1979). Shvedkov, E.L., Rovinsky, D.Y., Zozulya, V.D., Brown, E.D. (Eds.). Kyiv, Naukova Dumka [in Russian].
9. EagleBurgmann. (2006). *Mechanical seal technology and selection*. URL: http://www.boyser.sk/prislusenstvo/EagleBurgmann.com
10. Elonka, S. (1956). *Take a look at to-day's mechanical seals*. Power.
11. Falaleev, S., Chegodaev, D. (1998). *Face-to-face contactless sealing of aircraft engines*. Moscow, MAI Publishing House [in Russian].
12. *Flow-Serve-Mechanical-Seals-Catalog (Borg Warner — Flowserve)*. (2022). https://www.mechanical seals.net/pdf/Flow-Serve-Mechanical-Seals-Catalog
13. Gabriel, R. (2011). The History of Pumps: How Seals Have Changed the Pump industry. *Pumps & Systems Magazine*, Birmingham, Alabama, USA.
14. Gaft, Y., Anoshko, V. (1980). *Stuffing box seals of dynamic pumps. Overview information*. Ser. XM-4. Moscow, TsINTIkhimneftemash [in Russian].

15. Gaft, Y. (1988). Technical and economic analysis of the use of various types of seals. *Proceedings of the V scientific-technical Meetings on sealing technology*, 62—63. Sumy [in Russian].
16. Gaft, J., Zahorulko, A., Martsynkovskyy, V., Kundera, Cz. (2012). Theoretical and experimental investigations of buffer face impulse seals. *11th EDF/Prime Workshop: Behavior of Dynamic Seals in Unexpected Operating Conditions*. http://doi.org/10.13140/RG.2.1.4062.9204
17. Golubev, A.I. (1976). Mechanical seals of rotating shafts. Moscow, Mashinostroenie [in Russian].
18. Golubev, A.I. and Kondakov, L.A. (Eds.). (1994). *Seals and sealing technology: reference book*. Moscow, Mashinostroenie [in Russian].
19. Grundfos. (2013). Mechanical shaft seals for pumps. URL: https://www.yumpu.com/user/dk.grundfos.com
20. Holling, J. (1983). Derivation of the mechanical wear equation. *Proceedings of the American Society of Mechanical Engineers. Ser.: Problems of friction and lubrication*, *105*(2), 55—63.
21. Hornschurch, H. (1937). U. S. Patent 2128744.
22. Key, W., Dickau, R., Carlson, R. (2004). Mechanical Seals with Wavy Faces for a Severe Duty NGL/Crude Pipeline Application. *Proceedings of the 21st International Pump Users Symposium, Turbomachinery Laboratory*, Texas A&M University, College Station, Texas, 77—87.
23. Kondakov, L. A. (1972). *Seals of hydraulic systems*. Moscow, Mashinostroenie. [in Russian].
24. Kragelsky, I., Mikhin, N. (1984). *Friction units of machines: Handbook*. Moscow, Mashinostroenie [in Russian].
25. Krevsun, E. (1998). *Mechanical sealers of rotating shafts*. Minsk, Arty-Flex [in Russian].
26. Krivoruchko D. (2013). *Mechanical processing of composite materials*. Sumy, University Book [in Ukrainian].
27. KSB. (2017). *Expertise you can trust: pumps, valves and services for nuclear power stations*. URL: https://www.ksb.com/en-sk/applications/energy-technology/nuclear-power-plants
28. Kuznetsov, E., Tverdokhleb, I., Chernov, A. (1989). Modern shutter mechanical seals of centrifugal machines shafts. *Current State and Prospects for the Development of Hydraulic Engineering in the XXI Century: Proceedings of an International Scientific and Technical Conference*, 193—194 [in Russian].
29. Lebeck, A. (1987). U. S. Patent 4836561.
30. Lebeck, A. (1991). *Principles and Design of Mechanical Face Seals*. New York.
31. Loenhout, G. (2005). *Mechanical Seals with Laser Machined Wavy SiC Faces for High Duty Boiler- and Steam Generator Feedwater Applications*. Flowserve Flow Solutions Division.
32. Ma, C., Bai, S., Peng, X. (2016). Thermo-hydrodynamic characteristics of spiral groove gas face seals operating at low pressure. *Tribology International*, *95*, 44—54. https://doi.org/10.1016/j.triboint.2015.11.001
33. Makarov, G. (1973). *Sealing devices* (2nd ed.). Leningrad, Mashinostroenie. [in Russian].
34. Marcinkowski, W., Kundera, Cz., Gaft, J. (2005). Double impulse seals. *Hydraulics and Pneumatics*, *5*, 8—11.

35. Martsinkovsky, V. (2005). Hermomechanics, its role in ensuring the efficiency and environmental friendliness of pumping and compressor equipment. *Bulletin of the Sumy State University. Series of technical sciences*, *1*(73), 5—10. [in Russian].
36. Martsinkovsky, V. (2005). Hydrodynamics of throttling channels. Sumy. [in Russian].
37. Martsinkovsky, V., Shevchenko, S. (2018). *Pumps of Nuclear Power Plants: Calculation, Design, Operation*. Shevchenko, S. (Ed.). Sumy, University Book Publishing House. [in Russian].
38. Martsinkovsky, V., Gaft, J., Zagorulko, A., Gromyko, B. (2003). Design and calculation of mechanical seals with self-adjusting clearance. *Papers presented at 17th International Conference on Fluid Sealing*. York, UK. 505—520.
39. Martsynkovskyy, V., Gaft, Y., Gromyko, B., Chernov, O. (2000). Development and application of double pulse gas-liquid seals. *Proc. of 16th International Conference on Fluid Sealing*. Brugge, Belgium. 255—260.
40. Martsynkovskyy, V., Zahorulko, A., Gudkov, S., Mischenko, S. (2012). Analysis of buffer impulse seal. *Procedia Engineering*, *39*, 43-50. https://doi.org/10.1016/j.proeng.2012.07.006
41. Mayer, E. (1978). *Face seals*. Moscow, Mashinostroenie [in Russian].
42. Mayer, E. (1982). *Mechanical seals*. (3rd ed.). (trans.). Dr. Nau, B.S. (Ed.). Butterworth Scientific, London-Boston.
43. Melnik, V. (2004). Calculation of deformations in the rings of an end pair when loading the mechanical seal assembly by a pressure difference. *Chemical and oil and gas engineering*, *8*, 28—31 [in Russian].
44. Melnik, V. (2002). Temperature field and temperature deformation of mechanical seal rings. *Chemical and oil and gas engineering*, *8*, 29-32 [in Russian].
45. Melnyk, V. (2008). *Mechanical seals of shafts. Reference book*. Moscow, Mashinostroenie [in Russian].
46. Melnyk, V. (2003). A simplified method of calculating the working characteristics of an end seal. *Chemical and oil and gas engineering*, *9*, 31—33 [in Russian].
47. Melnyk, V. (2004). Heat generation in a turbulent flow of a compactable medium from disk friction in a face seal chamber. *Chemical and oil and gas engineering*, *12*, 28-29 [in Russian].
48. Miller, A. (1992). *People, Products and Progress: The Durametallic Story*. The Pricilla Press, Allegan, Michigan.
49. Mueller, H., Nau, B. (1998). *Fluid sealing technology*. New York, Marcel Dekker Inc.
50. Muller, H. (1990). *Sealing of moving machine parts*. Waiblingen, Media publisher.
51. Müller, M.; Šleger, V.; Čedík, J.; Pexa, M. (2022). Research on the Material Compatibility of Elastomer Sealing O-Rings. *Polymers*, *14*, 3323. https://doi.org/10.3390/polym14163323
52. Nau, B. (1980). Experimental observations and analysis of film characteristics of mechanical sealing. *Friction and lubrication problems*, *3*, 84—93.
53. Qiu, Y., Khonsari, M. (2012). Thermohydrodynamic Analysis of Spiral Groove Mechanical Face Seal for Liquid Applications. *Journal of Tribology*, *134*(2): 021703. http://dx.doi.org/10.1115/1.4006063
54. Rabinovich, E. (1981). Magnitude, spread and application of wear coefficient. *Proceedings of the American Society of Mechanical Engineers. Ser.: Problems of friction and lubrication*, *103*(2), 12—19.

55. Schlichting, H., Gersten, K. (2016). *Boundary-Layer Theory*. Springer, Berlin, Heidelberg, 29-49. https://doi.org/10.1007/978-3-642-85829-1_2
56. Schmitz, C. (1947). *Mechanical Seals*. Crane Packing Co. Ltd., USA.
57. Schoenherr, K. (1965). *Design Terminology for Mechanical End Face Seals*. SAE Paper No. 650301.
58. Shevchenko, S., Shevchenko, O., Radchenko, M. (n.d.). Assessment of Sealing Systems Impact on the Vibration and Environmental Safety of Rotary Machines. *Proc. of the Interdisciplinary Conference on Mechanics, Computers and Electrics (ICMECE 2022)*, Barcelona, Spain, ID 427.
59. Shevchenko, S. (2020). Computational method for mechanical seal as a dynamic system. *Electronic modeling*, *45*(5), 66—81. https://doi.org/https://doi.org/10.15407/emodel.42.05.066
60. Shevchenko, S. (2023). *Sealing systems and dynamics of centrifugal machines*. Kyiv, Akademperiodyka. https://doi.org/10.15407/akademperiodyka.479.266
61. Shevchenko, S., Chernov, A. (2020). Development of pulse mechanical seal calculation methods on the basis of its physical model construction. *Eastern-European Journal of Enterprise Technologies*, *3*(*2*(105)), 58-69. https://doi.org/10.15587/1729-4061.2020.206721
62. Shevchenko, S., Gaft, Y. (2020). *Stuffing box seals of dynamic pumps*. Shevchenko, S., (Ed.). University Book Publishing House [in Russian].
63. Shevchenko, S., Shevchenko, O. (2020). Improvement of Reliability and Ecological Safety of NPP Reactor Coolant Pump Seals. *Nuclear and Radiation Safety*, *4*(88), 47—55. https://doi.org/10.32918/nrs.2020.4(88).06
64. Skakov, M., Kurbanbekov, Sh., Koyanbaev, Y., Baklanov, V., Miniyazov, A., Mukhamedzhanova, R. (2015). Siliconized Graphite Production Technology. *Proceedings of the 2015 AASRI International Conference on Circuits and Systems*. Atlantis Press, 215—218. https://doi.org/10.2991/cas-15.2015.51
65. Stevenson, R. (1939). U. S. patent 2321871.
66. Vargaftik, N.B. (1972). *Handbook of Thermophysical Properties of Gases and Liquids*. Moscow, Nauka [in Russian].
67. Vasilytsov, E. (1974). *Non-contact seals*. Leningrad, Mashinostroenie [in Russian].
68. Wilkinson, J. (1913). U. S. Patent 1063633.
69. Williams, J. (2005). *Engineering Tribology*. Cambridge University Press, Cambridge.
70. Yu, Z., Shevchenko, S., Radchenko, M., Shevchenko, O., Radchenko, A. (2022). Methodology of Designing Sealing Systems for Highly Loaded Rotary Machines. *Sustainability*, *14*(23):15828. https://doi.org/10.3390/su142315828
71. Zagorulko, A. (2015). Theoretical and experimental researches of end shutter pulsed compacted with discrete supply. *Eastern-European journal of advanced technologies*, *4*(7), 45—52.
72. Zhu, W., Wang, H., Zhou, S. (2014). Research on sealing performance of hydrostatic pressure mechanical seal. *Journal of Marine Science and Technology*, *22*(6), 673-679. https://jmstt.ntou.edu.tw/journal/vol22/iss6/2

AUTHORS

SERHII SHEVCHENKO was born in 1961 and graduated from the Kharkiv Polytechnic Institute (KhPI) in 1984 (specialty: "Hydraulic machines and means of automation"). In 1990, he defended his Ph. D thesis on the topic "Development and research of new designs of stuffing-box seals for NPP pumping equipment". He worked at the research laboratory of machines' vibration reliability at the theoretical mechanic department of the Sumy branch of KhPI (later Sumy State University) as a research associate from 1984 to 1994 (as a junior researcher since 1986, as a senior researcher since 1991), participated in the development for the Aircraft technology and NPP. Since July 2020, he has been a senior researcher at the G.E. Pukhov Institute for Modelling in Energy Engineering of the National Academy of Sciences of Ukraine (IPME). In June 2023, he defended his doctoral (Doctor of Engineering) thesis on the topic "Mathematical models of processes in the sealing systems of centrifugal machines". The area of S. Shevchenko's research related to the methods of development of sealing theory and vibration reliability of centrifugal machines.

OLEKSANDR CHERNOV was born in 1963 and graduated from the Sumy Branch of the Kharkiv Polytechnic Institute in 1985 (specialty: "Hydraulic machines and means of automation"). In 1995, he defended his Ph. D thesis on the topic "Development and optimization of impulse mechanical seals for high-speed turbopump units of liquid jet engines". He worked as a researcher at the research laboratory of machines' vibration reliability at the theoretical mechanic department of the Sumy branch of KhPI (later Sumy State University) from 1987 to 1995. From 1996 to 2001, he worked as a lecturer and senior lecturer at the Department of General Mechanics and Dynamics of Machines of Sumy State University. From 2002 to 2003, he was the head of department No. 7 of VNDIAEN in Sumy. From 2004 to the present day, he is the director of "KB UKRSPETSMASH" LLC, Sumy. The direction of scientific and industrial activity of O. Chernov related to the development, production, and improvement of mechanical seals of various centrifugal machines (pumps, compressors, etc.)

Розглянуто фізичні засади та розроблено сучасні методи розрахунку контактних торцових ущільнень. Описано принцип роботи, методи розрахунку та особливості конструювання безконтактних торцових ущільнень. Представлені сучасні технології та матеріали, що застосовуються під час виробництва торцових ущільнень. Запропоновано напрями удосконалення торцових ущільнень. Проведено аналіз конструкцій та особливості експлуатації торцових ущільнень енергетичних насосів. Виявлено основні причини виходу з ладу та розроблено систему обслуговування і ремонту торцових ущільнень.

Монографія допоможе фахівцям у галузі ущільнювальної техніки і конструкторам насосного обладнання. Вона буде корисною фахівцям, які займаються експлуатацією та обслуговуванням відцентрових насосів, а також студентам енергомашинобудівних спеціальностей ЗВО.

Наукове видання

НАЦІОНАЛЬНА АКАДЕМІЯ НАУК УКРАЇНИ
ІНСТИТУТ ПРОБЛЕМ МОДЕЛЮВАННЯ В ЕНЕРГЕТИЦІ
ім. Г.Є. ПУХОВА НАН УКРАЇНИ

ШЕВЧЕНКО Сергій Станіславович
ЧЕРНОВ Олександр Євгенович

ТОРЦОВІ УЩІЛЬНЕННЯ ЕНЕРГЕТИЧНИХ НАСОСІВ

Англійською мовою

Редактор-коректор *О.В. Нікітченко*

Художнє оформлення *Є.О. Ільницького*

Технічне редагування *Т.М. Шендерович*

Виготовлення ілюстрацій *О.В. Нікітченко*

Комп'ютерна верстка *С.В. Кубарєва*

Підп. до друку 22.05.2024. Формат 70 × 100/16. Гарн. Minion Pro.
Ум. друк. арк. 16,66. Обл.-вид. арк. 16,49. Тираж 100 прим. Зам. № 7289.

Видавець і виготовлювач Видавничий дім "Академперіодика" НАН України
01024, Київ, вул. Терещенківська, 4

Свідоцтво про внесення до Державного реєстру суб'єктів видавничої справи серії ДК № 544 від 27.07.2001 р.